Solid-supported boronic acid conjugates for sugar and glycopeptide recognition

Peter Christopher Chisnall

Doctor of Philosophy

ASTON UNIVERSITY

October 2008

ASTON UNIVERSITY

Solid-supported boronic acid conjugates for sugar and glycopeptide recognition

A thesis submitted by Peter Chisnall B.Sc. (Hons) for the degree of
Doctor of Philosophy
October 2008

Abstract

The Fmoc synthetic strategy is based on the step wise coupling of *N*-α-Fmoc-protected amino acids to resin-bound amino functional groups through activation of the free carboxy group. Subsequent cleavage of the *N*-α-Fmoc protecting group yields the amino group of the newly coupled residue, allowing the process to be repeated to form peptide chains.

The Fmoc synthetic strategy was employed to synthesise two identical combinatorial peptide libraries on a hydrophilic PEG-PS resin. One library was appended with boronic acid moieties at two positionally-fixed locations. Successful inclusion of the boronic acid units was confirmed using a novel UV fluorescent colorimetric assay employing carminic acid as the dye compound.

A study of the effect had by the resin-bound peptides bearing boronic acid groups on the binding characteristics of vancomycin, a medically relevant antibiotic glycoprotein, was conducted. In all, 132 library compounds were tested for their binding affinity with vancomycin, via immobilisation of the glycopeptide onto the solid support through hydrogen bonding or complexation with the boronic acid moieties. Subsequent cleavage via acidolysis afforded vancomycin containing solutions which were quantified by growth inhibition of methicillin susceptible *Staphylococcus aureus*. Comparison of the diameters of the resultant zones of inhibition and those produced by vancomycin of known concentrations afforded a means of calculating the vancomycin concentration of the cleavage solutions, and thereby determining the binding affinity of vancomycin to each peptide sequence.

Five peptide sequences and twenty one of the peptidyl-boronic acid sequences showed zones of inhibition, demonstrating their reversible affinity for vancomycin. Three peptide sequences showed zones of inhibition in both libraries. The presence of boronic acid was therefore shown to impart, enhance, detract and remove the affinity of vancomycin to a range of resin-bound peptide sequences.

Keywords

Solid Support Resins; Boronic acid; Carbohydrate recognition; Vancomycin; Combinatorial peptide library

Acknowledgements

I would like to thank Dr. Andrew Sutherland for his constant help, guidance, support and enthusiasm throughout a project which did not begin life under his supervision, and Dr. Dierdre Pearce for the initial invitation to return to her research group.

I am also grateful to Mrs. Karen Farrow for her tireless efforts with performing low and high resolution mass spectrometry data. I would like to thank Dr. Mike Perry for his help and guidance with NMR spectroscopy, and to Dr. Sahar Al-Malaika and her research group for the use of their 'golden gate' FTIR apparatus.

I would especially like to thank Dr. Dave Nagel for the considerable time and energy he spent making the biological assays such a success. This thanks extends to Dr. A. V. Hine and the rest of her research group, and to Dr. Peter Lambert and the microbiology department for the extended use of their facilities and expertise.

I would also like to thank Dr. David J. Evans, Dr. Kevin Treacher, Dr. John Liddell and all of those at Avecia and Reaxa whose expertise, guidance and support were of great value to the project and to me personally.

Thank you to my friends and members of the Sutherland research group, Siobhan Cummins, Katy Parker, Jon Behrendt, and Steve Ryley, all of whom made life in the lab more enjoyable.

I would like to thank my brother David for his help with the numerous mathematical problems encountered over the years.

I would also like to thank Ian Henderson, whose patience, tolerance and humour know no bounds.

Finally I would like to thank my Mum, Dad and Nina for their unwavering support.

List of Contents

List of Tables

List of Figures

List of Reaction Schemes

List of Mechanisms

List of Pictures

List of Equations

List of Spectra

Abbreviations

(br)	Broad
(m)	Medium
(s)	Strong
(w)	Weak
1°	primary
2°	secondary
3°	tertiary
AA	Amino acid
Ac_2O/AcOAc	Acetic anhydride
AcO	Acetate
AcOH	Acetic Acid
AIBN	Azo-*iso*-butrylnitrile
AIDS	Acquired immunodeficiency disease
AMPS	Aminomethyl(poly)styrene
APCI-MS	Atmospheric pressure chemical ionisation mass spectrometry
Ar	Aromatic
ATR	Attenuated Total Refraction
Bn	Benzyl
Boc	*tert*-Butoxycarbonyl
CD	Circular Dichromism
$CDCl_3$	deuterated chloroform
CMPS	Chloromethyl(poly)styrene
CMS	Chloromethylstyrene
d	Doublet
Dansyl	5-dimethylaminonaphth-1-ylsulfonyl
DBU	1,8-Diazabicyclo[5.4.0]undec-7-ene
DCB	2,6 dichlorobenzoyl chloride
DCC	N,N-dicyclohexylcarbodiimide
DCM	Dichloromethane
Dde	1-(4,4-Dimethyl-2,6-dioxocyclohexylidene)ethyl
DIPEA	N,N-diisopropylethylamine
DMAP	4-Dimethylaminopyridine
DMF	N,N-Dimethylformamide
DMSO	Dimethyl sulfoxide
DMT	4,4'-Dimethoxytrityl
DNA	Deoxyribonucleic acid
DVB	1,4-Divinylbenzene

E. Coli	*Escherichia Coli*
EI	Electron Ionisation
Eqn.	Equation
eqv.	Molar Equivalents
EtOAc	Ethyl Acetate
FAB	Fast Atom Bombardment
FITC	Fluorescein isothiocyanate
Fmoc	9-Fluorenylmethoxycarbonyl
FTIR	Fourier Transform Infra Red Spectroscopy
H_2O	Water
HBTU	2-(1H-Benzotriazole-1-yl)-1,1,3,3-tetramethylaminium hexafluorophosphate
HCl	Hydrochloric acid
HIV	Human immunodeficiency virus
HOBt	N-Hydroxybenzotriazole
HPLC	High Performance Liquid Chromatography
HRMS	High Resolution Mass Spectrometry
Hz	Hertz
inh.	inhibition
IR	Infrared
m	Meta
m.p.	Melting Point
MeCN	Acetonitrile (methyl cyanide)
MeOH	Methanol
MHz	Megahertz
MIC	Minimum inhibitory concentration
MMT	4-Mono-methoxy trityl
mol	Mole
MS	Mass Spectrometry
MSSA	Methicillin susceptible *Staphylococcus aureus*
Mtt	methyltrityl
MW	Molecular weight
NHS	N-Hydroxysuccinimide
NMR	Nuclear Magnetic Resonance
o	Ortho
°C	Centigrade
p	Para
PBA	Phenylboronic acid
PEG	Poly(ethylene glycol)
PEG-PS	Poly(ethylene glycol)-Polystyrene

PET	Photoinduced Electron Transfer
Ph	Phenyl
ppm	Parts per million
PS	Cross-Linked Polystyrene
PVA	Polyvinyl alcohol
PyBOP	Benzotriazole-1-yl-oxy-tris-pyrrolidino-phosphonium hexafluorophosphate
R_f	Retention factor
Rink amide MBHA	4-(2',4'-dimethoxyphenyl-Fmoc-aminomethyl) phenoxyacetamido-norleucyl-p-methylbenzhydrylamine resin.
s	Singlet
sat.	Saturated
S_N1	Unimolecular Nucleophilic Substitution
S_N2	Bimolecular Nucleophilic Substitution
SPOC	Solid Phase Organic Chemistry
SPOS	Solid Phase Organic Synthesis
SPPS	Solid Phase Peptide Synthesis
SPS	Solid Phase Synthesis
Sty	Styrene
t	Triplet
TBTU	2-(1H-Benzotriazole-1-yl)-1,1,3,3-tetramethylaminium tetrafluoroborate
tBu	tertiary butyl
TEA	Triethylamine
TFA	Trifluoroacetic Acid
THF	Tetrahydrofuran
TIPS	Triisopropyl silane
TLC	Thin Layer Chromatography
TNBS	2,4,6-trinitrobenzenesulfonic acid
Tos-Cl	*p*-toluenesulfonyl chloride
Tos/Tosyl	*p*-toluenesulfonyl
Trt	Trityl (triphenylmethyl)
UV/VIS	Ultra Violet/ Visible light Spectroscopy

Amino Acids

Ala	A	Alanine
Arg	R	Arginine
Asn	N	Asparagine
Asp	D	Aspartic acid
Cys	C	Cysteine
Gln	Q	Glutamine
Glu	E	Glutamic acid
Gly	G	Glycine
His	H	Histadine
Iso	I	Isoleucine
Leu	L	Leucine
Lys	K	Lysine
Met	M	Methionine
Nle	*	Norleucine (* non-natural amino acid)
Phe	F	Phenylalanine
Pro	P	Proline
Ser	S	Serine
Thr	T	Threonine
Trp	W	Tryptophan
Tyr	Y	Tyrosine
Val	V	Valine

Chapter 1

Introduction

Introduction

1.1 Carbohydrates in Nature

Carbohydrates are everywhere. Glucose **1-4**, when considered in its polymeric cellulose form **5**, is the most abundant organic molecule on the planet[1]. The traditional view of the role of carbohydrates in nature ranges from being an energy source in organisms through to being the actual building blocks of the organisms themselves, for example the β-(1-4) polymer in cellulose **5** or the α-(1-4) glucose polymer in starch **6**.

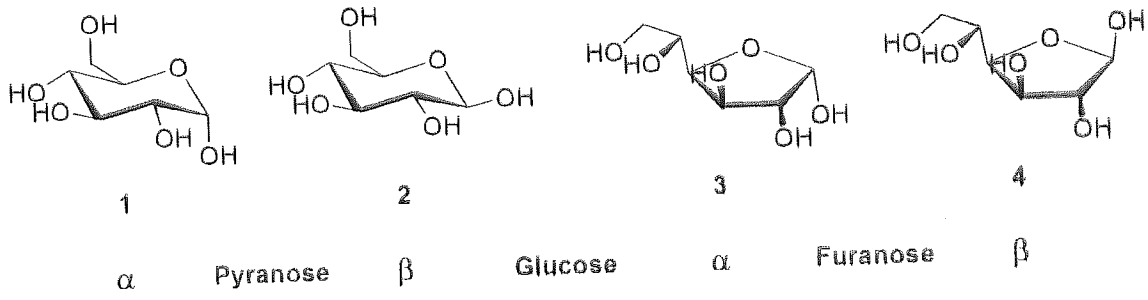

Figure 1: Anomers of glucose displayed in both furanose and pyranose ring forms.

However, they play an even more active role in the way cells and organisms function, being utilised for biological communication events that control processes such as egg fertilisation, microbial infection, inflammation and cancer growth[1]. Indeed without the sugars present in DNA and RNA, life itself could not come to pass.

1.1.1 Energy

Glucose is an important fuel for organisms. In mammals, glucose is the only fuel the brain uses under non-starvation conditions and is the only fuel available to red blood cells[2]. Glycolysis and fermentation are processes used by cells to generate energy from glucose. Under anaerobic conditions, glucose is converted, via phosphorylation and isomerisation, into pyruvate and ATP which results in a release of energy. Pyruvate can then be fermented to lactate or ethanol to produce more energy. Under aerobic conditions, pyruvate can be completely oxidised to CO_2 via the Krebs cycle, yielding much more ATP and energy than the anaerobic process.

When instant energy is not immediately required, glycogen serves as an energy storage medium for animals. Dietary carbohydrates not required for immediate use are converted into glycogen by the body for short-term storage, or fat for longer term storage. Glycogen contains a complex three-dimensional structure with both α-1,4' and α-1,6' glycosidic links between glucose units, numbering up to 100,000 in total[3]. Glycogen synthase constructs a glycogen chain of α-1,4 linkages. A second enzyme breaks an α-1,4 link and converts it into a α-1,6 link in order to introduce a greater degree of branching. This heavy branching increases the solubility but also the number of ends so that it can be made and degraded more rapidly than if it was linear[2].

Most of the glycogen molecule can be degraded by the enzyme glycogen phosphorylase. Glycosidic links between C1 of the terminal residue and C4 of the adjacent residue are cleaved to yield glucose 1-phosphate. This can be reversibly converted to glucose 6-phosphate and utilised during glycolysis[2].

1.1.2 Structural Carbohydrates

Polysaccharides consist of hundreds or thousands of repeating monosaccharide units linked together by glycoside bonds. They have no free anomeric hydroxyls (except

for the chain ends) and are therefore stereochemically fixed, showing no mutarotation[3]; the change in specific rotation of a monosaccharide due to spontaneous inter-conversion between the α and β forms until an equilibrium is reached.

Cellulose **5** is a polymer of D-glucose in which the anomeric centre of each unit is linked to the oxygen at position 4 of next unit. The bond in this instance conforms to β stereochemistry. Thousands of glucose units form to create a single molecule with several molecules combining to form large structures held together by hydrogen bonds. Cellulose is used primarily in nature in microfibrils, the basic structural units of cell walls in plants, which impart strength and rigidity.

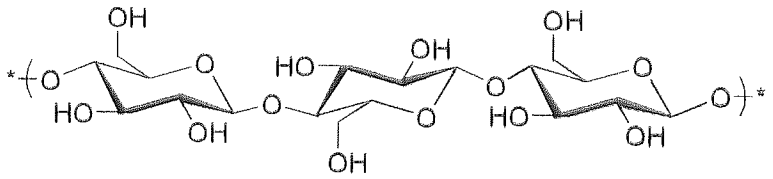

5

Figure 2: Cellulose 5, a 1,4'-*O*-(β-D-glucopyranoside) polymer of 2

Changing the stereochemistry of the glycosidic bond from the β to the α orientation gives rise to the polysaccharide starch **6**. When starch is eaten, *glycosidase* enzymes catalyse the hydrolysis of glycosidic bonds and release individual molecules of glucose. Like most enzymes, *glycosidase* is highly specific in function and only operates with the α-glycosidic bond in starch, leaving the β-glycoside links in cellulose unbroken[3]. Accordingly, humans can metabolise starchy foods such as grains and potatoes, but are unable to process the cellulose of grasses and leaves. Starch is one of the primary sources of glucose for humans.

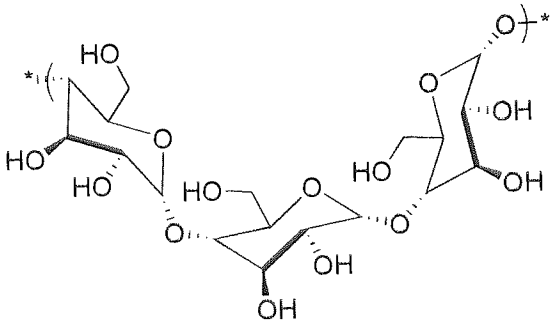

6

Figure 3: Starch 6, a 1,4'-*O*-(α-D-glucopyranoside) polymer of 1

Chitin **8** is structurally similar to cellulose and is also chemically inert and strong. It is based on the *N*-acteylglucosamine unit **7** of glucose and is used to make the exoskeletons of arthropods, e.g. shellfish and insects.

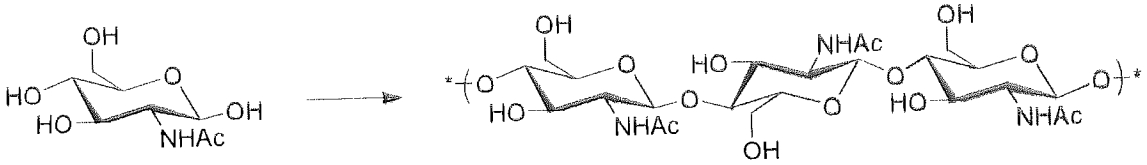

7 8

Figure 4: Chitin 8, a 1,4'-*O*-(β-D-*N*-acetylglucosaminopyranoside) polymer of 7

1.1.3 Amino-sugars

As well as in chitin, amino sugars are also found in antibiotics such as streptomycin and gentamicin[3].

Polysaccharides consisting of amino sugars, such as glucosamine and galactosamine, are often utilised on the surfaces of animal cells and in the extracellular matrix[2]. The repeat units of these polysaccharides also contain at least one sugar that has a negatively charged carboxylate or sulfate group. These glycosaminoglycans are usually attached to proteins to form proteoglycans. Proteoglycans are used as lubricants and structural components in connective tissue, mediate adhesion of cells

to the extracellular matrix and bind factors that stimulate cell proliferation. Some act as anticoagulants, while others, such as vancomycin, act as antibiotics. Proteoglycans are a type of glycoprotein.

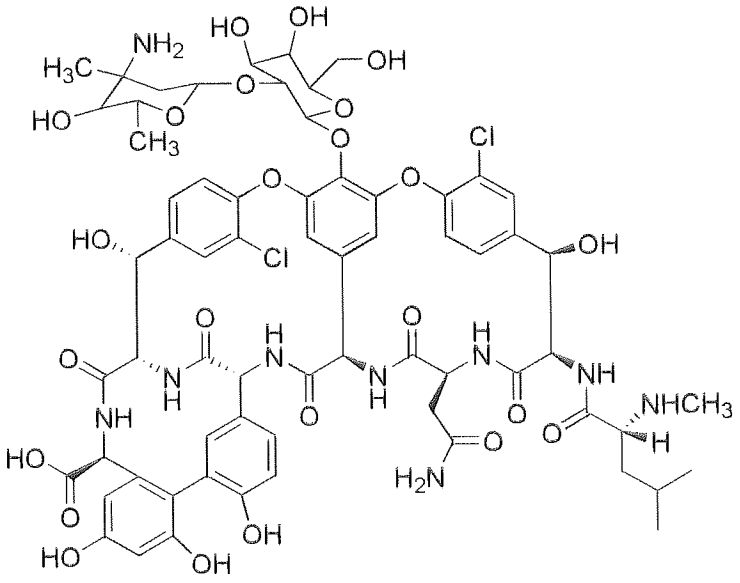

9

Figure 5: The antibiotic vancomycin 9 containing an amino-sugar.

1.1.4 Glycoproteins

Glycoproteins are a range of proteins that contain oligosaccharide chains (glycans) which are covalently attached to their polypeptide side-chains via asparagine (N-linked) or through serine or threonine (O-linked). They are often components of cell membranes, playing a variety of roles such as cell adhesion and biochemical labelling.

Carbohydrates are well suited to this labelling role due to the enormous variety afforded by relatively few compounds. A simple disaccharide compound consisting of carbohydrates **A** and **B** has two sequences; **AB** and **BA**. Each disaccharide can then be differentiated by the nature of the linkages; 1-1, 1-2, 1-3, 1-4 and 1-6. The stereochemistry at the anomeric centre allows each saccharide to adopt different anomeric forms enabling further encoding. Add to this other variables such as ring

size (furanose or pyranose) and modification of the hydroxyl groups (e.g. sulfation, phosphorylation, methylation, or acylation) and the number of permutations begins to increase exponentially.

While a sequence of 6 DNA bases (from a pool of 4; A, C, G, T) provides 4096 (4^6) different combinations, and the 20 natural amino acids can form 64 million (20^6) permutations of hexamer, the variety afforded by carbohydrates allows the construction of a sequence of 6 saccharides to occur in over one trillion (1×10^{12}) ways[1].

The differences afforded by diverse combinations of carbohydrate give rise to a variety of properties. They can alter solubility, change the antigenic nature of a protein and protect against protein-degrading enzymes.

Proteins of the same backbone can express different forms of glycosylation, called glycoforms. Unlike protein synthesis or DNA replication there appears to be no mechanism for proof reading and correcting differently labelled glycoproteins, therefore they occur in mixtures, with each glycoform having a unique property. It has been suggested[1] that these allow the body to provide a vast spectrum of activities.

A good example of this is the structural differences between the ABO blood groups in humans. Carbohydrates are attached to glycoproteins and glycolipids on the surfaces of red blood cells. Each blood type present cells with their own unique sugar combination, termed A, B and O. The O antigen is a common foundation to all antigen types, while A and B differ with the addition of one extra monosaccharide; either *N*-acetylgalactosamine (for A) or galactose (for B)[2].

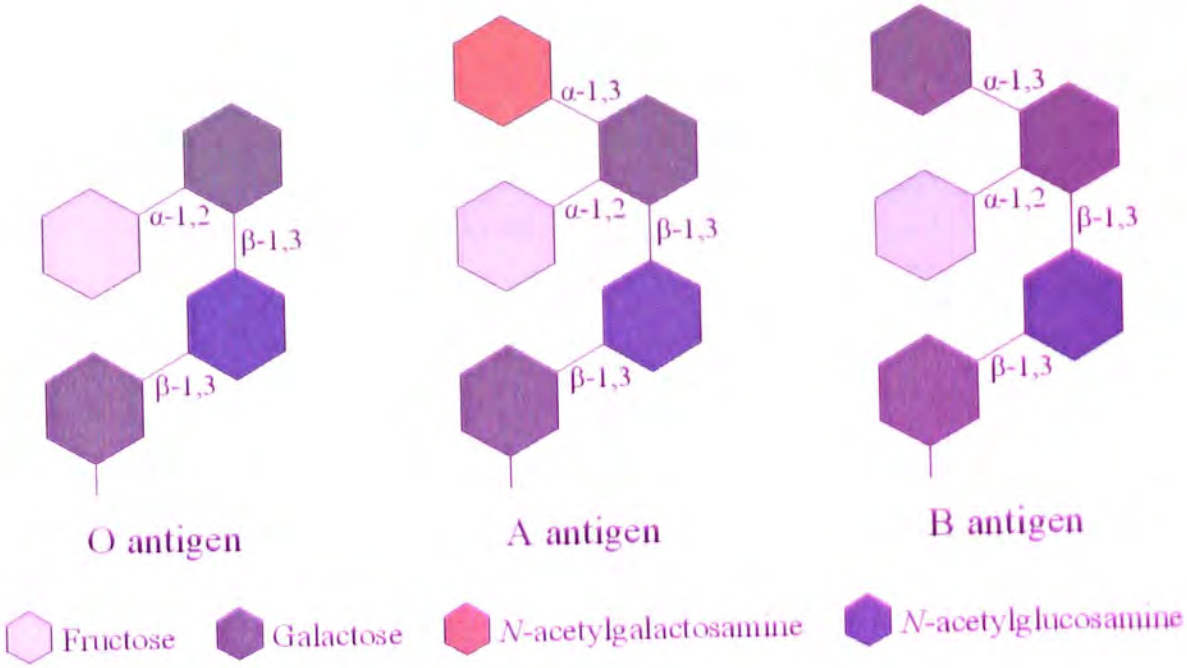

Figure 6: Structures of A, B and O oligosaccharide antigens[2]

These structures have important implications for blood transfusions, whereby the introduction of antigens not normally present can trigger an immune response. Conversely, this diversification of blood affords a mechanism of ensuring the entire human species does not fall foul to a single parasitic agent.

The sugar labels also convey information about the protein they are covalently attached to. Proteins are glycosylated and folded in the *endoplasmic reticulum* and *Golgi complex* of a cell[2]. As proteins are folded within these organelles, enzymatic action changes the glycosylation of the protein. Lectins bind to those carbohydrate sequences corresponding to unfolded proteins and prevent the protein from leaving the ER for the Golgi, while correctly folded proteins are allowed to move forward unhindered. Thus, in this instance, carbohydrates are used as a barcode, whereby the encoded information is used to identify incorrect folding during a 'quality control' check.

1.1.5 Infection by microorganism

Carbohydrate recognition can also be used as the introductory route of infection. The influenza virus[2], the bacteria that causes stomach ulcers (*Helicobacter pylori*) and the

parasite protozoan that causes Chagas' disease (*Trypanosoma cruzi*)[1] all depend on the binding ability between the sugar, sialic acid, and lectins.

1.1.6 Carbohydrates of medicinal value

Carbohydrates also have the ability to protect against infection. Human milk is full of compounds containing sialic acid; an *N*-acetyl substituted hexose with a nine-carbon backbone, also known as N-Acetylneuraminic acid. It has been theorised that their function is to act as decoys, with foreign organisms in the gut binding to these compounds rather than the glycoproteins on the cells of the digestive tract[1].

With some intervention from man, carbohydrate compounds can also be turned into powerful, active medicines. DNA and RNA are both compounds containing the carbohydrate ribose. Some important medicines act by resembling these structures, including two important anti-HIV drugs; Zidovudine (AZT) **10** and Lamivudine (3-TC) **11**.

AZT is synthesised from the nucleoside of thymine, 2'-deoxyribonucleic acid deoxythymidine **12**. The secondary alcohol of the 2-deoxyribose can be converted to an azide via a number of synthetic routes[4]. In the body, AZT is readily converted into the corresponding nucleotide. Due to its resemblance with the natural 2'-deoxyribonucleic acid deoxythymidine, it is incorporated into chains of newly formed HIV DNA by *reverse transcriptase*.

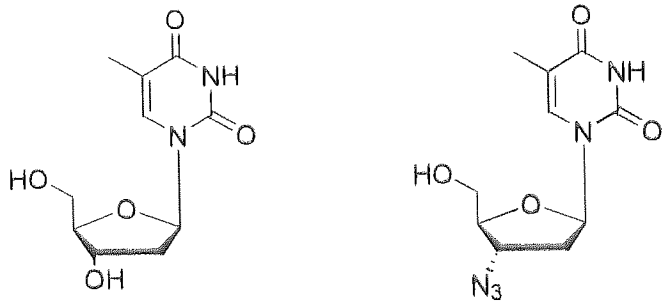

12 10

Figure 7: Left; 2'-deoxyribonucleic acid deoxythymidine 12, Right; AZT 10

The DNA chain is synthesised from the 5' to the 3' end by the stepwise addition of nucleotides through nucleophilic attack by the 3'-hydroxyl group of the primer towards the innermost phosphorus atom of the incoming deoxynucleoside triphosphate[2]. Since AZT does not contain a 3'hydroxyl group, having been replaced by the non-nucleophilic alkyl azide[3], the nascent chain is prevented from further elongation, resulting in a failed synthesis.

Lamivudine works on exactly the same principle, although is employed in place of a cytosine nucleoside **13.**

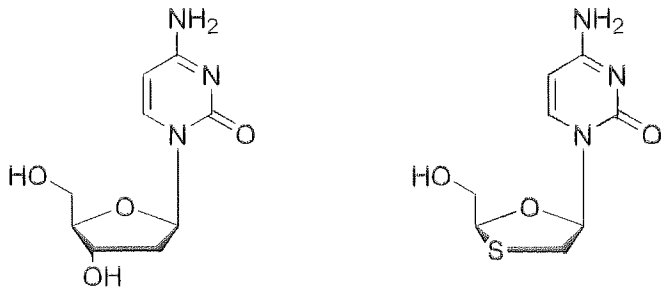

13 **11**

Figure 8: Left; 2'-deoxyribonucleic acid deoxycytosine 13, Right; 3-TC 11

1.2 Recognition of carbohydrates in nature

1.2.1 Lectins

As previously noted, lectins are the molecules utilised by organisms to recognise and decipher the encoding of carbohydrate sequences. Lectins are proteins that bind to specific carbohydrate sequences with a high degree of specificity. The binding occurs in the carbohydrate recognition domain (CRD) through hydrogen bonding between carbonyl groups of the protein and the hydroxyl groups of the sugar substrates[1]. Binding between a single sugar and the CRD is very weak, however when the number of sugars of the correct type and orientation combine, there is an

enormous increase in the affinity and specificity of the lectin. The specificity is such that there is usually only one way that a particular branched oligosaccharide can fit efficiently into the CRD. A lectin usually contains two or three binding sites for carbohydrate structures.

The main role of lectins in animals is to facilitate cell-cell interactions. The carbohydrates expressed on the surface of one cell interact with the lectins expressed on the surface of another. Each individual interaction is relatively weak; however the composite total for all of the combined interactions provides a strong binding force.

One class of lectin, requiring the presence of calcium, are called selectins and are responsible for the inflammatory response. They form rapidly on the inner surfaces of blood vessels (endothelia; E-selectins) and platelets (P-selectins)[2], and bind strongly to carbohydrates. This binding causes white blood cells (leucocytes) to bind to the walls of the blood vessels at the point of injury, where they pass through to the surrounding tissue[1].

1.3 The affinity of boronic acid for diols and saccharides

When it was discovered by Kuivila *et al.*[5] that boronic acids could alter the solubility of saccharides, there was an explosion of interest in the topic, which continued over the next few decades. Research over recent years has concentrated on making selective chemical sensors to demonstrate the event of binding between the boronic acid and carbohydrate[6,7,8,9,10,11,12].

Kuivila *et al.*[5] postulated the formation of a cyclic boronate ester **16**, although this had been disputed in the past[13]. More recent studies have shown the strong binding of boronic acids to compounds containing 1,2- and 1,3-*cis* diols in basic media through the formation of covalent bonds, results in the formation of cyclic esters[8,14,15].

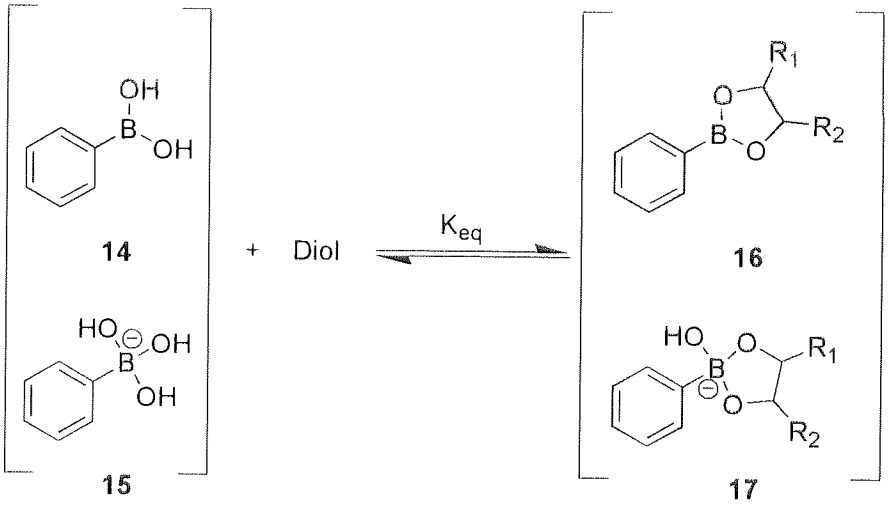

Figure 9: Boronate ester formation[14]

John Lorand and John Edwards published the first quantitative measures of boronic acid-saccharide binding in 1959[16], determining the selectivity of phenylboronic acid **14** to saccharides (Table 1). The adjacent rigid *cis*-diols of saccharides form stronger cyclic esters than simple acyclic diols such as ethylene glycol[17,18]. The selectivity order is retained across all monoboronic acids.

Table 1: Stability constants of polyol complex with phenylboronic acid[18].

Polyol	Boronic acid **17** (log *K*)
D-Fructose	3.64
D- Galactose	2.44
D-Mannose	2.23
D-Glucose	2.04
Ethylene glycol	0.44

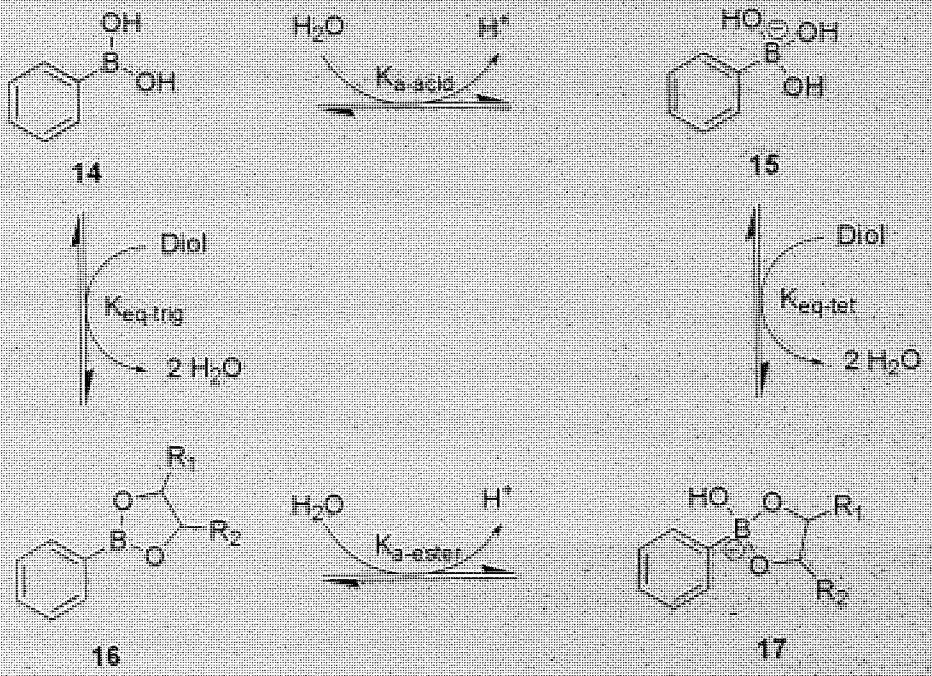

Figure 10: The relationships between phenylboronic acid and its diol ester[18].

In aqueous systems, a solvent water molecule can bind to the sp^2 boronic acid **14**. At higher pH values this solvent is deprotonated and forms an sp^3 hybridised, tetrahedral boronate **15**. As the bond angle is compressed from 120° (sp^2) to 108° (sp^3) the pK_a of the boronate ester **17** is lowered, so that in effect, it becomes more acidic than the boronic acid **14**[18]. While the geometry of the boronic acid and boronate ester are not in doubt, work by Springsteen and Wang[14] has recently begun to dispel some commonly held views, exemplified by Liu *et al.*[19], that boronic acids with lower pK_a values have higher affinities.

Table 2: The pK_a of phenylboronic acid and five boronate esters[14].

Boronic acid or ester	pK_a
Phenylboronic acid **14**	8.8
Fructose ester	4.6
Sorbitol ester	5.7
Glucose ester	6.8
Sucrose ester	7.5
Ethylene glycol ester	8.2

In 2002, Springsteen and Wang[14] utilised a three component competitive assay developed in 2001[20], containing Alizarin Red S. (ARS), phenylboronic acid and a diol compound, to study this and other commonly held beliefs.

It had been thought that a higher pH favoured binding of a boronic acid and a diol, that the pH needed to be above the pK_a of the boronic acid to see meaningful binding, and that the more acidic boronic acids would bind more tightly to diols than the more basic boronic acids.[19,21].

There are three acids in the process of boronic acid binding; the boronic acid itself, the ester which is often more acidic than the acid, and the diol. Although simple alcohols have pK_a values around 16, vicinal diols are often more acidic with glucose and fructose have pK_a values of around 12[22]. It was proposed that the optimal binding would occur at pH values between the pK_a values of the boronic acid and diol[19].

The results of Springsteen and Wang in 2002[14], which were extended further in 2004[22], show that the ranking of the binding constants among different boronic acids with a given diol (at physiological pH) did not always follow the trend of the boronic acid pK_a values. Instead it is related to both the pK_a values of the boronic acid and the diol, although in an imprecise manner which cannot be directly predicted. Additionally, the ranking of the binding constants was dependant on the pH of the solution, with optimal binding not necessarily occurring at pH values above the pK_a of the boronic acid. They surmise that, when viewing binding constants, it is critical

to consider the specific conditions of each individual situation, particularly the pH of the solution under which the binding constants were determined.

Understanding these binding affinities is important when considering the design of boronic acid based sensors tasked with binding with diols.

1.4 Boronic acid based saccharide sensors

Stable boronic acid based saccharide receptors offer the possibility of creating saccharide sensors that are selective and sensitive to a chosen saccharide. This selectivity has seen them involved in applications as sensors for saccharides, as nucleotide and carbohydrate transporters and as affinity ligands for the separation of carbohydrates and glycoproteins[23].

Selectivity to a particular carbohydrate depends on the precise placement of recognition motifs of the receptor in the correct position and orientation for optimal binding with the guest. Arylboronic acids form stable complexes with a variety of sugars and thus are not useful as specific receptors for a single sugar type.

Large, complex saccharide structures afford many positions of attachment, allowing only substrates with a complementary complexity, such as lectins, to bind selectively. Nature uses proteins as its basis for specific receptors. The proteins made up of a sequence of amino acid units can be tailored to adopt specific orientations in solvents such as water, where the folding is driven by the tendency of hydrophobic residues to be folded internally away from the water molecules[2].

The recognition of smaller molecules, with a limited number of recognition motifs can be more challenging. Yang *et al.*[24] approached the problem with multiple boronic acid units with positionally fixed orientations to one another. Appending a conformationally strained fused ring system with two boronic acid moieties in positions complementary to the α-1,2 and 4,6 hydroxyl groups of glucopyranose afforded an affinity for glucopyranose 400 times that of the other sugars tested.

The approach was an unqualified success, although it relied heavily on computational modelling to predict the orientation of the diol units in solution as well the complementary geometric arrangement of the receptor. While current computer-modelling capabilities may be able to predict the conformations of monosaccharides with accuracy, their ability to accurately predict the complex conformations adopted by sequences of polysaccharides is difficult to confirm.

Another approach is to incorporate a degree of flexibility into the receptor. While the binding selectivity displayed will not be as absolute, a small amount of inbuilt flexibility may provide a margin for error; making small allowances for any inaccuracies in the design produced by less-than-perfect computer modelling.

1.5 Examination of recognition events

1.5.1 Circular dichromism

Bis-boronic acid compounds such as **18** and **19** have been used to bind saccharides in a 1:1 fashion at its head and tail, with the previously flexible receptor forming a rigid complex. The asymmetric orientation of the aryl boronic acids when immobilised by the complex allows for examination by circular dichromism[25,26,27]. This technique allows the study of carbohydrates that are not fluorescent and are only weakly chromophoric.

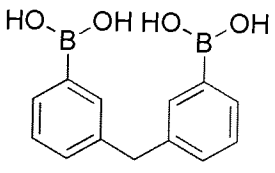

18

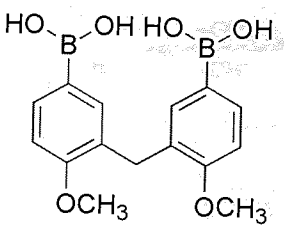

19

Figure 11: Examples of Bis-boronic acid compounds which yield complexes which have been examined by CD[27]

1.5.2 PET receptors

Synthetically produced photoinduced electron transfer (PET) receptors have been widely used in fluorescence sensing applications for monitoring binding events[28,29,30,31,32]. PET sensors usually adopt the format of an arylboronic acid linked to a fluorophore by a short spacer. Binding of the receptor to a diol creates changes in the oxidation/reduction potential of the system, which can register as a change in fluorescence. The incorporation of an amine group into the sensor (**20**) produces two major effects; boronic acids can complex with sugars at neutral pH instead of the high pH usually required to generate the boronate anion from simple boronic acids. Secondly, the amine controls the intensity of the fluorescence quenching of the system through PET.

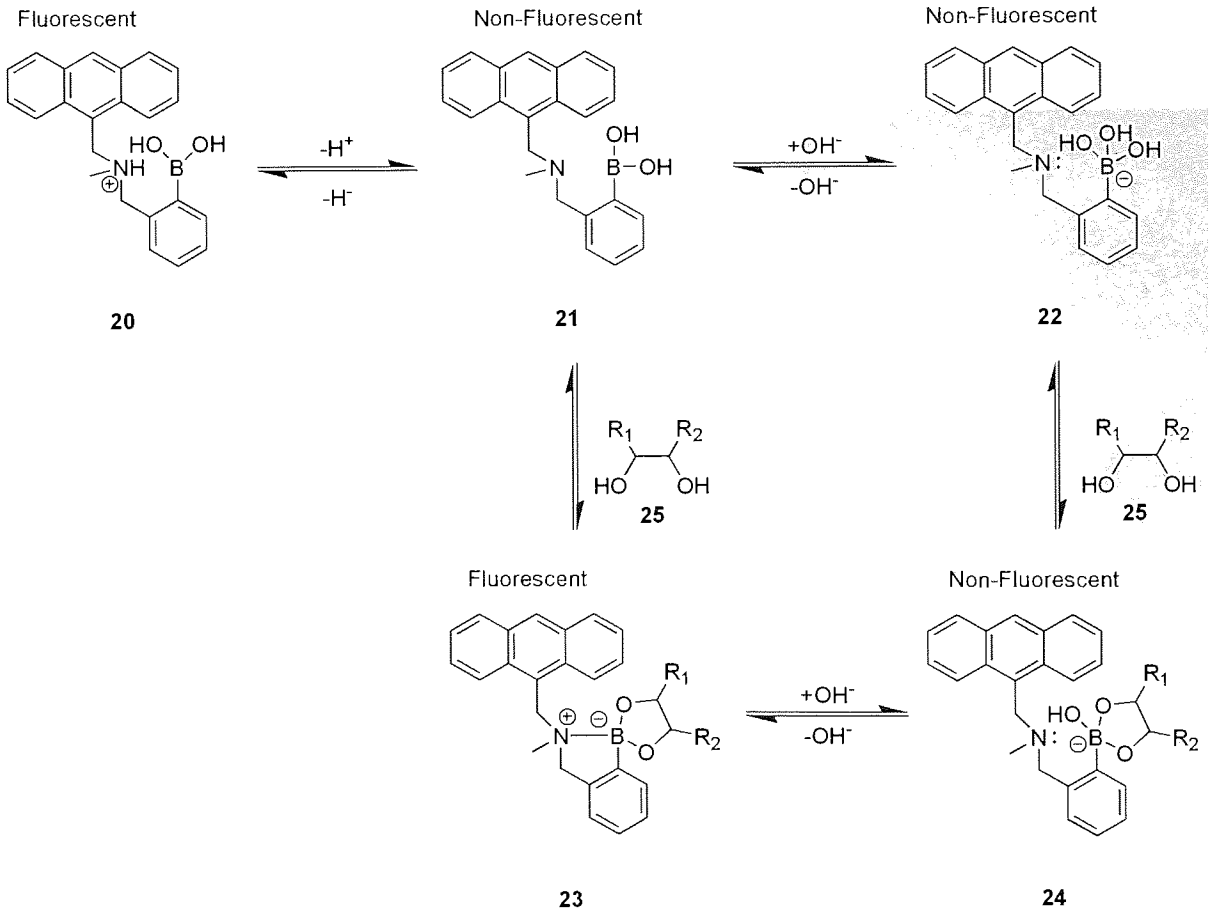

Figure 12: The effect of saccharide complexation with the PET sensor 20 with the differing forms of boronic acid formed at different pH levels.

When sugar **25** is added to **21**, the amine becomes bound to the boron atom and the electrons are unavailable to transfer and quench the fluorescence, resulting in the fluorescent species **23**. When the pH increases to a level which changes the boronic acid to the tetrahedral configuration **24**, the boron-amine bond is broken resulting in quenching to reoccur, even though the saccharide is still bound. This system is often described as an 'off-on' fluorescence sensor.

Introduction of a second boronic acid to form bis-boronic acid PET sensors has also been documented[33,11,34]. Sensor **26**[6] allows the monitoring of two possible sugar binding modes; a two to one complex of sugars (**28**) or two a 1:1 chelating complexes (**27** & **29**). It has been reported[6] that the positioning of the boronic acid groups of **26** allows it to display selectivity for D-glucose over other monosaccharides.

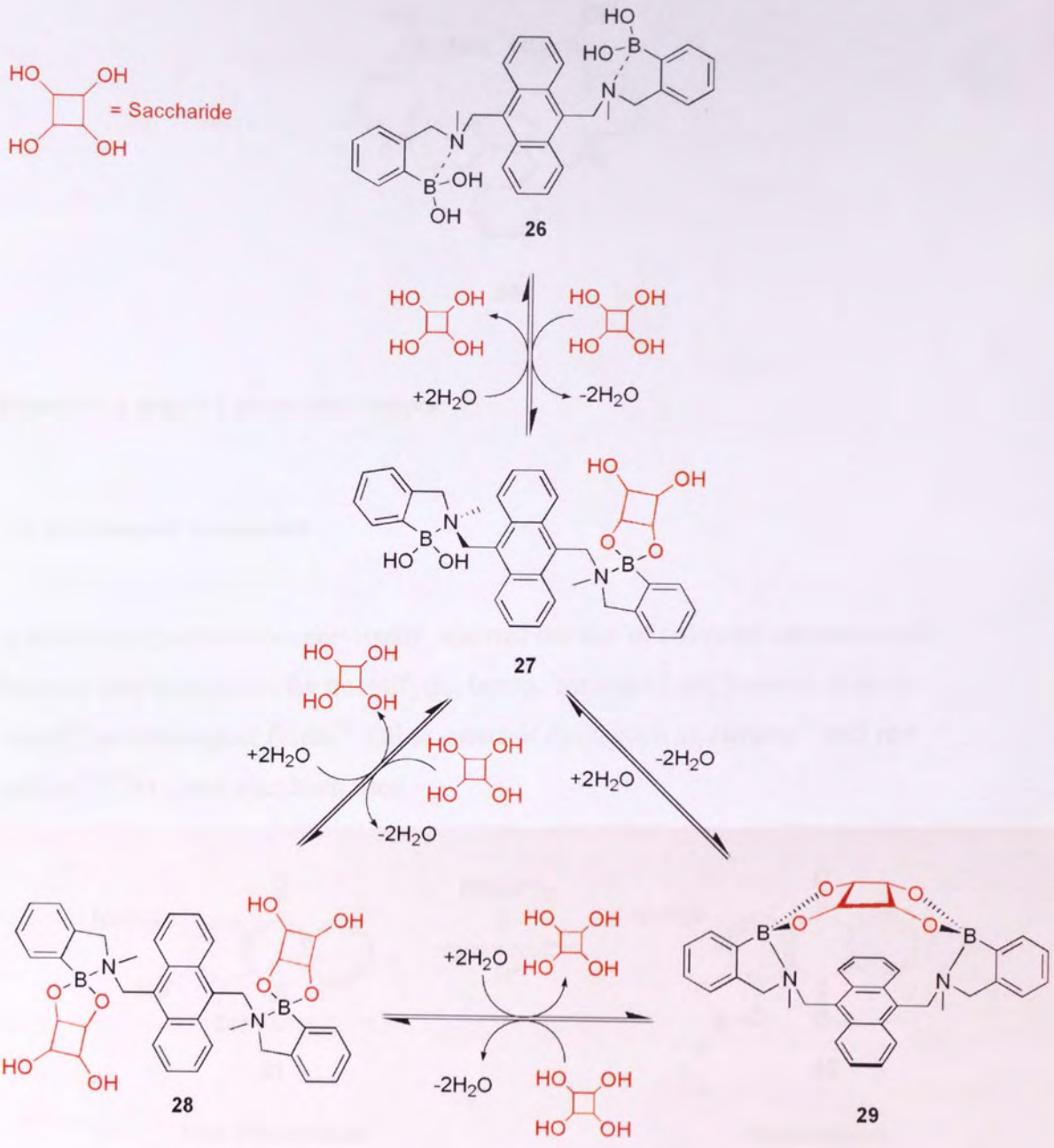

Figure 13: Bis-boronic PET receptor 26 forming complexes with one or two monosaccharides[6]

1.5.3 Non-PET receptors

The binding of a monosaccharide to the non-PET receptor **30** in a 1:1 ratio creates a rigid molecular complex[15]. The binding event affects the fluorescence properties of the incorporated fluorophore, however to a lesser degree than the comparable bis-boronic acid based on PET quenching.

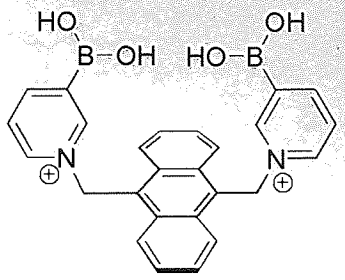

30

Figure 14: A non-PET bis-boronic receptor

1.5.4 Coloured receptors

A number of papers have previously reported the use of coloured carminic acid-boronic acid complexes for quantifying boron, boric acid and boronic acids in water[35] and biological fluids[36]. Other catechol dyes, such as alizarin[37] and red sulfate[14,20] **31**, have also been used.

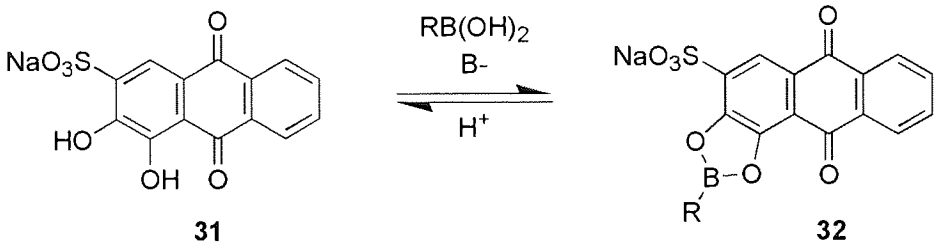

31 **32**

Non-Fluorescent **Fluorescent**

Figure 15: The alizarin red sulfate 31 catechol yields complexes with boronic acid to form complex 32.

Boronic acid azo dyes **33-36** have been used as internal charge transfer (ICT) sensors to study the interactions of boronic acids and sugars[7,8,27,38,39].

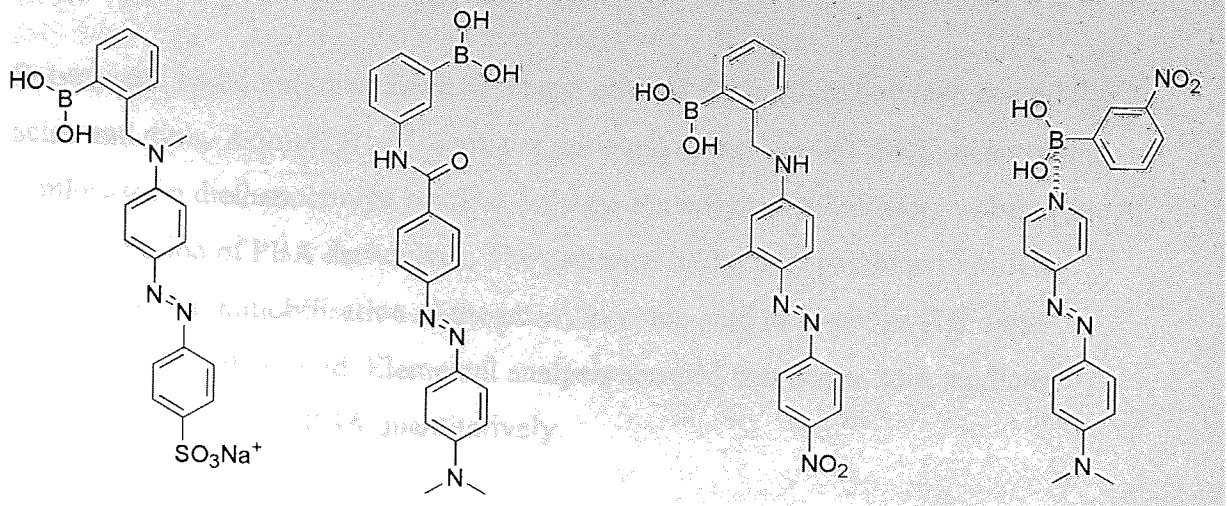

33 34 35 36

Figure 16: Boronic acid azo dyes 33-36

The shift in pK_a on binding of the boronic acid with the saccharide creates electronic changes which are transmitted to the neighbouring amine moiety, which in turn creates a change in the colour of the ICT chromophore.

1.5.5 Other methods

Many additional techniques have been used for examining the recognition of binding events including liquid crystalline systems[40], porphyrin-based receptors[27] and metal coordination receptors[41,42].

1.5.6 Polymeric receptors

Arylboronic acids have been added to the *N*-ε-position of polylysine polymeric chains[43,44]. The complexes formed with the saccharides significantly affected the higher-order structures of the polylysine chain. Subsequent addition of a fluorescent tag allowed the initial results recorded by CD to be confirmed. The information revealed that the complexation around the saccharides initiated the formation of α-helix, β-sheets, β-turns or random coil arrangements. These studies are of particular interest given the biological significance of the higher order structures of peptides.

Polystyrene based polymers have also been utilised for binding between boronic acids and diols. Arimori *et al.*[45] took the principle of the 'on-off' PET receptor and synthesised a diethanolamine pendant polystyrene polymer **37** in order to be of use in the preparation of PBA derivatives. The presence of the nitrogen lone pair of the amine enabled immobilisation of the phenylboronic acid to occur in THF with approximately 60 % yield. Elemental analysis showed that acetic acid mediated acidolysis cleaved the PBA quantitatively.

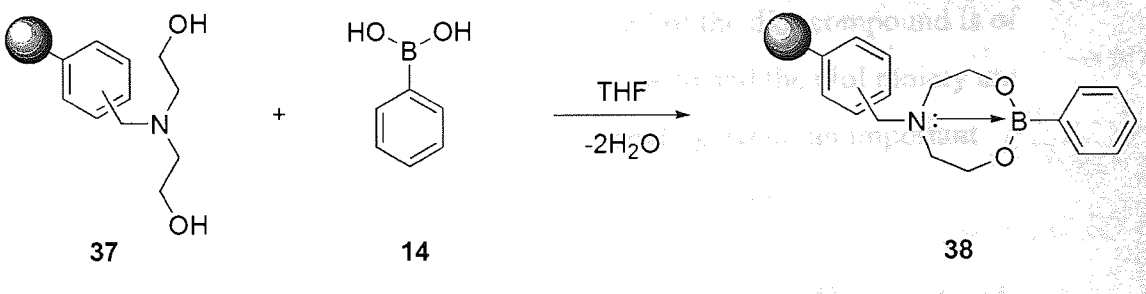

37 **14** **38**

Reaction Scheme 1: Loading of diethanolamine pendant polystyrene resin 37 with phenylboronic acid 14

Yang *et al.*[46] synthesised a catechol bearing polystyrene polymer **39** from Merrifield resin to extract boronic acid species from solution. The aims of the Yang study were again to use the solid support as a purification tool to assist with the isolation of boronic acid derivatives destined for a variety of uses, and secondly, to produce an immobilised catecholborane solid support reagent. Catechol compounds have been shown to have the highest affinity with boronic acid[14].

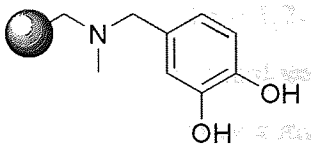

39

Figure 17: Catechol pendant polystyrene resin 39

Formation of the polymer-catechol/boronic acid complexes across a range of solvents occurred yields of 61-90 % (as assessed by %N elemental analysis) when using 0.8 equivalents of the phenylboronic acid derivatives. Higher temperature and a large excess of boronic acid drove the attachment to completion. Acetic acid mediated acidolysis cleaved the complex to give pure products as assessed by ^{1}H NMR. The resin was tested for recyclability, which was deemed excellent; showing no loss in efficiency after the resin had undergone a neutralisation process with base washings.

In both of these studies, the quantitative 'release' of the diol compound is of significance as it indicates that both the boronic acid and the diol moiety are regenerated and ultimately unchanged by the binding event; an important consideration for diols within biologically active molecules.

In a reversal of the approaches described above, Stones *et al.*[47] worked with polymer-bound arylboronic acids. Due to the structural and conformational complexity of any oligosaccharide target, they adopted a combinatorial strategy, based on screening large numbers of library receptor compounds. Each library compound was synthesised from a set of amino acids using the Fmoc-based peptide strategy on a diamine-derivatised trityl resin before being reduced. *O*-methylamino phenylboronic acid was adopted due to the ability of the B-N coordination to facilitate binding at neutral pH[18,17]. This choice of boronic acid also afforded a means of monitoring the binding through PET-induced fluorescence via the incorporation of anthracene (**Section 1.5.2; PET receptors**).

Four disaccharides, each possessing at least three 1,2- or 1,3-*cis* diol units were evaluated for binding. The study demonstrated that small differences in the structure of the units between library compounds can have a major effect on the stability of the resulting complex. A trend was also observed for a preference toward electron-poor arylboronic acid substituents when different electron donating or withdrawing groups were incorporated.

The adoption of combinatorial methods presents a convenient way of synthesising and screening many compounds without the need for powerful computational facilities or protracted synthesis requirements and comes closest to mimicking the recognition mechanisms of natural systems.

1.6 Fmoc-based Solid Phase Peptide Synthesis

The idea of anchoring a nascent peptide chain to an insoluble polymeric support was first established by Robert Merrifield[48]. He attached the first amino acid to an insoluble polymer. Subsequent amino acids were added sequentially. Once the entire peptide chain had been synthesised it released from the polymer via acidolysis.

The advantages of this method are considerable. The complicated purification of the product after each synthetic step is replaced by a simple washing procedure. The polymer remains attached to the resin so that loss of product is completely avoided. At the same time, the yield for each individual step can be increased by driving the reaction with a large excess of reagents; an important consideration in syntheses involving a large number of steps. Finally, this method can be automated.

Of vital importance is the need to prevent unwanted chain propagation. Performing coupling reactions in the absence of any protecting groups leaves the products open to react and produce undesired mixtures of products. Figure 18 shows a range of products which can arise during the coupling of an unprotected amino acid to a solid support resin.

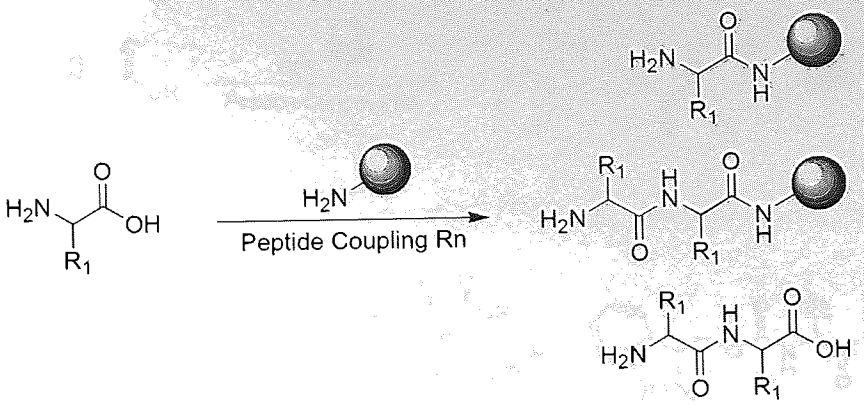

Figure 18: The absence of an amine protecting group allows the possibility of self coupling to occur on-bead and in solution, leading to multiple reaction products and impurities.

The desired product (top right) can be produced along with a resin showing uncontrolled propagation (middle), a result of a second sequential coupling to the resin or a single coupling of a short peptide (bottom) formed in solution. As chain assembly continues, incomplete reactions, side reactions or impurities will accumulate and contaminate the final product.

The Fmoc protecting strategy commences with the C-terminal of an Fmoc-protected amino acid being anchored to the solid support resin. The temporary Fmoc protecting group present at the amino group can be selectively removed, allowing the coupling of a single Fmoc-protected amino acid to take place. An excess of the amino acid is introduced, driving the reaction forward to produce high yields. The presence of the Fmoc group on the second amino acid prevents unwanted chain propagation during the coupling reaction, ensuring product purity. Excess reagents can then be removed by washing to enable the process to be continued in a step wise manner as required.

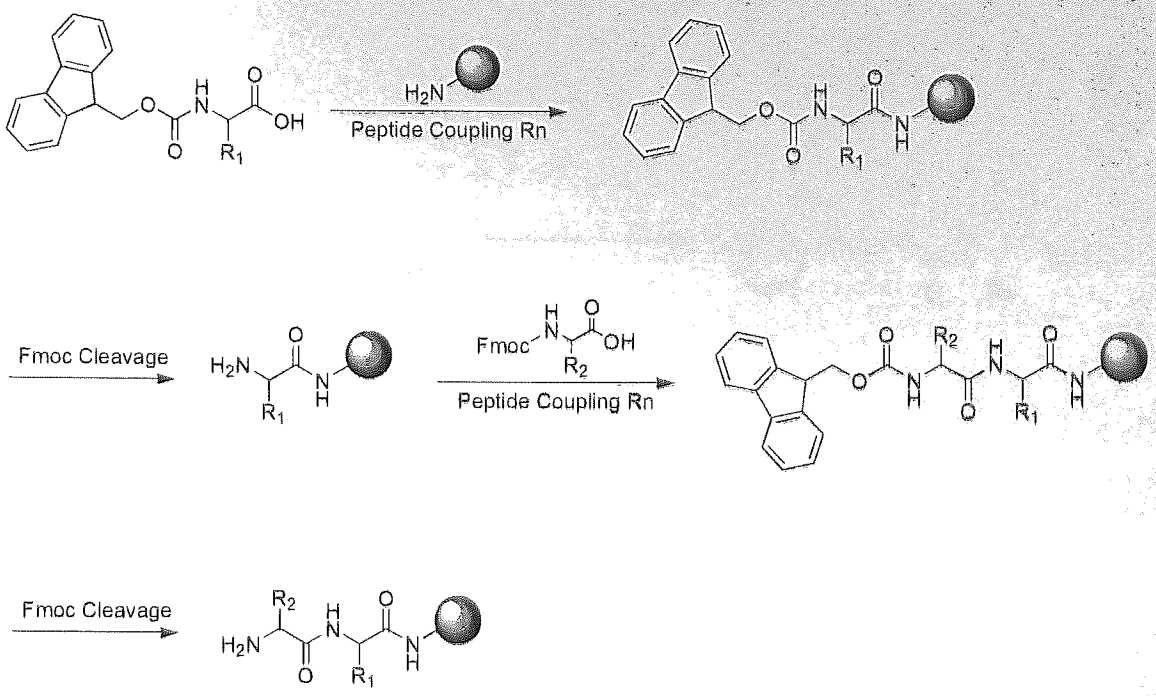

Reaction Scheme 2: Addition of an Fmoc-protected amino acid to a solid support resin, followed by step-wise deprotection and the addition of a subsequent amino acid.

Upon complete assembly, the product can be simultaneously cleaved of additional side-chain protection and released from the resin. The acidic conditions generally required for this last step ensure that the basic conditions of Fmoc cleavage and amino acid couplings do not precipitously cleave the peptide from the support.

1.6.1 Introduction of the Fmoc protecting group

The Fmoc solid phase synthetic strategy is based on an orthogonal protecting group strategy, using the base-labile *N*-Fmoc group to protect the α-amino group of an amino acid[49].

Introduction of the Fmoc protecting group to an amino acid usually occurs via the Schotten-Baumann method using the Fmoc-chloroformate[50]. Attack on the acyl chloride by the electron pair of the incoming amine results in S_N2 nucleophilic acyl substitution of the chlorine with the amine to yield the *N*-α-Fmoc protected amino acid (Mechanism 1).

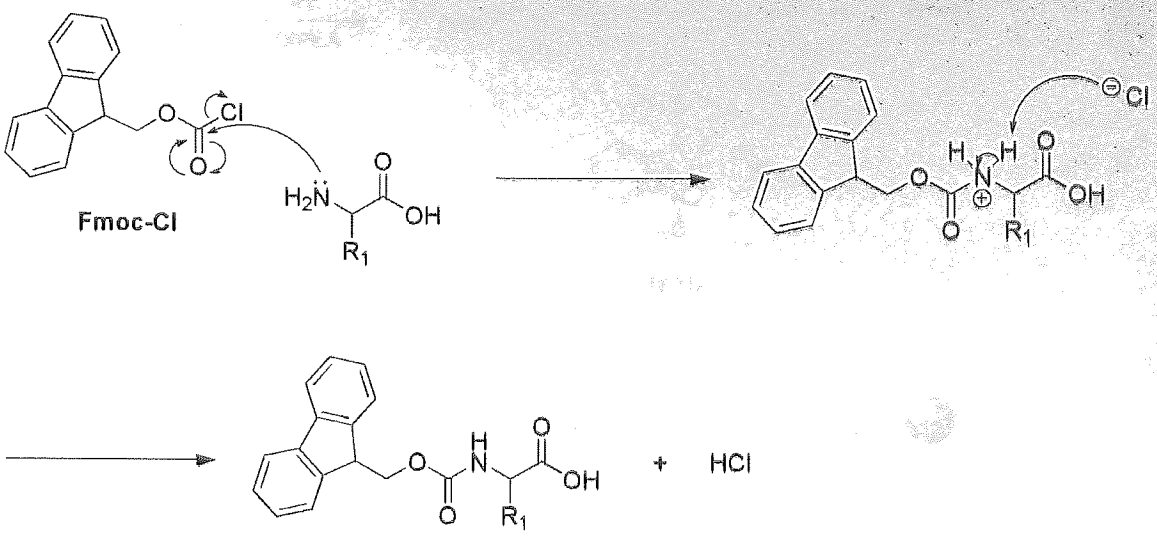

Mechanism 1: Fmoc Chloride reacts with an amino acid to afford the *N*-α-Fmoc protected amino acid.

1.6.2 Chain propagation

The step wise addition of *N*-α-Fmoc amino acids onto solid support usually involves the *in situ* generation of an activated carboxy group. To ensure complete coupling, an excess of the activated amino acid derivative is used in the coupling reaction. The time required to perform reactions depends on the activating species, but for highly reactive agents, such as those generated using aminium/phosphonium based derivatives, the reaction is usually completed in less than 30 minutes[51].

Many methods of generating the activated carboxy group have been investigated. Carbodiimides such as DIC or DCC[51], pentafluorophenyl esters[52] and acid fluorides[53] have all been used, but in recent years, aminium and phosphonium based derivatives have become the preferred method for the *in situ* generation of the activated carboxy group[51].

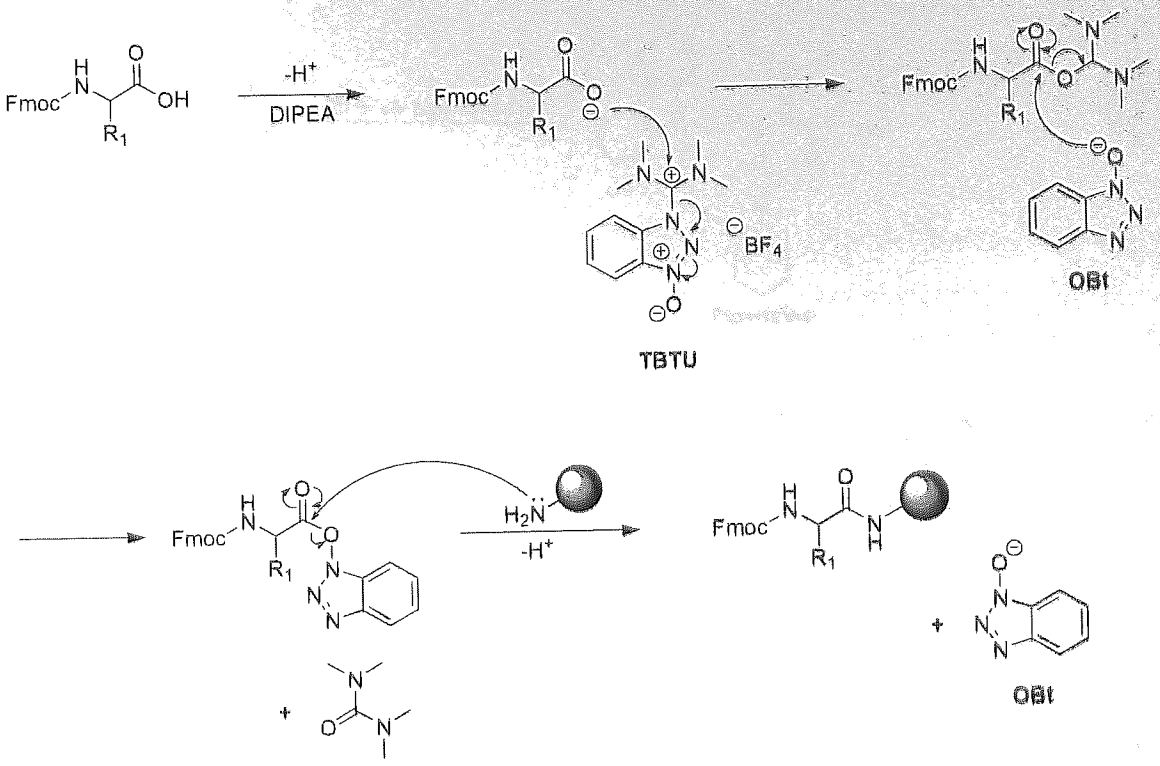

Mechanism 2: Aminium (formerly known as uronium) derivative mediated peptide coupling reaction. This example shows TBTU, but the mechanism for generating *in situ* carboxyl activation is the same for the HBTU derivative and the PyBOP phosphonium derivative.

The reagents which are most regularly used include PyBOP[54], TBTU[55] and HBTU[56]. These easily convert the Fmoc-amino acids into the corresponding OBt esters in the presence of a tertiary base such as DIPEA. The analogous OAt derivatives can also be generated by derivatives such as HATU[57] and PyAOP[58]. These are used in an identical manner but have been shown to give superior results with respect to coupling efficiencies and the prevention of enatiomerisation[58].

1.6.3 Removal of the Fmoc protecting group

The Fmoc group is very stable to acidic reagents, but it is rapidly removed with secondary amines[49,59] at room temperature. Piperidine (20 % in DMF) is considered to be the routine cleavage solution[51].

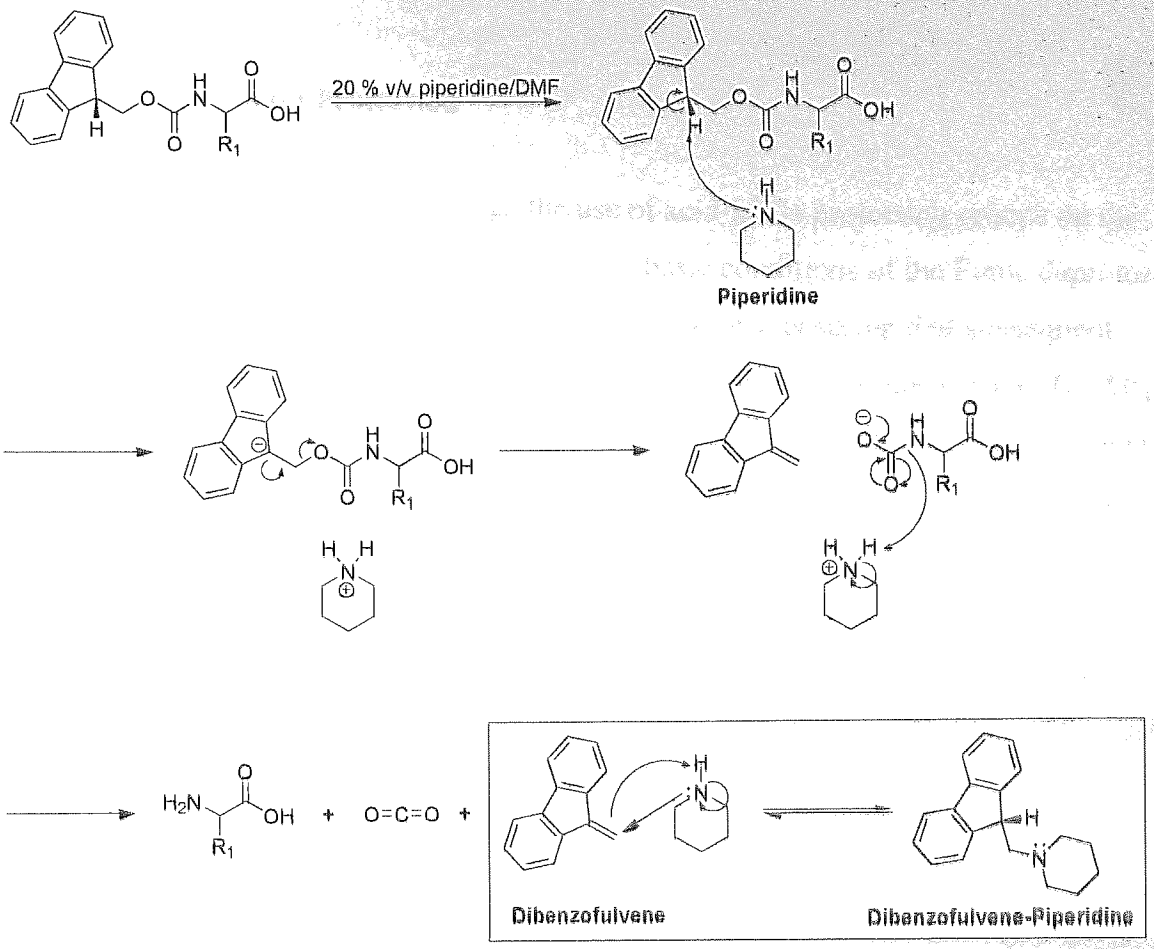

Mechanism 3: Piperidine mediated cleavage of the Fmoc group from an *N*-α-Fmoc-amino acid.

The piperidine deprotonates the fluorene ring to generate the cyclopentadiene type intermediate which quickly goes on to form the dibenzofulvene (DBF). DBF can then establish an equilibrium with piperidine by scavenging it to form the DBF-piperidine adduct[51]. The strong UV absorbance of the DBF offers the potential for monitoring the course of the deprotection reaction.

At this point, coupling of additional amino acid residues can ensue using the technique previously described, until the desired sequence has been completed and is ready for cleavage.

1.6.4 Side Chain Protection

Orthogonality is afforded through the use of acid-labile protecting groups on the side-chains of functionalised residues. The basic conditions of the Fmoc deprotection enables the retention of acid labile protecting groups, ensuring that subsequent coupling reactions can only occur at the desired position. Groups such as Trt, Mtt, OtBu, Boc, and tBu are most commonly employed[51], however there are a large range of groups available. Furthermore, there are a number of groups available which afford selective deprotection (such as Dde[60]), thereby enabling modification of individual side chains. For routine synthesis, all of the protecting groups used are readily removed with TFA, although the exact conditions are specific each protected amino acid[51]. In addition, TFA cleavage has the added advantage of simultaneously cleaving the peptide sequence from the solid support resin[51].

1.7 Summary

- Carbohydrates are biologically important molecules, serving many functions within organisms.
- Glucose is an important source of energy.
- Polysaccharides serve many purposes from energy storage to physical scaffolding.
- The large array of carbohydrate forms affords a vast possibility of combinations.
- Organisms use different carbohydrate combinations for structural differentiation and to encode information about proteins.
- Substitution of the hydroxyl groups in some nucleosides can result in reverse transcriptase inhibitors of great importance.
- Lectins are proteins that recognise carbohydrates and selectively bind to specific arrays of carbohydrates.
- Boronic acids bind to *cis*-1,2- and *cis*-1,3-diols.

- Boronic acid binding to carbohydrates is not constant across all sugars and displays a natural preference toward some complexes.
- Boronic acids can be manipulated to alter and enhance this selectivity.
- Boronic acids have been appended to increase the pH range over which they can bind to diols.
- There are numerous methods for monitoring the binding of boronic acids with sugars.
- Polymers appended with boronic acids have been shown to alter their higher-order structures as a result of boronic acid binding.
- Polymer supports have been used to scavenge boronic acid compounds from solution.
- Combinatorial strategies have been employed to study boronic acid/sugar interactions.

1.8 Aims and Objectives

The aim of the research was to answer a number of fundamental questions which were raised at the beginning of the project;

1) Can a polymer-based recognition motif be synthesised, such that it can reversibly bind to carbohydrates?
2) Can such a recognition motif be modified, so that it has a greater affinity for particular carbohydrates?
3) Can such a recognition system be used to reversibly bind glycosylated peptides without compromising their biological activity?
4) Can a moiety with a proven affinity for particular a glycopeptide have its selectivity altered by design, such that it enhances the binding to a specific glycopeptide?
5) Can such a recognition system be used as a means of purifying one glycopeptide from a mixture of glycopeptides with differing glycosylation?

Carbohydrates serve a huge array of functions in nature. By mimicking lectins and producing synthetic methods of recognising carbohydrate sequences, the potential to collect huge amounts of information about glycobiology of cells, encompassing information from protein folding within cells to identifying potential disease and bacterial pathways along with identifying target sites for directed therapy.

This thesis describes early attempts to design a series of simple, resin-bound, synthetic lectin analogues. Construction of the lectins would be based around Fmoc-amino acid synthetic strategies, employing boronic acid as the recognition motif. Combinatorial library methods would enable simultaneous screening of lots of different compounds to enable the identification of sequences demonstrating increased selectivity for specific carbohydrates or glycopeptides..

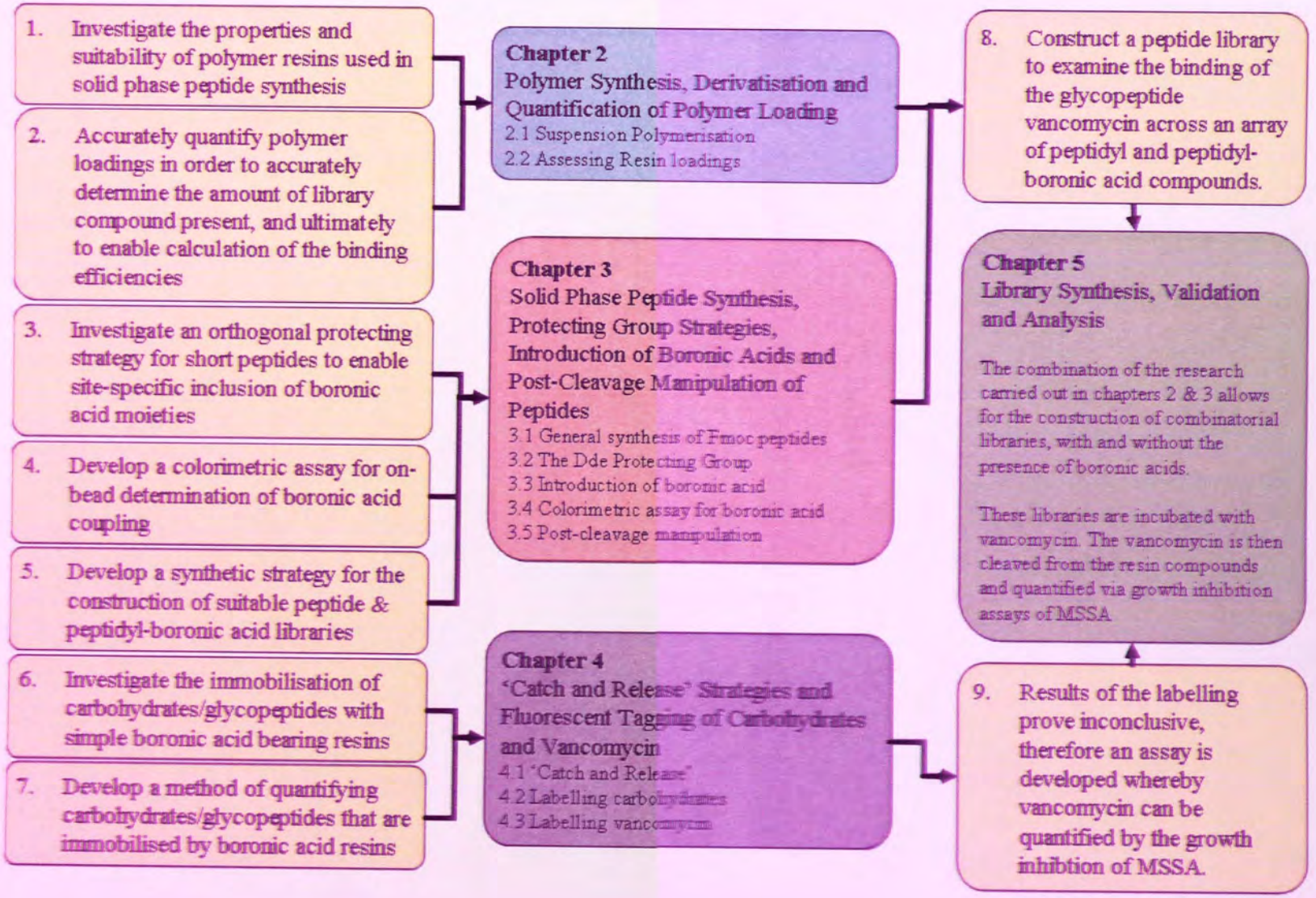
1. Investigate the properties and suitability of polymer resins used in solid phase peptide synthesis
2. Accurately quantify polymer loadings in order to accurately determine the amount of library compound present, and ultimately to enable calculation of the binding efficiencies
3. Investigate an orthogonal protecting strategy for short peptides to enable site-specific inclusion of boronic acid moieties
4. Develop a colorimetric assay for on-bead determination of boronic acid coupling
5. Develop a synthetic strategy for the construction of suitable peptide & peptidyl-boronic acid libraries
6. Investigate the immobilisation of carbohydrates/glycopeptides with simple boronic acid bearing resins
7. Develop a method of quantifying carbohydrates/glycopeptides that are immobilised by boronic acid resins
Chapter 2
Polymer Synthesis, Derivatisation and Quantification of Polymer Loading
2.1 Suspension Polymerisation
2.2 Assessing Resin loadings
Chapter 3
Solid Phase Peptide Synthesis, Protecting Group Strategies, Introduction of Boronic Acids and Post-Cleavage Manipulation of Peptides
3.1 General synthesis of Fmoc peptides
3.2 The Dde Protecting Group
3.3 Introduction of boronic acid
3.4 Colorimetric assay for boronic acid
3.5 Post-cleavage manipulation
Chapter 4
'Catch and Release' Strategies and Fluorescent Tagging of Carbohydrates and Vancomycin
4.1 'Catch and Release'
4.2 Labelling carbohydrates
4.3 Labelling vancomycin
8. Construct a peptide library to examine the binding of the glycopeptide vancomycin across an array of peptidyl and peptidyl-boronic acid compounds.
Chapter 5
Library Synthesis, Validation and Analysis
The combination of the research carried out in chapters 2 & 3 allows for the construction of combinatorial libraries, with and without the presence of boronic acids.
These libraries are incubated with vancomycin. The vancomycin is then cleaved from the resin compounds and quantified via growth inhibition assays of MSSA
9. Results of the labelling prove inconclusive, therefore an assay is developed whereby vancomycin can be quantified by the growth inhibtion of MSSA.

Chapter 2

Polymer Synthesis, Derivatisation and Quantification of Polymer Loading

Polymer Synthesis and Derivatisation and Quantification of Polymer loading

The following chapter describes the synthesis of Merrifield resin, Quadragel resin and their amine derivatives. The chapter then goes on to describe a comparative study of the commonly employed methods for quantifying the loading values of solid polymer supports.

2.1 Suspension polymerisation and on-bead chemistry

The solid support resin is a crucial component in any solid phase organic chemistry (SPOC) or solid phase peptide synthesis (SPPS) strategy. A vast array of resins for use in SPOC and SPPS are commercially available, but as with all 'buy off the shelf' products, choice is limited to those resins which are financially viable for the manufacturers. These commercial resins, each with their own unique properties, offer a good, generic approach to SPPS however they may not provide the exact resin characteristics required for a specific reaction. In order to integrate particular properties into a resin it may often be desirable to synthesise the resin itself.

Of the different polymerisation techniques, suspension polymerisation is best suited for producing larger size beads (35-750 μm) which are the mainstay of SPOC and SPPS[61]. An organic phase consisting of the monomers, any cross-linking moiety and a free radical initiator is added to an aqueous phase which usually contains a suspension stabiliser such as PVA. The resultant mixture is stirred vigorously. Heating initiates the generation of free radicals which begins the polymerisation process. If a chemically functionalised resin is to be produced, theoretical loadings are calculated on the basis of monomer composition of the organic phase. Post-reaction washing is essential to remove irregularly shaped particles which have broken up due to the stresses of the mechanical shearing within the reaction vessel, known as 'fines'.

Synthesis of polymer resins is often referred to as a 'black art'. Even when using the same batch of raw materials, reaction vessels and conditions it can be difficult to synthesise a polymeric resin consistently. The shape and size distribution of the polymer beads can vary dramatically with each synthesis, and although each reaction proceeds with the same amounts of starting materials, there is no sure way to predict reaction yields.

Table 3: Advantages and disadvantages in employing solid polymer supports for chemical reactions

Advantages On Solid Phase	Disadvantages On Solid Phase
Reagents can be used in excess without purification difficulties	Not as well developed as standard chemistry
Simple purification of the product via washing and filtration	Additional steps required for linkage and cleavage from resin
Solid phase resins commercially available	Limited types of supports
Automation of synthesis possible	Not as simple to monitor reactions
Split and mix possible	

The biggest advantage of synthesis on solid support is the ability to drive a reaction to completion by utilising large excesses of reagents. Once the reaction is complete, purification can be achieved by simple filtration with subsequent washings with a variety of solvents to ensure complete removal of all unreacted starting materials and any by-products formed by the reaction. Significantly, reactions on solid supports enable the utilisation of "split and mix" synthesis. Split and mix or recombine synthesis is useful as it facilitates the rapid and synthetically economic production of a large number of different compounds that are then available for screening[62].

2.1.1 Chloromethyl(poly)styrene (2 % *p*-divinylbenzene (DVB) crosslinked) (Merrifield's Resin) 43

To enable comparison to be made with a commercially available resin, Quadragel resin **59**, it was decided to synthesise Merrifield's resin 'in house'. Synthesis of

Merrifield's resin allowed for the subsequent derivatisation of the polymer into one upon which useful chemistry could be performed. 4-Vinylbenzylchloride is commonly used as a co-monomer in the synthesis of Merrifield's resin due to its ready availability and low cost. The benzylic chloride group, while stable to the polymerisation process, can readily be displaced as it is a good leaving group, allowing subsequent chemistry to be performed on the resin.

Polymerisation was carried out using standard suspension polymerisation reaction conditions (**Chapter 7.2: Experimental**). 4-Vinylbenzylchloride **42**, DVB **41** and styrene **40** along with azo-*iso*-butrylnitrile (AIBN) initiator were mixed to create the organic phase. The aqueous component was made up of PVA solution (1 % w/v in water). After the polymerisation reaction the beads were extensively washed with copious amounts of water to remove the bulk of the 'fines'. When the polymer was exposed to a variety of solvents it displayed the reversible swelling/collapsing characteristics associated with this type of gel polymer.

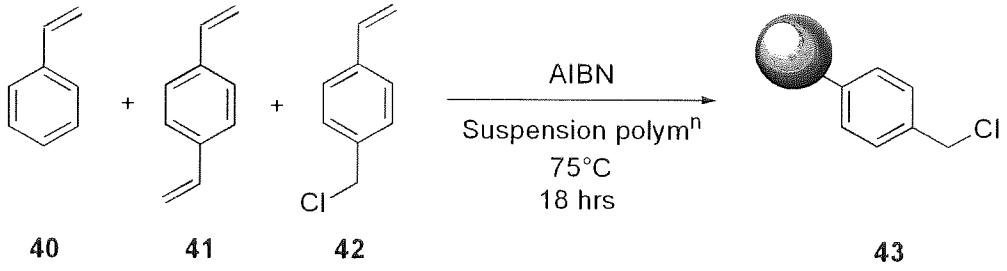

Reaction Scheme 3: Synthesis of Chloromethyl(poly)styrene 43

The title compound was isolated in a yield of 42 % by weight, with 95 % of the resin beads being sized (by sieves) between 150 and 250 μm in diameter. Analysis by ATR-FTIR showed peaks corresponding to both aromatic and aliphatic C-H stretches (3028 and 2922 cm^{-1} respectively). Benzene ring stretches were visible at 1598 and 1493 cm^{-1}. A CH_2 wag specifically from a CH_2-Cl was visible at 1265 cm^{-1} indicating the successful integration of the 4-vinylbenzyl chloride into the resin.

2.1.2 Phthalimido-protected Aminomethyl(poly)styrene 44

A simple, two-step synthetic route allows for the conversion of the benzylic chloride into an amine to give an amino-functionalised resin. The amino-functionalised resin was selected as the target as it allows for direct coupling with amino acids utilising proven synthetic methods. In the first step of the conversion the benzylic halide of the functionalised polymer resin **43** is converted into a phthalimide group to yield the phthalimide-protected amine resin **44**.

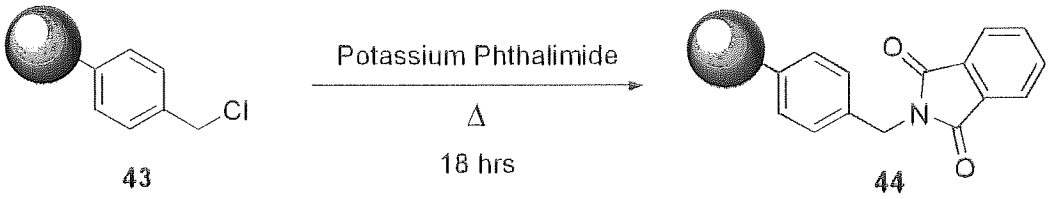

43 44

Reaction Scheme 4: Synthesis of Phthalimido-protected aminomethyl(poly)styrene

Potassium phthalimide was used to ensure the complete reaction of all of the reactive benzylic chloride groups. After reaction, the system was placed under an inert atmosphere and refluxed overnight. Upon cooling the yellow polymer was washed exhaustively to ensure complete removal of the excess potassium phthalimide and the potassium chloride by-product.

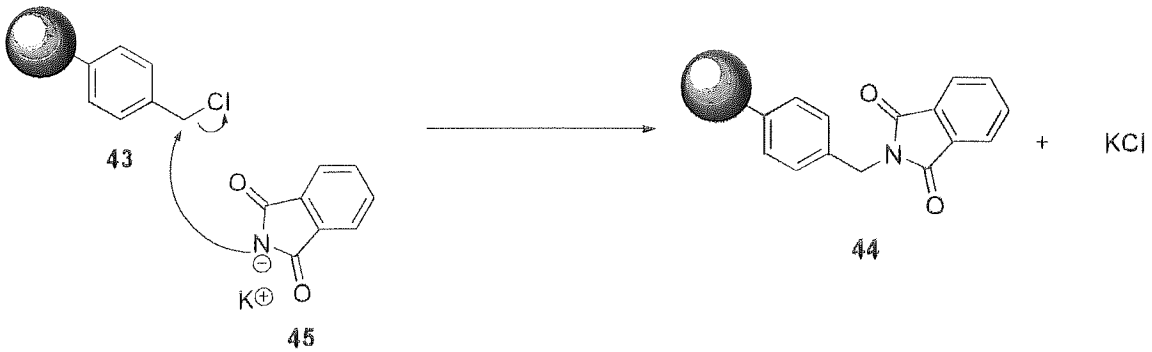

43 45 44

Mechanism 4: S_N2 displacement of halogen by phthalimide nucleophile

The title compound **44** was isolated in 94 % yield. Although the reaction efficiency is below the ideal value of 100 % which *should* be achievable when using SPOC, it can be said to have gone to completion. Utilising thermodynamically good solvents during the reactions caused the resin to swell, however, even in its swollen state, it is very likely that not every benzylmethylchloride group was positioned within the polymer matrix in such a way in which it could react with the incoming reagent. Chain entanglement and steric hindrance play a role in masking some of the reactive sites which in turn produce a below 'idealised' reaction yield. The infra red spectrum of the compound was consistent with the desired product. Strong peaks at 1716 cm^{-1} and a weak signal at 1771 cm^{-1} are indicative of the carbonyl groups present within the imide group.

2.1.3 Aminomethyl(poly)styrene (AMPS) 46

In the second step of the conversion, the amine functionalised resin **46** was prepared using the Ing-Manske modified version of the Gabriel Amine synthesis[63]. The traditional Gabriel amine synthesis reaction utilises water with a hydroxide donor to ring open the imide, forming phthalic acid and the desired amine.

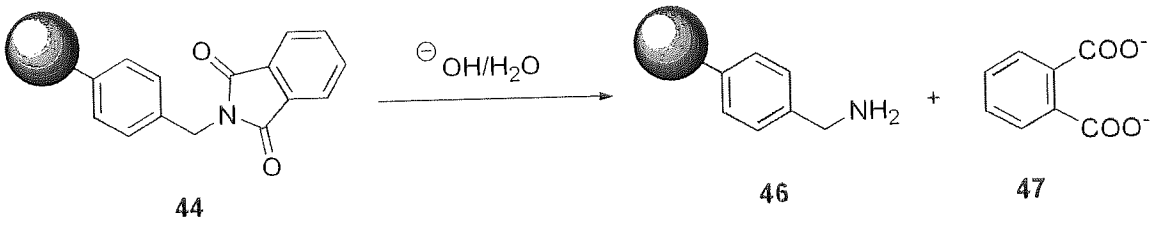

44 **46** **47**

Reaction Scheme 5: Traditional Gabriel amine synthesis reaction

This is an impractical method of reducing this particular type of resin due to the hydrophobic nature of the base resin. As the reacting sites are dispersed throughout the polymer matrix it is necessary for the resin to swell effectively in order for the reagents to permeate through to the reactive sites. Studies have shown that Merrifield's resin fails to show any significant swelling in water[64] and mass-water

uptake assays demonstrate that Merrifield's resin is completely hydrophobic[65]. As such the Ing-Manske variant of the Gabriel procedure was employed.

Merrifield's resin has been shown to be highly swellable in THF[65,66]. For the reaction, 1,4-dioxane was selected as an aprotic substitute to THF[66]. Accordingly, resin **44** was suspended in 1,4 dioxane and reacted with hydrazine monohydrate[63]. After a period of equilibration the system was placed under reflux. Periodic sampling of the beads allowed the progress of the reaction to be followed with on-bead Kaiser staining test[67]. Upon completion of the reaction the polymer beads were again washed with a variety of solvents before being dried to constant weight.

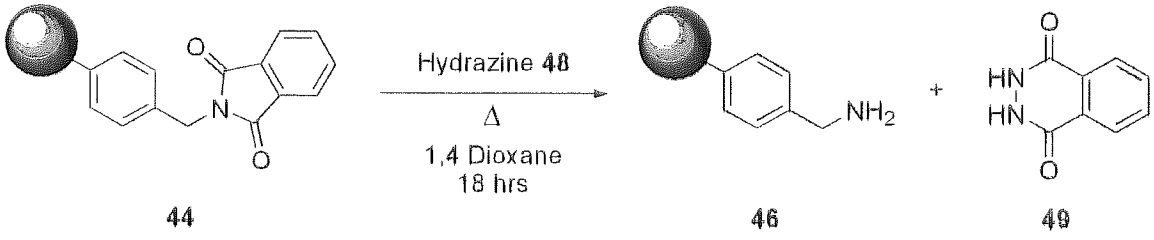

44 46 49

Reaction Scheme 6: Formation of AMPS 46 and phthalhydrazide 49 via the hydrazine-mediated reduction of 44

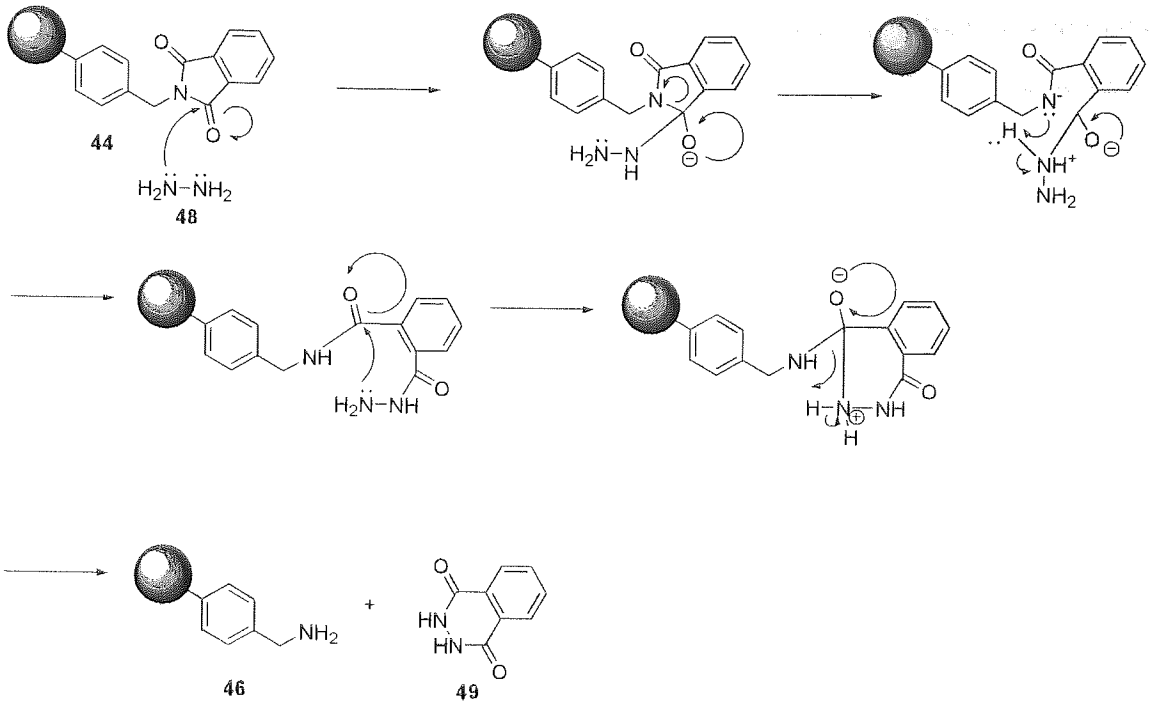

Mechanism 5: Hydrazine is used to generate the amine resin 46 from the corresponding phthalimide

Amino-functionalised resin **46** was afforded in a 97 % yield, giving the AMPS **46** a loading of 1.0 mmol/g. Characterisation by infra red spectroscopy confirmed the disappearance of signals associated with the carbonyl groups contained within the imide moiety (1771 & 1716 cm^{-1}), definitively showing that the phthalimide group had been displaced. There is no absolute certainty that a peak corresponding to the primary amine is present. An NH_2 deformation is known to occur in primary amines between 1650 and 1590 cm^{-1}, however this region is also where you would expect signals associated with the stretching of a benzene ring. Although IR is not considered quantitative, it is reasonable to assume that any signal arising from the amine is swamped by the much more abundant benzene ring systems within the polymer sample which is being analysed. The resin was subject to two on-bead colorimetric assays, 2,4,6-trinitrobenzenesulfonic acid (TNBS)[68] and Kaiser[67] assays, both of which indicated the presence of amines.

Safety restrictions at the Reaxa worksite, where some practical work was conducted, prevented the use of hydrazine. Accordingly, an alternative reagent was required.

Later reductions utilised methylamine (40 % w/v in water), with its lower toxicity[69], as the reducing agent[66]. Reactions proceeded at room temperature, with agitation of the beads in the aqueous methylamine/dioxane solution occurring over 72 hours to take account of the lower temperature and hence reactivity of the reagent.

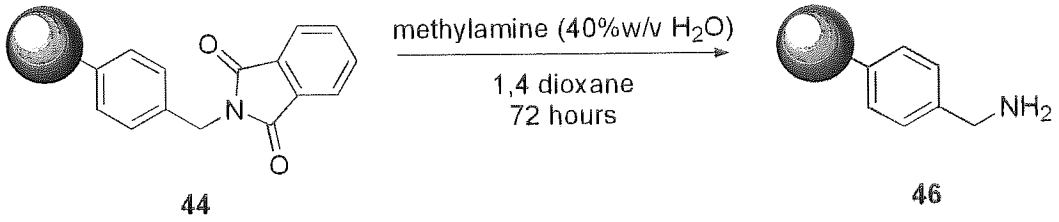

44 **46**

Reaction Scheme 7: Synthesis of AMPS 46 via the reduction of 44 with methylamine

Reaction progress was again monitored by on-bead colorimetric assay. ATR-FTIR spectroscopy for the product via the methylamine route gave a spectrum that was identical to that of the hydrazine route. Reaction efficiencies were comparable to the hydrazine route at 98 %.

2.1.4 Quadragel Resin 59

The synthesis and derivatisation of the Merrifield's resin enabled the polymerisation reaction protocols to be established, and for derivatisation methods to be tested and enhanced. However, it was realised from the outset that Merrifield's resin and its derivatives would not be suited to the water-based conditions[64] that would be required for combinatorial assays developed for use with carbohydrates and glycosides. It was therefore desirable to synthesise a polymer which had a greater affinity to water. TENTA-GEL and ARGO-GEL are commercially available supports which have successfully been used for SPOC[65,70]. These are constructed by grafting poly-(ethylene glycol) directly onto the solid support via a benzylic ether bond[71,72,73]. Reaxa had recently patented a PS-DVB based resin containing a short polyethylene glycol (PEG) chain upon which chemistry could be performed[74]. The presence of the PEG chain enhances the water compatibility of the resin in comparison to Merrifield-based resins. Unlike the commercially available resins

TENTA-GEL and ARGO-GEL, the PEG is introduced into a monomer unit used as a co-monomer in the synthesis of Quadragel. PEG is largely inert[75], chemically robust[71] and can impart both organic and aqueous compatibility[65]. Generation of the PEG-containing monomer began with the stoichiometric addition of half an equivalent of trityl chloride **52** to a commercially available tetraethylene glycol$_4$ unit, **50**. This enabled just one of the two primary hydroxyl groups to be protected, yielding the mono tritylated PEG derivative **51**. The remaining free hydroxyl group of the monotritylated PEG **51** was then converted into the tosylate **55**. Pre-treatment of acetoxystyrene with potassium hydroxide produced the 4-vinyl phenolate anion **54** which undergoes S_N2 substitution with the tosyl group of monotrityl-monotosylated tetraethylene glycol **55** to yield the Quadragel monomer **56**.

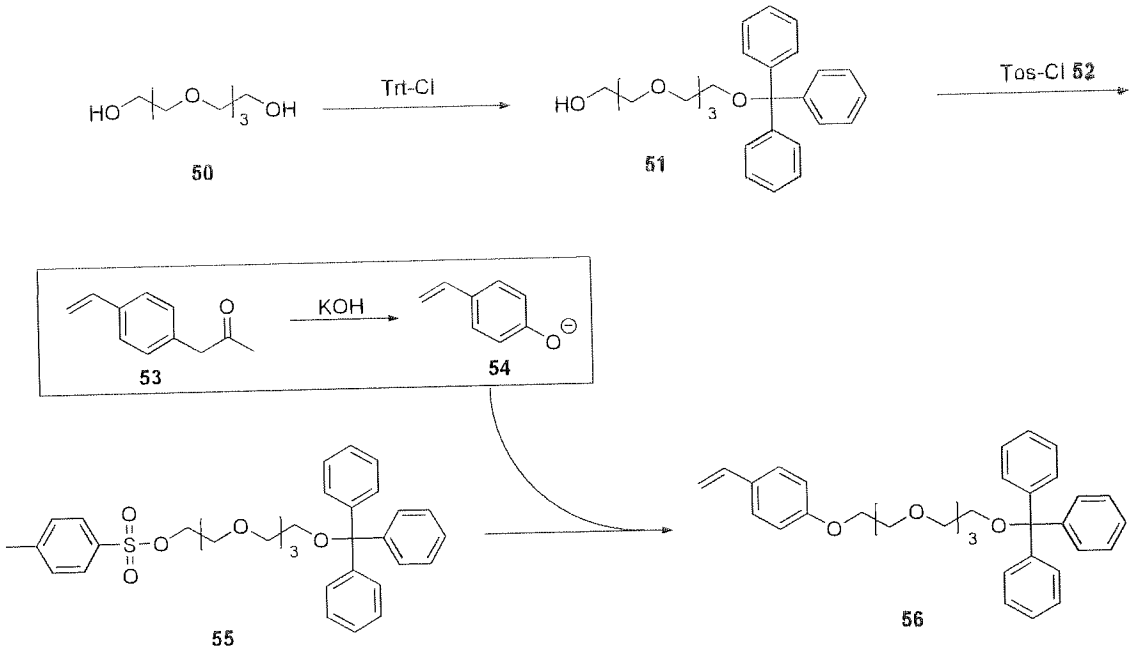

Reaction Scheme 8: Synthetic route to obtain the Quadragel monomer 56

Polymerisation of Quadragel monomer **56** was carried out using standard suspension polymerisation reaction conditions (**Chapter 7: section 7.2**). The Quadragel monomer was mixed with DVB, styrene and lauroyl peroxide initiator to create the organic phase. The aqueous phase consisted of 2.5 % w/v PVA solution with sodium chloride (2.5 % w/v) to increase the ionic potential of the aqueous phase and ensure

the organic and aqueous phases remain immiscible, even with the presence of a 'hydrophilic' PEG component in the organic phase.

Analysis of the product resin **57** by ATR-FTIR indicated the presence of aromatic and aliphatic C-H stretches at 3025 and 2921 cm^{-1} respectively. The PEG units gave rise to a C-O-C ether stretch at 1244 cm^{-1}. No evidence existed for the presence of a primary alcohol, indicating that the trityl protecting group had remained in place during the polymerisation reaction. This was confirmed by subjecting a small sample of beads (1-3 mg) to neat TFA, and observing a bright yellow supernatant, consistent with the trityl cation in solution. The presence of the trityl group throughout the polymerisation reaction helps the PEG chain to maintain the immiscibility of the polymerisation components and provide an area of exclusion which enlarges its 'cone of mobility'.

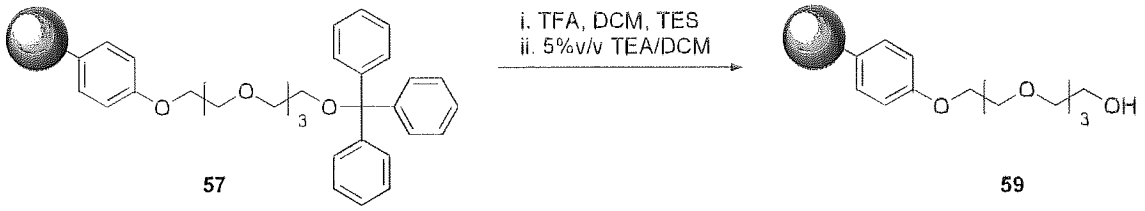

57 59

Reaction Scheme 9: Detritylation of polymerised monomer 57 to form Quadragel Resin 59

Removal of the trityl group post-polymerisation was carried out by subjecting resin **57** to a resin-compatible TFA cleavage solution containing a cation scavenger (1 TFA: 14 DCM: 0.4 TES) for 4 hours. IR analysis of the product resin showed a strong carbonyl signal at 1788 cm^{-1} indicating that, perhaps unsurprisingly, the trityl protecting group had been replaced with a trifluoroacetate, donated from the cleavage mixture. The lack of any signal due to the hydrogen bonding of the terminal –OH groups lent extra weight to this theory.

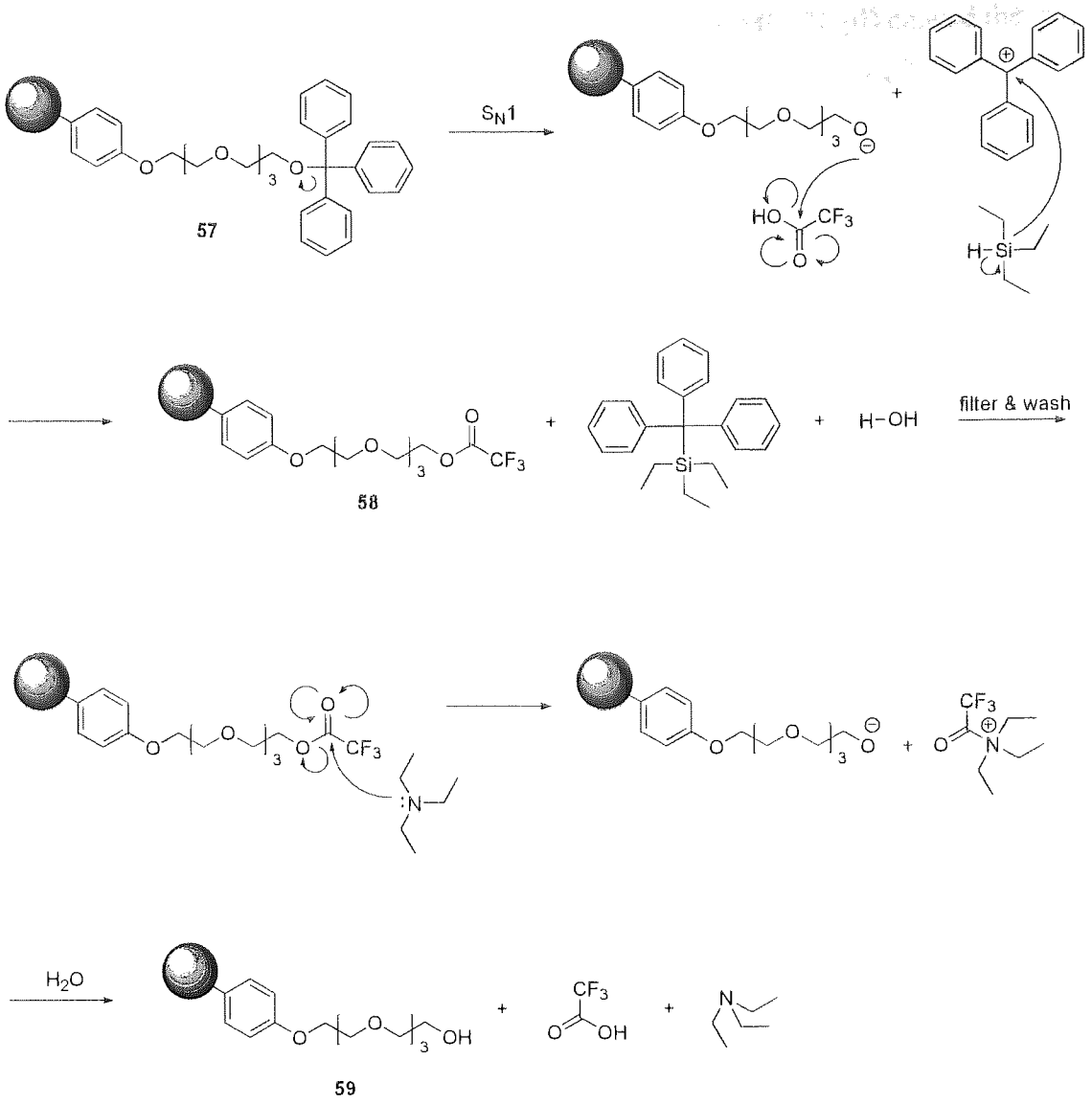

Mechanism 6: Detritylation of polymerised monomer 57 to form Quadragel resin 59

Subsequent suspension and stirring of the resin in 5 % v/v TEA/DCM solution overnight removed the trifluoroacetate, and yielded the target resin **59**.

The sample of Quadragel resin **59** was dried to constant weight and isolated in an overall yield of 61 %. The IR spectrum obtained from a sample of resin **59** exhibited the broad signal of a hydrogen bonded O-H stretch at 3391 cm^{-1}. Peaks at 3026 and 2921 cm^{-1} confirmed the presence of aromatic and aliphatic C-H bonds respectively. Benzene ring stretches are seen at 1602 and 1493 cm^{-1}, while the C-O-C ether stretch is present as a medium strength peak at 1244 cm^{-1}. Subsequent incubation with

Alizarin Red (1% in DMF; 20 µl) and 10 % v/v DIPEA/DMF (20 µl) caused the beads to stain red indicating the presence of terminal hydroxyl groups[76].

2.1.5 Quadragel-Tosylate 60

Again, the ultimate aim of the derivatisation of the resin is the introduction of a terminal amine group. It is not possible to directly introduce the phthalimide group directly on to the alcohol functionality of the Quadragel resin **59**. Therefore an additional activation step was required, which converted the alcohol into a moiety which could be displaced by the phthalimide anion. Alcohols react with *p*-toluenesulfonyl chloride to yield alkyl tosylates. These compounds behave much like alkyl halides, with the tosyl group undergoing S_N2 substitution readily[3]. Accordingly, it was decided that tosylation of resin **59** with subsequent displacement by phthalimide followed by reduction would yield the Quadragel resin as a primary amine.

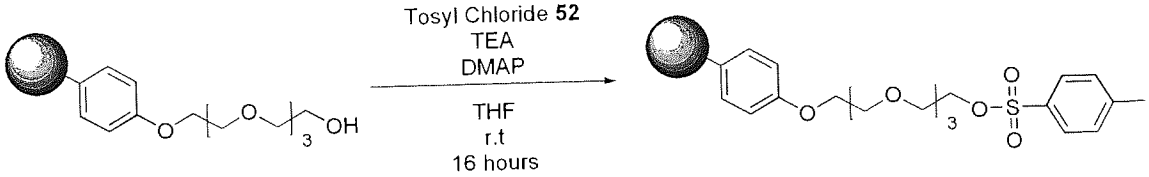

59 **60**

Reaction Scheme 10: Tosylation of Quadragel Resin 59 to form Quadragel-Tosylate 60

Quadragel resin **59** was mixed with TEA and an excess of *p*-toluenesulfonyl chloride to generate the corresponding Quadragel tosylate **60**. The resin was suspended in THF, to which was added a solution of DMAP in TEA. TEA was utilised as a non-nucleophilic base to prevent reaction with any other species, while DMAP was used as a catalyst. *p*-Toluenesulfonyl chloride (5.45 equivalents) was dissolved is THF and added slowly to the resin suspension, maintaining the temperature below 5 °C. After the complete addition of the *p*-toluenesulfonyl chloride solution the mixture was brought back up to room temperature and stirred overnight. Subsequent filtration

of the beads and thorough washing to remove unreacted and excess materials yielded the target compound, which was dried to constant weight.

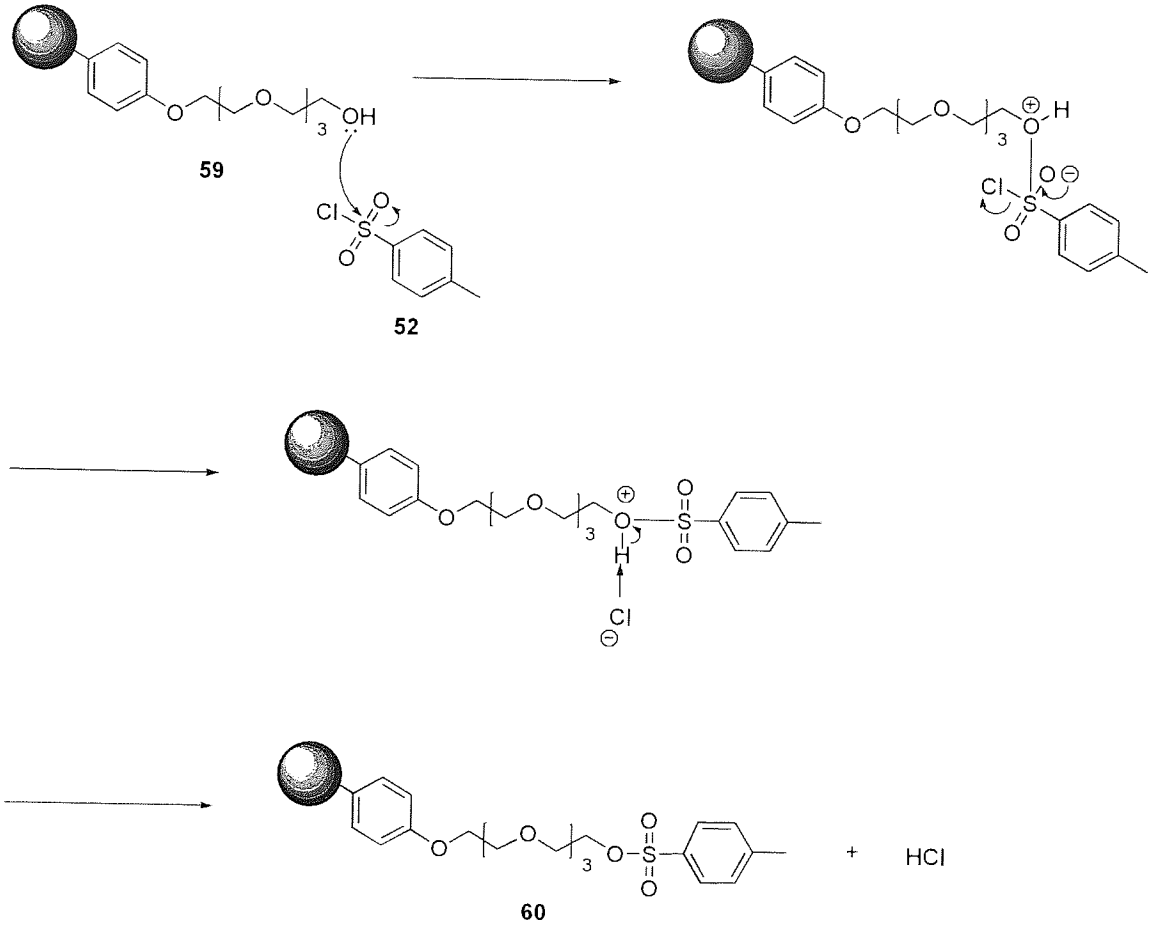

Mechanism 7: Tosylation of resin 59 to yield resin 60

The target resin was dried to constant weight and isolated in 99.8 % yield. Analysis of the product resin **60** by ATR-FTIR showed the emergence of strong peaks at 1358 cm^{-1}, the antisymmetric SO_2 stretch, and at 1175 cm^{-1}, the corresponding symmetric stretch. A strong signal associated with an S-O-C stretch is seen at 918 cm^{-1}, while the medium C-S stretch is observed at 663 cm^{-1}. Elemental analysis showed that sulfur was responsible for 2.4 % of the composition by weight. Loading by sulphur analysis was determined to be 0.87 mmol/g, a slight increase from the theoretical value of 0.79 mmol/g.

2.1.6 Phthalimido-Protected Quadragel 61

The Quadragel tosylate **60** was suspended in a solution of potassium phthalimide (5 equivalents) in DMF. The suspension was refluxed overnight to allow the S_N2 substitution of the phthalimide group to occur. Filtration and subsequent washing of the resin yielded resin **61**, the phthalimide derivative of the Quadragel base resin.

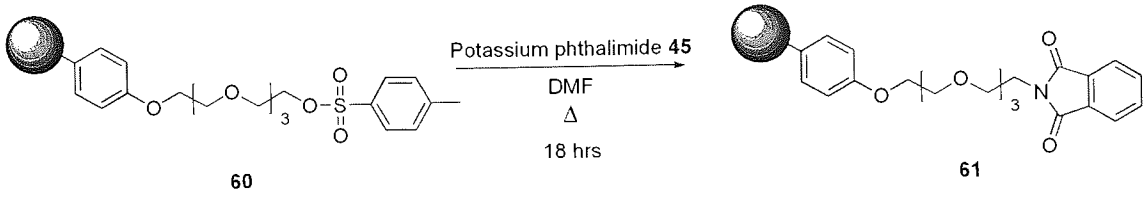

60 61

Reaction Scheme 11: Substitution of the tosyl activating group from 60 with phthalimide to yield resin 61.

Phthalimido-protected Quadragel **61** was isolated in 98 % yield after drying. The IR spectrum obtained from analysis of resin **61** showed the disappearance of the IR signals consistent with a tosyl group. In addition, the emergence of signals indicative of a phthalimide moiety indicated a successful transformation. The spectrum exhibited a very strong peak at 1712 cm^{-1} and another weaker signal at 1773 cm^{-1}, signals typical of imides, where the high-frequency signal is weaker and sometimes obscured[77].

2.1.7 Quadramine 62

Resin **61** was suspended in 1,4 dioxane and subjected to agitation with aqueous methylamine at room temperature for 72 hours[66]

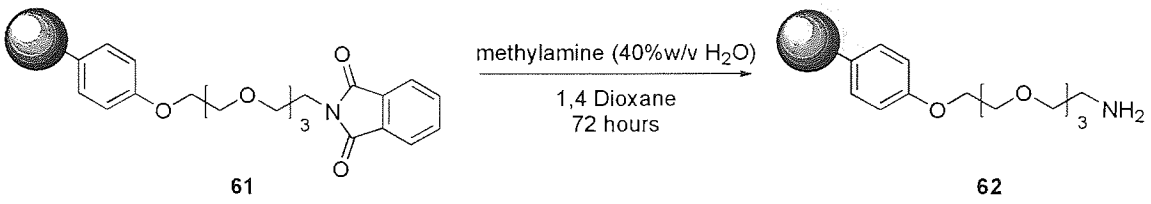

61 62

Reaction Scheme 12: Synthesis of Quadramine resin 62 via the reduction of 61 with methylamine

The resultant product, Quadramine resin **62**, was isolated in 99 % yield. The molecular weight difference between the hydroxyl resin **59** and the amine resin **62** is zero, giving resin **62** the same loading as the Quadragel resin **59** of 0.87 mmol/g. A spectrum obtained by ATR-FTIR analysis exhibited signals similar to the Quadragel resin **59**. The important difference between the two spectra is the absence of a broad peak associated with the hydrogen bonded –OH groups in resin **59**. All other signals are consistent with the base resin; peaks at 3025 and 2919 cm^{-1} show the presence of aromatic and aliphatic C-H bonds respectively. Benzene ring stretches are seen at 1601 and 1492 cm^{-1}, while the C-O-C ether stretch is present as a medium strength peak at 1244 cm^{-1}. The lack of any carbonyl signals in the IR spectrum of resin **62** indicated successful removal of the phthalimide group. The presence of primary amine groups was confirmed by TNBS[68] and Kaiser[67] assays.

The overall efficiency for the 3 step conversion of Quadragel resin **59** to Quadramine resin **62** was greater than 97 %, which highlights the benefits of utilising solid supports for multi-step chemical synthesis.

2.2 Comparative resin loading as assessed by Fmoc release, elemental analysis and mass balance

2.2.1 Introduction

Recently, there have been discussions about the validity of results obtained by utilizing the various reported 9-fluorenylmethoxycarbonyl (Fmoc) release assay techniques[78]. Assay methods are frequently published and amended or quickly superseded by another protocol. Literature sources from the same year often cite differing methods for performing the quantification. Each research group will no doubt have its preferred method, but this produces frequent instances of disputed results within and between research groups. The industrial ramifications are perhaps more important, especially for processes undertaken on the manufacturing scale. Many pharmaceutically relevant compounds such as peptides and pharmaceutically relevant precursors are produced using solid phase synthesis (SPS) and solid phase peptide synthesis (SPPS) technologies. Without accurate assessment of polymer loadings, these entities are being synthesised in either lower yield and in an impure form, as by-product formation occurs if insufficient reagents are employed, or at unnecessarily higher levels of cost, as excess raw materials are utilised needlessly. This is especially relevant with the current focus on producing cheap medication for the developing world. For example, each year hundreds of kilos of the anti-HIV drug T20 (Fuzeon®)[79] are produced, by Roche, predominantly using SPPS. Accurately determined polymer loading values could significantly reduce the environmental burden from waste, and additionally the amounts of raw materials required, which in concert, could lower the overall production cost of producing these pharmaceutically relevant molecules.

The aim of the study was to establish the optimal method for determining the loading of a resin for application in Fmoc-based peptide synthesis especially cGMP manufacturing. Accordingly, we set out to provide an impartial comparison of a number of commonly employed techniques used widely to quantify substitution

levels of resins within SPS and SPPS. The current study comprises past and most recent Fmoc release protocols, elemental analysis and mass balance. In each case we sought to assess the validity and reproducibility of each technique, and to gain some indication as to how the results obtained from each technique compare with one another for a range of resins. These results have also been compared with theoretically calculated loading values obtained by monomer composition calculations or residual ion analysis.

2.2.2 Materials and methods

2.2.2.1 Resins

Two batches of 2 % cross-linked chloromethyl(poly)styrene resin (75-150 μm diameter) were employed in this study. Resin **43** was synthesised 'in-house' (Aston University) using a standard suspension polymerisation procedure (**section 2.1**)[80,61]. The second batch of chloromethyl(poly)styrene resin **43a** was manufactured by Reaxa. 2-Chlorotritylchloride polystyrene resin **63** was obtained from Merck Biosciences. Prior to attachment of amino acids the resins **43**, **43a** and **59** were converted into their corresponding amino-functionalised derivatives **46**, **46a** and **62** using a standard Ing-Manske modification of the Gabriel reaction[63] described in **section 2.1** and **chapter 7, section 7. 2**

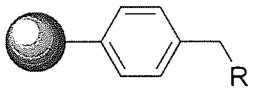

43	R=Cl	(Aston)
43a	R=Cl	(Reaxa)
46	R=NH_2	(Aston)
46a	R=NH_2	(Reaxa)
64	R=NHCO-Met-NHFmoc	(Aston)
64a	R=NHCO-Met-NHFmoc	(Reaxa)
65	R=NHCO-Met-Met-NHFmoc	(Aston)
65a	R=NHCO-Met-Met-NHFmoc	(Reaxa)

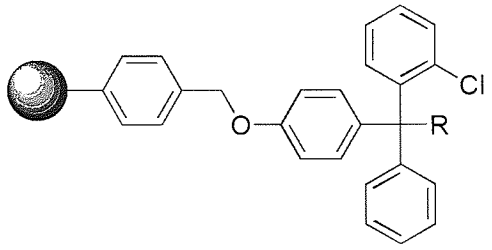

63	R=Cl
66	R=OCO-Met-NHFmoc
67	R=OCO-Met-Met-NHFmoc
68	R=OCO-Met-Phe-Gly-Gly-Tyr(tBu)-NHFmoc
69	R=OCO-Met-Met-Phe-Gly-Gly-Tyr(tBu)-NHFmoc

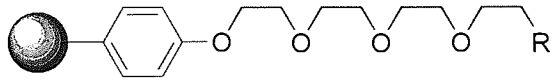

59	R=OH
62	R=NH_2
70	R=NHCO-Met-NHFmoc

Figure 19: Structures of the SPPS resins and resin-bound compounds

2.2.2.2 Methods - Peptide synthesis[51,81]

The peptidyl sequences were synthesised in a stepwise manner employing the widely recognised PyBOP/HBTU/TBTU technique[51]. Precise reaction conditions are described in detail in **chapter 7, section 7.2.**

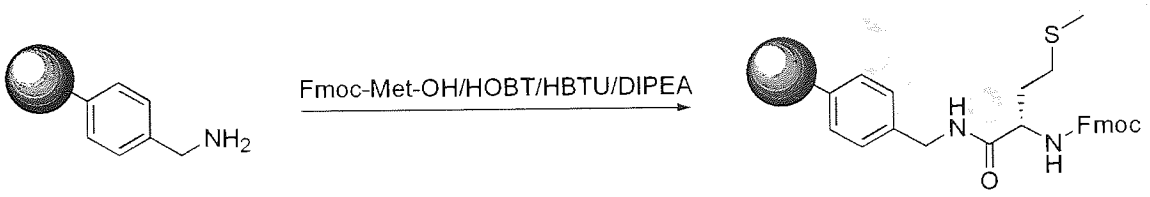

46/46a

64/64a

Reaction Scheme 13: HOBT/HBTU coupling of Fmoc-Met-OH to AMPS 46/46a to yield 64 (64 & 64a)

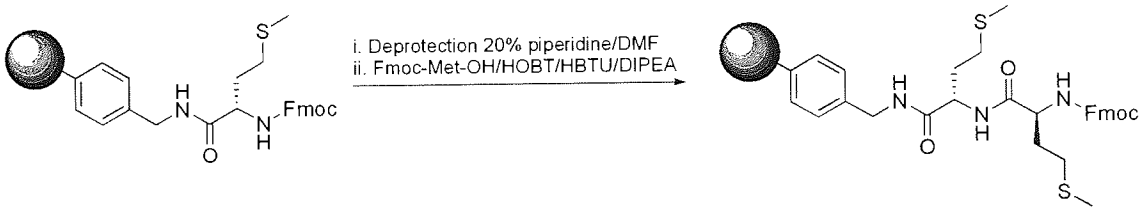

64/64a

65/65a

Reaction Scheme 14: HOBT/HBTU coupling of Fmoc-Met-OH to 64 to yield derivative 65 (65 & 65a)

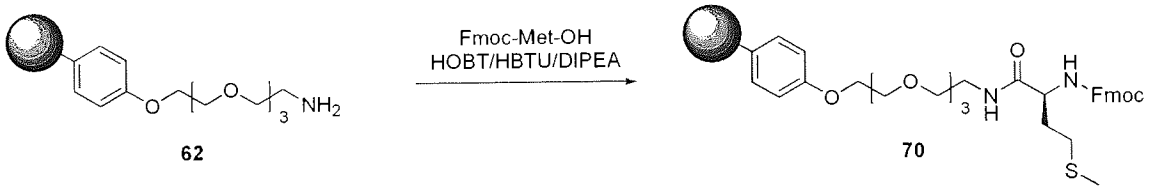

62

70

Reaction Scheme 15: HOBT/HBTU coupling of Fmoc-Met-OH to 62 to yield derivative 70

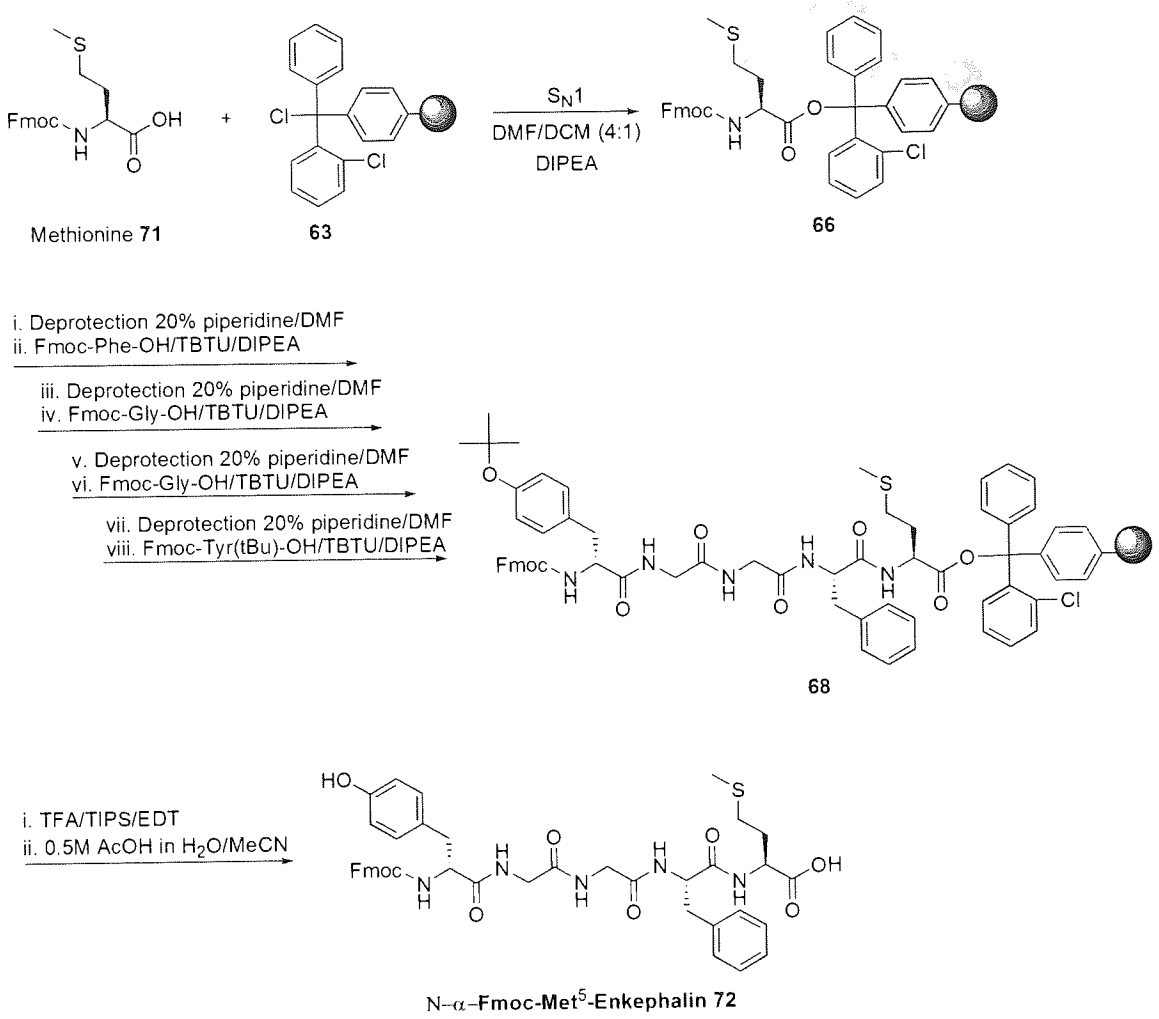

Reaction Scheme 16: Synthesis of compound 68 and subsequent cleavage of the resultant peptide *N*-α- Fmoc-[Met^5]-Enkephalin-OH 72.

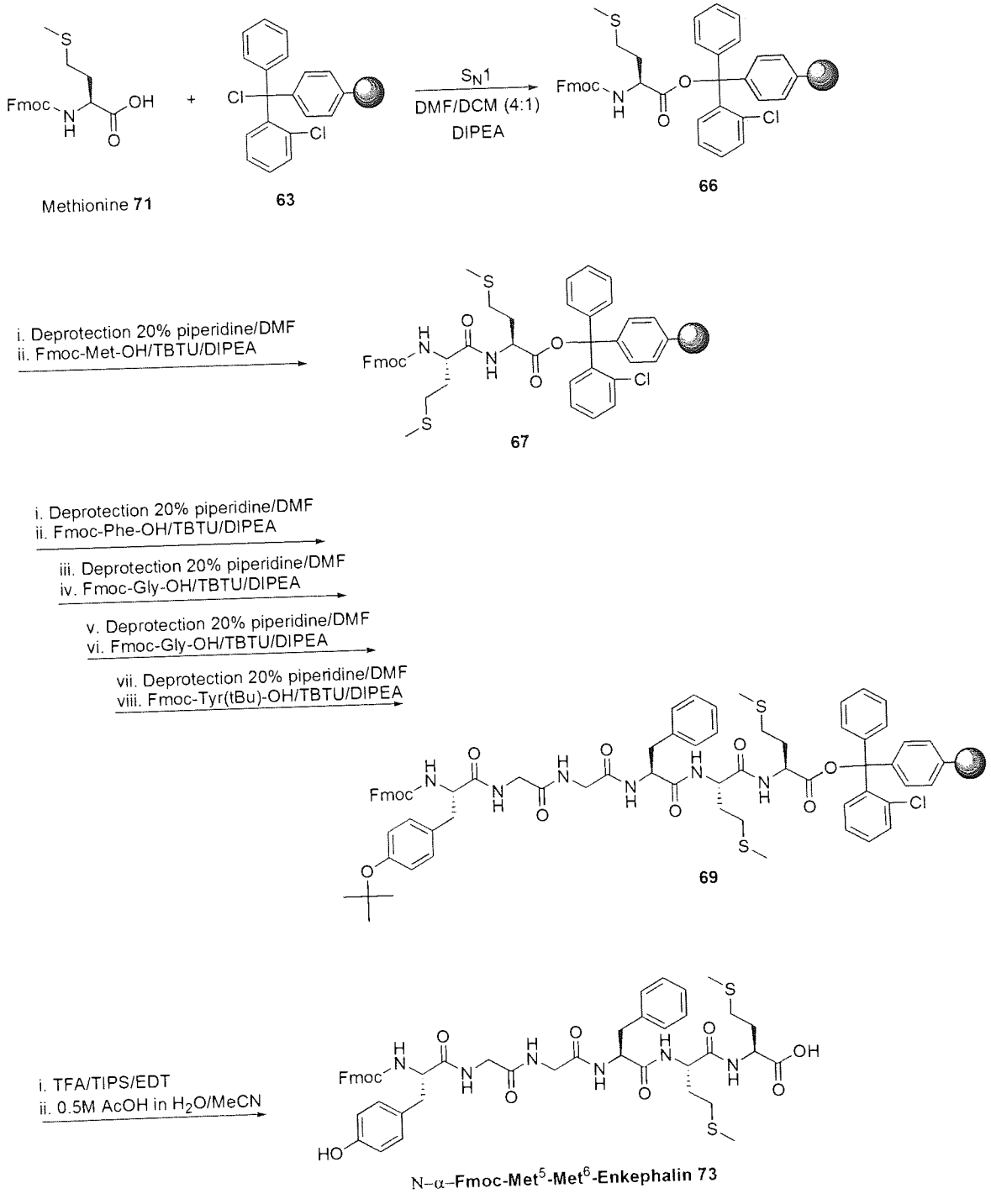

Reaction Scheme 17: Synthesis of compound 69 and subsequent cleavage of the resultant peptide *N*-α- Fmoc-[Met^{5}Met^6]-Enkephalin-OH 73.

2.2.2.3 Calculation of resin loadings

2.2.2.3.1 Calculation of resin loadings by Fmoc release assay using published equations

The following published equations were employed to calculate the resin loadings.

Equation 1[82]

$$loading(mol/g)_{290nm} = \frac{Abs_{piperidine/DMF}}{mass\ of\ resin(mg)} \text{x} \frac{1}{1.65}$$

Equation 2[78]

$$loading(mol/g)_{294nm} = \frac{Abs_{DBU/DMF}}{mass\ of\ resin(mg)} \text{x} 142.14$$

Equation 3[78]

$$loading(mol/g)_{305nm} = \frac{Abs_{DBU/DMF}}{mass\ of\ resin(mg)} \text{x} 163.96$$

2.2.2.3.2 Calculation of resin loadings by Fmoc release assay using extinction coefficients determined "in-house"

Using the extinction coefficients obtained from the calibration protocols above the loading of the resins were recalculated using the following equations.

Equation 4

$$Abs = \varepsilon cl$$

Where Abs = absorbance, ε = extinction coefficient ($L \cdot mol^{-1} \cdot cm^{-1}$), c = concentration of Fmoc ($mol \cdot L^{-1}$), and l = path length (cm) and is equal to 1.

Equation 5

$$n = cv$$

Where n = number of moles of Fmoc, v = volume of solvent in the cuvette (cm^3)

Combine (Equation 4) & (Equation 5):

Equation 6

$$n = \frac{Abs}{\varepsilon} v$$

By definition:

Equation 7

$$loading(mol/g) = \frac{n}{mass\ of\ resin}$$

Therefore:

Equation 8

$$loading(mol/g) = \frac{\frac{Abs}{\varepsilon} v}{mass\ of\ resin}$$

In neither the previously published[78,82] nor the "in-house" calculations is the mass increase of the resin resulting from the covalent attachment of each amino acid taken into account. A more accurate procedure, the 'mass balance' method, which takes into account the additional mass of coupled amino acids, is discussed below in **section 2.2.3.7**.

2.2.3 Results

2.2.3.1 Loading values established by the uncalibrated piperidine-mediated Fmoc cleavage procedures[82]

Initially, the loading of the two chloromethyl(poly)styrene resins **43** and **43a** was determined by subjecting ~3 mg samples (accurately weighed) of derivatives **64, 64a, 65** and **65a** to the Fmoc release assay using the small-scale piperidine-based method described in **section 7.2.14**. For each sample, measurement of the absorbance at 290 nm was performed in quadruplicate and the average reading employed in conjunction with Equation 1 to give the loading value for that sample. The experimental results and the theoretical loading values were calculated on the basis of monomer composition utilised in resin synthesis (Table 4). Larger scale analyses were also performed on samples of ~17 mg of derivatives **64, 64a, 65** and **65a** (accurately weighed). The larger-scale study was performed in an identical fashion to the initial procedure (Table 5).

Table 4: Loadings of resins 43 and 43a determined by piperidine-mediated Fmoc release from ~3 mg samples of derivatives 64, 64a, 65 and 65a (accurately weighed) employing method 7.2.14 in conjunction with Equation 1. All calculations are based upon the UV/vis maxima obtained for the DBF-piperidine adduct at 290 nm.

Resin	Derivative	Theoretical loading (mmol / g)[a]	Experimental loading calculated using Equation 1 (mmol / g)
43	**64**	1.00	0.520
43	**65**	1.00	0.310
43a	**64a**	1.20	0.370
43a	**65a**	1.20	0.330

[a] Theoretical loadings are calculated on the basis of the monomer composition utilised in resin synthesis for resin **43**, and residual chloride ion content for resin **43a**.

Table 5: Loadings of resins 43 and 43a determined by piperidine-mediated Fmoc release from ~17 mg samples of derivatives 64, 64a, 65 and 65a (accurately weighed) using method 7.2.14 in conjunction with Equation 1. All calculations are based upon the UV/vis maxima obtained for the DBF-piperidine adduct at 290 nm.

Resin	Derivative	Theoretical loading (mmol / g)[a]	Experimental loading calculated using Equation 1 (mmol / g)
43	**64**	1.00	0.621
43	**65**	1.00	0.496
43a	**64a**	1.20	0.473
43a	**65a**	1.20	0.373

[a] Theoretical loadings are calculated on the basis of the monomer composition utilised in resin synthesis for resin **43**, and residual chloride ion content for resin **43a**.

2.2.3.2 Construction of Fmoc concentration vs. absorption calibration curves in a piperidine/DMF solvent system

The concentration of Fmoc (M) which caused deviation from linearity in a plot of concentration versus absorption at 290 and 300 nm was determined for cleavage conditions employing piperidine (Figure 20). This graph summarises the results obtained from the study of three different Fmoc protected amino acids (Fmoc-Gly-OH, Fmoc-Met-OH and Fmoc-Nle-OH) over a large concentration range (Figure 20). The range of concentrations where Beer-Lambert Law remains linear can then be expanded (Figure 21).

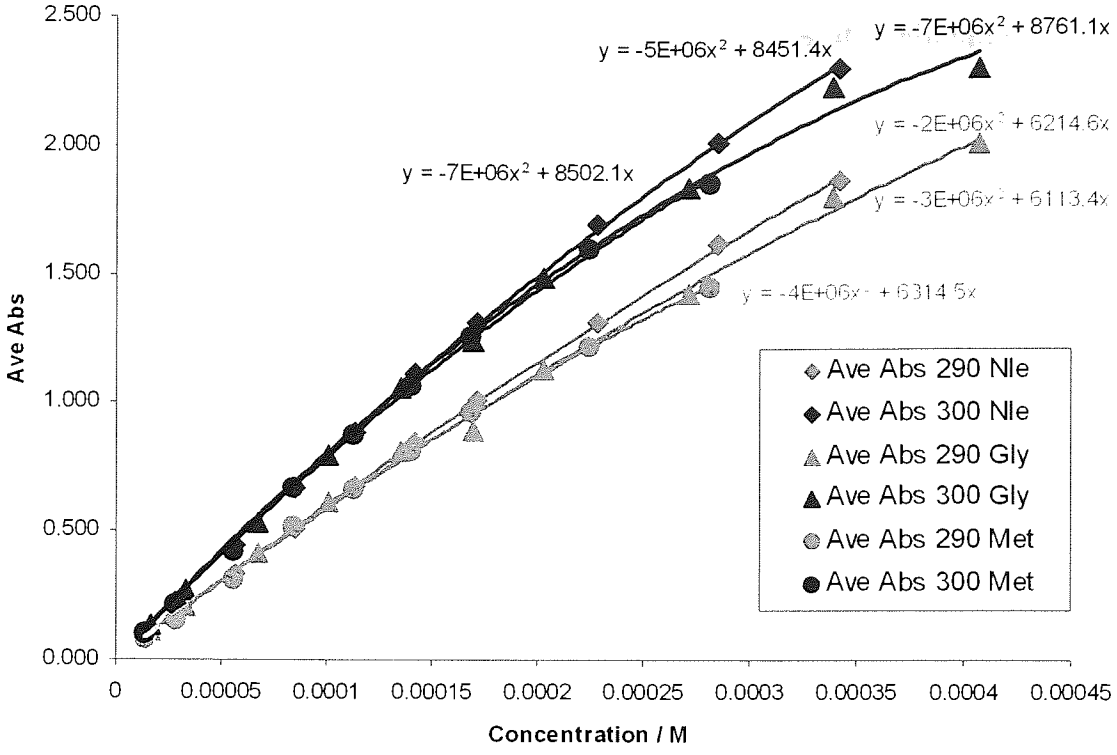

Figure 20: Calibration curve of Fmoc concentration vs. absorbance at 290 and 300 nm via cleavage with 20 % v/v piperidine/DMF.

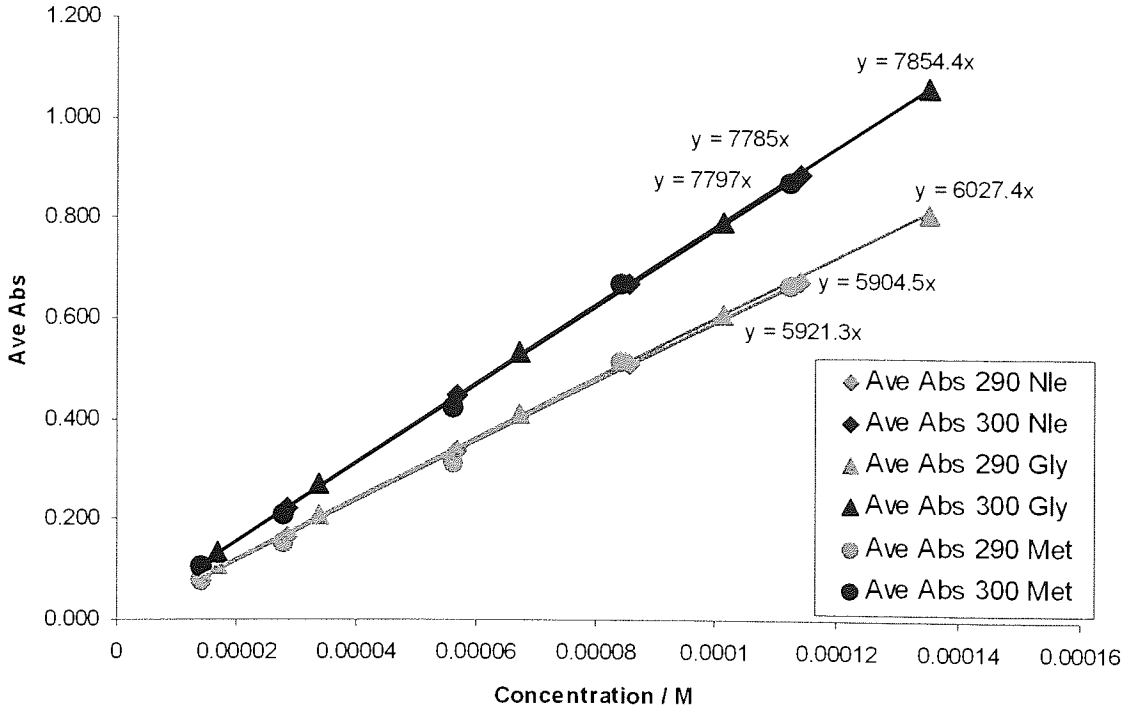

Figure 21: Linear region of the calibration curve of Fmoc concentration vs. absorbance at 290 and 300 nm via cleavage with 20 % v/v piperidine/DMF.

The extinction coefficient of the released dibenzofulvene (DBF)-piperidine adduct was determined for each amino acid at 290 and 300 nm from each of the calibration curves in Figure 21. (Table 6).

Table 6: Extinction coefficients determined for the DBF-piperidine adduct in 20 % v/v piperidine in DMF at 290 and 300 nm

Amino Acid	$\varepsilon_{piperidine/DMF}$ at 290 nm	$\varepsilon_{piperidine/DMF}$ at 300 nm
Fmoc-Gly-OH	6027	7854
Fmoc-Met-OH	5921	7797
Fmoc-Nle-OH	5904	7785

2.2.3.3 Loading values established by the calibrated piperidine-mediated Fmoc cleavage procedures

The calculated extinction coefficients for the DBF-piperidine adduct obtained for Fmoc-Gly-OH were used in conjunction with Equation 8 to enable calibrated loadings to be calculated for resins **43** and **43a**. Experimental values obtained via both the small-scale and the large-scale piperidine-mediated Fmoc release assays are displayed below (Table 7 & Table 8).

Table 7: Loadings of resin 43 and 43a determined by piperidine-mediated Fmoc release from ~3 mg samples of derivatives 64, 64a, 65 and 65a (accurately weighed) using method 7.2.15 in conjunction with Equation 8. All calculations are based upon the UV/vis maxima obtained for the DBF-piperidine adduct at 290 nm.

Resin	Derivative	Theoretical loading (mmol / g)[a]	Experimental loading calculated using Equation 8 (mmol / g)
43	**64**	1.00	0.426
43	**65**	1.00	0.251
43a	**64a**	1.20	0.305
43a	**65a**	1.20	0.268

[a] Theoretical loadings are calculated on the basis of the monomer composition utilised in resin synthesis for resin **43** and residual chloride ion content for resin **43a**.

Table 8: Loadings of resin 43 and 43a determined by piperidine-mediated Fmoc release from ~17 mg samples of derivatives 64, 64a, 65 and 65a (accurately weighed) using method 7.2.15 in conjunction with Equation 8. All calculations are based upon the UV/vis maxima obtained for the DBF-piperidine adduct at 290 and 300 nm.

Resin	Derivative	Theoretical loading (mmol / g)[a]	Experimental loading calculated using Equation 8 290 nm (mmol / g)	Experimental loading calculated using Equation 8 300 nm (mmol / g)	Average Experimental loading (mmol / g)[b]
43	**64**	1.00	0.510	0.518	0.514
43	**65**	1.00	0.407	0.407	0.407
43a	**64a**	1.20	0.393	0.397	0.395
43a	**65a**	1.20	0.306	0.304	0.305

[a] Theoretical loadings are calculated on the basis of the monomer composition utilised in resin synthesis for resin **43** and residual chloride ion content for resin **43a**. [b] Average experimental value of the loading calculated at 290 nm and 300 nm for each resin.

2.2.3.4 Loading values established by the uncalibrated DBU-mediated Fmoc cleavage procedure

The loading of the two chloromethyl(poly)styrene resins **43** and **43a** were also determined by subjecting derivatives **64, 64a, 65** and **65a** to the DBU-mediated Fmoc release assay[78] referred to in **section 7.2.14**. For each sample, the absorbance readings were recorded in quadruplicate at 294 and 305 nm. Using the average reading at each wavelength in conjunction with Equation 2 or Equation 3 gave the loading values for that sample. In addition the loadings of base resins **63** and **59** were determined in an identical manner by analysis of derivatives **66-70** (Table 9).

Table 9: Loadings of resins 43, 43a, 63 and 59 determined by DBU-mediated Fmoc release from ~50 mg samples of derivatives 64, 64a, 65, 65a, 66-70 (accurately weighed) using method 7.2.14 in conjunction with Equation 2 and Equation 3. All calculations are based upon the UV/vis maxima obtained for DBF at 294 and 305 nm.

Resin	Derivative	Theoretical loading (mmol / g)[a]	Experimental loading calculated using Equation 2 294 nm (mmol / g)	Experimental loading calculated using Equation 3 305 nm (mmol / g)	Average Experimental loading (mmol / g)[b]
43	**64**	1.00	0.546	0.578	0.562
43	**65**	1.00	0.400	0.423	0.412
43a	**64a**	1.20	0.400	0.420	0.410
43a	**65a**	1.20	0.304	0.320	0.312
63	**66**	1.20	0.607	0.645	0.626
63	**67**	1.20	0.556	0.589	0.573
63	**68**	1.20	0.453	0.479	0.466
63	**69**	1.20	0.402	0.426	0.414
59	**70**	0.89	0.612	0.648	0.630

[a] Theoretical loadings are calculated on the basis of the monomer composition utilised in resin synthesis for resins **43** and **59** and by residual chloride ion content for resin **43a**. Resin **63** utilised the loading value reported by the manufacturer.

[b] Average experimental value of the loading calculated at 294 nm and 305 nm for each resin.

2.2.3.5 Construction of Fmoc concentration vs. absorption calibration curves in a DBU/DMF solvent system

A second set of calibration curves were then constructed for the cleavage conditions employing DBU, (Figure 22). As with Figure 21 this graph summarises the results obtained from the study of three different Fmoc protected amino acids (Fmoc-Gly-OH, Fmoc-Met-OH and Fmoc-Nle-OH) over a concentration range of 0 to 0.15 mmol. Again each data point is the average of four separate absorption readings.

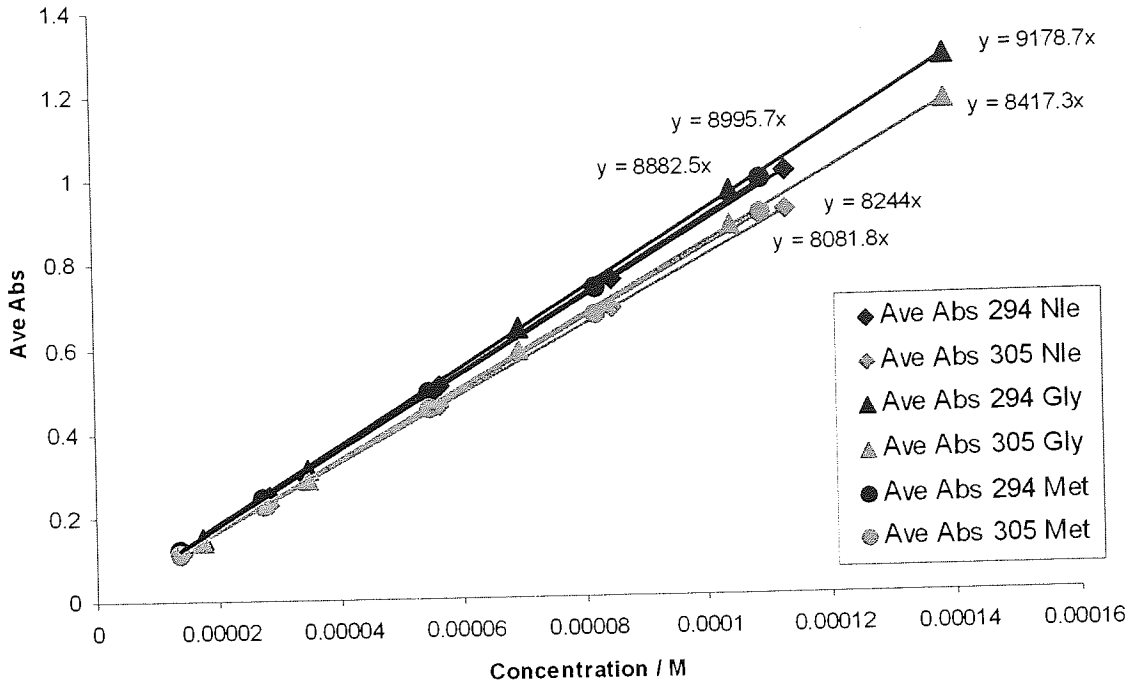

Figure 22: Calibration curve of Fmoc concentration vs. absorbance at 294 and 305 nm via cleavage with 2 % v/v DBU/DMF

The extinction coefficient of the released DBF was determined for each amino acid at both 294 and 305 nm from each of the calibration curves in Figure 22. (Table 10).

Table 10: Extinction coefficients determined for DBF

Amino Acid	$\varepsilon_{DBU/DMF/MeCN}$ at 294 nm	$\varepsilon_{DBU/DMF/MeCN}$ at 305 nm
Fmoc-Gly-OH	9179	8417
Fmoc-Met-OH	8996	8244
Fmoc-Nle-OH	8883	8082
Average[a]	9019	8248

[a] Average value of the extinction coefficient at either 294 or 305 nm for the three amino acids studied

2.2.3.6 Loading values established by the calibrated DBU-mediated Fmoc cleavage procedures

The two average calculated extinction coefficients determined for DBF in 2% v/v DBU in DMF at both 294 and 305 nm were used in conjunction with Equation 8 to enable calibrated loadings to be calculated for resins **43, 43a, 63** and **59** within the DBU-mediated Fmoc release assay of derivatives **64, 64a, 65, 65a, 66-70**, (Table 11).

Table 11: Loadings of resins 43, 43a, 63 and 59 determined by DBU-mediated Fmoc release from ~50 mg samples of derivatives 64, 64a, 65, 65a, 66-70 (accurately weighed) using method 7.2.16 in conjunction with Equation 8. All calculations are based upon the UV/vis maxima obtained for DBF at 294 and 305 nm.

Resin	Derivative	Theoretical Loading (mmol / g)[a]	Experimental loading calculated using Equation 8 294 nm (mmol / g)	Experimental loading calculated using Equation 8 305 nm (mmol / g)	Average Experimental Loading (mmol / g)[b]
43	**64**	1.00	0.798	0.801	0.800
43	**65**	1.00	0.586	0.586	0.586
43a	**64a**	1.20	0.585	0.583	0.584
43a	**65a**	1.20	0.445	0.444	0.445
63	**66**	1.20	0.880	0.887	0.884
63	**67**	1.20	0.807	0.810	0.809
63	**68**	1.20	0.657	0.659	0.658
63	**69**	1.20	0.583	0.587	0.585
59	**70**	0.89	0.888	0.891	0.890

[a] Theoretical loadings are calculated on the basis of the monomer composition utilised in resin synthesis for resins **43** and **59** and by residual chloride ion content for resin **43a**. With resin **63** the reported manufacturing loading was utilised.

[b] Average experimental value of the loading calculated at 294 nm and 305 nm for each resin.

2.2.3.7 Loading values established by % elemental composition and mass of released product following bulk scale synthesis of derivatives 68 and 69

The loadings of resins **43, 43a, 63 and 59** were also determined by elemental combustion analysis (%S and %N) of resin derivatives **64, 64a, 65, 65a, 66-70** (Table 12). Additionally, the loading of resin **63** was determined from the actual mass isolated after cleavage of crude Fmoc-[Met^5]-Enkephalin-OH and Fmoc-[Met^5Met^6]-Enkephalin-OH peptides from derivative resins **68** and **69** respectively, (Table 12). In this study the scale of the syntheses and cleavages were sizable, facilitating accurate weighings (see **section 2.2.4.3**).

Table 12: Loadings of resins 43, 43a, 63 and 59 determined by elemental combustion analysis and of resin 63 by isolated mass of crude cleaved peptide.

Resin	Derivative	Theoretical loading (mmol / g)[a]	Loading based on %S (mmol / g)	Loading based on %N (mmol / g)	Loading based on isolated peptide mass (mmol / g)
43	**64**	1.00	0.964	1.230	
43	**65**	1.00	0.978	1.543	
43a	**64a**	1.20	1.079	1.819	
43a	**65a**	1.20	0.934	1.543	
63	**66**	1.20	0.741	0.819	
63	**67**	1.20	0.764	0.813	
63	**68**	1.20	0.780	0.749	0.64
63	**69**	1.20	0.730	0.715	0.72
59	**70**	0.89	0.867	0.906	

[a] Theoretical loadings are calculated on the basis of the monomer composition utilised in resin synthesis for resins **43** and **59** and by residual chloride ion content for resin **43a**. With resin **63** the reported manufacturing loading was utilised.

2.2.4. Discussion

In order to reduce raw material expenditure within manufacturing processes involving synthesis upon solid supports, it is imperative that the loading of the support employed is known accurately. It was therefore necessary to evaluate a number of alternative methods for assessing resin loading. Specifically these were 1) piperidine-mediated Fmoc release, 2) DBU-mediated Fmoc release, 3) elemental analysis and 4) actual mass of product released from a support. Our findings with regards to each of these methods are given below.

2.2.4.1 Piperidine-mediated Fmoc release assay

Since their inception, Fmoc protected amino acids have been routinely utilised for solid phase peptide synthesis. It is the facile removal of the *N*-Fmoc protecting group with secondary amines[49,59] and the ready commercial availability of the desired amino acid building blocks, in large quantities, that has promoted Fmoc SPPS as the method of choice for cGMP manufacturing. The Novabiochem catalogue (Merck Biosciences Ltd.) is a highly respected and widely used technical reference source, especially within industry. A simple method for determining resin loading by Fmoc release employing 20 % v/v piperidine in DMF is provided[82] and was performed herein.

The reported method relies upon treating small amounts of resin (~3 mg) with a 20 % v/v piperidine in DMF solution and measuring the resultant UV absorbance of the DBF-piperidine adduct at 290 nm. The loading of the resin is then determined simply by inserting the measured absorbance value into Equation 1. When this procedure was performed on the Fmoc-Met **64** and Fmoc-Met-Met **64a** derivatives of resin **43**, loading values of 0.52 mmol / g and 0.31 mmol / g were obtained (Table 4). It was surprising to witness the size of the discrepancy between these two values as the assemblies were deemed near quantitative by Kaiser monitoring studies. In addition, Fmoc-Met-Met **65** was derived directly from Fmoc-Met **64.** Even taking

into consideration the weight gain from resin derivative **64** to resin derivative **65** the experimental loading value calculated from this piperidine-mediated Fmoc release assay value was questionable. Indeed, both values were significantly lower than the theoretical loading value expected for resin **43** based upon the monomer composition used in its construction (1.00 mmol / g). Initial thoughts were that the construction of 'in-house' resin **43** had not proceeded satisfactorily. However, when analogous commercial resin **43a** was converted into derivatives **64a** and **65a** and these derivatives assayed in identical fashion, similar low-value loading results were obtained (Table 4).

The small amount of resin employed in this first assay procedure coupled with the accuracy of the balance (typically a four-point balance is standard in most laboratories) used to weigh the resin sample means that there is a significant potential for error. To try and reduce this discrepancy the piperidine-mediated Fmoc release assay was repeated on derivatives **64, 64a, 65** and **65a** using a more substantial mass of resin (~17 mg). Interestingly, the results obtained here gave values which were uniformly higher yet still significantly lower than the theoretical values (Table 5).

A further source of potential error was that the loading values were calculated, in both the small and large scale piperidine-mediated procedures, using Equation 1 which contains a pre-determined multiplication factor. This factor takes into account standard cuvette size, extinction coefficient, etc. but was calculated on a different instrument to the one used to generate our data (Table 4 and Table 5). Additionally it was not clear which amino acid had been employed for the purposes of calibration in the published study, and indeed whether or not the extinction coefficient is amino acid dependent.

Accordingly, to eliminate these potential sources of error, a number of calibration curves were constructed utilising *N*-Fmoc-Gly, Met and Nle protected amino acids. Firstly, it was necessary to determine whether the Beer-Lambert law deviated from linearity and if so, at what concentration of Fmoc (M) this occurred. In addition to taking absorbance readings at 290 nm, further readings were taken at the second absorption maxima of the DBF-piperidine adduct at 300 nm. The absorbance vs.

concentration plot shows deviation from linearity as concentration increases (Figure 20), but is linear for each of the three amino acids up to concentrations of 0.15 mM at both 290 and 300 nm (Figure 21). Furthermore, at low amino acid concentrations these plots appear to be amino acid independent (Figure 21). Accordingly, the calculated extinction coefficients for Fmoc-Gly-OH at 290 and 300 nm were used in all subsequent calculations involving piperidine-mediated release of Fmoc.

Surprisingly, the loading values from the calibrated small scale assays (Table 7) are uniformly lower than those obtained from the uncalibrated small scale procedure (Table 4). However, due to the large degree of error we believe is inherent in the small scale procedure, these values were not deemed reliable enough for further scrutiny. The loading values obtained from the larger scale calibrated procedure (Table 8) were also uniformly lower than those obtained from the uncalibrated procedure (Table 5). Since there is such good correlation between the two sets of data obtained for the large scale calibrated procedure (Table 8) we believe this data most accurately represents the loadings of the resins **43** and **43a** as assessed by a piperidine-mediated Fmoc release assay.

2.2.4.2 DBU-mediated Fmoc release assay

Recently, a general consensus has formed that DBU/DMF should be used as the preferred cleavage solution in Fmoc release assays[78,83,84,85]. Protocols have been published for measuring the concentration of the sole DBF product produced via the DBU cleavage (as opposed to the product equilibrium potentially encountered when using piperidine) by UV spectroscopy[86], HPLC[87], and GC[88].

The UV spectroscopic method described by Gude et al[78] is founded upon cleaving the Fmoc group with 2 % v/v DBU in DMF. Resin loadings are calculated by recording the UV-Vis absorbance maxima at one of two wavelengths (294 nm or 305 nm) in conjunction with Equation 2 and Equation 3 respectively. This procedure was applied to establish the loadings of resins **43, 43a, 63** and **59.** Analysis of resins **43** and **43a** was undertaken to enable comparison with the piperidine-mediated assay results and additionally with **63** and **59** to establish the general applicability of the

assay, as resin **63** and types analogous to **59** are most likely to be encountered presently in the bulk manufacture of peptides.

There is relatively close agreement with the two sets of data recorded at 294 and 305 nm (Table 9). This concurrence is such that it appears reasonable to average the two values to obtain a single loading value for each derivative **64, 64a, 65, 65a,** and **66-70**. Comparison of these individual loadings for derivatives **64, 64a, 65** and **65a** also appears to be in accord with values obtained from the calibrated large-scale piperidine-mediated Fmoc release assay (Table 8).

In light of the previous finding that the construction of a set of calibration curves for the piperidine-mediated assay resulted in apparently more reliable data, a similar set of calibration curves was constructed for the DBU-mediated Fmoc release process (Figure 22). Here, as with the piperidine-mediated process, a linear response was observed for all three amino acids studied (Fmoc-Gly, Fmoc-Met and Fmoc-Nle) at 294 and 305 nm. Linearity was observed up to concentrations approaching 0.15 mM. However, unlike the piperidine-mediated deprotection procedures, it appears that this time there is a degree of amino acid dependence, albeit a relatively small one. Consequently, for the calibrated loading calculations, the average values of the extinction coefficients at 294 nm ($\varepsilon = 9019$, Table 10) and 305 nm ($\varepsilon = 8248$, Table 10) were used in all subsequent calculations.

When the averaged extinction coefficients at 294 and 305 nm were used in conjunction with Equation 8 in the analysis of derivatives **64, 64a, 65** and **65a**, the agreement between the calculated loading values at 294 and 305 nm is excellent (Table 11). Indeed, these findings highlight an improved procedure to that in which data sets are obtained employing a non-calibrated method (Table 9). It is important to note that the loading values calculated using the calibrated DBU procedure are uniformly higher than those obtained using the non-calibrated method, and generate results which have greater agreement with the theoretically calculated loadings. This observation was replicated exactly in the analysis of derivatives **66-70**.

2.2.4.3 Elemental analysis

The loadings of derivatives **64, 64a, 65, 65a,** and **66-70** were also investigated by combustion analysis to provide the percentage elemental composition of each resin sample. Specifically, determination of the percentage content of S and N was imperative to avoid overlap with the polymer composition. For each derivative the mass of the compound coupled to the base resin (weight gain) was taken into account to provide loading values based on the abundance of sulphur and nitrogen in the sample (Table 12).

In this study, sulphur content provides an excellent measure of loading when used in conjunction with sulphur containing residues such as the amino acids Cys or Met. Sulphur is not present in the base resins **43, 43a, 63** or **59** and so any atoms of sulphur present must necessarily arise directly as a result of the successful covalent attachment of sulphur-containing molecules. This was verified by comparison with samples of aminomethyl(poly)styrene resins **46** and **46a** that had undergone the coupling procedure *without* the activating agents being present in the reaction mixture. The sulphur content of these samples was found to be negligible (< 0.1 %, the limit of detection) and showed that the presence of sulphur was the result of successful covalent attachment and not simply due to encapsulation/precipitation of methionine by or within the resin.

Loading values can also be calculated from the nitrogen content. This is entirely valid for derivatives **64a, 65a, 66-70** which were manufactured using a peroxide initiator (e.g. lauroyl peroxide). However, this method is inappropriate for the analysis of derivatives **64** and **65** since azobis-*iso*-butyronitrile (AIBN) was used in the construction of resin **43**. This azo-based initiator can itself supply nitrogen atoms (from the nitrile moieties) to the polymer matrix comprising the resin.

2.2.4.4 Mass of released product

Probably the most appropriate method for determining the loading of a resin for utilisation in bulk-scale SPPS manufacture is to propagate a "real" batch of it in the bulk-scale synthesis of a peptide. Subsequent release and isolation of the crude peptidic material (before purification) will indicate a true loading value for the batch of starting resin. To best enable a direct comparison of such a "real" loading value with the values obtained from each of the analytical assays described above it was decided to synthesise two pharmaceutically relevant peptides which are known to assemble in a facile manner. Accordingly, assemblies of Fmoc-[Met^5]-Enkephalin-OH and Fmoc-[Met^5Met^6]-Enkephalin-OH were undertaken using standard Fmoc protocols. The same base resin **63** was utilised for both syntheses and in each case the synthesis was conducted at a scale relevant to industrial peptide production (~5.00 g of resin **63,** theoretical scale ~6 mmol). Additionally, the use of a significantly large scale of synthesis enabled the mass of released peptide, following cleavage, to be determined accurately. Upon cleavage and subsequent critical reverse phase HPLC analysis the crude Fmoc-[Met^5]-Enkephalin-OH product was determined as >95% pure. This met the necessary criteria as truncated or deletion peptide impurities would affect the calculation. From the gross mass of released Fmoc-[Met^5Met^6]-Enkephalin-OH from resin **63** the experimental loading capacity of the base resin was determined as 0.72 mmol / g. Similarly, in the separate synthesis of the peptide Fmoc-[Met^5]-Enkephalin-OH of identical purity, the experimental loading value was determined as 0.64 mmol / g.

It is most likely that the result derived from the synthesis of the Fmoc-[Met^5]-Enkephalin-OH is inaccurate. The syntheses of both Fmoc-[Met^5]-Enkephalin-OH and Fmoc-[Met^5Met^6]-Enkephalin-OH utilised the same base resin **63,** and both resin-based derivatives **68** and **69** gave similar elemental sulphur results with loading values greater than 0.7 mmol / g. It is thus most likely that one of the amino acid coupling reactions utilised in the synthesis of derivative **68,** subsequent to the original methionine coupling, did not proceed quantitatively, reducing the yield of final product. Subsequent cleavage resulted in an anomalously low loading value for the base resin **63** being obtained.

2.2.4.5 Comparison of methods

It is reasonable to suggest that determining the resin loading on the basis of gross mass of product isolated after cleavage is the most appropriate method since this is the "real" loading value and will mimic any process performed at scale. However, this value is arrived at only after the completion of a protracted synthetic procedure and thus is of little practical use within day-to-day laboratory undertakings where results are required quickly. From a practical and economic viewpoint this method is only appropriate if there is a very strong need to reduce the overall cost of the production process, for example by employing less molar equivalents of reagents, reducing solvent consumption, etc. In this instance the results strongly indicate that one or more trial scouting assemblies at an appropriate scale should be undertaken to accurately quantify the loading of a bulk batch of starting resin.

Of the pre-production methods of analysis evaluated in the studies it can be concluded that elemental analysis, most especially of %S, gives loading values which most accurately reflect the "real" loading values obtained through the measurement of gross mass of released product. Clearly it is not always possible to incorporate sulphur-containing residues at an early stage in a synthesis, if at all. In these instances the most appropriate use of elemental analysis would appear to be to establish the loading of a bulk batch of resin by coupling methionine or cysteine to a small sample of resin and subjecting it to S elemental analysis. The loading value obtained in this manner should then be utilised in all subsequent syntheses involving that batch of resin.

Of the UV-based assay procedures evaluated, the calibrated DBU-mediated procedure gives loading values which most closely relate to our "real" value. If a non-calibrated method must be selected then again this should be the DBU-mediated process since the loadings established using this method were found to be closer to our "real" values than any of the piperidine-mediated methods. In practice, the analytical time required to perform the calibrated DBU-mediated study is obviously longer than that required to perform the uncalibrated process. Therefore the labour cost of the process to an industrial user is greater when using the calibrated method.

However and critically, in employing this more accurate means of resin loading determination, one may obtain a more appropriate yield of product to be made on any given batch of resin and hence alleviate raw material waste. Thus costs in terms of labour are more than likely going to be offset by the economic feasibility of the process. From the results obtained in this study it is clear that the piperidine-mediated cleavage methods are best avoided.

In summary, it appears from this study that there is a good correlation between establishing a resin loading by S elemental analysis and by performing a calibration of Fmoc release products in a DBU/DMF solvent system when compared with the actual amount of material isolated after cleavage from the resin. Since the DBU-mediated Fmoc release results do not take into account mass gain as the mass of material coupled to the base resin increases, the disparity between the measured loading value and the true loading value will increase. Conversely, since the elemental analysis method takes into account the mass increase due to the covalent attachment of amino acids, it has to be regarded as the most accurate pre-production method for determining resin loading values. Ideally for assessing a batch of resin, these two methods should be used in concert with a small sample of the material being converted into the Fmoc-Met or Fmoc-Cys derivative and subjected to both modes of analysis. For small scale syntheses where the financial implications of the resin loading are not so vital, and where S is not incorporated within the initially immobilised species, a calibrated DBU method would appear to be the most time and cost effective method.

Chapter 3

Solid Phase Peptide Synthesis, Protecting Group Strategies, Introduction of Boronic Acids and Post-Cleavage Manipulation of Peptides

Solid Phase Peptide Synthesis, Protecting Group Strategies, Introduction of Boronic Acids and Post-Cleavage Manipulation of Peptides.

The following chapter describes the synthesis of the Dde protecting group and the subsequent Dde-protected *N*-α-Fmoc-Lysine-OH, and methods for incorporating phenylboronic acid onto peptidyl-resin compounds. A colorimetric assay for determining the presence of on-resin boronic acid moieties is also described. The chapter concludes with a description of peptide synthesis strategies which would afford short peptide sequences capable of binding to the antibiotic vancomycin. These sequences are designed to act as control sequences in subsequent library studies.

3.1 General synthesis of Fmoc peptides

The construction of peptides on a solid-support has numerous advantages over the equivalent solution synthesis. Separation of the intermediate peptides from excess reagents can be accomplished through simple filtration and washing processes without the need for complex purification techniques. Such treatment greatly reduces the time and effort required to synthesise a peptide sequence. The use of excess reagents may be employed to drive reactions to completion. Losses of a valuable product are minimised as the peptide is attached at all times to the solid support. Handling is also greatly improved.

Since Fmoc-protected amino acids are readily available and the coupling/deprotection procedures employing these building blocks are very well established, Fmoc-based chemistry has become the standard manner by which peptides are constructed.

3.1.1 Pre-reaction swelling

To enable reactions to occur throughout the entire solid support matrix it is vital that the solid support is pre-swollen. In all the examples described below, each resin sample was weighed into a glass column containing a glass sinter (porosity 4) and swollen in DMF for one hour prior to its initial use.

3.1.2 Coupling step

Aminium/phosphonium activation methods were used as the standard method of *in situ* carboxyl activation. PyBOP, HBTU and TBTU were all used at points during the research, as techniques and quantities were honed and perfected to suit individual needs. The reactivities of analogous aminium and phosphonium derivatives are essentially equivalent[51]. PyBOP was favoured during early peptide synthesis as it had been widely and successfully used within the research group, however the high cost of this reagent led to a gradual shift towards it being replaced by HBTU. A period of secondment to the Reaxa laboratories saw the use of TBTU as the preferred activation agent. On returning to the University laboratory TBTU was adopted as the coupling agent of choice to enable synchronisation with our collaborators.

Coupling methods incorporating PyBOP utilised equimolar amounts of coupling agent and each amino acid, where each component was used in a four fold excess relative to the resin. Six molar equivalents of DIPEA (relative to the resin) were also used and the coupling mixture was dissolved in the minimum amount of DMF. HBTU reactions in which PyBOP was replaced with HBTU utilised the same reagent ratios. Couplings following the TBTU methodology incorporated different ratios of TBTU (2.35 eq.), amino acid (2.5 eq.) and DIPEA (3.0 eq.) with respect to the resin. Again the minimum amount of DMF was used to solubilise the coupling system. These reagent ratios were deemed to be 'standard couplings' and used as such throughout unless otherwise stated.

The coupling solutions were pre-mixed and added to the vessel containing the resin. These reaction mixtures were agitated gently at room temperature. Coupling times were minimised and deemed to have reached full completion within 20 mins. After this time, a Kaiser colorimetric assay was performed on a small sample of beads to determine the successful coupling of the Fmoc-amino acid. Upon confirmation, the reaction solution was drained from the resin which was then washed with DMF (10 aliquots). Propagation of the chain continued by i) removal of the *N*-Fmoc protecting group with 20 % v/v piperidine in DMF (2 washes, 3 & 7 mins. respectively) and ii) further coupling. After the final coupling and deprotection steps, the deprotection solution, containing any remaining dibenzofulvene adduct, was drained and the resultant resin washed with DMF (10 x 30 ml). At each stage of the synthesis qualitative removal of the Fmoc group was confirmed with a positive Kaiser test for free primary amines.

After completion of the synthesis, the peptide could be cleaved or prepared for the coupling of any ensuing amino acid.

3.1.3 Storage

Should a synthetic procedure require more than one day to complete, the resin was deemed suitable for overnight storage at room temperature after the coupling stage or after the removal of the Fmoc protecting group. After the prescribed washes with DMF, further washes with DCM (10 aliquots) and MeOH (5 aliquots) were performed. The collapsed resin that resulted from this treatment was covered and allowed to air-dry overnight. Overnight storage in this manner necessitated the resin to be swollen for one hour in DMF prior to use in a manner analogous to the initial swelling process.

3.1.4 Cleavage from the solid support resin

If a cleaved peptide sequence was desired, the sequence was cleaved from the resin via acidolysis. The peptidyl resin was incubated with a pre-mixed solution of

TFA/EDT/TIPS (95/2.5/2.5, 10.0 ml) over 90 mins[51]. After this time the spent resin was removed by filtration and the filtrate concentrated under reduced pressure to a greatly reduced volume of <10 % the original volume. The crude peptidic cleavage products were precipitated by addition of diethyl ether or a mixture of ether and hexane. The precipitate was collected either through centrifugation or filtration through a DVPP membrane filter cloth, and allowed to air dry for one hour before being shell frozen in water. Solvents were removed by lyophilisation to yield a fluffy, drawn-out peptide.

3.2 The Dde protecting group

3.2.1 2-Acetyldimedone (Dde-OH) 76

The Dde-OH group is a quasi-orthogonal protecting group which may be removed selectively by treatment with 2 % hydrazine in DMF[60] or hydroxylamine[89]. These reagents do not remove more conventional protecting groups such as BOC and other acid labile groups. The inclusion of Dde in the library synthesis would allow for the incorporation, at a specific point of attachment, of a boronic acid unit onto the side chain of the peptide sequence, while maintaining the full protection of other side groups. Although commercially available Dde-protected amino acids exist, they are expensive and thus an attempt was made to generate these materials in-house.

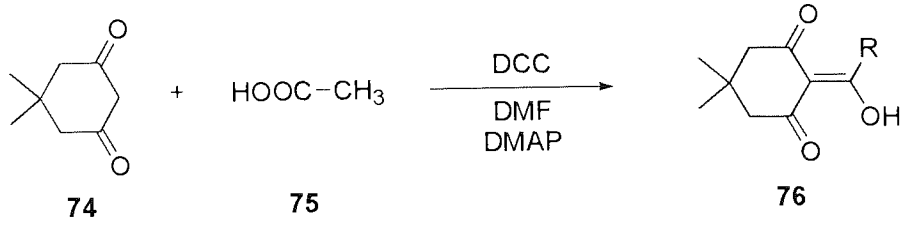

74 75 76

Reaction Scheme 18: DCC coupling of dimedone 74 and acetic acid 75 to form of the Dde protecting group 76.

A DMAP catalysed, *N,N'*-Dicyclohexylcarbodiimide (DCC) mediated coupling reaction between dimedone **74** and acetic acid **75**[90] resulted in the formation of Dde-OH **76** (Mechanism 8).

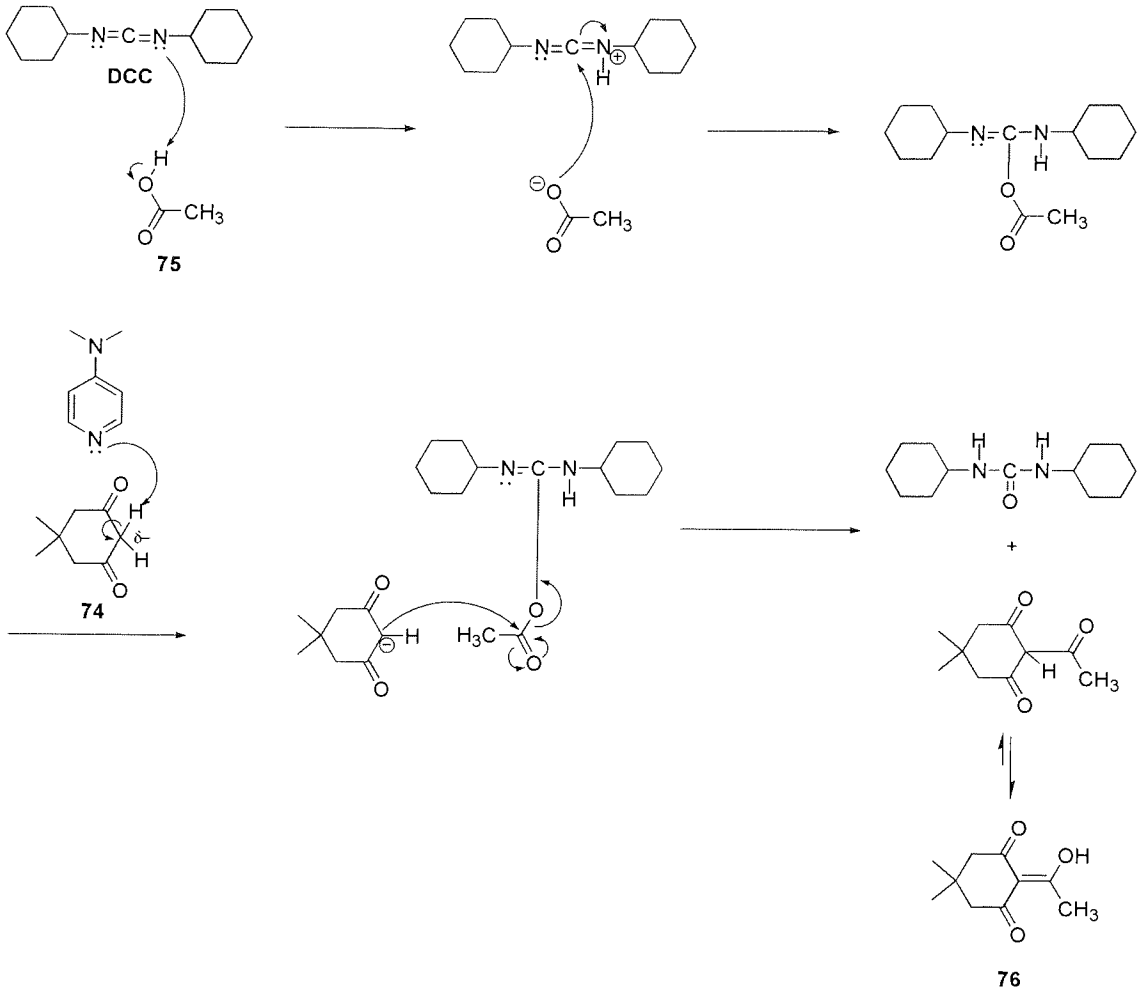

Mechanism 8: Synthesis of the Dde-OH protecting group 76 via DCC coupling of dimedone 74 and acetic acid 75.

As the mechanism shows, this reaction requires a 1:1 ratio of carboxylic acid to DCC, therefore the reaction can be followed by the cessation of precipitation of the urea by-product. After aqueous work up, the product was extracted into saturated sodium hydrogen carbonate solution and thus separated from any excess dimedone. Neutralisation allowed for re-extraction into DCM, after which the solvent was removed to yield the crude product as a thick yellow oil with a yield of 60 %. TLC

analysis indicated contamination with DMAP, which was subsequently removed by column chromatography (100 % DCM) to afford Dde-OH **76** in a yield of 29 %.

Interestingly, within this particular molecule the enol tautomer is more stable than the keto tautomer due to the enhanced stability afforded by intramolecular hydrogen bonding between the hydroxyl group of the enol and the *cis*-ketone group on the ring structure.

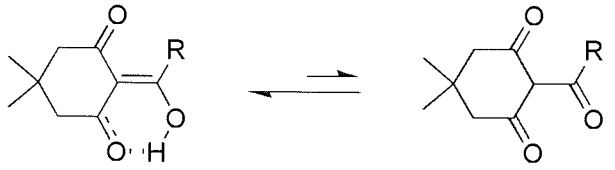

Figure 23: Equilibrium bias of Dde-OH 76 towards the enol tautomer due to intramolecular stabilisation.

All spectroscopic analysis of the product **76** was fully consistent with the structure of Dde-OH. HRMS provided excellent correlation with the target mass. The infra red spectrum showed a complicated carbonyl region. The β-diketone (carbons 4 and 4', Figure 24) in the enolic form give rise to a strong signal at 1560 cm^{-1}. The ketone *trans* to the hydroxyl group gives a strong signal at 1668 cm^{-1}, at a slightly lower frequency than a usual ketone due to the unsaturated, conjugated nature of the molecule. Strong signals at 1444 and 1370 cm^{-1} are symmetric and antisymmetric CH_3 deformations respectively. The ^1H NMR of **76,** (Spectra 1) is consistent with the desired product, and shows agreement with previously obtained NMR data[90].

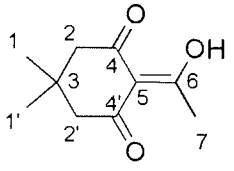

Figure 24: Numerically labelled structure of Dde-OH 76

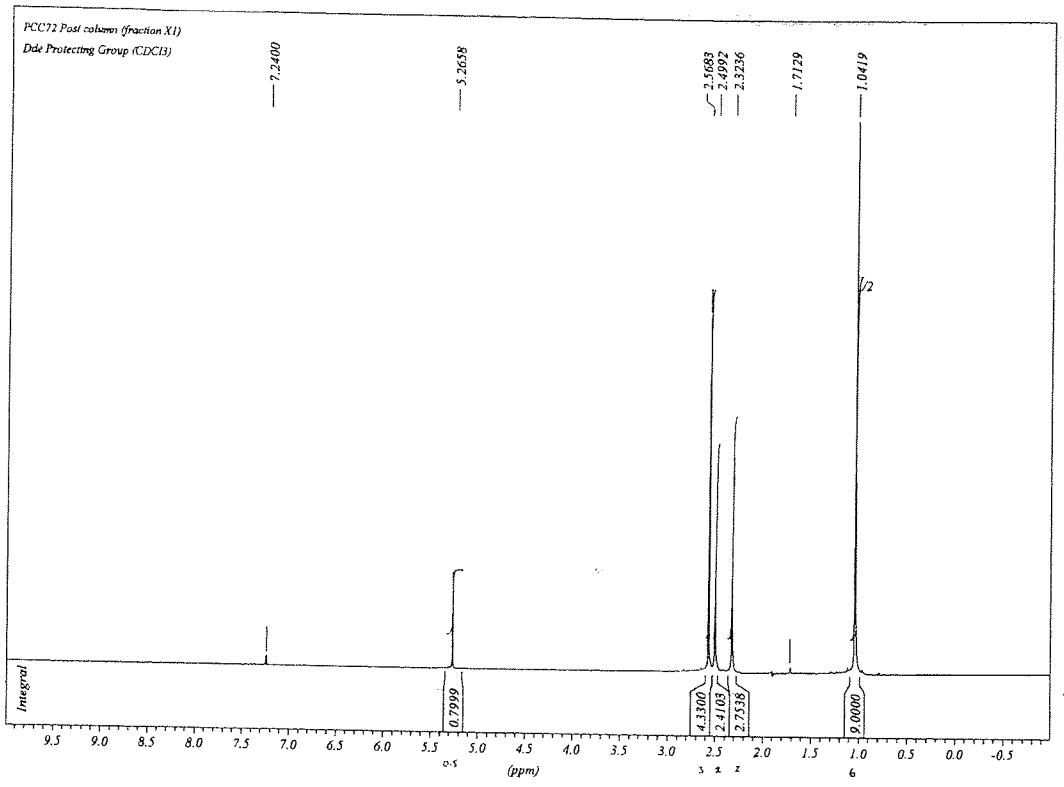

Spectra 1: ^{1}H NMR of Dde-OH 76

The singlet at δ 1.04 ppm corresponds to the two methyl groups **H-1** and **H-1'**. The third methyl group **H-7** is shifted downfield due to its proximity to the enol group and is responsible for the singlet at δ 2.57 ppm. As expected, the integral of this peak is half of that obtained for the peak at δ 1.04 ppm. **H-2** and **H-2'** give rise to peaks at δ 2.32 ppm and 2.50 ppm, although there is no method of identifying which protons correspond to which peak. The signal at δ 5.27 ppm is a product of the equilibrium between the enol and ketone forms. The integral value of 0.5 protons indicates a 50:50 split between the two tautomeric forms of the Dde product. In the β-diketone the proton from the hydroxyl group moves to position **H-5** giving rise to a new CH signal not present when **C-5** has a quaternary nature within the enol form. The signal is a long way upfield of standard aliphatic protons due to its positioning between the 3 electron withdrawing ketones **C-4 & 4'** and **C-6**.

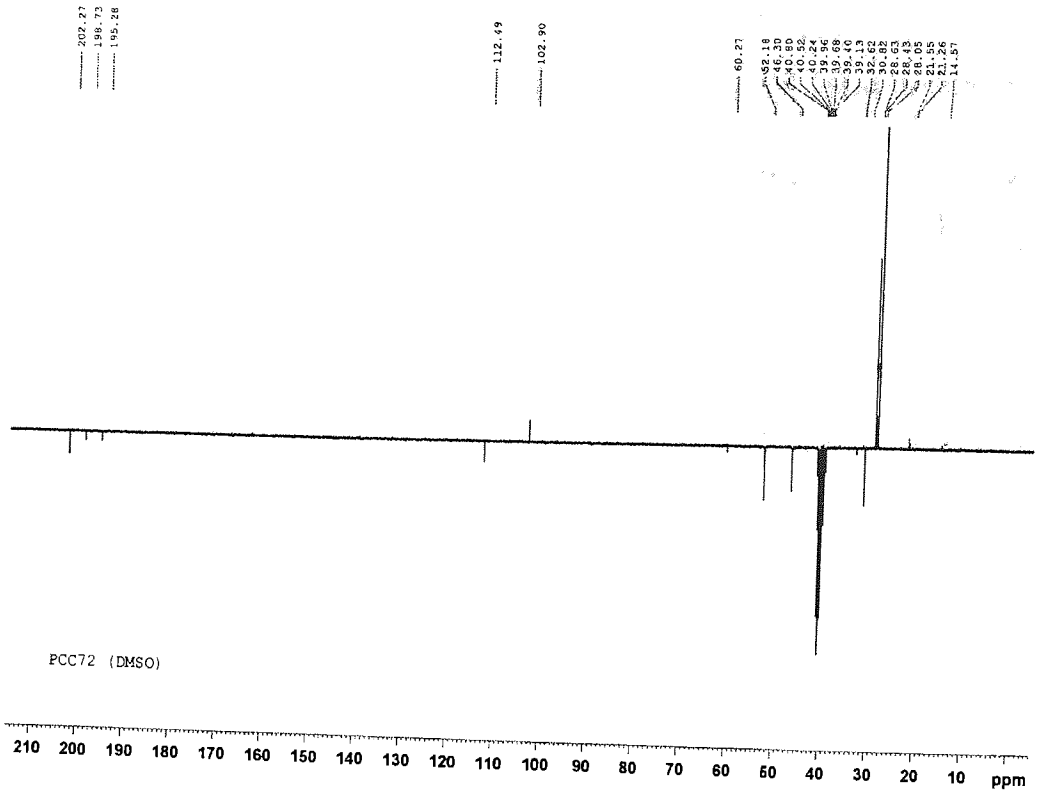

Spectra 2: ^{13}C NMR of Dde-OH 76

Analysis of the ^{13}C NMR spectra (Spectra 2) revealed 9 signals. **C-1 & 1'** appear as overlapping signals at δ 28.05 ppm. **C-3**, a quaternary carbon, appears on the $-y$ axis within PENDANT at δ 30.82 ppm. In a similar fashion to the ^{1}H NMR, the signals for **C-2 & 2'** occur at slightly different ppm shifts (δ 46.8 ppm & 60.27 ppm) but it is not possible to definitively assign them. This is also true of **C-4 & 4'** which give rise to signals at δ195.3 ppm & 198.7 ppm. **C-6** is present at δ 202.3 ppm. The success of the reaction is confirmed by the signal of **C-5** at δ 112.5 ppm, showing the extra shift upfield caused by the electron withdrawing enol in addition to the two α-ketones. (Dimedone has a shift of ~ δ 102 ppm for **C-5**[91]). Tautomerism to the β-diketone accounts for the second signal for **C-5** at δ 102.9 ppm. The CH signal moves downfield with the removal of the electron-withdrawing enol, and changes to the $+y$ axis on the PENDANT scan.

3.2.2 N^{α}-Fmoc-Lysine ε-1-(4,4-dimethyl-2,6-dioxo-cyclohexylidene)-ethylamine (Fmoc-Lys(Dde)-OH 78

Fmoc-Lys-OH **77** reacts readily with Dde-OH **76** to afford the N^{ε}-1-(4,4-dimethyl-2,6-dioxo-cyclohexylidene)-ethyl derivative **78**, a compound with orthogonal protection which can be incorporated into a library using standard Fmoc synthesis.

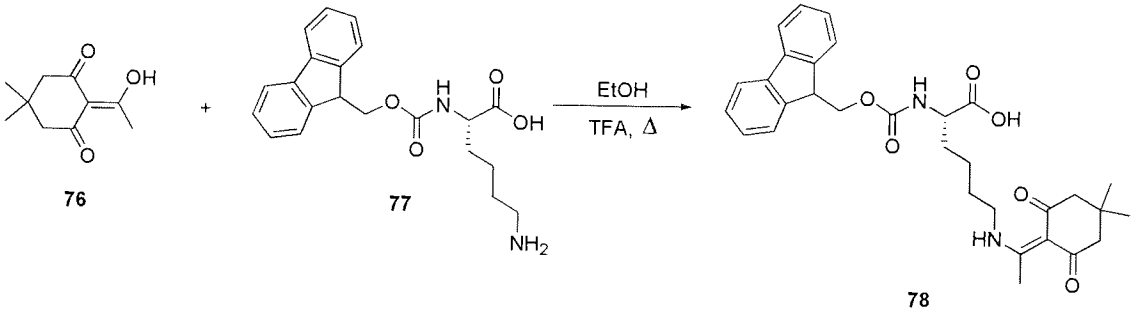

Reaction Scheme 19: Protection of the N^{ε} side chain of Fmoc-Lys-OH 77 with Dde-OH 76

Dde-OH **76** was dissolved in ethanol and added to half an equivalent of Fmoc-Lys-OH **77**. The mixture was refluxed with a catalytic amount of TFA to promote nucleophilic attack by the Lysine onto the double bond of Dde (Mechanism 9). Evaporation of the mixture gave the crude product which was reconstituted in ethyl acetate. Unreacted Fmoc-Lys-OH **77** and aqueous soluble impurities were removed by extraction with an aqueous wash. The crude mix was then triturated in hexane, dissolving any unreacted Dde-OH **76** in the mixture. The remaining mixture was then dissolved in ethyl acetate and precipitated from a large volume of hexane to remove any last trace of Dde-OH **76**. Collection of this precipitate should have afforded the pure title compound.

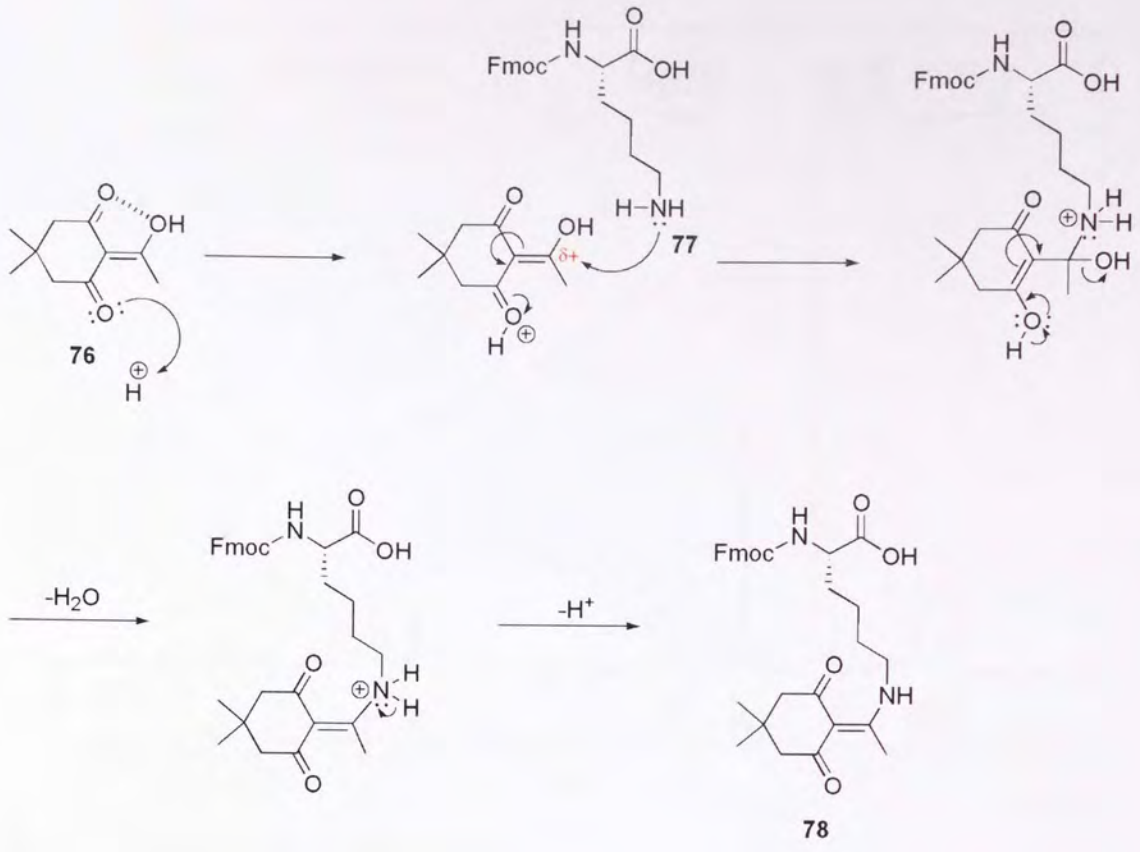

Mechanism 9: Protection of the N^{ε} side chain of N^{α}-Fmoc-Lys-OH 77 with Dde-OH 76

The compound was synthesised in an extremely poor yield of 1.3 %. LRMS & HRMS confirmed the presence of a compound with the correct mass, and FTIR was consistent with a compound possessing the correct functional groups. However analysis by ^{1}H NMR (Spectra 3) was less convincing, especially when compared with a spectrum obtained from a commercial sample.

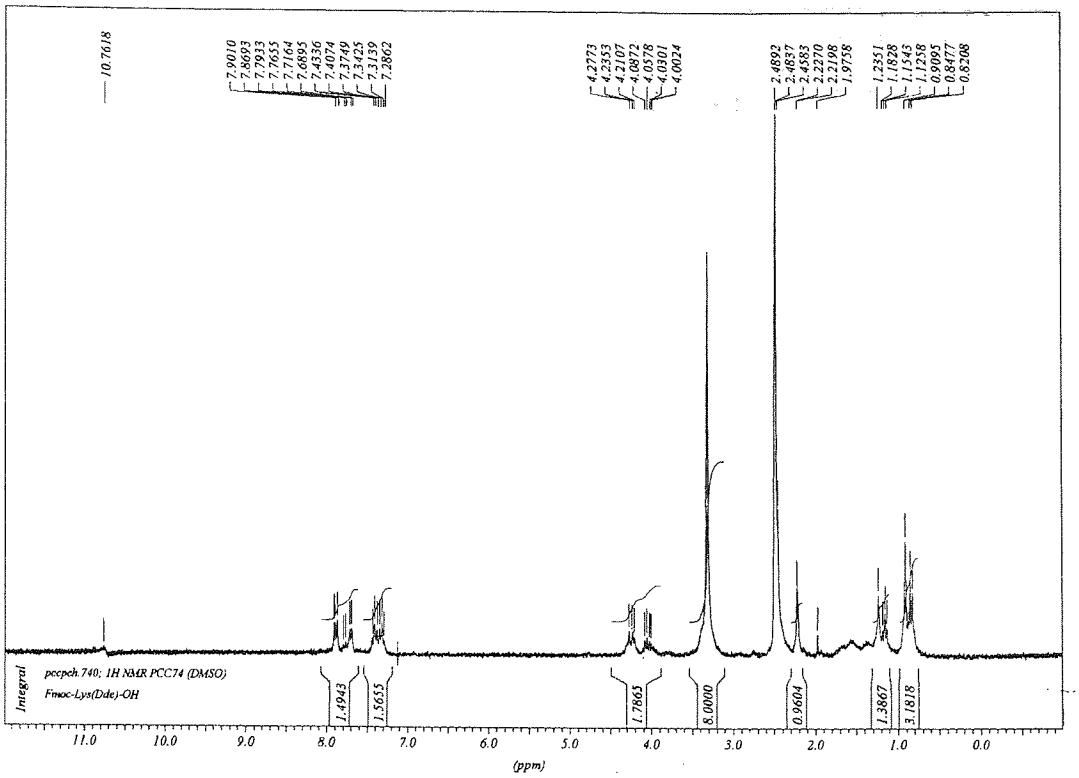

Spectra 3: ^{1}NMR of Fmoc-Lys(Dde)-OH 78

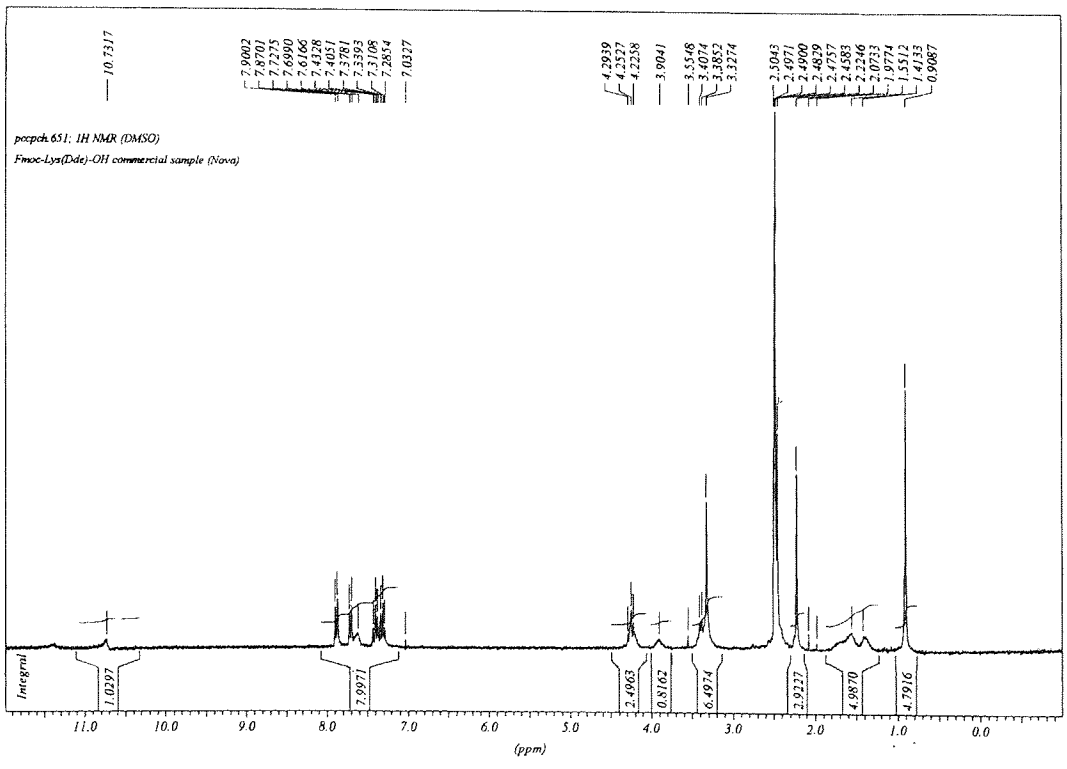

Spectra 4: ^{1}NMR of Fmoc-Lys(Dde)-OH (commercial sample)

Broadly speaking, the spectra look very similar but there are some important distinctions. Within the commercial sample (Spectra 4), the two methyl groups attached to C-4 of the Dde ring give rise to a 6H singlet, while the synthesised compound has a singlet and a doublet in the same region (δ ~ 1.0 ppm). The synthesised material also has too large a signal associated with the alkyl side chain of the lysine (δ ~ 3.0 ppm), whereby there is a 2:1 ratio of alkyl protons to the aromatic protons of the Fmoc group (δ ~ 7 ppm), rather than the 1:1 ratio it should exhibit. ^{13}C NMR did not contain any of the quaternary carbon signals seen in Dde-OH **76**, and not enough signals throughout the spectrum. The synthesis was repeated twice more, the second attempt giving similar results, while the third failed to produce any product at all. The quality of the starting materials was called into question, however the third attempt utilised freshly opened ethanol and TFA, while analysis of the Fmoc-Lys-OH **77** confirmed it was pure. Extremely poor yields, coupled with a lack of definitive proof of success led to the abandonment of the synthesis. For the subsequent combinatorial library synthesis it was decided to utilise a commercial sample of Fmoc-Lys(Dde)-OH.

3.3 Introduction of phenylboronic acid

Boronic acids have been used widely in artificial receptors for carbohydrates with great success[17,27,24,92,93]. Additionally they have been shown to have important biological affects[94] and have been implicated in enabling efficient drug delivery through organic membranes[95,96]. By generating an array of library of compounds, all of which contained a boronic acid moiety, it was hoped that some of the library compounds would enable specific glycosylated proteins (such as vancomycin) to be both recognised and bound selectively.

Throughout this study 4-carboxyphenylboronic acid was utilised as the boronic acid-containing building block. This reagent was selected as it was deemed a good candidate for boronic acid incorporation via facile amide bond forming coupling reactions to amine bearing library compounds. Accordingly, all incorporations of boronic acid were conducted using this particular reagent. For ease, any future

experimental reference to the 'boronic acid' is taken to mean the amide coupled phenylboronic acid moiety, and these terms will be used interchangeably in the following discussion.

Fmoc-Glycine-OH was coupled to AMPS **46** using the standard PyBOP coupling procedure. Subsequent deprotection (20 % piperidine in DMF) afforded the deprotected product **79**. This product served as the test resin to enable the optimum method of boronic acid attachment to be determined. Glycine was incorporated in this test resin to act as a small spacer unit. It was thought that the extra distance between the amine group and the polymer matrix may help to increase the yield of subsequent coupling reactions.

Two methods of synthesis were explored, i) conversion of 4-carboxyphenylboronic acid into the corresponding acyl chloride with oxalyl chloride, followed by *in-situ* coupling to the amine, and ii) a standard amino acid coupling reaction. Both methods would result in the formation of the amide bond between the two reactive species.

3.3.1 Acyl Chloride intermediate 81

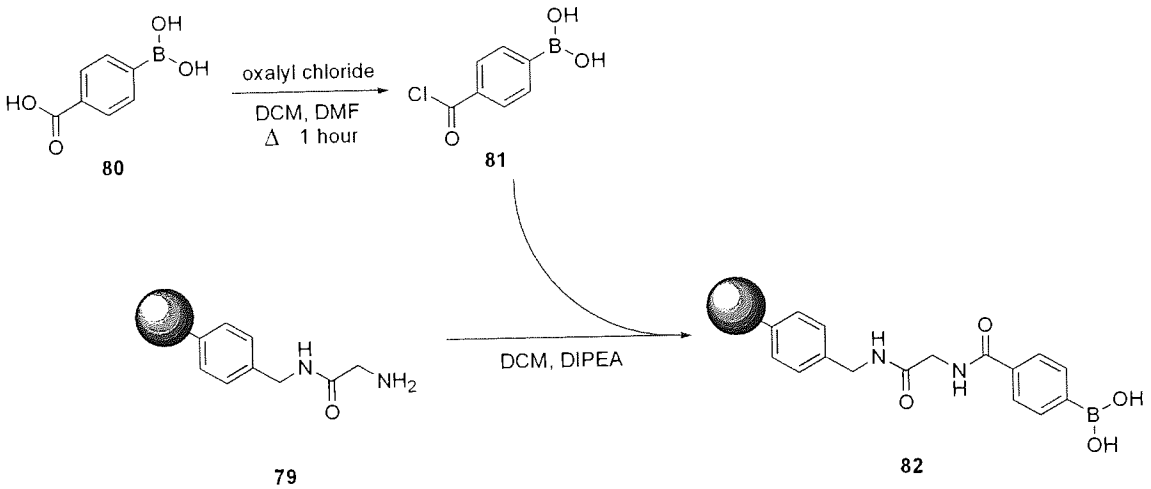

Reaction Scheme 20: 21 reacted in situ with the acyl chloride intermediate 81 of the 4-carboxyphenylboronic acid.

4-Carboxyphenylboronic acid **80** was reacted with oxalyl chloride in the presence of a catalytic amount of DMF under anhydrous conditions to produce the acyl chloride intermediate **81**.

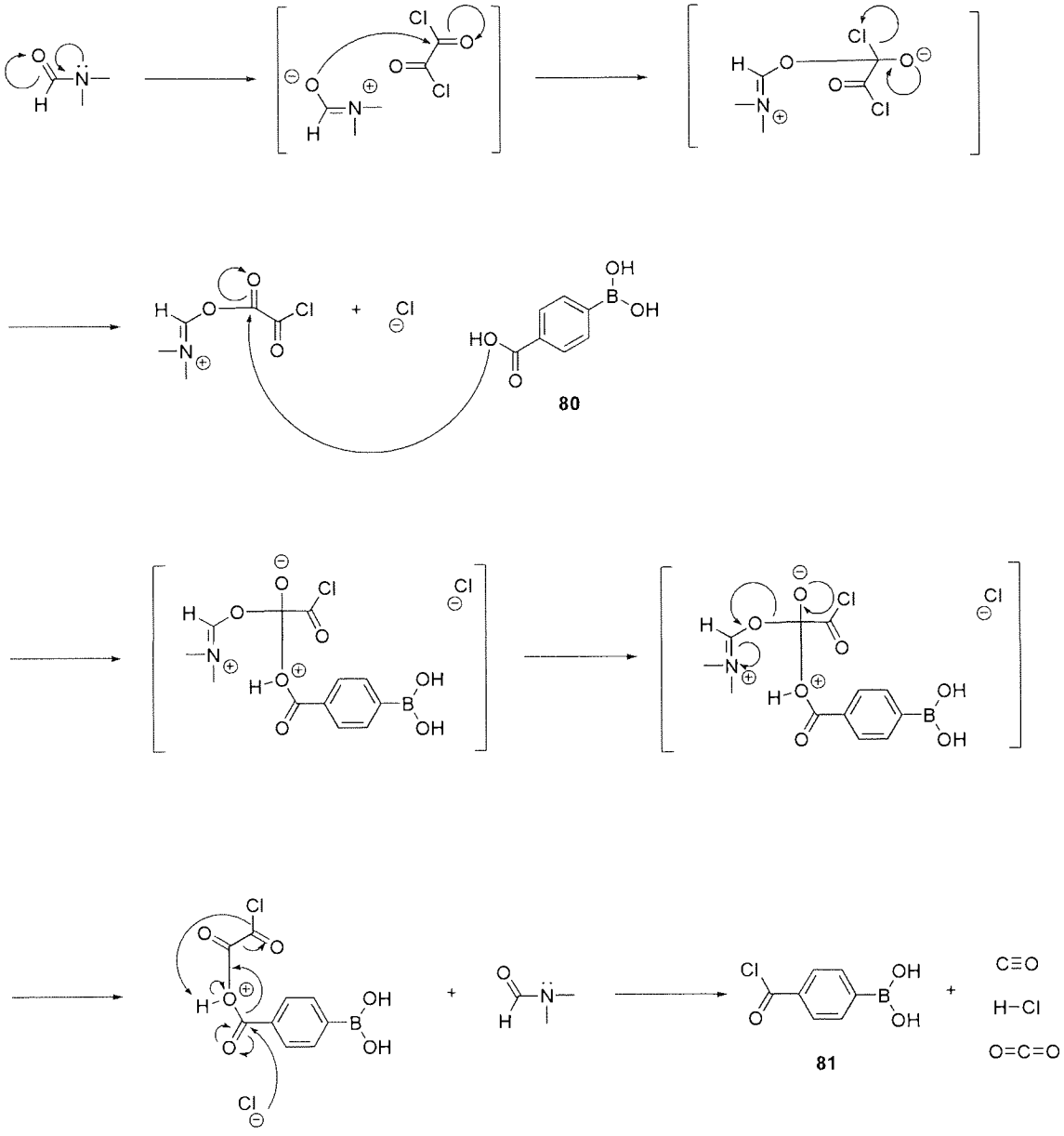

Mechanism 10: DMF catalysed chlorination of 4-carboxyphenylboronic acid 80 utilizing oxalyl chloride, to produce 81

Resuspension of the acyl chloride intermediate **81** in DCM allowed for high swelling to take place of resin compound **79**. Subsequent nucleophilic acyl substitution

proceeded smoothly with displacement of the chlorine by the incoming amine of **79** yielding the desired boronic acid **82** and hydrogen chloride. After the reaction the beads were filtered and washed with successive aliquots of DCM, THF, water and methanol and dried to constant weight to yield an orange resin **82**.

The scale of the reaction was such that any mass change was immeasurable, and thus the reaction yield incalculable. Infra red analysis of the compound was inconclusive, however the orange colouration of the beads, which could not be removed with washing, was deemed to indicate that the reaction had failed to proceed as planned. Due to the relative complexity of the reaction and the fact that it was effectively a two-step synthesis, the investigation of this method was halted while the success of the coupling using the PyBOP was assessed.

3.3.2 PyBOP Coupling

One of the issues highlighted by the oxalyl chloride method was the lack of definitive proof as to the success of the coupling procedure. Analysis by IR spectroscopy proved inconclusive as it was difficult to assign the B-O stretch (expected at 1380-1310 cm^{-1}) due to its relative weakness compared to the stretches associated with the polymer matrix. An amide signal was present in the spectrum (1654 cm^{-1}), although this can be attributed to the amide of the coupled glycine, just as it can to the linkage to the phenylboronic acid. It was therefore decided to abandon this method of coupling 4-carboxyphenylboronic acid to **79** and instead construct the peptidic adduct on a cleavable resin, enabling post cleavage analysis, in particular mass spectroscopy.

Rink Amide MBHA Resin was used as the polymer support for the construction of the short peptide sequence H_2N-Lys(Boc)-Ala-Gly-Rink Amide MBHA **83**. When cleaved, this short peptide sequence would provide a mass sufficiently above the limit of detection of the mass spectrometer.

Fmoc-Glycine-OH, Fmoc-Ala-OH and Fmoc-Lys(Boc)-OH were sequentially coupled to the deprotected Rink Amide MBHA resin **83** using the standard Fmoc

approach discussed previously (**section 3.1**) to afford **85**. 4-Carboxyphenylboronic acid (4 equivalents) was then dissolved in DMF and added to peptide-bearing resin **85** in the presence of PyBOP (4 eq.) and DIPEA (6 eq.) to yield the target compound **86**. Subsequent cleavage of the boronic acid derived peptide utilising TFA/TIPS/H_2O (95:2.5:2.5) followed by precipitation from diethyl ether afforded the crude peptidic product **87** as a colourless fluffy solid in a 98.4 % yield.

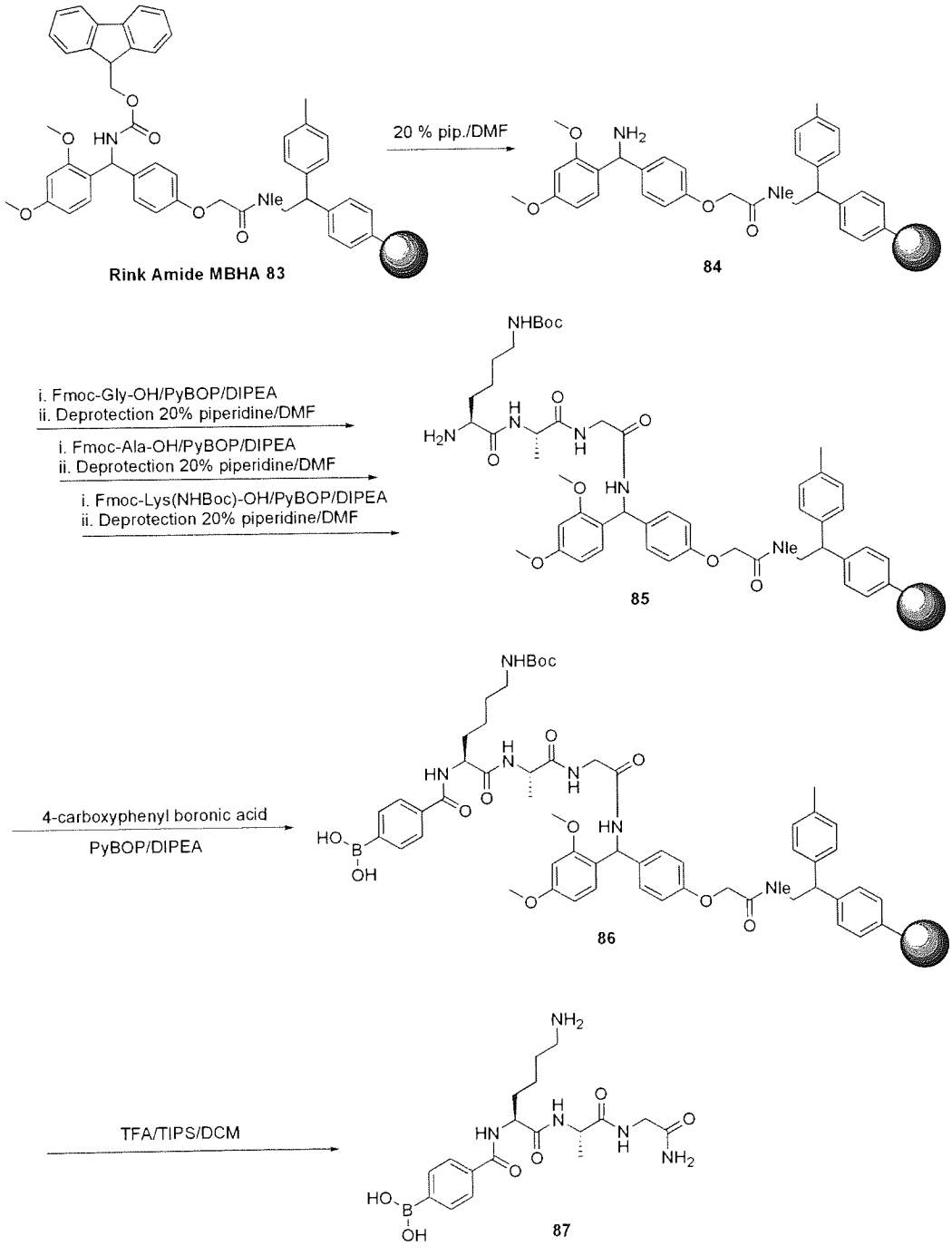

Reaction Scheme 21: Synthesis of 86 followed by TFA mediated cleavage to yield peptide 87

Analysis of the cleaved material by HPLC showed the presence of 2 compounds, with yields of 98.4 % and 1.5 %. The two HPLC fractions were collected and submitted for analysis by mass spectroscopy, which gave the mass of the major fraction as 420 (ES-; $[M-H]^-$), 423 (ES+; $[M+H]^+$) and 445 (ES+; $[M+Na]^+$). This corresponds extremely well with the target mass of 421 for boronic acid containing peptide **87**. The mass of the adduct, had it not contained the boronic acid unit, would have been much lower at 272.

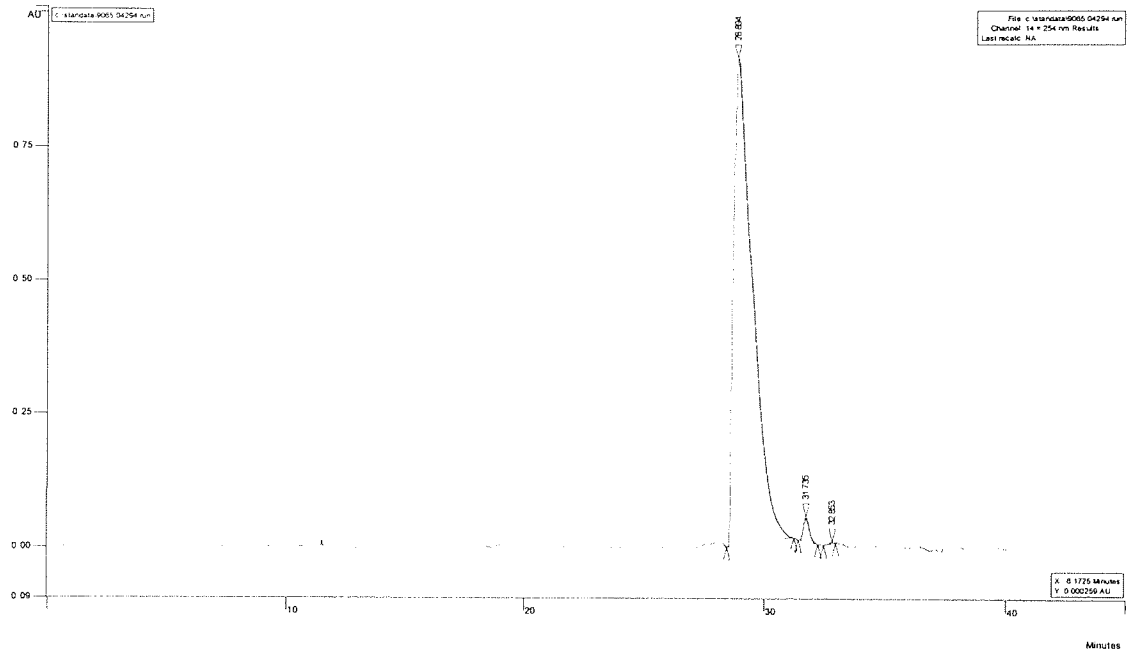

Figure 25: HPLC analysis of peptide 87

The combined HPLC/MS analysis showed that the incorporation of boronic acid could be achieved through an easy one-step route with near quantitative results, making this the preferred method of incorporating boronic acid units into peptidic systems.

3.3.3 Quadramide-phenylboronic acid 88

4-Carboxyphenylboronic acid was coupled to Quadramine resin **62** to provide a boronic acid-functionalised polymeric resin **88**. This simple model would enable the stability of resin-bound boronic acid to be tested and binding studies to be carried out with model carbohydrates without the effects of any amino acid interactions.

4-Carboxyphenylboronic acid was coupled to Quadramine resin **62** utilising standard TBTU methodology to yield Quadramide-phenylboronic acid **88** in a 96 % yield (on the basis of mass).

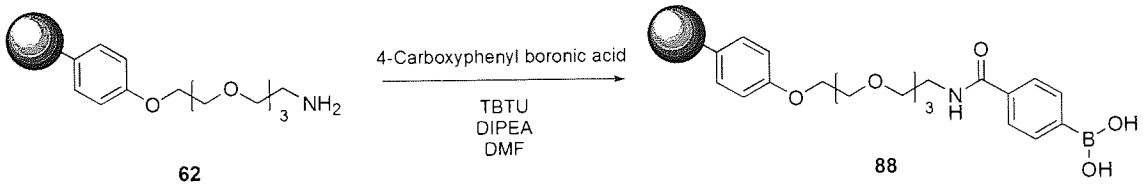

Reaction Scheme 22: Coupling of 4-Carboxyphenylboronic acid to Quadramine 62

Analysis by ATR-FTIR suggested the successful formation of the target product. A strong signal at 1661 cm^{-1} indicated the presence of a carbonyl group attributable to the secondary amide formed in the reaction. The B-O stretch at 1348 cm^{-1} is visible, but weaker than expected, and hydrogen bonding of the boronic acid units is evidenced by the medium-strength broad signal at 3356 cm^{-1}. The starting resin **62** did not possess any hydrogen bonding. All other signals are attributable to the base resin, with signals representing aromatic and aliphatic C-H stretches (3026 and 2919 cm^{-1} respectively), a benzene ring stretch at 1602 cm^{-1}, and C-O-C ether stretches at 1244 and 1107 cm^{-1}.

3.3.4 Stability of the boronic acid moiety

The stability of the boronic acid moiety to reagents and solvents commonly utilised in peptide synthesis was examined to determine whether or not the boronic acid

would 'survive' the library synthesis unmodified. The introduction of the boronic acid would occur at a point in the synthesis prior to the removal of the acid-cleavable protecting groups. Knowledge of its behaviour upon exposure to these materials would allow a strategy to be constructed whereby any adverse effects could be avoided.

A small quantity (3-5 mg) of resin **88** was exposed separately to TFA, piperidine, DBU, DMF, DCM, TIPS, DIPEA, TEA, acetic anhydride, methanol and a mix of TFA/DCM (50:50). Each of the 11 aliquots was incubated for 1.5 hours, the maximum time any peptide coupling/deprotection sequence is performed. After removal of the supernatant, the resin samples were dried and submitted for ATR-FTIR analysis for comparison with the starting Quadramide-phenylboronic acid **88**.

As expected, incubation with DMF, DCM, TIPS, DIPEA, TEA and methanol had no affect on the resin, with the IR spectra directly overlaying that of the starting resin.

Incubation with piperidine caused a dramatic change in the IR signal (Spectra 5). There is an increase in the relative intensity of the aliphatic CH_2 stretch at 2930 cm^{-1} verses the aromatic CH groups contained within the polymer matrix. This is corroborated by the increased intensity of the signal at 1451 cm^{-1} consistent with an aliphatic CH_2 scissors vibration. A strong signal at 3432 cm^{-1} is consistent with the presence of an N-H stretch from the piperidine. (The N-H stretch usually falls between 3500 and 3450 cm^{-1} however it falls at a lower frequency in saturated heterocyclics such as piperidine[77]). The same batch of resin was washed with copious amounts of DCM and subjected to a second FTIR scan. The second scan showed complete removal of all signals associated with the presence of piperidine, leaving the spectra (Spectra 6) identical to that of the starting resin **88**.

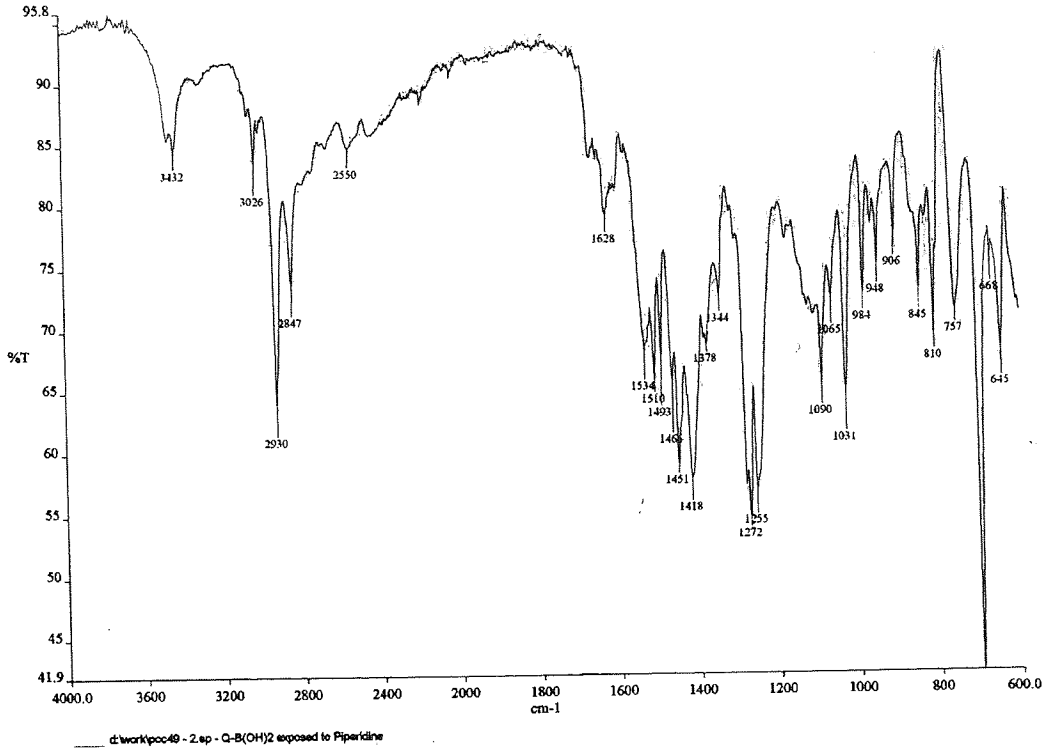

Spectra 5: ATR-FTIR analysis of Quadramide-phenylboronic acid 88 after incubation with piperidine

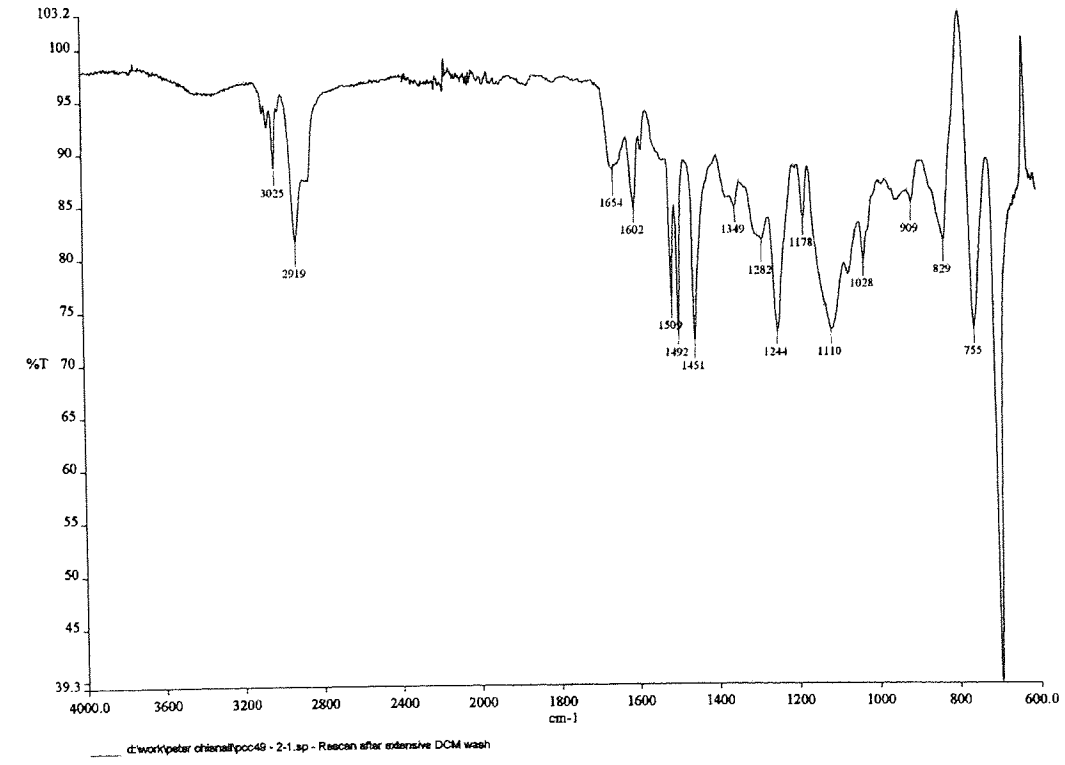

Spectra 6: ATR-FTIR analysis of Quadramide-phenylboronic acid 88 after incubation with piperidine and subsequent DCM wash

Incubation with DBU also caused a large change in the FTIR spectra of the resin (Spectra 7). The imine signal was observed as a very strong signal at 1620 cm^{-1}.

Again the batch of resin was washed with copious amounts of DCM and subjected to a second FTIR. In a similar fashion to piperidine, all traces of DBU were removed after washing the resin.

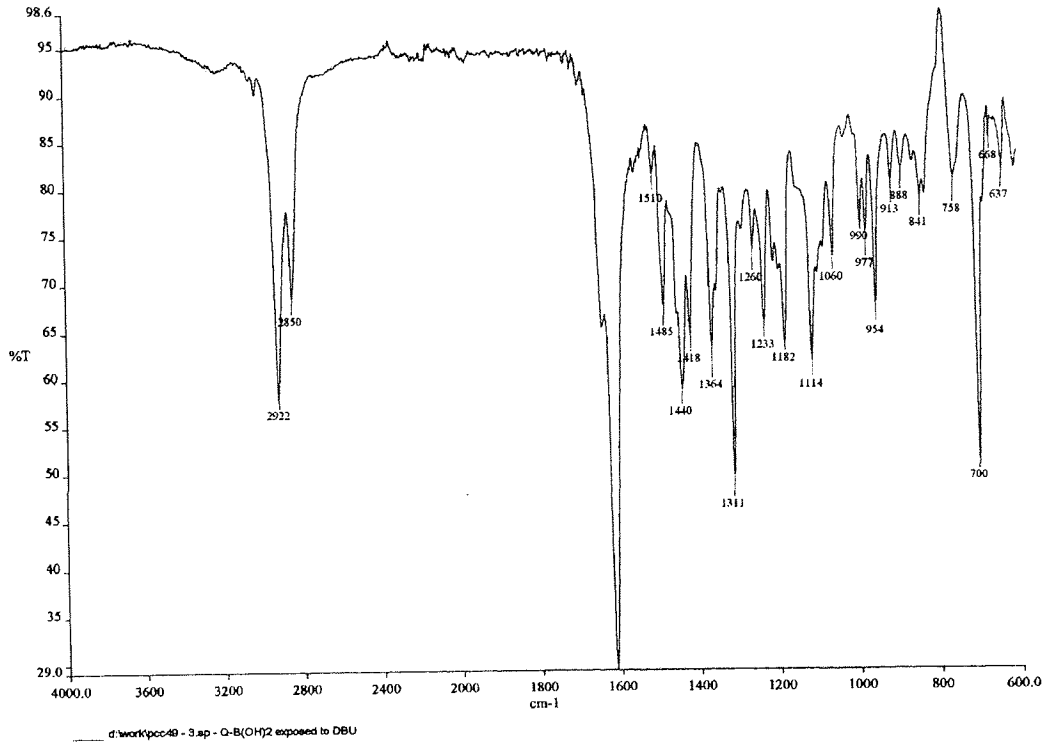

Spectra 7: ATR-FTIR analysis of Quadramide-phenylboronic acid 88 after incubation with DBU

The spectra of the resin which had undergone incubation with acetic anhydride (Spectra 8) had a number of differences from that of the base resin. Esterification of the boronic acid is the expected result of any reaction and this is supported by the strong carbonyl signal at 1752 cm^{-1}. The strong antisymmetric C-O-C of the PEG contained within the polymer backbone is also visible at 1180 cm^{-1}. Acetic acid would be the by-product of the esterification process. The presence of another strong signal at 1823 cm^{-1} could indicate the presence of a carbonyl group attached to an electronegative element, or the presence of residual acetic acid trapped within the

polymer matrix. Since acetic anhydride is only utilised in the capping procedure it would not be utilised after the inclusion of the boronic acid, and its use in the presence of phenylboronic acid is therefore avoidable.

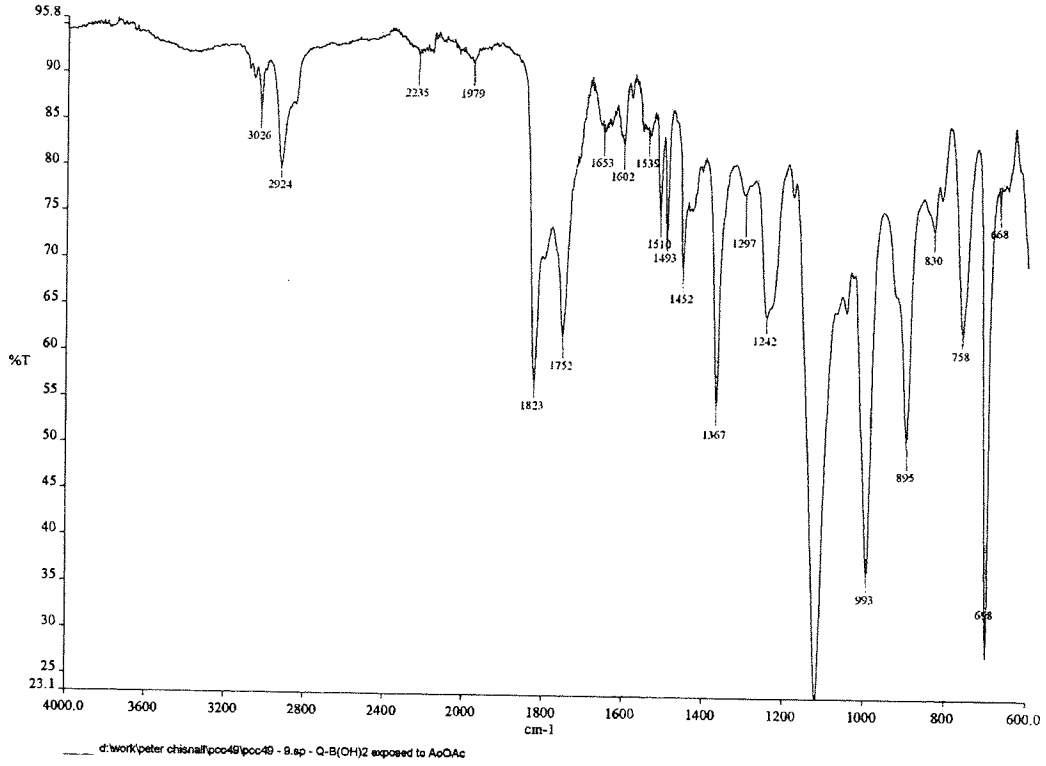

Spectra 8: ATR-FTIR analysis of Quadramide-phenylboronic acid 88 after incubation with acetic anhydride

It is hypothesised that incubation of the Quadramide-phenylboronic acid with 100 % TFA (Spectra 9) resulted in the formation of an trifluoromethyl ester link with the boron, similar to that discussed in the deprotection of Quadragel **59** (**section 2.1.4**). The signal corresponding to the C=O groups is at a high frequency (1781 cm^{-1}) which is typical of a halo ester due to the electronegativity of the halogen. The boronic acid is linked to the polymer via a secondary amide bond and this linkage is still evident at 1660 cm^{-1}. Treatment with 50 % TFA in DCM yielded the same result.

Spectra 9: ATR-FTIR analysis of Quadramide-phenylboronic acid 88 after incubation with 100 % TFA

Unsurprisingly, copious washing with DCM was ineffective at breaking the ester links. Accordingly, a process involving incubating with 5 % v/v TEA/DCM solution was initiated which resulted in the disappearance of the TFA associated peak. Although the trifluoromethyl ester was not produced during the synthesis of the boronic acid-peptide **87**, the observation of its presence in Spectra 9 caused concern. It was decided that the wash with TEA would be incorporated into any library construction to remove the possibility of trifluoroacetate formation interfering with subsequent library studies.

3.4 A Colorimetric assay for the identification of Boronic acid on solid support

Colorimetric assays have an important place within the fields of SPS/SPPS. They allow a rapid determination of the success of a reaction to be made and do not require expensive instrumentation. As the dyes have employed a degree of

selectivity, it is possible to show that the end group attached to the SPS resin has changed by incubating the resin with a dye both before and after the reaction step. Moreover, by exposing aliquots of the resin to a number of dyes, an absolute determination of end group is possible. The Kaiser Test[67,97] is a well documented example for following the progress of peptide couplings by showing the presence or lack thereof of an amine group.

A number of papers have previously reported the use of carminic acid in quantifying boron, boric acid and boronic acids in water[35] and biological fluids[36]. Sensitivity of detection was found to be as low as 0.4 ppm in water, was relatively unaffected by foreign ions and found to be reproducible over a range of boron concentrations.[35] It is noteworthy that to date, no literature source describes the carminic acid-based sensing of a boronic acid moiety on a solid support. In the current study it was hoped that a colorimetric assay, based upon carminic acid, could be developed which would allow for rapid, on-bead determination of the presence/absence of boronic acids.

3.4.1 Experimental

The colorimetric assay was performed on various derivatives of two types of SPPS resin to determine consistency. The first base resin was a Rink Amide MBHA Resin (0.78 mmol/g), while the second was Quadragel resin **59** (0.89mmol/g). Boronic acid-based derivatives of these two resins, **86** and **88**, have been described above.

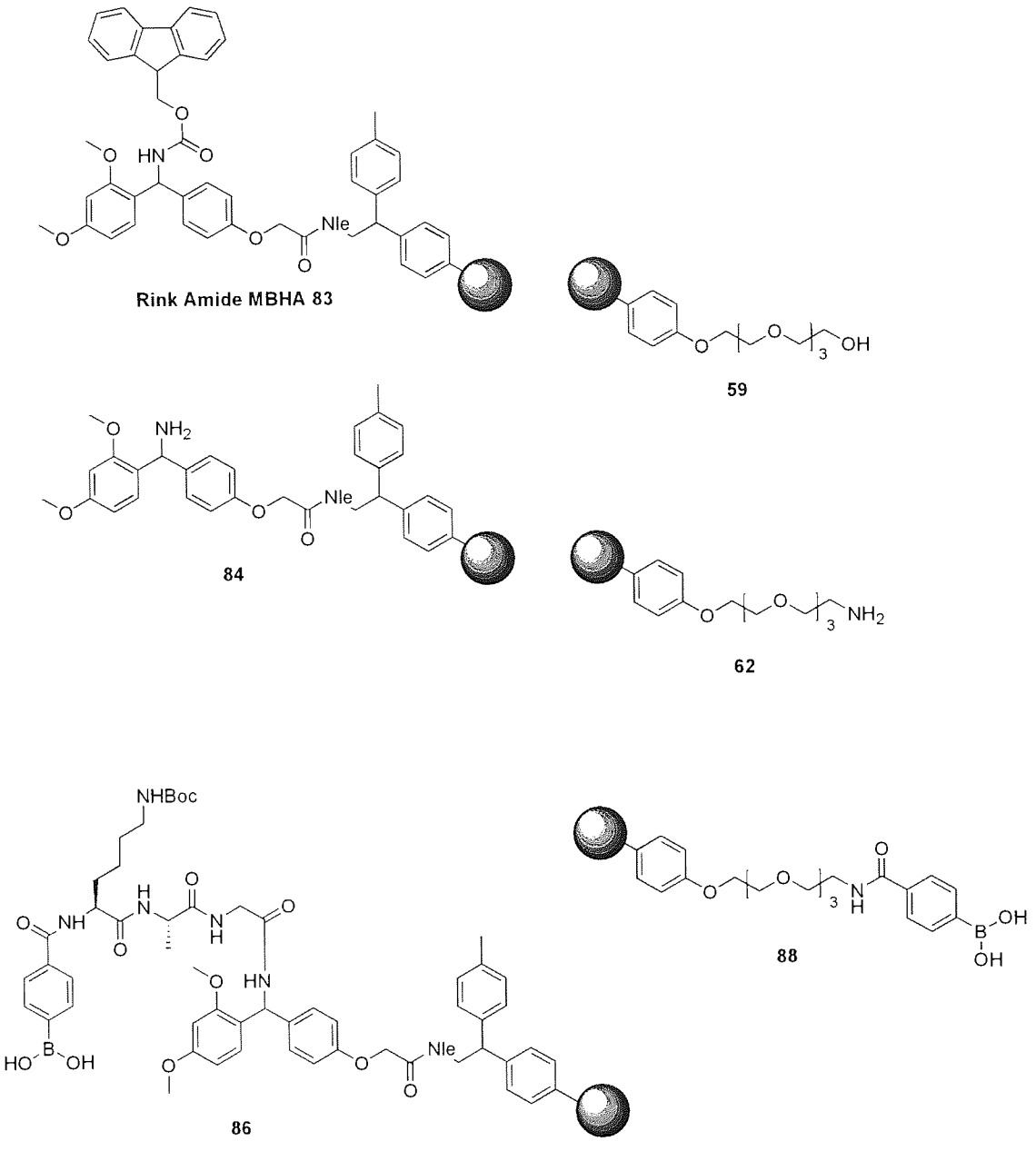

Figure 26: Compounds tested within the colorimetric assay.

3.4.2 Dye Compounds

2 drops of the dye solution (1 % w/v in DMF) followed by 2 drops of 10% v/v *N,N*-diisopropylethylamine (DIPEA) in DMF were added to each sample of polymer beads (~1-3 mg).

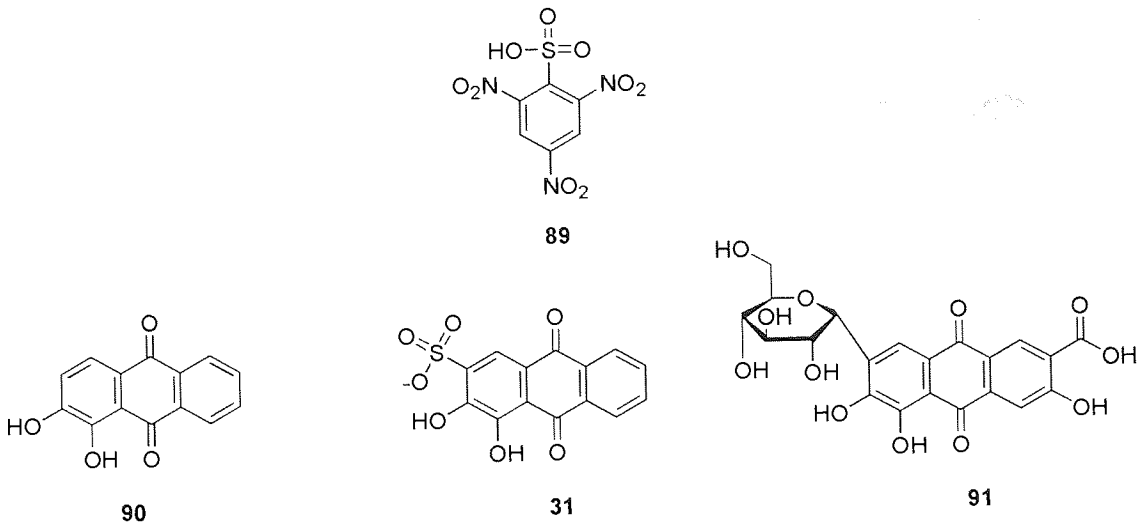

Figure 27: Dye compounds. TNBS 89 indicates the presence of primary amines[68]; Catechol based dyes: Alizarin 90; Alizarin Red Sulphate 31 (has been used to detect boronic acid[14]); Carminic acid 91 (used to detect Boron).

3.4.3 Colorimetric Results

A small amount (~1-3 mg) of Rink amide MBHA resin **83** along with derivatives **84** & **86** were swollen with 10 % DIPEA in DMF (20 µl) and incubated with each of the four dye compounds (20 µl, 1 % w/v in DMF). The resin samples were incubated for 3 minutes before being diluted to 1.5 ml with water. Successive removal of the supernatant and dilution with water was carried out until the supernatant ran colourless. The beads were allowed to dry and the colour of each was recorded. Quadragel **59** was included as a control sample to compare the specific geometry of the boronic acid moiety to disparate, mobile hydroxyl groups that have the potential to come together in space and pass close to the dye molecule.

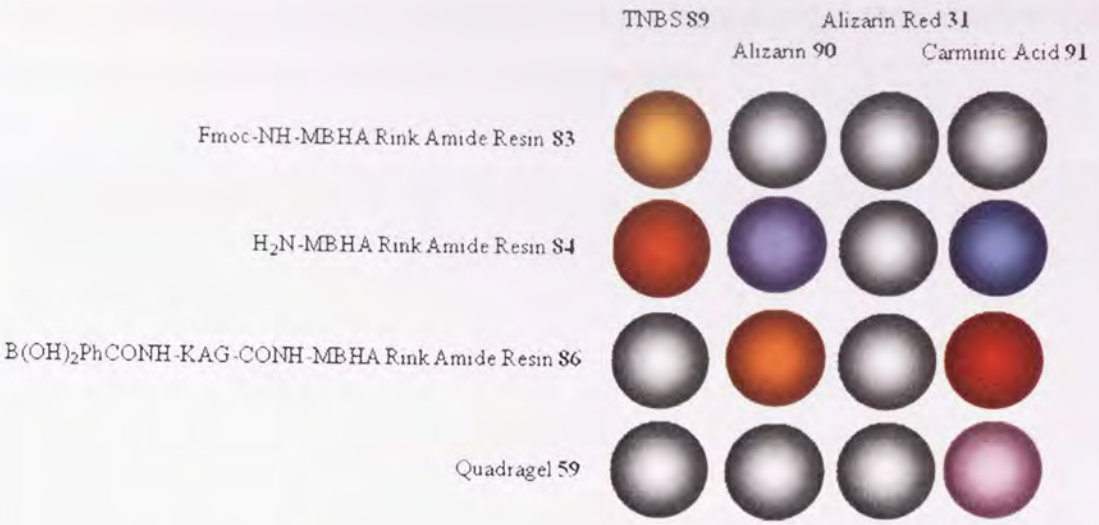

Figure 28: Colour matrix showing the approximate colouration (natural light) of the derivatives after incubation with each respective dye compound.

Alizarin red caused no colour change in any of the samples. TNBS **89** caused colouration of the amine bearing compound, although a slight colouration was also observed on the Fmoc-protected sample, indicating the possibility of a small number of unprotected sites. Alizarin **90** reacted with both the amine and boronic acid derivatives, producing a distinguishable colour change between the two. Carminic acid **91** showed the same distinct change of colour. Carminic acid did give the control Quadragel **59** a slight colouration, however the intensity was insignificant in comparison to the resin bearing boronic acid moieties. Indeed the Quadragel loading of 0.89 mmol/g exceeds that of the boronic acid derivative **86** which has a loading of approximately 0.77 mmol/g, indicating that the affinity of the carminic acid to Quadragel is negligible.

A second matrix was created, this time concentrating on derivatives of Quadragel **59**. Quadragel **59**, Quadramine **62** and Quadramide-phenylboronic acid **88** were swollen with 10 % DIPEA in DMF (20 µl) and incubated with the same four dye compounds (20 µl, 1 % w/v in DMF). In addition, approximately 1-2 mg of each derivative was mixed with the other derivatives (pre-incubation) in four separate pots. Each pot was then incubated with one of the dyes in the same manner as the 'uniform' samples. The purpose was to see if the presence of one type of compound would have an

overriding effect on the others, or whether each compound within the mixture would behave as they had done within the 'uniform' samples.

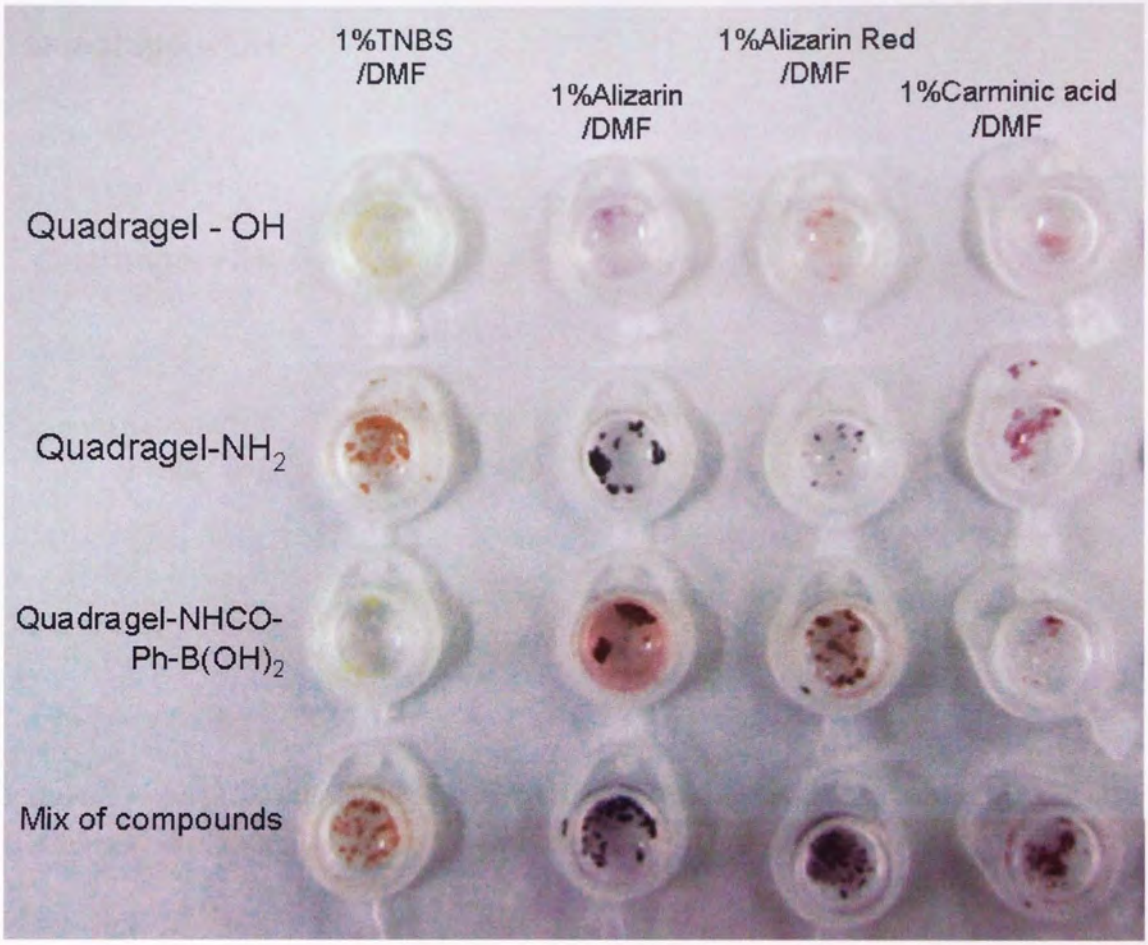

Picture 1: Colour matrix of Quadragel-based compounds incubated with a variety of dyes, viewed in natural light. Rows descending; Quadragel 59, Quadramine 62, Quadramide-phenylboronic acid 88, mix of the 3 derivatives. Photographs were taken with a Fuji FinePix F10 6.3M pixel camera. Photographs were taken without flash. Photographs taken under long wavelength UV (UV-B) conditions have an ISO 1600 rating.

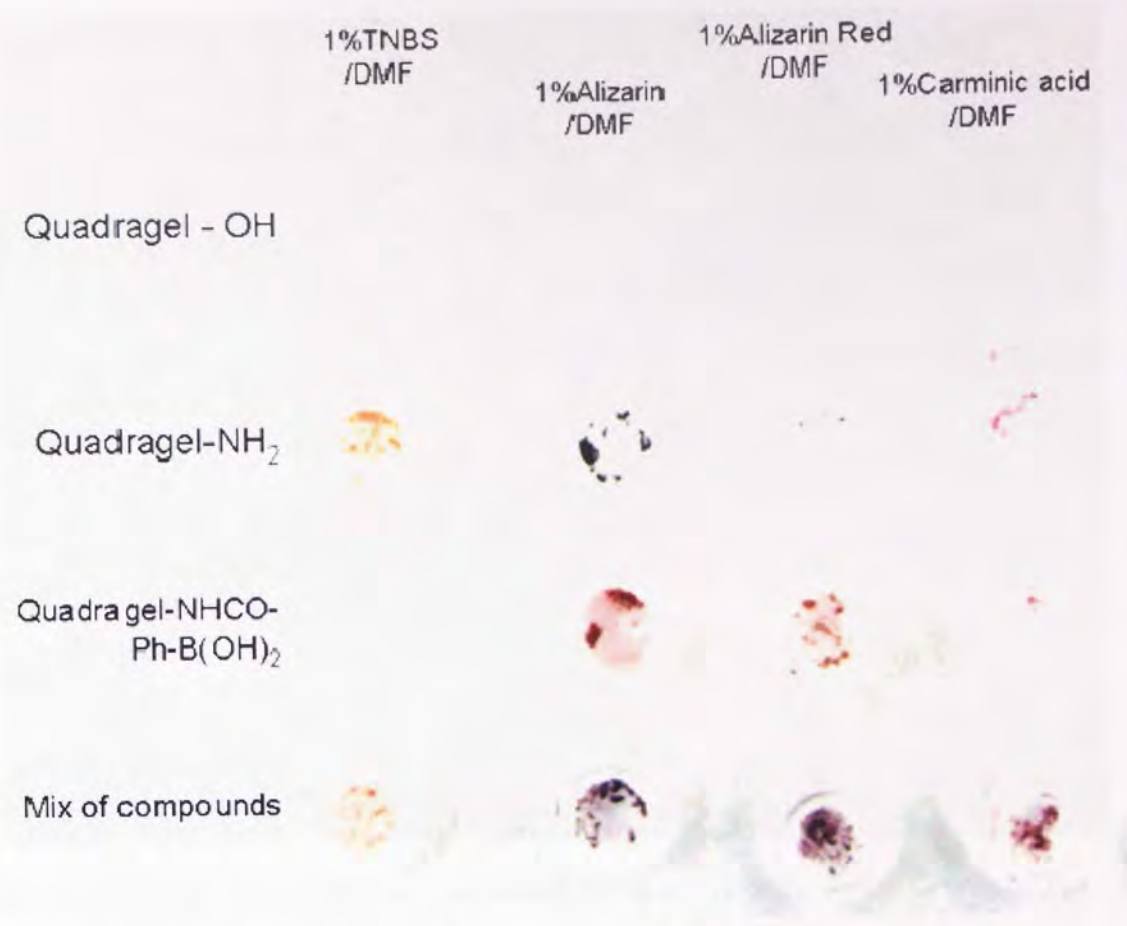

Picture 2: Picture 1 seen through a high contrast filter. Rows descending; Quadragel 59, Quadramine 62, Quadramide-phenylboronic acid 88, mix of the 3 derivatives.

Quadragel **59** can be seen to have reacted with all of the dyes, but again the intensities are much lower than the derivatives **62** and **88**, and the resin samples are not at all visible through the high contrast filter (Picture 2). Alizarin reproduces the colour shift from blue to orange observed in the first matrix (Picture 1). The incubations with Alizarin Red this time produce colour changes, with results similar to those observed with Alizarin. The carminic acid moiety reacted with both the amine and boronic acid derivatives, but unlike in the first matrix, each of the resin-dye complexes produces a red-pink colour, with very little difference in intensity to enable differentiation between the two compounds. The assays involving the mixtures of resins highlighted the selectivity of each of the four dyes, with particular derivatives reacting in a specific manner with the dyes to produce coloured beads which are readily distinguishable from one another.

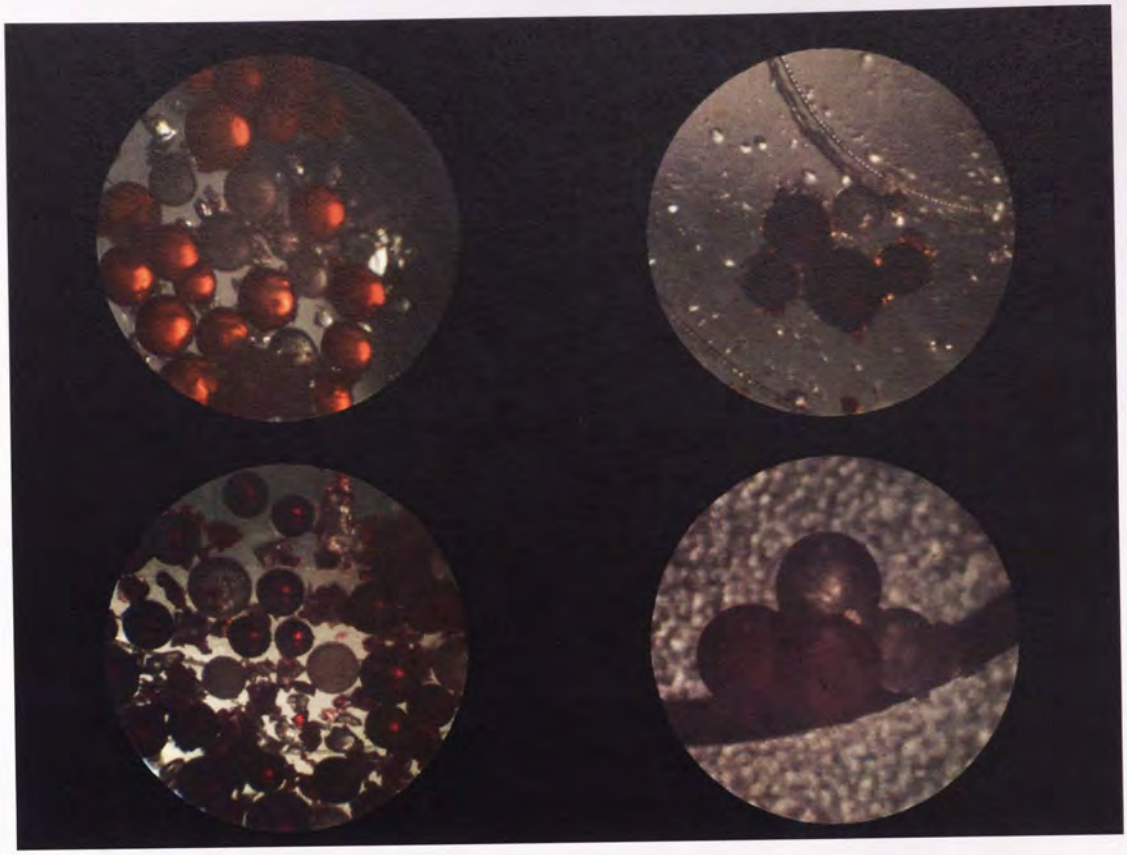

Picture 3: Photographs of the mixed resin samples (Picture 1; row 4), 50x magnification. Top left (clockwise) TNBS stain 89 (Orange = Amine), Alizarin stain 90, Carminic acid stain 91, Alizarin Red stain 31. In each photograph at least two resin derivatives can be distinguished from one another on colour alone.

Unfortunately it is exceedingly difficult to distinguish the three compounds in each mixed sample. Under the TNBS staining conditions colourless resins could be Quadragel **59** or the boronic acid derivative **88**. The catechol dyes produce colours which, when mixed, are barely distinguishable. The only certainty in each is the colourless Quadragel **59**.

It has been reported that the alizarin red-boronic acid complex can fluoresce[20]. Springsteen and Wang[14] postulate that formation of the boronate ester removes the fluorescence quenching mechanism which in turn leads to an increase in the fluorescence of the system.

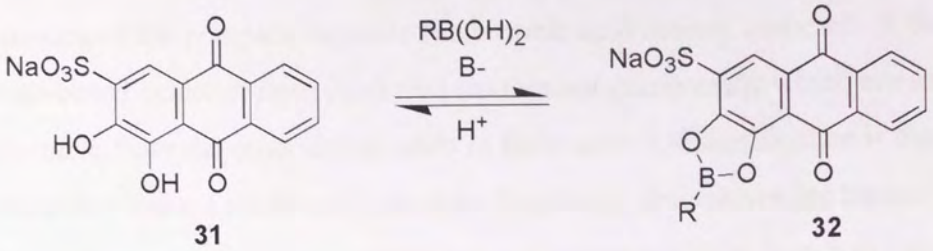

31 32

Non-Fluorescent Fluorescent

Reaction Scheme 23: Dye-boronic acid complex yields the fluorescent anthracene-based catechol.

Observation of the colour matrix presented in Picture 2 under UV-B illumination showed highly fluorescent species.

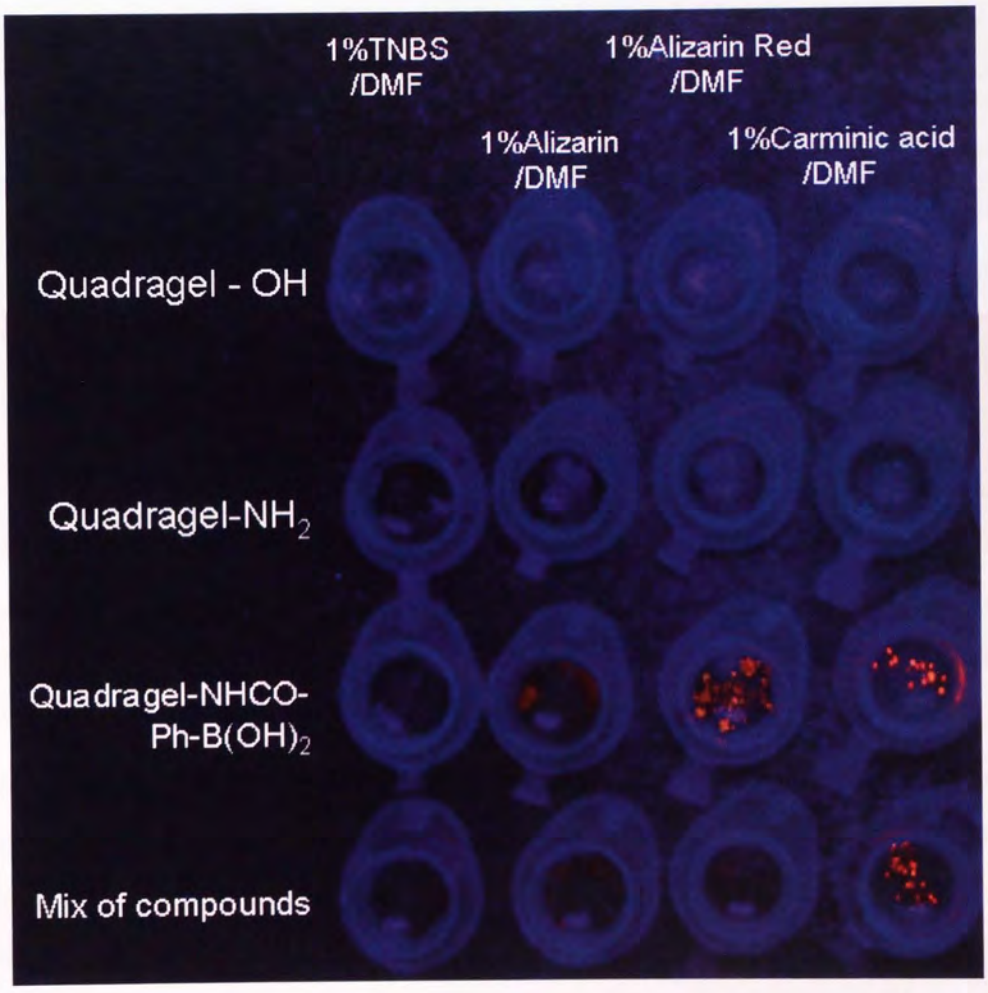

Picture 4: Colour matrix of Quadragel-based compounds incubated with a variety of dyes, viewed under long-wavelength (UV-B) UV light. Rows descending; Quadragel 59, Quadramine 62, Quadramide-phenylboronic acid 88, mix of the 3 derivatives. Photographs taken under long wavelength UV (UV-B) conditions have an ISO 1600 rating.

The formation of the complex between the boronic acid moiety and each of the anthracene-based catechol dyes produced fluorescent compounds which are easily distinguishable from the other compounds in the matrix. Of significance is the observation that when a mixture of the three Quadragel derivatives are treated with the respective dyes, all except the carminic acid appear to suffer from a quenching effect. Picture 5 clearly shows that the mixed 'pot' (far right) contains both fluorescent and non-fluorescent beads which have the potential to be separated by mechanical means. This ability to fluoresce in the presence of other compounds is the cornerstone of any future application based on the use of carminic acid as the standard detection method for use during the incorporation of boronic acids onto solid supports.

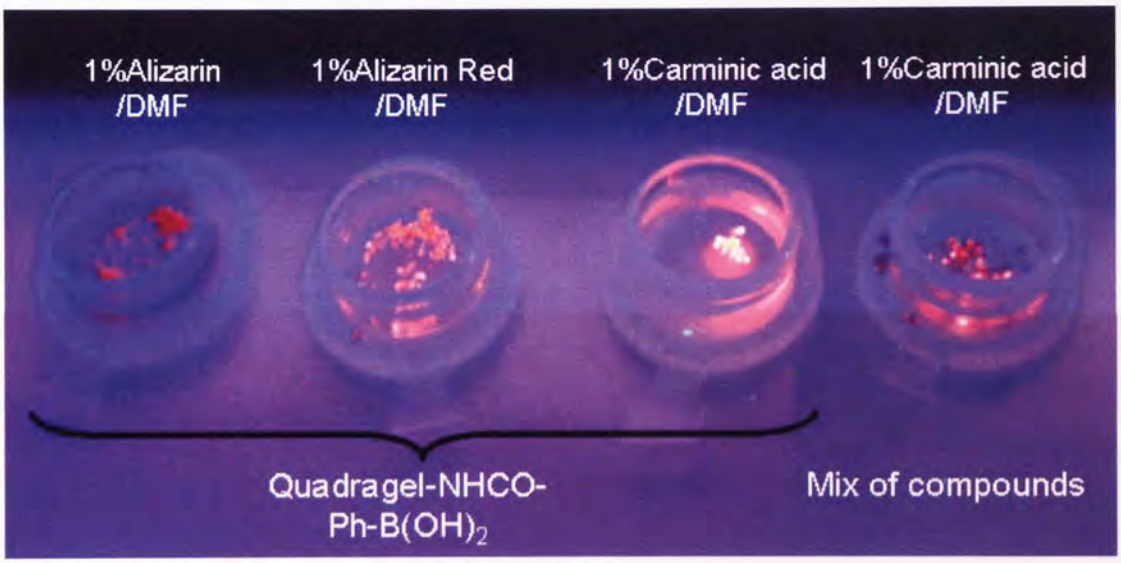

Picture 5: Close view of the 4 matrix positions which fluoresce under UV-B light (Picture 4). Photographs taken under long wavelength UV (UV-B) conditions have an ISO 1600 rating.

The reproducibility of the assay was extremely good, with synthesis of Quadramide-phenylboronic acid **88** being successfully followed on over five separate occasions. Accordingly, carminic acid staining assays can be used to distinguish hydroxyl, amine and boronic acid functionalised beads in complex mixtures using very simple colour-based methodology. As a result, in subsequent studies, this technique was used in conjunction with other colorimetric assays, FTIR and MS (where appropriate) to determine the successful incorporation of the 4-carboxyphenylboronic acid onto solid support resins.

3.5 Post-cleavage manipulation and rotation of peptides

Vancomycin was selected as the glycoprotein target due to the biological importance of this antibiotic, its commercial availability, low cost and well established recognition motif. Vancomycin inhibits the synthesis of cell walls by forming complexes with peptides terminating in D-alanyl-D-alanine at the carboxy terminus[98,99,100]. In model studies, D-alanine can easily be incorporated into peptide sequences as it is readily available in its *N*-α-Fmoc-protected form. More complicated, in terms of synthesis, is the requirement for the free end of the peptide to be the carboxy terminus.

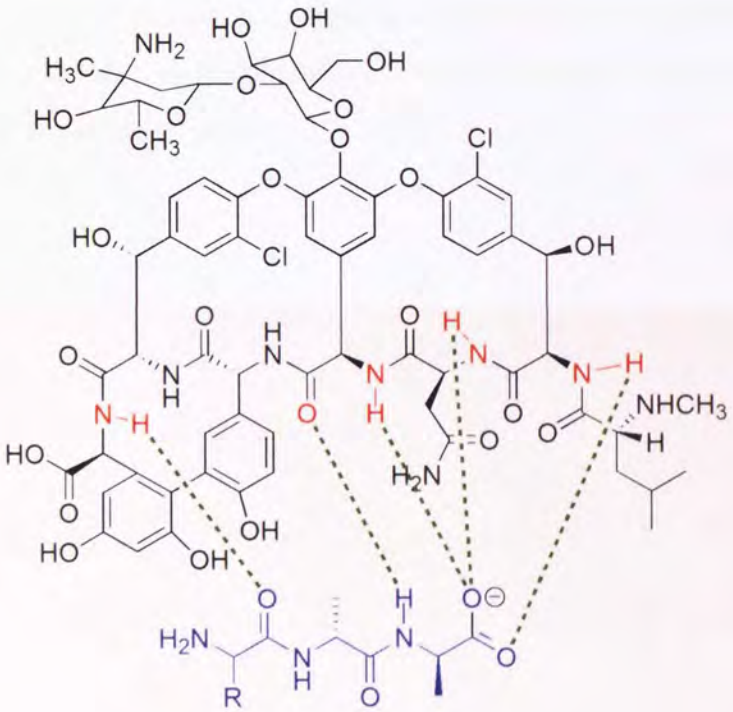

Figure 29: Hydrogen bonding of Vancomycin 9 to a short peptide sequence ending with AA_1-D-Ala-D-Ala at the carboxy terminal[101].

Standard Fmoc protocols create a stepwise addition of a resin-bound amine to a free carboxylic acid, resulting in another resin-bound amine (subject to deprotection). *N*-α-Fmoc-protected amino acids are of much greater desirability to the peptide chemist due to their cheap and ample supply and their ease of use. In order to present

a free carboxy terminus using Fmoc methodology, any peptide sequence would need to be synthesised in reverse order, cleaved from the resin and then reattached at the amine terminus to a different resin.

3.5.1 Synthetic strategy 1

The first strategy to be investigated involved synthesising a model tetrapeptide using Fmoc chemistry on a 2-chlorotrityl chloride PS support **63** and subsequently cleaving the synthesised Fmoc-protected peptide from the support. It was envisaged that tritylation of the carboxylic acid, followed by piperidine mediated cleavage of the Fmoc protecting group would yield an amine functionalised peptide which could then be attached to a carboxy resin. Lysine was included in the peptide sequence to provide a point of attachment for boronic acid units if desired, while glycine was added to act as a small spacer unit.

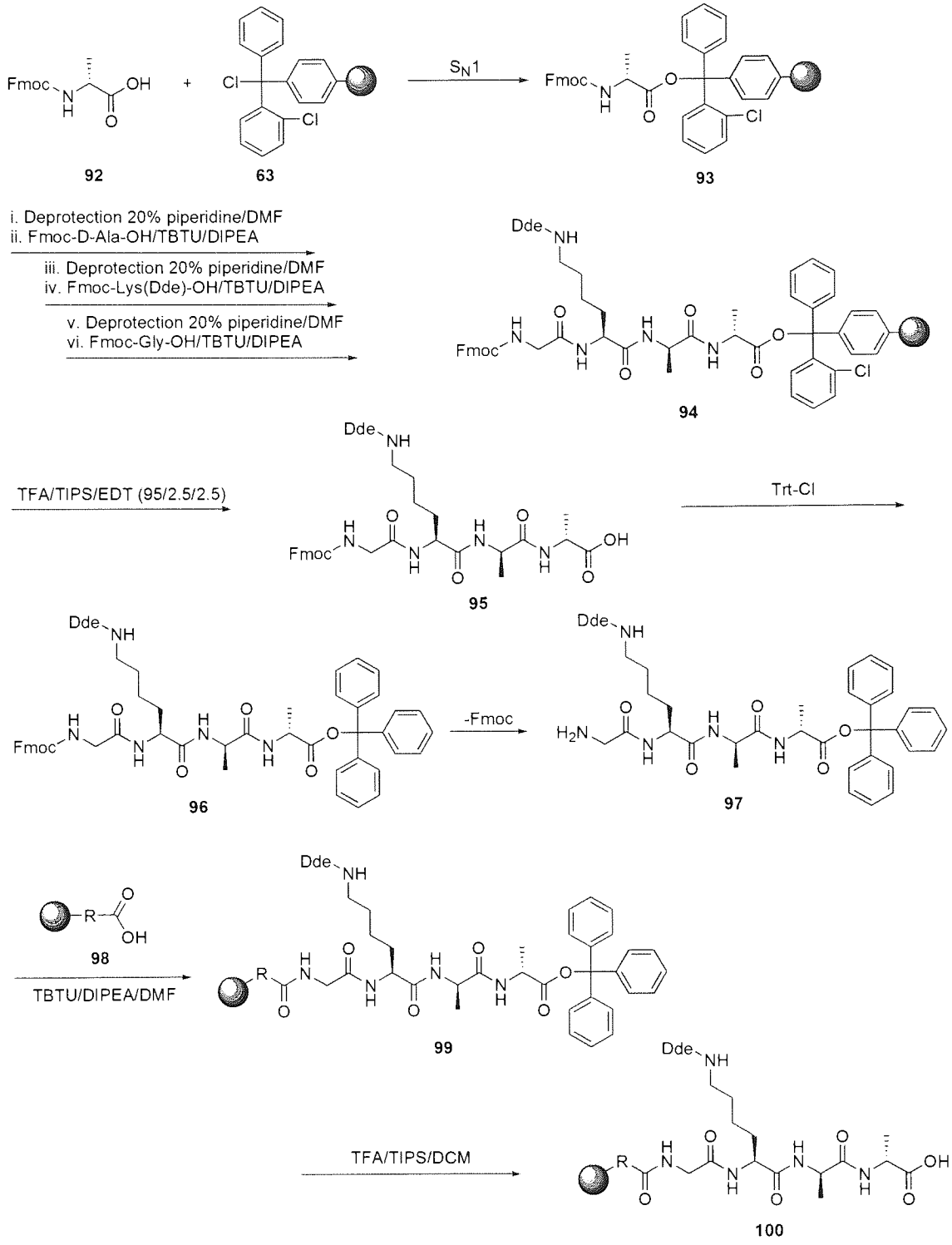

Reaction Scheme 24: Planned synthetic route of a carboxyl-bearing peptide using Fmoc methodology.

3.5.2 Fmoc-Glycine-Lysine(Dde)-D-Alanine-D-Alanine-OH 95

The first amino acid in the sequence was added to the 2-chlorotrityl chloride PS support **63** via a facile S_N1 reaction. The remaining amino acids were added sequentially utilising standard Fmoc-chemistry and TBTU/DIPEA coupling conditions. The peptide sequence Fmoc-Gly-Lys(Dde)-D-Ala-D-Ala-OH **95** was cleaved from the resin by treatment with TFA and isolated in an 80 % yield as a white fluffy solid. Analysis by mass spectrometry identified a compound with the same mass as the target sequence.

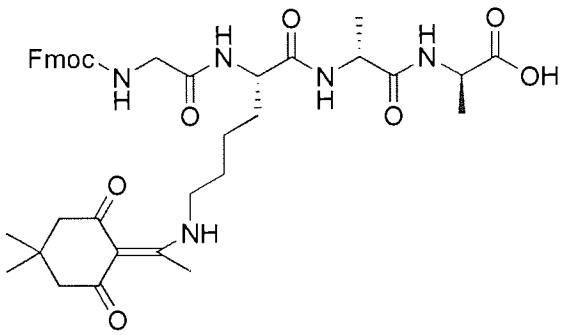

95

Figure 30: Fmoc-NH-Gly-Lys(Dde)-D-Ala-D-Ala-OH 95

The next stage of the synthesis involved tritylation of **95** to yield **96**. Tritylation was undertaken using the same strategy which initiated the on-resin synthesis, namely displacement of the chlorine from trityl chloride via an S_n1 reaction.

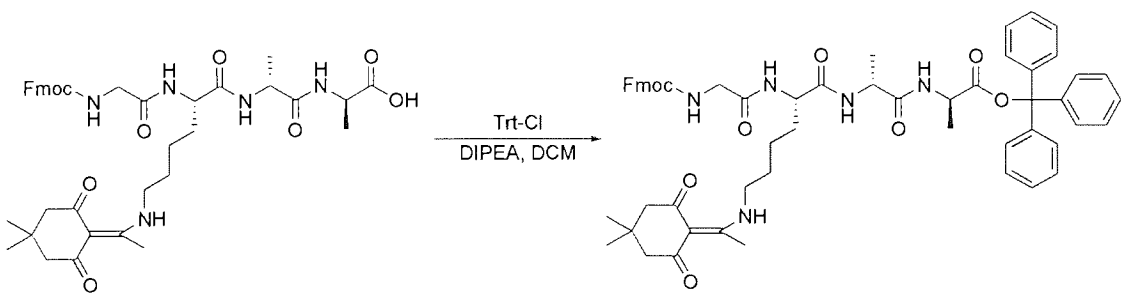

95 **96**

Reaction Scheme 25: Tritylation of peptide 95 to yield the trityl protected peptide 96.

The peptide was dissolved in DCM and added to a solution of trityl chloride (1.1 eq.) and DIPEA (3 eq.) in DCM (1 ml). After stirring for an hour the solution was concentrated under reduced pressure to a volume < 1 ml. The crude peptidic cleavage products were precipitated from diethyl ether (10.0 ml) triturated and collected by filtration through a DVPP membrane filter cloth. Analysis of the precipitate by ^{1}H NMR showed no aromatic protons associated with either the Fmoc or trityl protecting groups. Subsequent analysis of the filtrate indicated that the reaction had failed. Mass spectrometry revealed peaks corresponding to the starting peptide sequence and its sodium and potassium adducts, as well as the trityl cation. ^{1}H NMR showed proton signals associated with Fmoc and trityl and also a doublet attributable to one of the alanine-methyl groups. The integration of these peaks highlighted an excess of trityl, greater than the 1.1:1.0 ratio of the reaction mixture. TLC analysis of the filtrate showed a single spot under UV with an R_f corresponding to the trityl group. Staining of the plate with TFA produced 3 yellow spots within the sample lane, each matched with a corresponding spot from the trityl chloride.

Picture 6: TLC analysis of 96 after attempted tritylation. Left to right; precipitate; filtrate; mixed lane; trityl chloride. Mobile phase: 100 % DCM; visualisation 100 % TFA.

From the various corroborating analyses it was concluded that the reaction had failed, with the likely reason being the presence of residual TFA from the resin-cleavage stage. As trityl groups are readily cleaved with the acid, any trace amount would undoubtedly prevent successful protection of the peptide. It was deemed likely that even if a pre-neutralisation step of the peptide was attempted, removal of all

traces of acid was unlikely to be successful, thereby compromising the success of the reaction. As a result this approach was abandoned.

3.5.3 Quadramide-butanoic acid 98

The first carboxy resin designed to be synthesised was Quadramide-butanoic acid **98**. This support was constructed by reaction of the Quadramine **62** with succinic anhydride **101** which caused ring opening of the anhydride and the formation of an amide bond[102].

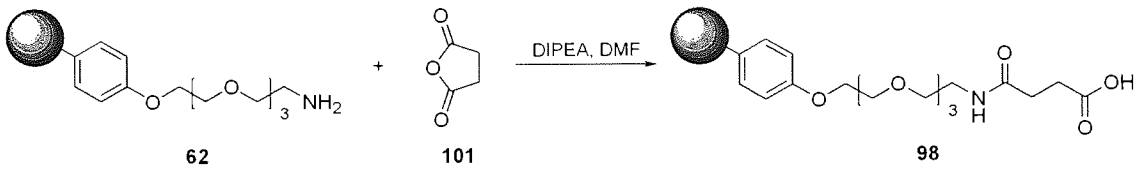

62 **101** **98**

Reaction Scheme 26: Ring opening of succinic anhydride 101 and subsequent formation of an amide bond to yield the carboxylic acid resin 98.

Quadramide-butanoic acid **98** was isolated in a 97 % yield. Analysis of the product by ATR-FTIR showed the formation of an amide with a strong signal at 1649 cm^{-1}. A second carbonyl signal corresponding to the carboxylic acid was visible at a higher frequency of 1727 cm^{-1}. A strong, broad signal at 3334 cm^{-1} showed a signal consistent with hydrogen bonding of the OH groups of the COOH moiety; something lacking in the starting resin **62**. A colourless result to the Kaiser colorimetric assay confirmed the absence of a primary amine due to reaction.

3.5.4 Synthetic strategy 2

With the failure of the tritylation method (Reaction Scheme 24) a new synthetic route using activated resin **107** was proposed. By pre-activating the carboxylic acid on the resin it is possible to ensure that only the amine terminal of the peptide reacts with the bead. As the reaction mixture contains no coupling agents, the reaction provides a

method of coupling which avoids the complication of possible self-coupling of the unprotected peptide sequence.

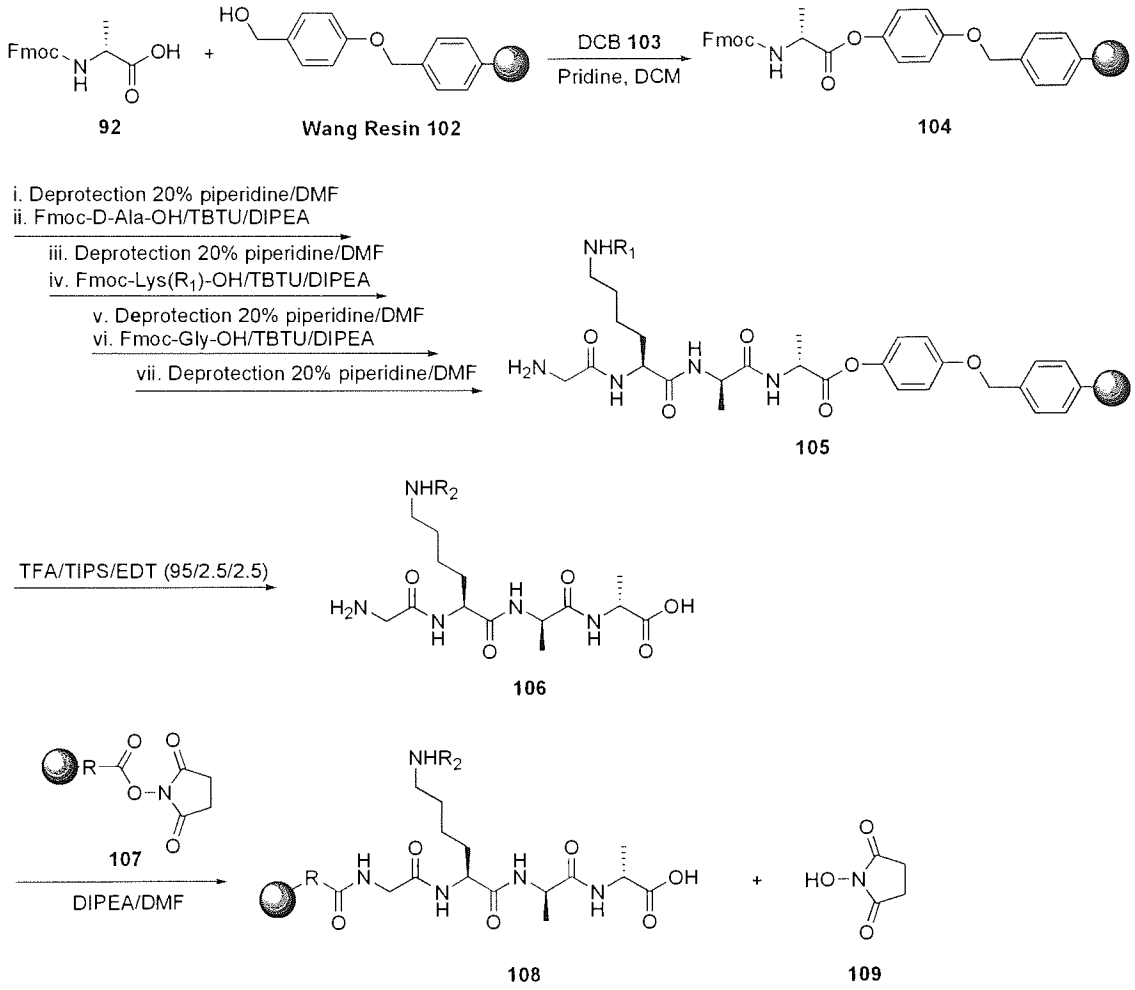

Reaction Scheme 27: Second synthetic route to achieving a carboxyl-bearing peptide using Fmoc methodology. Treatment of a carboxyl functionalised resin 112 with *N*-hydroxysuccinimide yields a 'pre-activated' resin 107. The peptide 106 reacts with the resin-bound carbonyl to form the amide bond and expels the hydroxysuccinimide in the process. If R_1 = Dde, R_2=Dde. If R_1 = Mmt, R_2=H.

3.5.5 H_2N-Glycine-Lysine(NH_2)-D-Alanine-D-Alanine-OH 106

To generate the peptide sequences for coupling to the *N*-hydroxysuccinimide activated resin **107**, an alternative synthesis was used to that described previously (**section 3.5.1**). For reasons of economy, the use of 2-chlorotrityl chloride

polystyrene resin **63** was abandoned in favour of the cheaper Wang resin **102**. The dichlorobenzoyl chloride **103** method of coupling Fmoc-amino acids to hydroxyl resins, such as Wang resin **102**, results in products virtually free of impurities arising from enantiomerisation and dipeptide formation[103,51]. Accordingly, this coupling methodology was adopted for all first stages of peptide synthesis constructed on Wang resin.

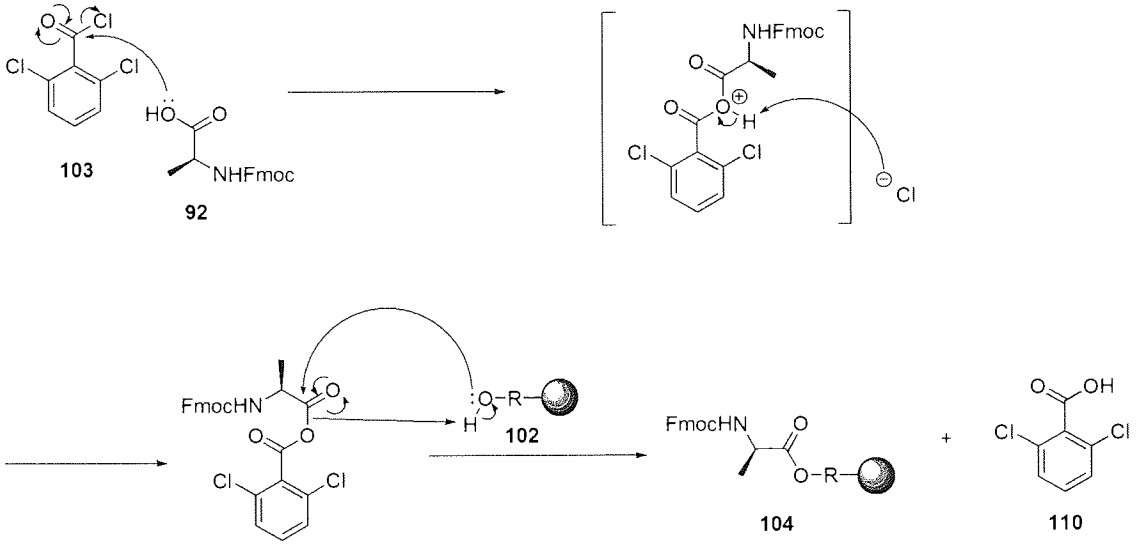

Mechanism 11: DCB mechanism for coupling Fmoc-Amino acids to hydroxyl resins.

After the first coupling procedure had been carried out, removal of the Fmoc protecting group followed by a Kaiser test confirmed the successful addition of the primary amino acid. Propagation of the chain was then performed in a stepwise manner employing TBTU/DIPEA methodology.

A short peptide sequence was constructed to demonstrate a proof of concept method, primarily focused on the practical requirements of the post-cleavage manipulation of short peptides. The high cost of the *N*-α-Fmoc-Lysine(Dde)-OH derivative made its inclusion in every sequence prohibitive. Accordingly, it was decided that use of the Dde protected amino acid in this high-risk methodology would not be cost-effective, and as such Fmoc-Lys(Mtt)-OH was utilised instead.

Cleavage of the target peptide from the resin was accomplished via TFA acidolysis with subsequent analysis by HRMS confirming the presence of a compound of the target mass.

3.5.6 Quadramide-PEG$_4$carboxylic acid 112

The concept of forming the carboxy-functionalised resin **98** was repeated, however the ring-opening reaction of succinic anhydride was replaced by coupling a poly(ethylene glycol) form of the bis-carboxylic acid as a method of increasing the overall hydrophilicity of the resin.

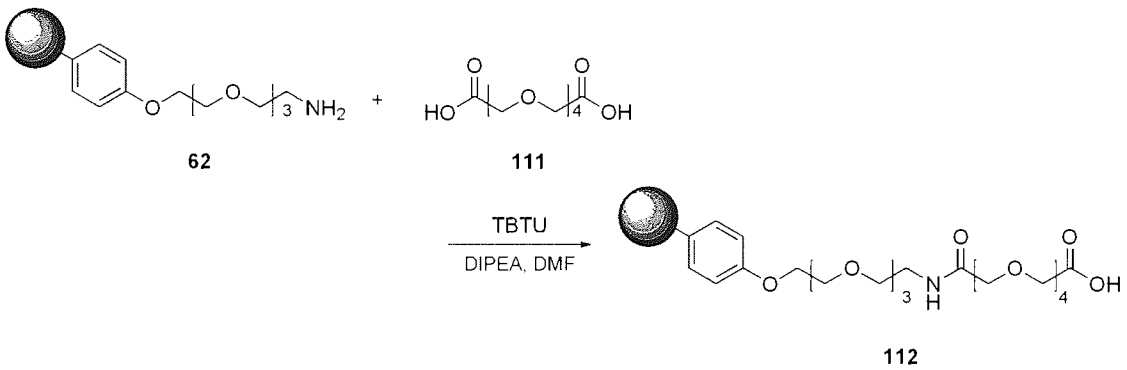

62 111 112

Reaction Scheme 28: Unlike 98, derivative 112 incorporates Poly(ethylene glycol) bis(carboxymethyl) ether as a way of increasing the overall hydrophilicity of the resin.

The target resin was isolated in a slightly reduced yield (when in comparison with **98**) of 95 %. The Kaiser test produced colourless beads indicative of a successful coupling to the amine which was confirmed by FTIR signals attributable to a secondary amide stretch at 1674 cm^{-1}. Signals for the hydrogen bonded –OH stretch (3364 cm^{-1}) and the carbonyl of the carboxylic acid (1750 cm^{-1}) were also present.

3.5.7 Quadramide-PEG$_4$carboxy-*N*-Hydroxysuccinimide 107

Resin **112** was treated with *N*-hydroxysuccinimide (NHS) to form the activated resin **107**, which would in turn react with the amine groups found on an incoming peptide through nucleophilic acyl substitution.

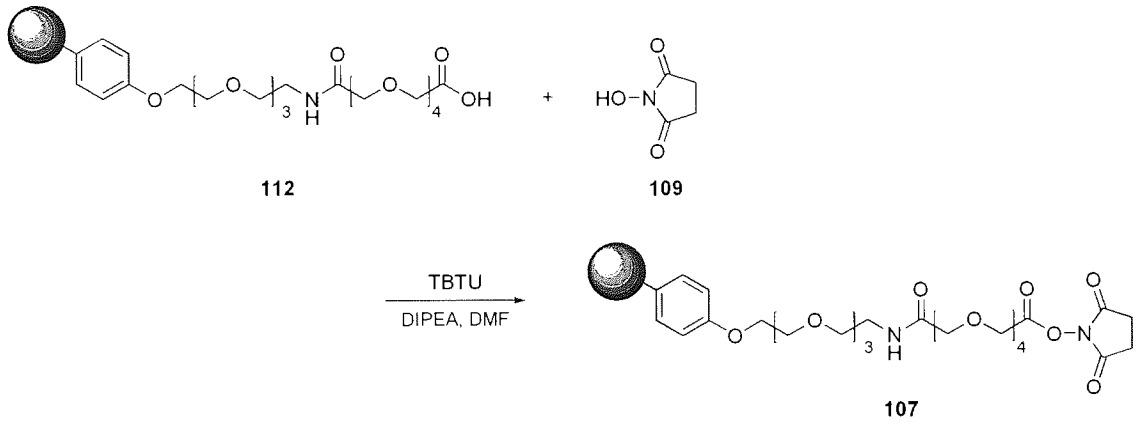

Reaction Scheme 29: Synthesis of a 'pre-activated' carboxy resin 107 using resin 112 and *N*-hydroxysuccinimide 109.

A solution of NHS (5 eq.), TBTU (12 eq.) and DIPEA (12 eq.) in DMF (2 ml) was added to resin **112**. Agitating overnight at room temperature afforded orange/brown beads. It was unclear how stable the resin would be to analysis, therefore the success of this reaction was determined by the production of any subsequent resin-peptide product.

3.5.8 Quadramide-PEG$_4$CONH-Peptide 108

The inclusion of Fmoc-Lys(Mtt)-OH in the construction of sequence **106** resulted in a peptide which contained two amine groups as cleavage from the resin also removed the ultra-labile 4-methyltrityl group. Any further reaction would afford two isomers. Spontaneous reaction of the peptide sequence with the NHS ester functionalised resin **107** was expected to produce attachment of the peptide at the *N*-α-glycine as well as

the *N*-ε-lysine, however the position of the resin in both derivatives is away from the D-Ala-D-Ala residue binding motif for vancomycin.

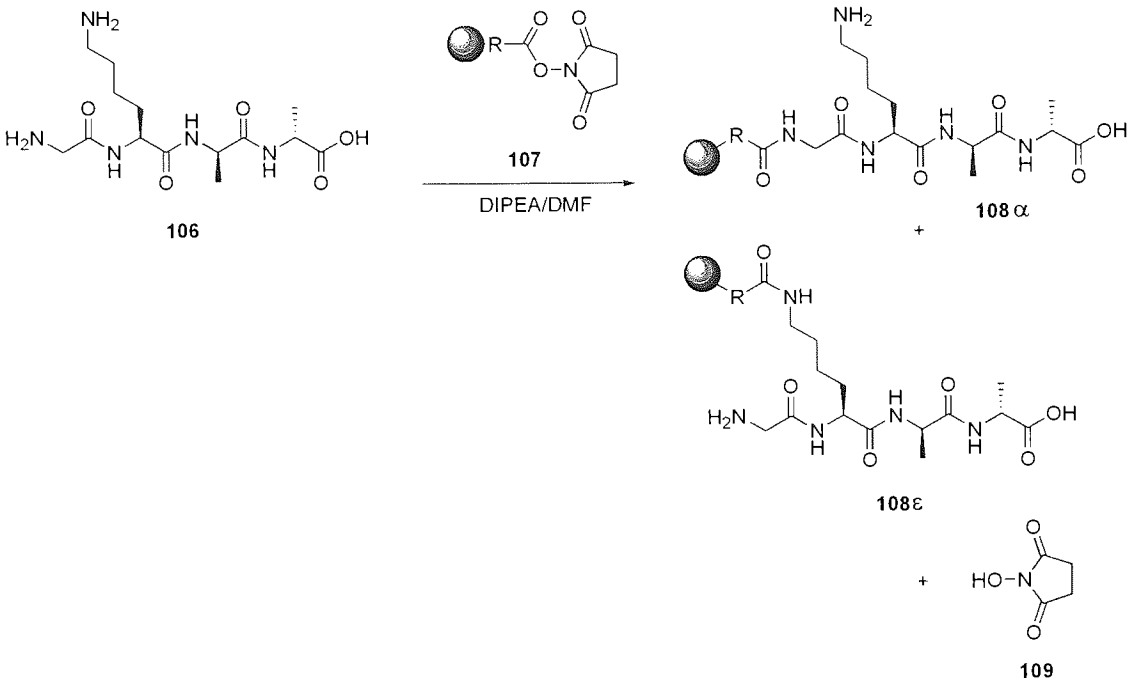

Reaction Scheme 30: The two possible products of the reaction with 106 with 107. Coupling position of peptide to the resin is denoted by α or ε.

The title compound was produced with an 11 % yield, although the measurement of such small mass increases (~2 mg) is inherently prone to error. Any starting resin would undergo hydrolysis to reform resin **112**. The reaction was followed by Kaiser assay which afforded blue beads, indicating the presence of the remaining primary amine groups in the peptide sequence which had not reacted with the resin.

The IR analysis broadly coincides with the expected analysis of the target compound. The only functional group present in the product and not the starting resin is the primary amine of either the glycine or lysine residues. Since the hydrogen bonded N-H stretch overlaps with the hydrogen bonded OH stretch (present in both base resin **112** and the products **108α/ε**) no definitive proof of reaction success can be elicited from the spectra.

3.5.9 Quadramide-PEG$_4$CONH-Peptide-Boronic acid 113

Addition of a boronic acid moiety was achieved though a TBTU coupling reaction. Due to the mixed starting products, two potential positions of attachment existed, the *N*-α-glycine and the *N*-ε-lysine.

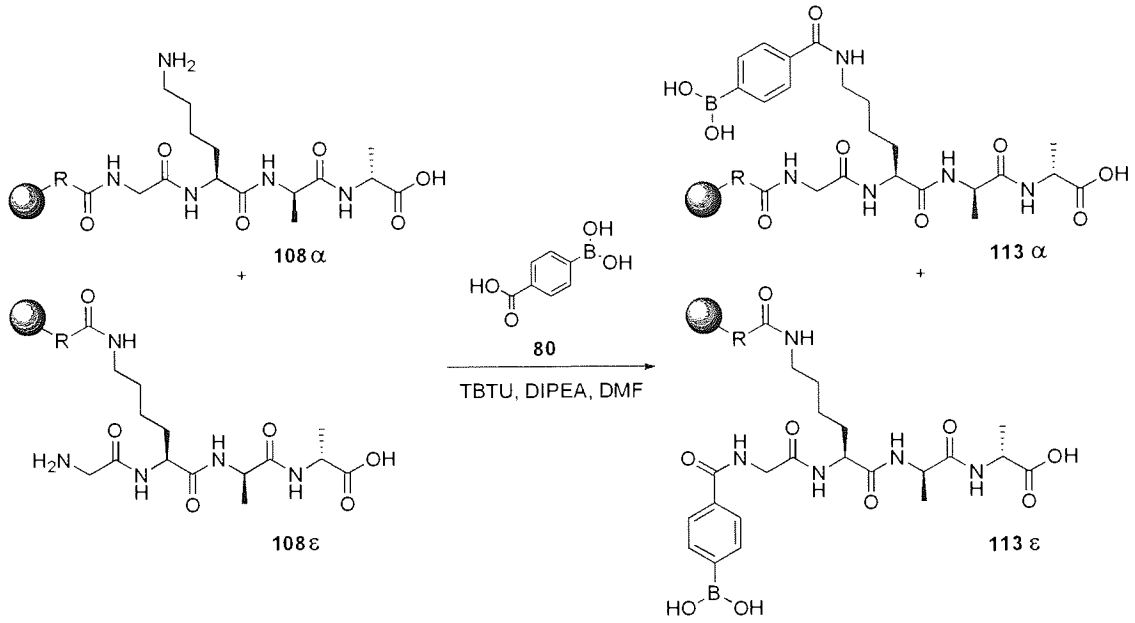

Reaction Scheme 31: Coupling of 4-carboxyphenylboronic acid 80 to peptidyl resin product 108 to yield the boronic acid functionalised compound 113 with the boronic acid coupling at both the α & ε amine groups. Coupling position of peptide to the resin is denoted by α or ε.

Attachment of the boronic acid was followed with on-resin colorimetric assays. The starting material was blue by both Kaiser and carminic acid tests. After successful coupling of the boronic acid the resultant resin was colourless by Kaiser test and red by carminic acid test. Beads treated with carminic acid also fluoresced under UV light.

Compound **113** has very few groups which enable differentiation between it and the starting resin **108**. The B-O stretch, which would allow such a determination, is not identifiable in the IR spectrum, and therefore offers no information about the progression of the reaction. Accordingly, success was attributed entirely on the basis of mass gain and colorimetric assay results.

The mass increase of 4 % associated with the coupling of the boronic acid would indicate that the 11 % yield of **108** was underestimated. Assuming the boronic acid coupled with the 96 % efficiency exhibited previously (Resin **88**), the yield calculated by mass increase due to boronic acid is 17 %. As previously discussed, the accurate measurement of masses of a few milligrams on standard 4-point balances is unreliable at best. Such numbers should therefore be reviewed with extreme caution. Accordingly, with reactions of this scale it is perhaps better to acknowledge that the reaction methodology was proved to be successful by colorimetric methods, rather than dwell on the absolute efficiency of the reaction.

Resin compounds **108α/ε** and **113α/ε** were added to the combinatorial library as stand-alone compounds to test the affinity of vancomycin for the 'reverse' free hydroxyl sequences.

Chapter 4

'Catch and Release' Strategies and Fluorescent Tagging of Carbohydrates and Vancomycin

'Catch and Release' Strategies and Fluorescent Tagging of Carbohydrates and Vancomycin

The following chapter describes the use of simple carbohydrates as model substrates to test the process for the binding and subsequent release of saccharides from solid supported boronic acid containing compounds. The chapter then goes on to describe attempts at labelling such compounds in a manner that would allow accurate quantification of the 'catch and release' process.

4.1 'Catch and release'

Boronic acids are well known to bind strongly to compounds containing 1,2- and 1,3-*cis* diols. Binding occurs through the formation of covalent bonds in the form of cyclic boronate esters[8,14,15]. Consequently, boronic acids have been used as the recognition motif in the construction of sensors for saccharides, as nucleotide and carbohydrate transporters and as affinity ligands for the separation of carbohydrates and glycoproteins[23]. The reversible formation of a cyclic boronate ester in basic conditions affords a method of immobilising a carbohydrate onto the surface of the solid support, a process which can be reversed at a later stage by acidification[17]. In the current study, simple carbohydrates in conjunction with Quadramide-phenylboronic acid **88** were used in a model study to test the binding characteristics of solid supported boronic acids in preparation for studies centred on vancomycin immobilisation (see **Chapter 5**).

4.1.1 'The catch'; Immobilisation of carbohydrates with Quadramide-phenylboronic acid 88

A range of carbohydrates were chosen for inclusion within this model study to encompass the main forms of saccharides; fructose (furanose), glucose (pyranose) and raffinose (an oligosaccharide comprised of both furanose and pyranose ring forms).

Prior to conducting any model on-bead complexation studies a solvent had to be selected. Pyridine was chosen as the solvent as it affords excellent resin swelling, complete dissolution of the carbohydrates chosen for study, and is sufficiently basic ($pK_a = 5.27$) to create the boronate anion[29] required for carbohydrate complexation. In addition, unlike buffer solutions, concentrating a pyridine solution does not cause the deposition of solid material within the polymer matrix, allowing the mass gain of a resin due to carbohydrate binding to be established accurately by a simple weighing procedure.

Table 13: Immobilisation rates of a furanose, pyranose and oligosaccharide onto Quadramide-phenylboronic acid 88.

Conjugate	Carbohydrate	Immobilised mass* /g	mmol	% of boronic acid sites filled
114	Fructose **117**	0.0849	0.589	74 %
115	Glucose **1**	0.0483	0.335	43 %
116	Raffinose **118**	0.1652	0.353	45 %

*Immobilised mass calculated from the measured mass gain of the resin.

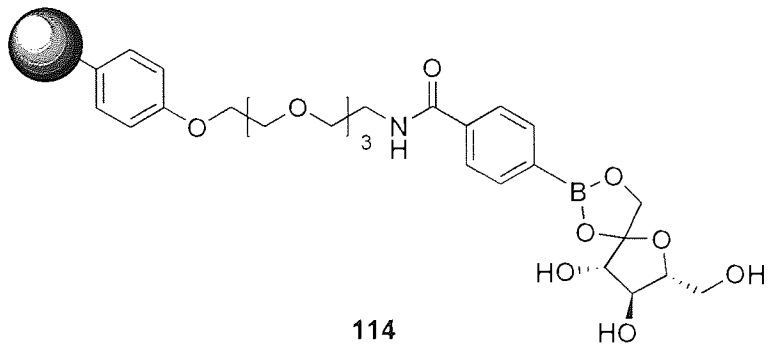

114

Figure 31: Immobilisation of fructose onto boronic acid-containing resin 88 to form complex 114

In an initial study the three different carbohydrates were incubated with Quadramide-phenylboronic acid **88**. As mentioned earlier (section **3.4**), boronic acid moieties may be visualised by staining with carminic acid. With all three carbohydrates, formation of the corresponding boronate ester meant that staining the resin conjugates with carminic acid resulted in virtually colourless beads.

Photo 1: Carminic acid staining of resin compounds. Left; Quadramide-phenylboronic acid 88. Right; Quadramide-phenylboronic acid-glucose complex 115 after the immobilisation procedure.

Fructofuranose **117** has one position of binding with boronic acid; at the 5,6-*cis* diol. C6 offers a point of free rotation, and is therefore not bound by the constraints of the ring. The other diols in the system adopt the *trans* configuration, whereby the adjacent hydroxyl groups are too far apart in space to be bridged by the incoming boronic acid.

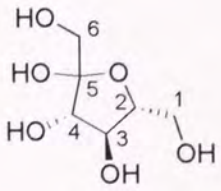

117

Figure 32: D-Fructofuranose 117

β-Glucose **2** does not contain a 1,2-*cis* diol. When the anomeric hydroxyl is in the α-position **1**, the 1,2-*cis* diol is formed at the anomeric centre. This equilibrium-dependent mutorotation may suggest the reason why the binding strength of boronic acids to glucose **1** is approximately half that of fructose **117**.

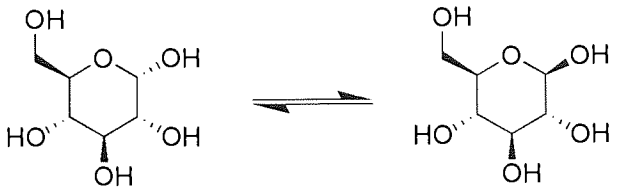

1 **2**

Figure 33: D-Glucopyranose in the α- (1) and β- (2) forms

Raffinose **118** has a D-glucose unit and a furanose unit, both without a *cis*-diol. The comparable rate of binding between the glucose and raffinose suggests that both undergo the same equilibrium-dependant mode of binding.

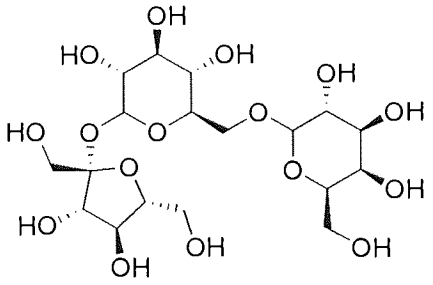

118

Figure 34: D-Raffinose 118

The results detailed in Table 13 correlate with a previous study[14,27] comparing the binding of a number saccharides to boronic acid in solution. The study of James *et al.* (1995) was more extensive than the current limited investigation, but the agreement would appear to show that the saccharide-binding trend remains unchanged between solution and solid supported boronic acids.

4.2.1 'The release'; liberation of the bound carbohydrate

Methods such as competitive displacement were considered as possible ways to release the bound carbohydrates, however these methods were ruled out as boronate ester complex stability has been shown to increase from simple acyclic diols to the rigid *cis*-diols of saccharides[8]. Acidolysis was therefore adopted as the preferred method of liberating the immobilised carbohydrate. In a previous study[17] it had been shown that the amount of phenyl boronic acid-fructose complex below pH 4 is negligible. Accordingly, an aqueous solution of citric acid (pH 3.0) was used to hydrolyse the boronic acid-carbohydrate complex. The compatibility of citric acid with biological systems was also considered (the citric acid cycle[2]), given the intended application of developing methodology for studying biologically relevant molecules such as vancomycin. THF was added to the cleavage solution to maintain the compatibility of the solvent system with the resin.

Table 14: Liberation rates of a furanose, pyranose and oligosaccharide.

Conjugate	Carbohydrate	Liberated mass* /g	mmol	% of carbohydrate liberated
114	Fructose **117**	0.0850	0.589	100 %
115	Glucose **1**	0.0482	0.335	100 %
116	Raffinose **118**	0.1650	0.353	100 %

*Liberated mass is calculated on the difference in resin mass pre and post acidolysis. % Liberation is based on the ratio of the number of moles cleaved to the number of moles immobilised.

The percentage of carbohydrate liberated by treatment with citric acid was calculated on the basis of the dried mass of the resin samples post-cleavage. The post-cleavage mass of the resin samples was compared to the pre-cleavage masses to obtain the mass of carbohydrate cleaved from the resin. The amount of carbohydrate cleaved was expressed as a percentage of that immobilised.

Calculating the yields from the isolated residue was deemed to be less accurate due to the presence of citric acid along with the possibility of pyridine salts, formed from residual pyridine associated with the resin following the immobilisation procedure.

The liberation of the different carbohydrates occurred quantitatively, with the mass of each resin sample returning to its pre-immobilisation mass. Staining of the post-cleavage resin samples with carminic acid (Photo 2) indicated the successful regeneration of the boronic acid moieties.

Photo 2: Carminic acid staining of resin compounds. Left; Quadramide-phenylboronic acid-glucose complex 115 after the immobilisation procedure. Right; Post-liberation with citric acid to yield boronic acid containing resin 88.

Analysis of the cleaved solutions by mass spectroscopy showed compounds with masses corresponding to the appropriate carbohydrate, along with citric acid. Resolving the NMR spectra of carbohydrates is notoriously problematic[104] and time consuming. Accordingly, the ^{1}H NMR data was collected for completeness, but not subjected to detailed scrutiny. In addition to the carbohydrate, each spectrum showed peaks corresponding to citric acid. Subsequent incubation of the cleaved raffinose solution with aminomethyl(poly)styrene **43** (employed as a scavenger resin), appeared to show a decrease in the concentration of the citric acid relative to the other signals, suggesting a direction for possible future purification efforts.

While the 'catch and release' process was shown to be successful, following the progress of the boronate ester forming reaction was not possible given the colourless nature of the immobilised species. Not only would the introduction of a chromophore aid in determining the end point of the reaction, but it would also afford a second method of quantification. Accordingly, steps were taken to try and generate labelled species for use in evaluating on-support boronic acid mediated carbohydrate sequestration.

4.2 Labelling Carbohydrates

Monitoring the capture and subsequent release of carbohydrates from the resin **88** by mass change is limited to instances where the change is of a sufficient size to be measurable. The scale of synthesis required to provide a high degree of accuracy effectively rules out the possibility of a large number of library compounds being quantified in this manner.

Fluorescent tagging of the carbohydrate binding partner was considered a method that would afford a simple, highly sensitive means of accurately measuring small amounts of a given compound. Accordingly, the tagging of both a series of carbohydrates and the antibiotic vancomycin were investigated.

4.2.1 D-Mannopyranosylamine-ethylamine 121

A method of attaching a hydroxylamine linker to an oligosaccharide has previously been reported[105]. The selective coupling was performed in methanol, using a strategy that allowed the use of unprotected sugars. Accordingly, the ratio of reagents (carbohydrate:diamine = 1:10) was adapted to favour the formation of the monosaccharide product.

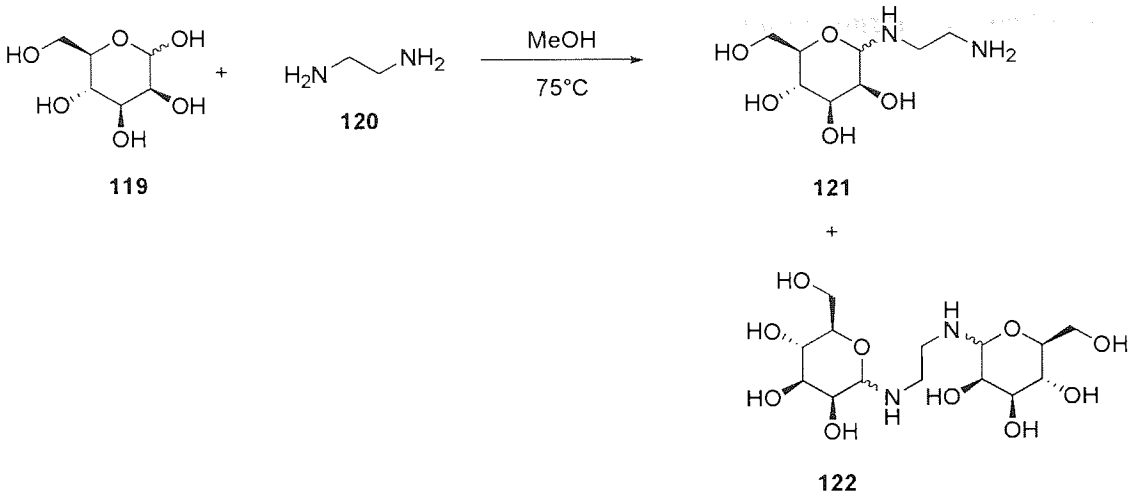

Reaction Scheme 32: Reaction of ethylenediamine 120 with mannopyranose 119 to yield D-Mannopyranosylamine-ethylamine 121 and its dimer, *N,N'*-di-α-D-mannopyranosyl ethylenediamine 122.

Analysis of the crude material by mass spectroscopy verified the presence of the two products; D-mannopyranosylamine-ethylamine **121** and the *N,N'*-di-α-D-mannopyranosyl ethylenediamine dimer **122**.

^{1}H NMR analysis of the crude material gave a well resolved spectrum, but as with all sugars, assignment of peaks proved to be incredibly difficult. The S_N1 nature of the nucleophilic substitution reaction creates mixed α and β anomers.

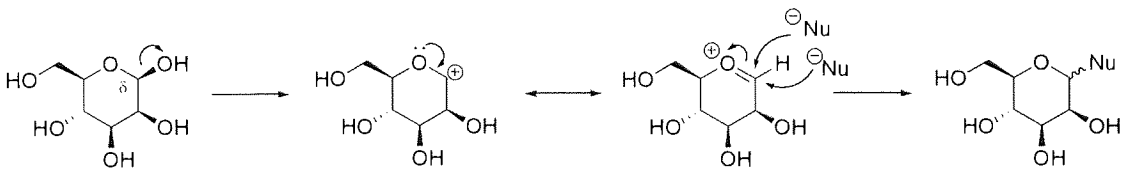

Mechanism 12: S_N1 pathway of a nucleophilic substitution reaction of a β-pyranose to form the product of unknown or mixed anomeric forms[1].

Each proton from an anomeric form produces its own multiplet signal that overlaps with those produced by the protons of the other anomer. The presence of any of the

disaccharide product will be a mixture of αα, αβ and ββ forms, further adding to the complexity of the spectra.

Experimentation with various TLC conditions was unable to identify a mobile phase that would provide the separation of the products with sufficiently good resolution to allow for purification. It was therefore decided to proceed with the fluorescent labelling, using the crude mixture obtained from the reaction with ethylenediamine. It was hoped that the resultant fluorescent products would be of sufficiently different polarities to the non-fluorescent compounds to afford good separation via column chromatography.

4.2.2 D-Mannopyranosylamine-ethyl-thioureido-fluorescein 125a

Isothiocyanates can undergo a nucleophilic addition reaction with primary amines to form thioureas, as observed in the initial stage of the Edman degradation[3]. Fluorescein isothiocyanate (FITC) **123** is a readily available fluorophore with a high extinction coefficient, which has been widely used for tagging amine compounds[106,107,108].

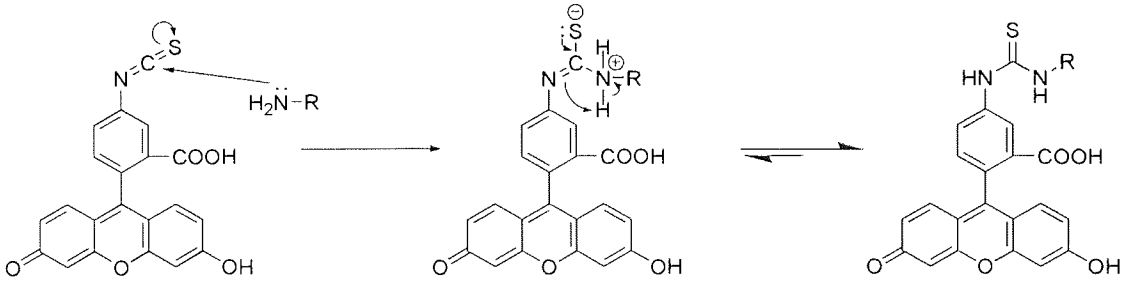

123 124

Mechanism 13: Nucleophilic addition of an amine functionalised moiety to fluorescein isothiocyanate 123. Tautomerisation affords the most stable thiourea form of the molecule.

Reacting FITC **123** with D-mannopyranosylamine-ethylamine **121** was expected to produce the fluorescent compound D-mannopyranosylamine-ethyl-thioureido-fluorescein **125a**. The *N,N'*-di-α-D-mannopyranosyl ethylenediamine **122**, also

present in the crude reaction mixture, was expected to remain unaltered in the presence of the isothiocyanate.

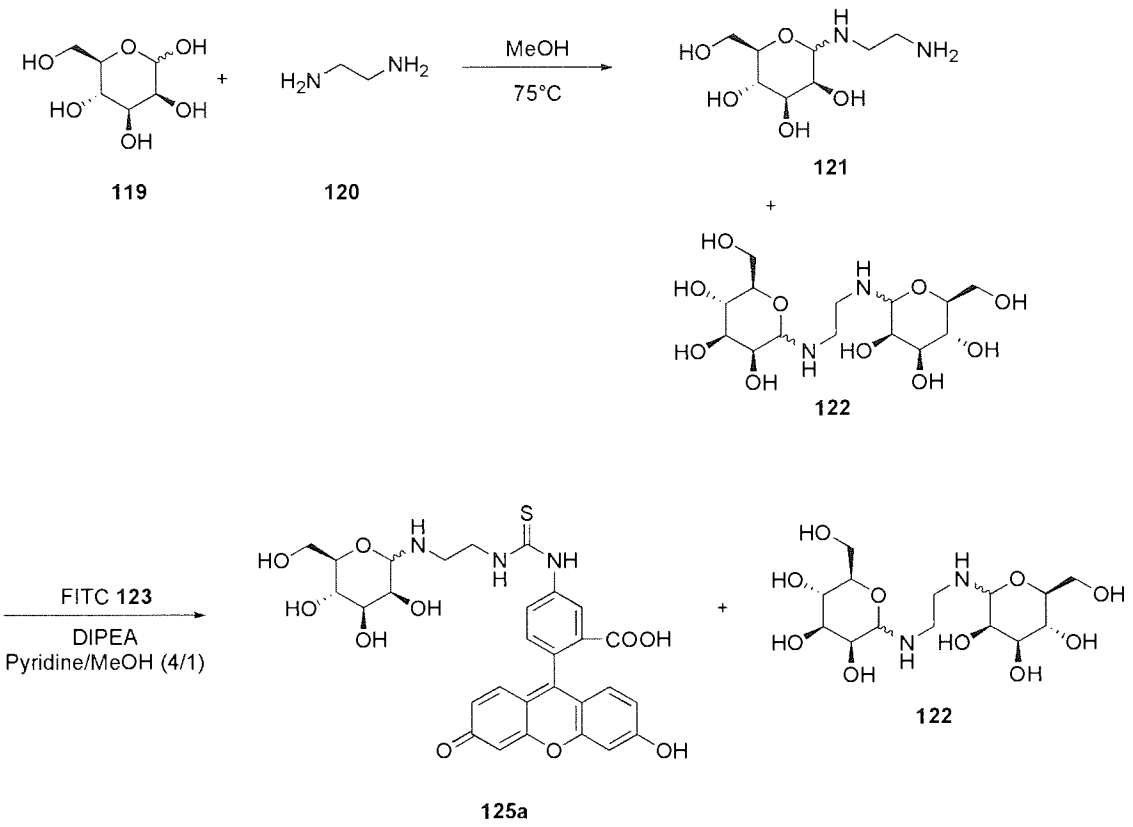

Reaction Scheme 33: Subsequent reaction of 121 with FITC yields a single fluorescent product 125a.

The presence of the fluorescent target compound was indicated by mass spectroscopy, which gave a peak at $m/z = 610$, corresponding to M^-. Unfortunately all other characterisation methods did not allow conclusive interpretation. The degree of separation in TLC analysis which was hoped for at the start of the synthesis could not be achieved, causing further purification attempts to be abandoned.

4.2.3 Thiocarbonyl ethylenediamine fluorescein 126

In a reversal of the initial synthetic route of the fluorescent pyrannosylamine derivative **125a**, fluorescein isothiocyanate **123** was reacted with ethylenediamine **120** via nucleophilic addition. In a variation of a previously reported synthesis[109], a

large excess of ethylenediamine was reacted with fluorescein isothiocyanate in order to favour the formation of the mono-fluorescein product **126**. While it was anticipated that the subsequent reaction with a carbohydrate would yield the same generic target compound **125**, the revised methodology was devised so that it would afford a general fluorescent marker which could be attached to any sugar molecule with an unprotected hydroxyl at the anomeric centre, via a one-step nucleophilic substitution.

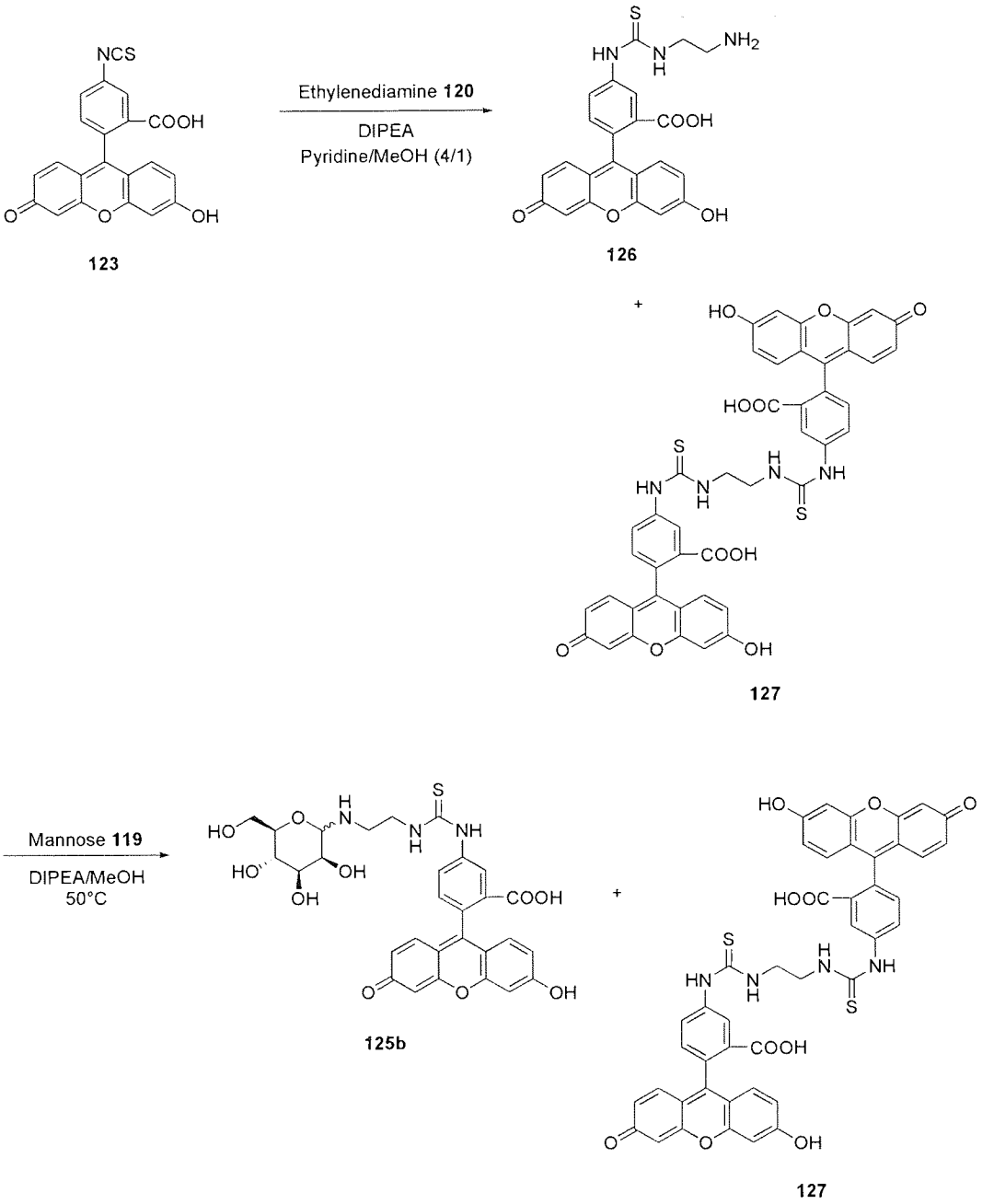

Reaction Scheme 34: Reaction of ethylenediamine 120 with fluorescein isothiocyanate 123 to yield the amine functionalised fluorophore 126 and di-fluorescein ethylenediamine 127. Subsequent reaction with mannose 119 yields a single mannopyranosylamine product 125b.

The presence of the target compound **126** was confirmed by HRMS, however the ^{1}H NMR spectrum was complicated by the presence of the di-fluorescein product **127**, and the resonance forms which fluorescein can adopt. Separation and purification of the thiocarbonyl ethylenediamine fluorescein **126** was not attempted. It was envisaged that reacting the crude mixture with mannose **119** would result in a

fluorophore/carbohydrate-fluorophore mixture which had the potential for purification by utilising Quadramide-phenylboronic acid **88** as a scavenger resin.

4.2.4 D-Mannopyranosylamine-ethyl-thioureido-fluorescein 125b

The formation of a single carbohydrate product **125b** from the reaction pathway afforded by utilising the fluorescein derivative **126** raised the potential for scavenging the carbohydrate product **125b** from the mixture. This approach was to have exploited the affinity that boronic acid compounds such as Quadramide-phenylboronic acid **88** have the for *cis* 1,2 or 1,3 diols often contained within sugars. Unlike the reaction pathway incorporating **121**, the by-product of this reaction (**127**) does not contain such a diol, so the practice of scavenging with boronic acid and subsequently cleaving would afford a process of enriching the fluorescent carbohydrate compound.

Accordingly, an attempt was made to couple thiocarbonyl ethylenediamine fluorescein **126** with mannopyranose **119**, using the reaction conditions previously used to attach the ethylenediamine linker to the monosaccharide[105]. Analysis by HRMS identified compounds with mass equal to that of the fluorescent monosaccharide **125b** and the di-fluorescein ethylenediamine **127**. An attempt was made therefore, to purify and enrich the fluorescent carbohydrate **125b** by the same 'catch and release' method successfully employed for the non-fluorescent carbohydrates. The Quadramide-phenylboronic acid resin **88** underwent an observable colour change during the pyridine-mediated incubation step, which was not removed by washing. This colour change was reversed during the citric acid-mediated cleavage step. Characterisation of the concentrated cleavage solution enabled citric acid to be identified, however NMR analysis failed to show any aromatic signals arising from protons within the fluorescein moiety. HRMS identified a compound with mass equal to citric acid, but not of the target compound or any likely fragmentation products.

Although purification of the target compound should, in theory, have been achievable by chromatography, the 'catch and release' technique is at the heart of the

methodology envisaged for the bioassays of combinatorial libraries in the end stage of the planned research. Accordingly, further purification was not attempted as compound **125b** was of little relevance beyond this test of the 'catch and release' technique.

4.3 Labelling vancomycin

Although characterisation of carbohydrates labelled in a similar manner had proved inconclusive, it was hoped that labelling of the vancomycin would be more fruitful. The synthesis and use of chromophore/fluorescent tagged vancomycin utilising *o*-phenylenediamine[110], BODIPY[111,112,113,114,115] and fluorescein derivatives[115,,116] has been previously reported. The addition of a diamine linker to vancomycin was attempted on the basis of a literature precedent[117], which would afford a position of attachment for a fluorophore.

4.3.1 Amino-butylamido-Vancomycin 129

Derivatisation of vancomycin via Reaction Scheme 35 has been previously described by Metallo *et al*[117] in 2003. The paper describes a method of creating a point of attachment on the vancomycin, enabling the subsequent coupling of the vancomycin-diamine conjugate to polyacrylamide. For the purposes of this study, interest lay in the potential to use this conjugate as a way of fluorescently labelling the vancomycin in a manner which should not compromise the bioactivity of the antibiotic.

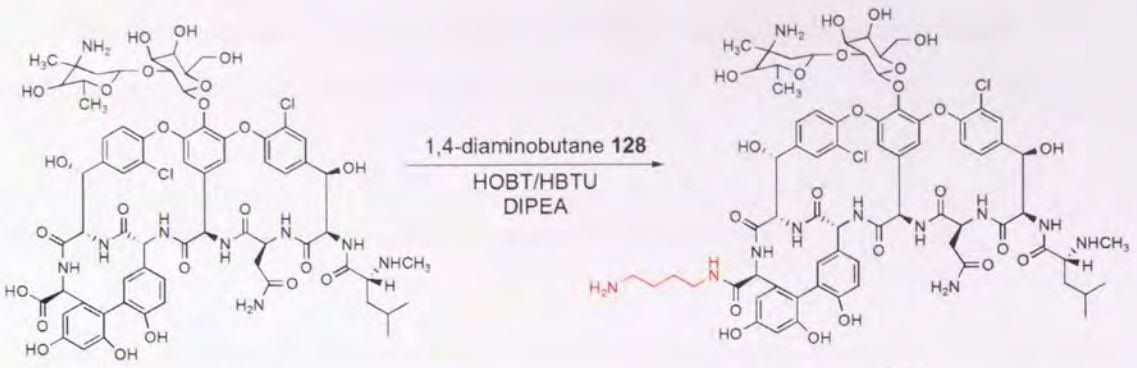

Vancomycin 9 129

Reaction Scheme 35: Coupling 1, 4-diaminobutane 128 to Vancomycin 9 via the activated vancomycin-ester intermediate afforded by HBTU to produce an amine functionalised derivative 129.

The coupling of 1,4-diaminobutane **128** and vancomycin **9** proceeded according to the prescribed method[117], whereby the precipitate obtained by adding DCM to the reaction mixture was filtered and washed with additional aliquots of DCM, before being dried to constant mass.

Analysis of the material by ^{1}H NMR spectroscopy gave a spectrum that had very poor resolution, which could not be improved upon. The similarity of the product to the starting vancomycin meant that the two compounds were not of sufficiently different polarities to be distinguished by R_f values or reactions of the spots to different staining techniques. Analysis by FTIR again resulted in the inability to distinguish the two compounds.

Initial attempts at obtaining the mass spectra also met with failure. No peaks were observed under standard atmospheric pressure chemical ionization (APCI) or electrospray conditions. Measurements obtained using the Fast Atomic Bombardment technique (FAB-MS) have previously been reported for vancomycin[118]. Accordingly, samples for FAB-MS were sent to Dr. P. R. Ashton at the University of Birmingham's School of Chemistry, a renowned expert on mass spectrometry, for analysis. Positive analysis of vancomycin, the target compound, and indeed all of the subsequent derivatives could not be achieved, even when

analysis was expanded to include a variety of other mass spectroscopy-based techniques available at Birmingham University.

4.3.2 Fluorescein-thioureido-butylamido-Vancomycin 130

Although it was not possible to characterise the vancomycin conjugate **129**, the crude product was carried forward and reacted with fluorescein isothiocyanate.

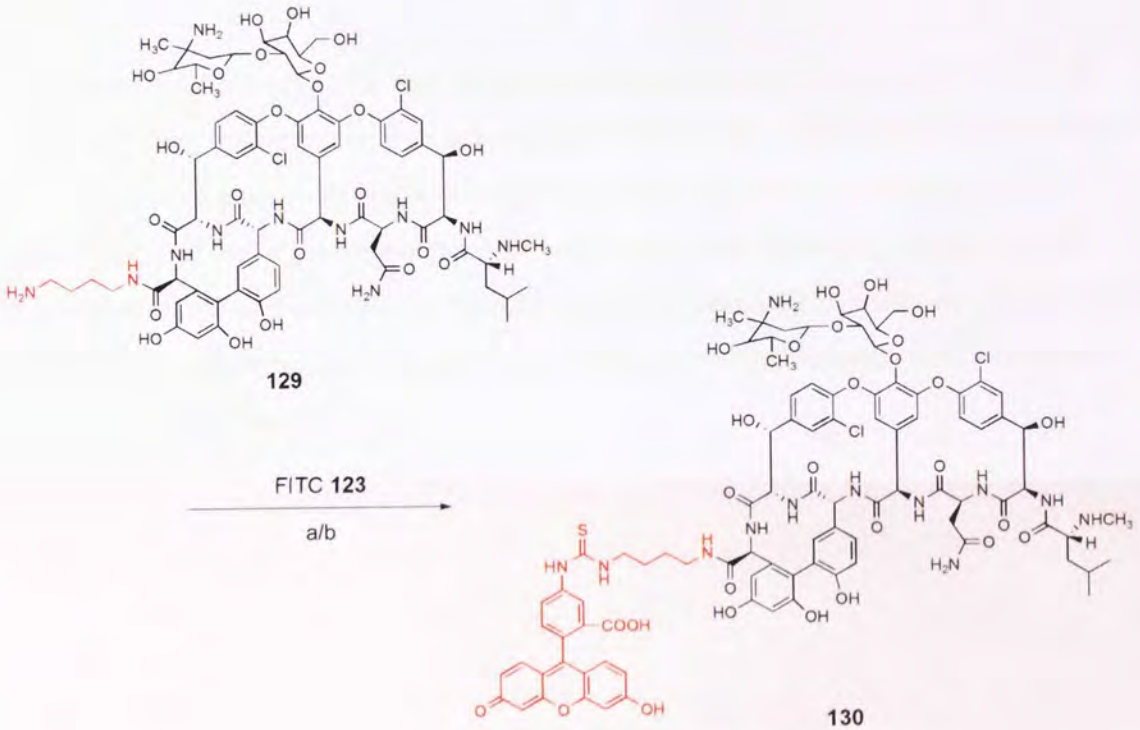

Reaction Scheme 36: Addition of FITC utilising two different sets of reaction conditions; a)[119] FITC (1.1 eqv. w.r.t. Vancomycin) Pyridine/water (3:1) with DIPEA; b) FITC, HOBT, HBTU, DIPEA (4:4:4:6 eqv. w.r.t. Vancomycin) in DMF. In both cases the fluorescent Vancomycin derivative is precipitated by adding a large volume of DCM to the reaction mixture.

The coupling of the fluorophore was performed in two different ways. Route a) was based a variation of the previously described method by Fernandéz *et al*[119] employing pyridine and DIPEA. Route b) follows a standard HBTU coupling procedure, most commonly used during peptide synthesis.

Characterisation for each fluorophore-vancomycin conjugate was attempted, but ultimately was unsuccessful. NMR spectra could not be produced with sufficient resolution to allow ready interpretation. FTIR peaks of medium intensity at 1111 cm^{-1} and 1114 cm^{-1} could arise from the formation of the thiourea, with the characteristic isothiocyanate signal (~2090 cm^{-1}) being absent from both samples. By itself however, infrared analysis cannot determine the success of the reaction.

4.3.3 Fluorescein-thioureido-ethylamido-Vancomycin 131

Labelling of the vancomycin was attempted using the same theory as the 'reversed' sugar labelling, whereby the thiocarbonyl ethylenediamine fluorescein **126** is reacted directly with vancomycin. Unlike the carbohydrate, vancomycin possesses a carboxylic acid moiety where attachment via amide bond formation could proceed. Activation of the carboxylic acid was afforded via a standard uronium activation step using HBTU, allowing the coupling to proceed in a manner analogous to a standard peptide coupling reaction.

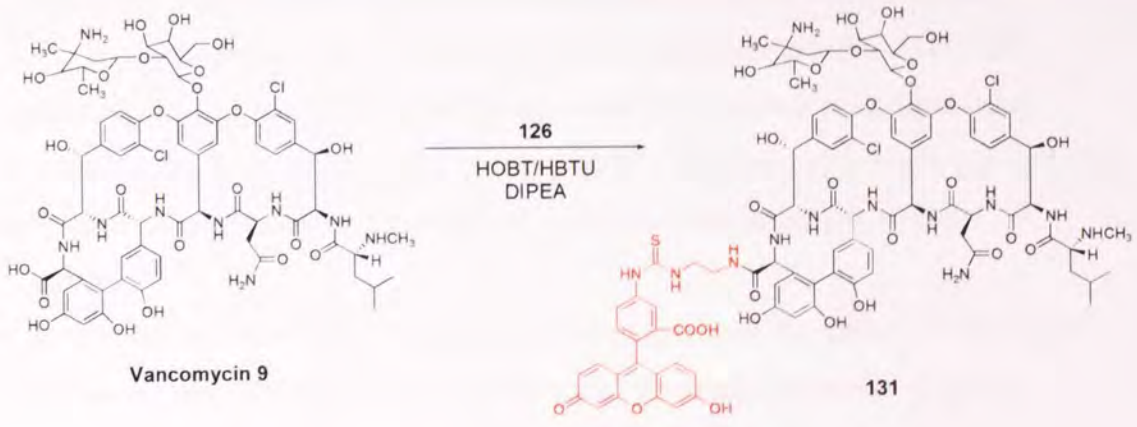

Reaction Scheme 37: Coupling of amino-ethyl-thioureido-fluorescein 126 to afford a fluorescent vancomycin derivative 131.

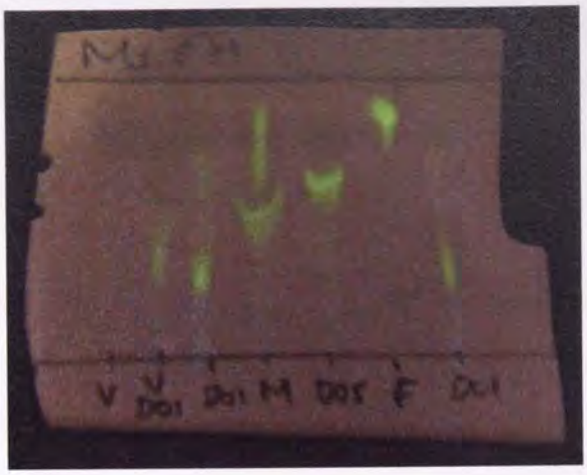

Photo 3: TLC (100 % MeOH); Left to right; Vancomycin, 126/vancomycin co-elution, 126, Mix lane, 131, FITC, 126.

TLC analysis suggested the successful formation of a fluorescent compound (lane 5) with $R_f = 0.63$. Lane 3 shows two spots, compound **126** ($R_f = 0.27$) and the di-fluorescein ethylenediamine **127** ($R_f = 0.70$). Vancomycin (lane 1) does not fluoresce, but co-elution with **126** (lane 2) produces a single spot with $R_f = 0.35$. Fluorescein isothiocyanate (lane 6) has an $R_f = 0.86$. The separation of the compounds shows that the product spot **131** does not correspond to FITC **123**, compound **126**, or the di-fluorescein compound **127**. Co-elution of the starting materials (lane 2) seems to 'slow' the separation of the two compounds **126** and **127** to produce a single spot, which is also distinct from the target compound.

Characterisation was unable to provide data that conclusively identified the target compound. Accordingly, it must be concluded that while the results suggest a measure of success, without proper characterisation of the various derivatives, successful labelling cannot be proved irrefutably.

The attachment of fluorescent markers to the saccharides and vancomycin was a logical step in the development of the final assay technique. Fluorescence provides a visual confirmation of success, and can be easily quantified. The inconclusive results regarding attachment of the fluorescein, along with the inability to purify any such compound would make quantification of subsequent libraries impossible. Question

marks over the nature of the fluorescent attachment also raise concerns. Fluorescein may have detrimental effects on the binding characteristics, either by preventing binding completely, or by causing the fluorescent antibiotic to be incomparable to previously published work on vancomycin binding.

Consequently, assessing the library screening by the quantification of fluorescent tags was deemed unsuitable. Subsequent assays use the natural, 'naked' form of vancomycin, and employ a different means of quantification.

Chapter 5

Library Synthesis, Validation and Analysis

Library Synthesis, Validation and Analysis.

The following chapter describes the synthesis of a library of peptidyl-resin compounds, along with a complementary boronic acid containing library. The chapter then goes on to describe the development of a bioassay, using vancomycin in conjunction with methicillin-resistant *Staphylococcus aureus*, to enable quantification of vancomycin binding to the array of library compounds.

5.1 Design of the combinatorial library

As described in **section 3.5**, vancomycin binding is based on the *N*-acyl-D-Ala-D-Ala-OH peptide sequence. Inclusion of Fmoc-D-Ala-OH was crucial to the validity of the library. Although post cleavage manipulation of the peptides could be used to afford the D-Ala-D-Ala-OH compound, the labour and time required to make even a modestly sized combinatorial library using this method would be prohibitive, especially given the calculated yields for **108** of <20 %. Accordingly, the Fmoc synthetic strategy was employed in the construction of the library, although this would ultimately lead to the reverse, D-Ala-D-Ala-NH_2 derivative being formed. Although it has been previously reported that such a derivative does not combine with vancomycin[98], this approach was deemed to be the only available method of generating a large number of library compounds. The presence of boronic acid moieties within the library also raised the possibility of a 'reverse' sequence binding to vancomycin. The unknown effect of adding boronic acid to a sequence acknowledged not to bind was of great interest and legitimised the adopted Fmoc synthetic strategy.

A simple tetrapeptide library consisting of sequences based on the **L-2** 'core' (Quadramine resin **62** with Gly and Lys(Dde) **78** residues attached) with the addition of a further 2 amino acids was designed. A range of amino acids were selected for inclusion in the library. Glycine was included as the linker to the base resin and therefore not included again in the sequence. Cysteine and methionine were omitted due to the presence of sulphur. Methionine can have major problems such as

alkylation and oxidation[120,51] while cysteine has the added challenge of the potential to form disulphide bridges.

Leucine, isoleucine and valine are nonpolar aliphatic molecules with very similar properties. Accordingly, leucine was chosen for inclusion at the expense of the other two. Although any peptide sequence will have some degree of secondary structure, proline was excluded due to the turns it introduces. The fused ring also introduces a significant degree of conformational rigidity which was deemed unlikely to be of benefit when trying to bind to the active site of the vancomycin molecule. In all, 8 amino acids were selected, covering a range of different amino acid side chains and thus properties (Figure 35).

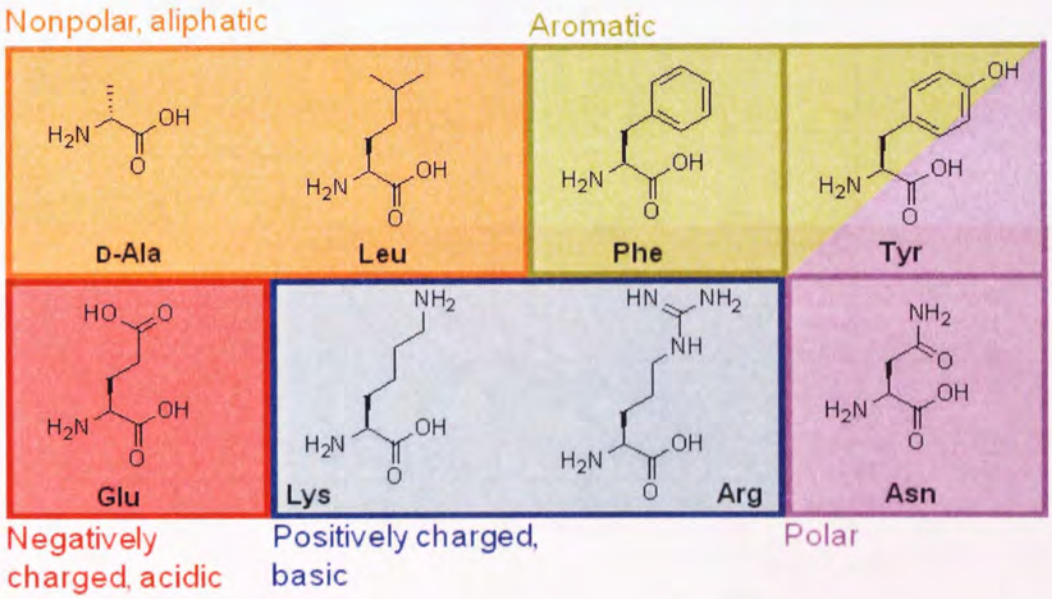

Figure 35: The range of properties of the 8 selected amino acids. Alanine is utilised as the D-enantiomer, whereas the other 7 amino acids are in the L-formation. Any subsequent reference to alanine for synthesis purposes is taken to explicitly mean D-Ala.

Coupling the **L-2** core to each of the eight amino acids generated eight compounds, each of which was coupled to each of the eight amino acids. This second coupling procedure generated 64 compounds (Figure 36). Dividing this library into two, and coupling boronic acid to one half of the compounds doubled the library total, affording 128 compounds for use in incubation assays with vancomycin (Figure 37).

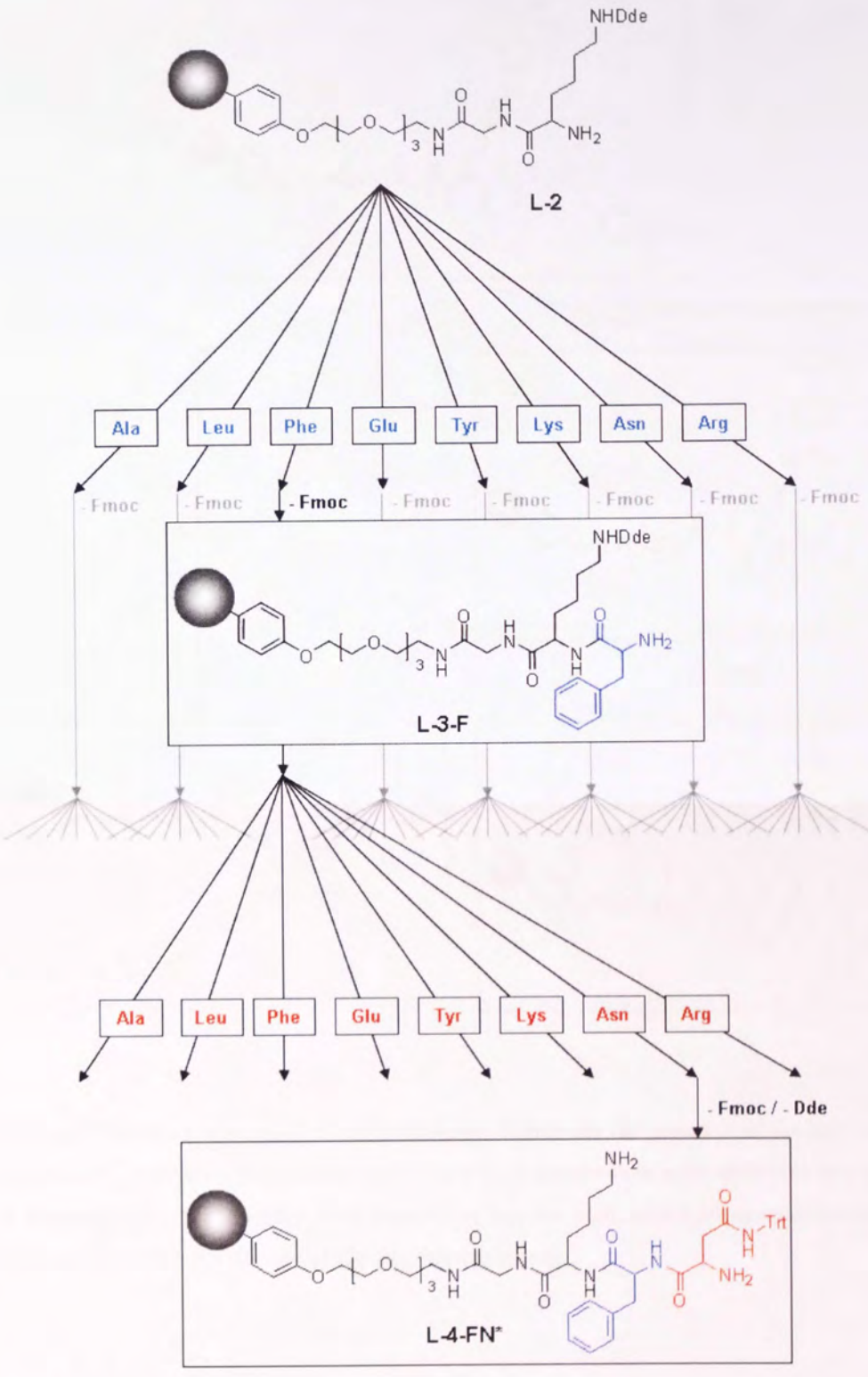

Figure 36: A schematic showing the synthetic route of one of the 64 possible compounds in the library. Attachment of a single 'blue' amino acid, followed by splitting and subsequent coupling of a 'red' amino acid affords the 64 combinations of 8 amino acids in a sequence of 2.

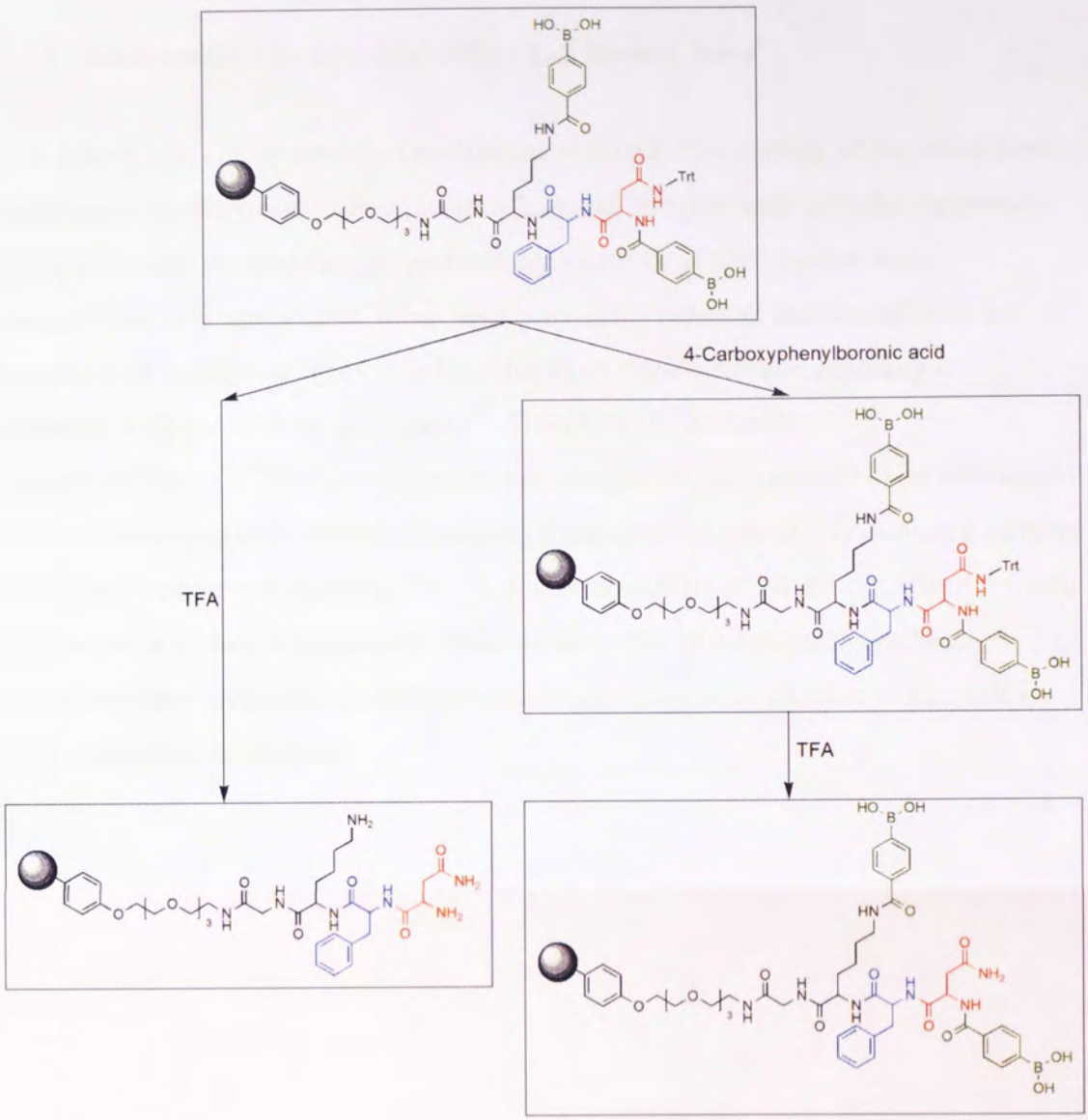

Figure 37: Designations which contain the letter B indicate the presence of boronic acid units at the *N*-α-AA_4 and *N*-ε-Lys amine groups. The 64 L-4 compounds were split into two and are used to generate a further 64 compounds containing boronic acid, which when combined with the original 64 afforded a library of 128 peptide sequences.

5.1.1 Quadramide-Gly-Lys(Dde)-NH_2 - L-2 library 'core'

The library was constructed on Quadramine resin **62**. The loading of the compound had been accurately established (**section 2.2**) and its agreement with the theoretical value identified the resin as one particularly suited to SPPS. Glycine was incorporated as a spacer unit. It has been previously reported that the affinity for vancomycin is affected by the third residue from the *c*-terminus, reaching an optimum with L-ornithine or L-lysine[98]. Therefore the inclusion of Fmoc-Lys(Dde)-OH **78** allowed for the introduction of boronic acid in an orthogonal manner in the presence of other protecting groups, while potentially avoiding adverse effects on vancomycin binding. The 'in-house' synthesis of **78** did not afford the title compound in a yield which would allow its inclusion in subsequent syntheses, therefore Fmoc-Lys(Dde)-OH **78** was purchased along with all other amino acids from a commercial supplier.

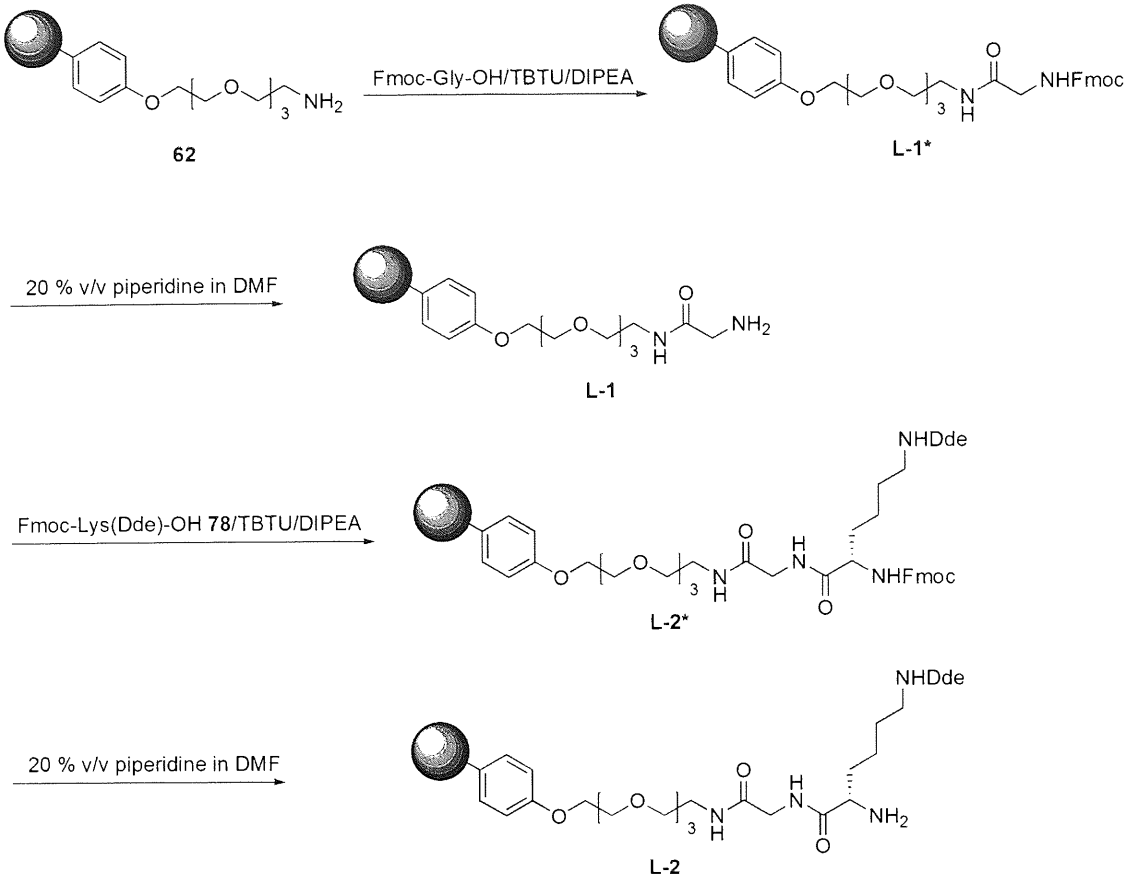

Reaction Scheme 38: Construction of library 'core' compound L-2. Compound designations follow a common rule; L denotes a library compound, the number denotes the number of amino acids attached to the base resin, 62. The presence of an asterisk denotes a peptide sequence which contains one or more protecting groups (not including Dde).

Quadramide-Gly-Lys(Dde)-NH_2 **L-2** was synthesised in a stepwise manner using the previously established TBTU method and isolated in a 100 % yield. Analysis by FTIR showed the successful addition of the Dde containing moiety, evidenced by a strong signal associated with the enol form of the diketone (1558 cm^{-1}). Removal of the *N*-α-Fmoc protecting group was confirmed by Kaiser resin assay and a broad IR signal at 3287 cm^{-1} attributable to the N-H stretch of a primary amine.

5.1.2 Library construction; L-3 sub library

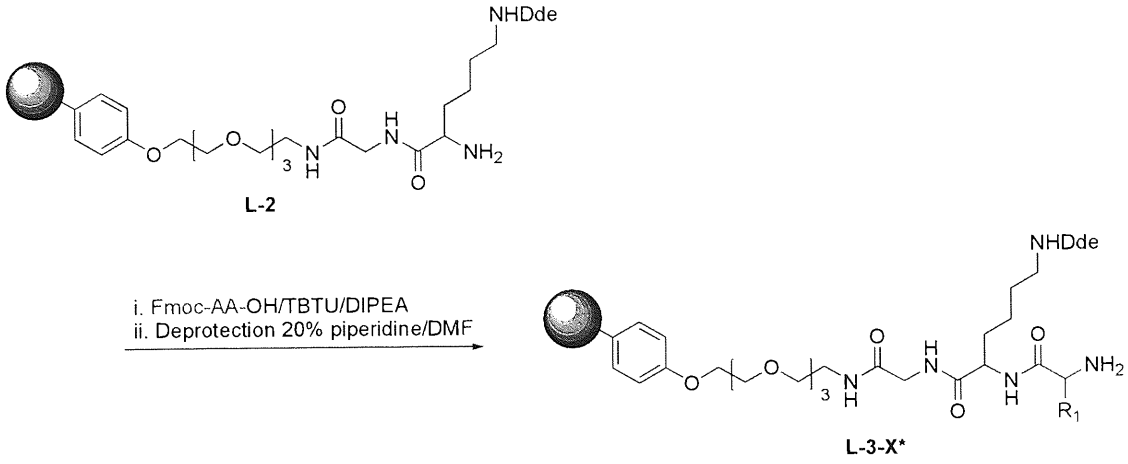

Reaction Scheme 39: Propagation of L-2 to form L-3-X*

Use of the Fmoc protecting group alongside the Dde group afforded orthogonality within the library precursor compound **L-2**. Accordingly, to maintain the ability for selective positioning of the boronic acid units, protecting groups which were orthogonally cleavable in the presence of both Fmoc and Dde were required. As both Fmoc and Dde are cleaved in basic conditions, the library synthesis employed acid labile protecting groups on the amino acid side chains.

Table 15: Amino acids utilised in the library synthesis, with conditions of side chain deprotection

Amino Acid	Cleavable unit	Cleavage conditions
Fmoc-D-Ala-OH	-	-
Fmoc-Leu-OH	-	-
Fmoc-Phe-OH	-	-
Fmoc-Glu(OtBu)-OH	tBu	90 % v/v TFA, 30 mins.[121]
Fmoc-Tyr(tBu)-OH	tBu	90 % v/v TFA, 30 mins.[122]
Fmoc-Lys(Boc)-OH	Boc	90 % v/v TFA, 30 mins.[123]
Fmoc-Asn(Trt)-OH	Trt	90 % v/v TFA, 30-60 mins.[124]
Fmoc-Arg(Pbf)-OH	Pbf	95 % v/v TFA, 30 mins.[125]

Library precursor compound **L-2** was divided into 8 equivalent aliquots of resin. Each of the 8 peptidyl-resin sequences, **L-2**, was extended by a further amino acid by employing the stepwise TBTU coupling methodology previously described to afford 8 different compounds. In each case, successful addition of the amino acid and subsequent removal of the Fmoc protecting group was confirmed by Kaiser resin test.

The 8 compounds, each with 3 amino acids coupled to the base resin **62**, were given the designation **L-3-X***. Since there is a common 'core' molecule, **L-2**, only the final amino acid (X) is specifically referred to in the compound designation. The asterisk denotes the presence of one or more unspecified protecting groups. For example, although after Fmoc deprotection the sequence **L-3-A** does not contain a protecting group, the asterisk designation is still utilised until it has also undergone treatment with TFA. This ensures that all compounds are treated equally throughout the synthesis and therefore the designation of this compound remains as **L-3-A*** for conformity.

5.1.3 Library construction; L-4 sub library

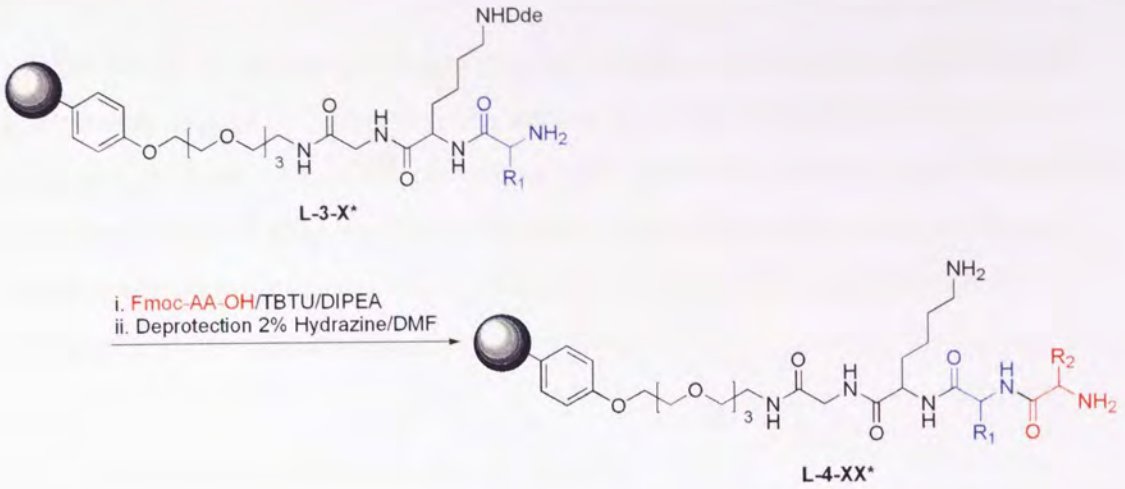

Reaction Scheme 40: Propagation of L-3-X* to form L-4-XX*

Each of the 8 library **L-3-X*** compounds was further divided into 8 equal aliquots of resin to afford a total of 64 batches of resin. Each of the 64 peptidyl-resin batches was extended by a single amino acid, again employing the stepwise TBTU methodology, to afford 8 different compounds within each of the 8 sub libraries. Successful addition of the amino acid was confirmed by a negative Kaiser resin test.

Simultaneous cleavage of the *N*-α-Fmoc and *N*-ε-Dde protecting groups was achieved by agitating each peptidyl-resin with 2 % v/v hydrazine in DMF. This provided each of the 64 compounds with two potential sites for reaction with 4-carboxyphenylboronic acid. The 64 different peptidyl-resin sequences were each divided in two to create 128 batches of resin. Half of these were employed in the construction of the **L-4B** sub library (see **Section 5.1.4**.).

The remaining half was treated with TFA to remove the remaining acid-labile protecting groups. Table 15 details the cleavage conditions for the 5 amino acids containing acid-labile groups. The highest concentration required is 95 % v/v TFA, while the longest incubation time is 60 minutes. To ensure complete deprotection and to ensure each library compound had been exposed to identical reaction conditions,

each of the 64 compounds was subjected to identical acidolysis conditions using a solution of 95 % TFA, 2.5 % TIPS & 2.5 % water for a total of 60 minutes.

Section 2.1.4 and **section 3.3.4** describe the formation of the trifluoromethyl ester group when using TFA. To ensure that any such moiety was eliminated from the library, each of the 64 **L-4-XX** compounds was incubated with a 5 % v/v TEA/DCM solution for 2 hours after the TFA mediated acidolysis procedure. Each resin was washed with copious amounts of DMF and DCM before being collapsed with methanol and dried to constant mass.

5.1.4 Library construction; L-4B sub library

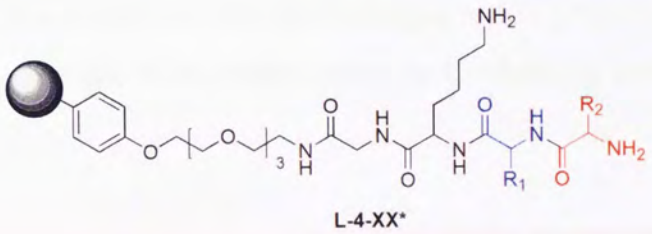

L-4-XX*

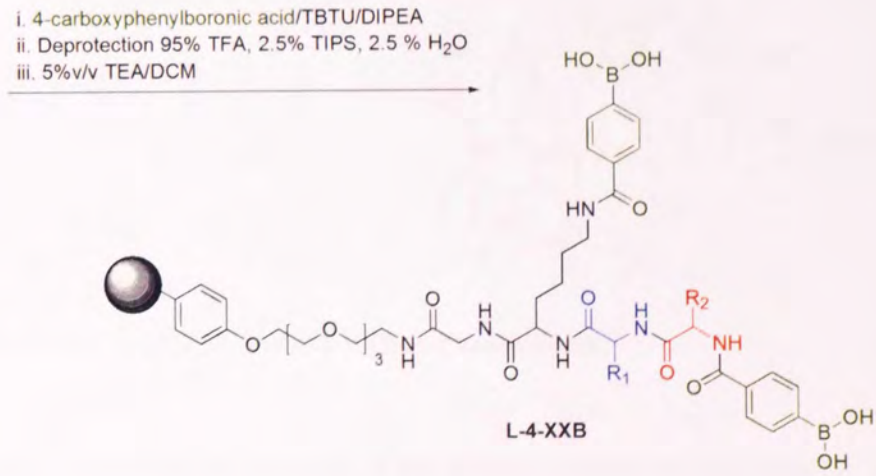

L-4-XXB

Reaction Scheme 41: coupling of 4-carboxyphenylboronic acid to L-4-XX* followed by TFA mediated acidolysis of the protecting groups of amino acids 3 & 4 to yield the L-4-XXB compounds.

4-Carboxyphenylboronic acid was coupled to each of 64 **L-4-XX*** utilising the TBTU methodology to yield the **L-4B*** sub library. Cleavage of the *N*-α-Fmoc and *N*-ε-Dde protecting groups created two positions of attachment of the boronic acid.

The binding motif of the L-4 library was to be based purely on the hydrogen bonding of vancomycin with the backbone of the library compound. Within the L-4B library, coupling of boronic acid to the formerly Dde-protected amine of the *N*-ε-lysine was performed in order to incorporate an additional binding moiety. Its position at the end of the lysine sidechain provided the maximum length between the boronic acid and the backbone, and gave the opportunity for the boronic acid to bind to the diols of the carbohydrate within the vancomycin. Given the relative sizes of the two binding components, it was hoped that any boronic acid binding would be able to act in combination with any hydrogen bonding between the vancomycin and the backbone of the library compound, enhancing the selectivity.

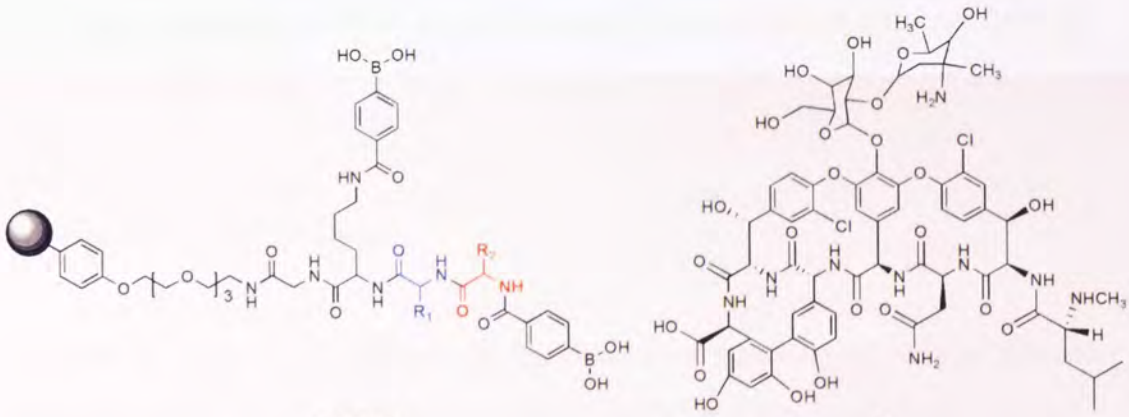

Figure 38: An indication of the similar sizes of L-4-XXB and vancomycin.

Conversely, it was also noted that the position of the boronic acid at the *N*-ε-lysine may give rise to steric hindrance. There was concern that the distance of the boronic acid from the peptide backbone may have been insufficient for the boronic acid to reach the *cis*-diol. This in turn, may have reduced the ability of the boronic acid to orientate correctly with respect to the diol. Accordingly, the presence of the boronic acid may then have become a hindrance, resulting in the blocking of the incoming vancomycin and preventing any hydrogen bonding with the peptide backbone.

In order to provide some certainty of boronic acid-vancomycin interaction, a second boronic acid moiety was incorporated at the *N*-α-amine of residue 4. Although its positioning with respect to the peptide would rule out the concomitant binding of vancomycin to the boronic acid and backbone, the different tertiary structures afforded by the extended peptide sequence would also generate a manner of selectivity, different to that of the L-4 library.

Accordingly, twice the number of moles of boronic acid, TBTU and DIPEA were used in these coupling reactions compared with the standard TBTU couplings. Deprotection was afforded in the same manner as for the **L-4** sub library. After incubation with 5 % v/v TEA/DCM, small samples of resin (~ 1 mg) from **L-4-AAB**, **L-4-LFB** and **L-4-LYB** were subjected to the carminic acid staining assay. Each resin-bound library compound displayed fluorescence upon exposure to UV-B light indicating both the successful coupling of the boronic acid, and that in each case it was free boronic acid residues which were present. Each batch of resin was washed with copious amounts of DMF and DCM before being collapsed with methanol and dried to constant mass.

5.2 Bioassay validation

The inability to positively characterise the fluorescent vancomycin adducts **130** and **131** required the development of a new method of monitoring and quantifying any binding of vancomycin to the array of peptidyl resins.

Vancomycin is a broad spectrum antibiotic that inhibits the growth of Gram-positive bacterial cells[117]. It exhibits a novel receptor-like mode of action, forming complexes with the *C*-terminal D-Ala-D-Ala peptide sequence, preventing its incorporation into the bacterial cell wall[99,126,127,128]. Accordingly, incubation of vancomycin solutions on bacterial plates supporting the Oxford strain (NCTC 6571, ATCC 9144) of methicillin-sensitive *Staphylococcus aureus* (MSSA) colonies would provide zones of inhibition where the vancomycin had diffused through the media. Such zones can be identified easily and quantified.

5.2.1 Incubation of simple resin compounds with vancomycin

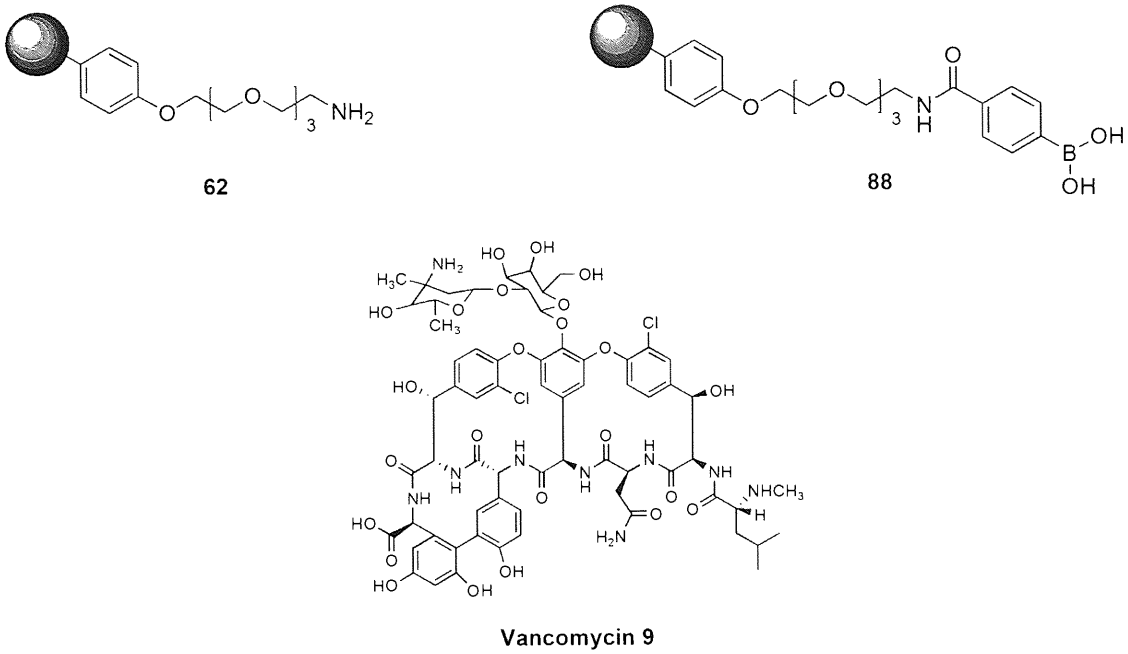

Figure 39: Compounds used for the purposes of the bioassay validation.

The affinity of boronic acid for vancomycin was tested with resin **88**, using resin **62** acting as a control. A solution of vancomycin in pyridine (2.2 mM, 15 ml, 0.033 mmol) was incubated with Quadramide-phenylboronic acid resin **88** (100 mg, loading 0.79 mmol/g, 0.079 mmol) and Quadramine resin **62** (100 mg, 0.89 mmol/g, 0.089 mmol) to afford vancomycin to end group ratios of 0.4:1.

The number of moles of vancomycin was significantly lower than the potential number of binding sites on the resin so that;

1) An excess of vancomycin would not drive the equilibrium in favour of binding.
2) It would be theoretically possible to 'pull' 100 % of the vancomycin from the solution.

The suspension was agitated at room temperature for 30 minutes before the solution was drained and the resin washed with copious amounts of pyridine via Soxhlet extraction for 4 hours. The vancomycin-resin conjugates **62V** and **88V** were then

dried to constant mass. A control of both resins was prepared by subjecting aliquots of **62** and **88** to an identical procedure in the absence of vancomycin.

The Quadramide-phenyl boronic acid-vancomycin conjugate **88-V** was isolated in a yield of 107.8 mg, a mass increase equivalent to 0.005 mmol of vancomycin. This corresponded to 15 % of the vancomycin available in the solution filling 5.6 % of the available boronic acid binding sites. By comparison, both control samples and conjugate **62-V** showed no mass increase, indicating that it was entirely due to the effect of vancomycin binding to the boronic acid units of resin **88**.

Figure 40 shows a general schematic of the incubation process with an example from the completed combinatorial library.

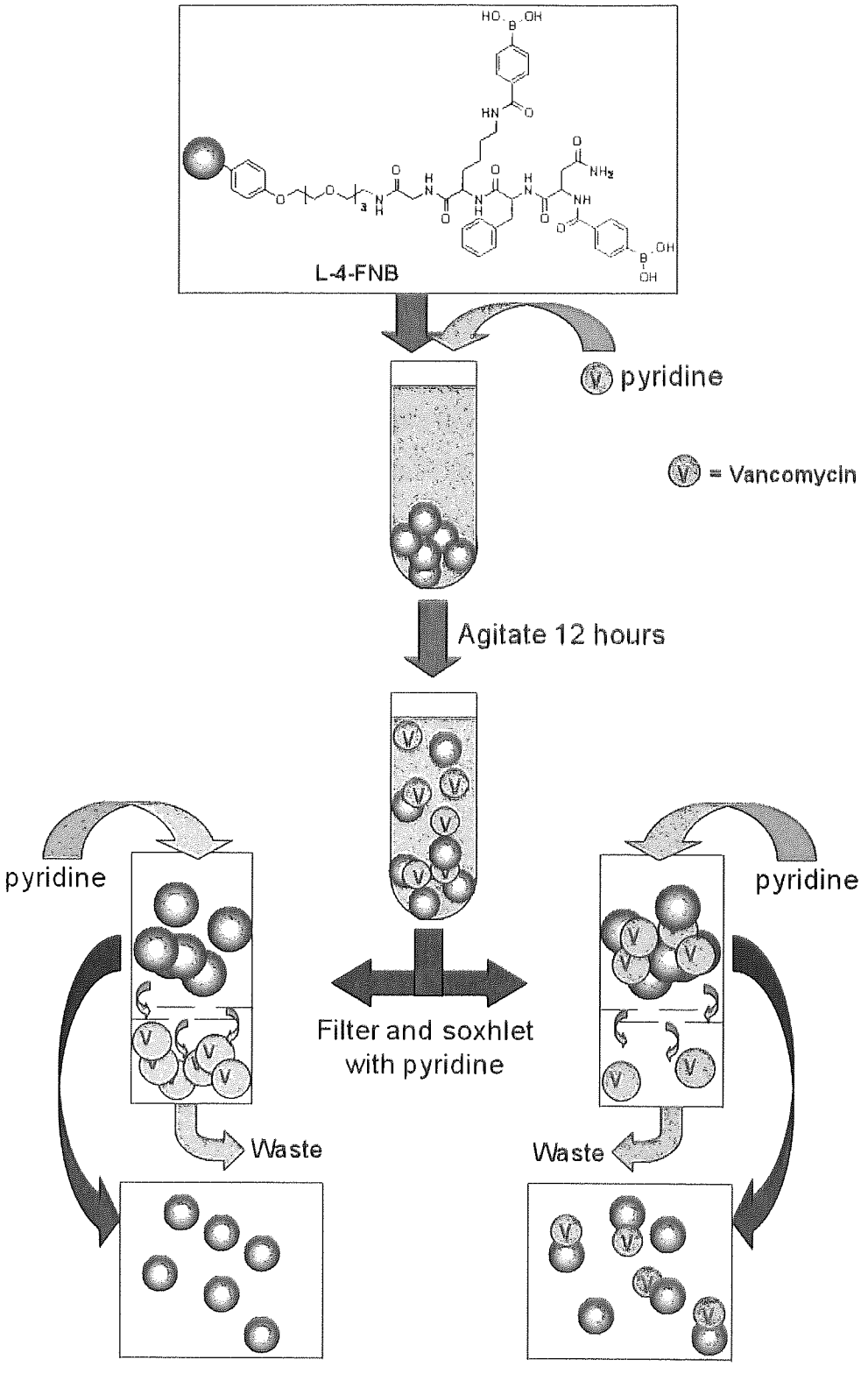

Figure 40: Schematic diagram of the process of incubating vancomycin with a library compound. Vancomycin can show no affinity for the compound (left) or bind to the peptide (right).

5.2.2 Cleavage of vancomycin from the resin

Prior studies with sugars had demonstrated the efficacy of a THF/citric acid solvent system in cleaving carbohydrate moieties from a boronic acid bearing resin; however the effects of such a solvent system on MSSA were unknown.

To test any such effects, the resins **62**, **62-V**, **88** and **88-V** (~5 mg) were incubated in variations of the solvent system (Table 16) for 2 hours. The beads were removed by filtration and the solvent taken to dryness. The citric acid along with any vancomycin was resuspended in the appropriate volume of water, to return the system to the original citric acid concentration.

Neutralisation was afforded by treatment with an aqueous solution of sodium hydrogen carbonate (18 mM). Due to the associated volume increase, the volume of the incubation samples was scaled-up accordingly to maintain the molarity of vancomycin in the assay.

Table 16: Incubation of cleavage solvent system with MSSA

Solvent system	Cleavage vol.	Resuspension	Neutralisation	Incubation vol.
2:1 THF/citric acid (1.5 mM)	1200 µl total	400 µl water	-	40 µl
2:1 THF/citric acid (1.5 mM) with neutralisation	1200 µl total	400 µl water	100 µl $NaHCO_3$ (18 mM)	50 µl
Citric acid (1.5 mM)	400 µl	400 µl water	-	40 µl
Citric acid (1.5 mM) with neutralisation	400 µl	400 µl water	100 µl $NaHCO_3$ (18 mM)	50 µl

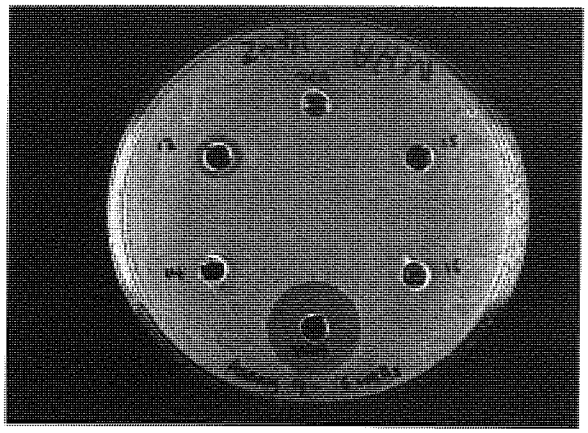

Figure 41: 2:1 THF/citric acid; Clockwise from top; Solvent, 88, 62, Vancomycin std (dissolved in solvent system to 0.67 mM), 62-V, 88-V.

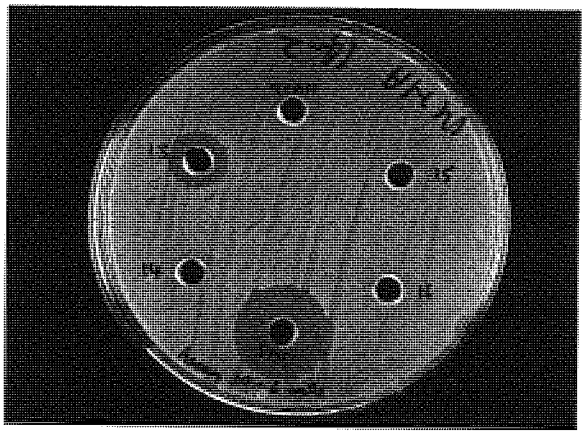

Figure 42: 2:1 THF/citric acid followed by neutralisation; Clockwise from top; Solvent, 88, 62, Vancomycin std (dissolved in solvent system to 0.67 mM), 62-V, 88-V

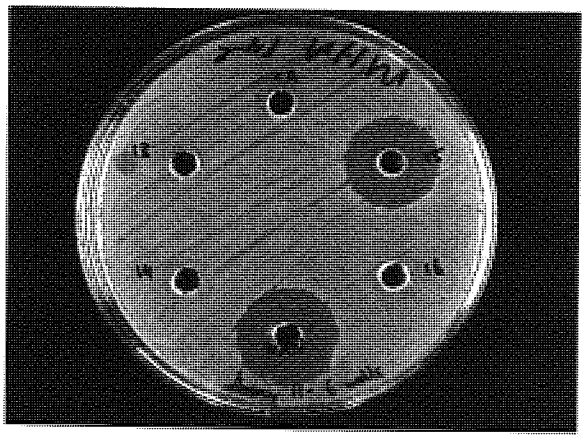

Figure 43: citric acid; Clockwise from top; Solvent, 88-V, 62, Vancomycin std (dissolved in solvent system to 0.67 mM), 62-V, 88.

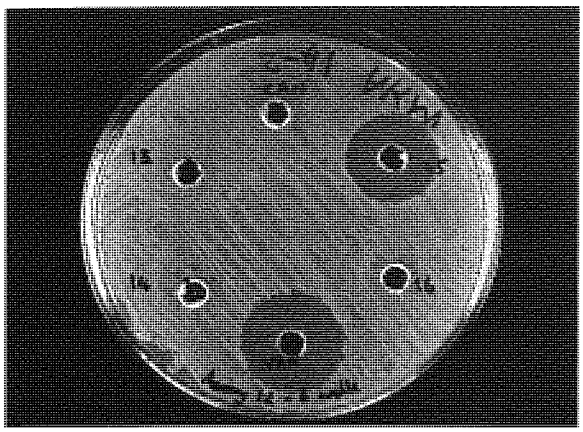

Figure 44: citric acid followed by neutralisation; Clockwise from top; Solvent, 88-V, 62, Vancomycin std (dissolved in solvent system to 0.67 mM), 62-V, 88.

The series of incubations demonstrated that each of the solvent systems employed were not toxic to MSSA. The citric acid solution (Figure 41, well: CA) showed no zone of inhibition, thereby negating the need for neutralisation. Inclusion of the THF component also appeared to have no adverse effects as Figure 41 and Figure 42 demonstrate.

Significantly, the four vancomycin standards (bottom well) still exhibited zones of inhibition, indicating that the solvent systems did not interfere with the biological activity of the antibiotic.

Of most importance are the results from the four samples of **88-V**. Each demonstrated that the biological activity of vancomycin was unaffected by the processes of being bound by the resin and subsequently cleaved from it. The results obtained from this preliminary study also provided good evidence that the idea and methodology of the biological assay was sound. It also indicated that vancomycin was not binding to the base resin. Diffusion of the substrates into the resin matrix had been a major concern prior to conducting the assay. Had this eventuality occurred, the results obtained would have been greatly complicated by diffusion vs. complex formation equilibria. Early trial assays had indicated this was potentially a major problem (data not presented), however switching from copious washing to an extended Soxhlet extraction proved that an adequate washing procedure readily prevented such problems.

Figure 45 shows a general schematic of the acid mediated cleavage process in a continuation of the example from Figure 40.

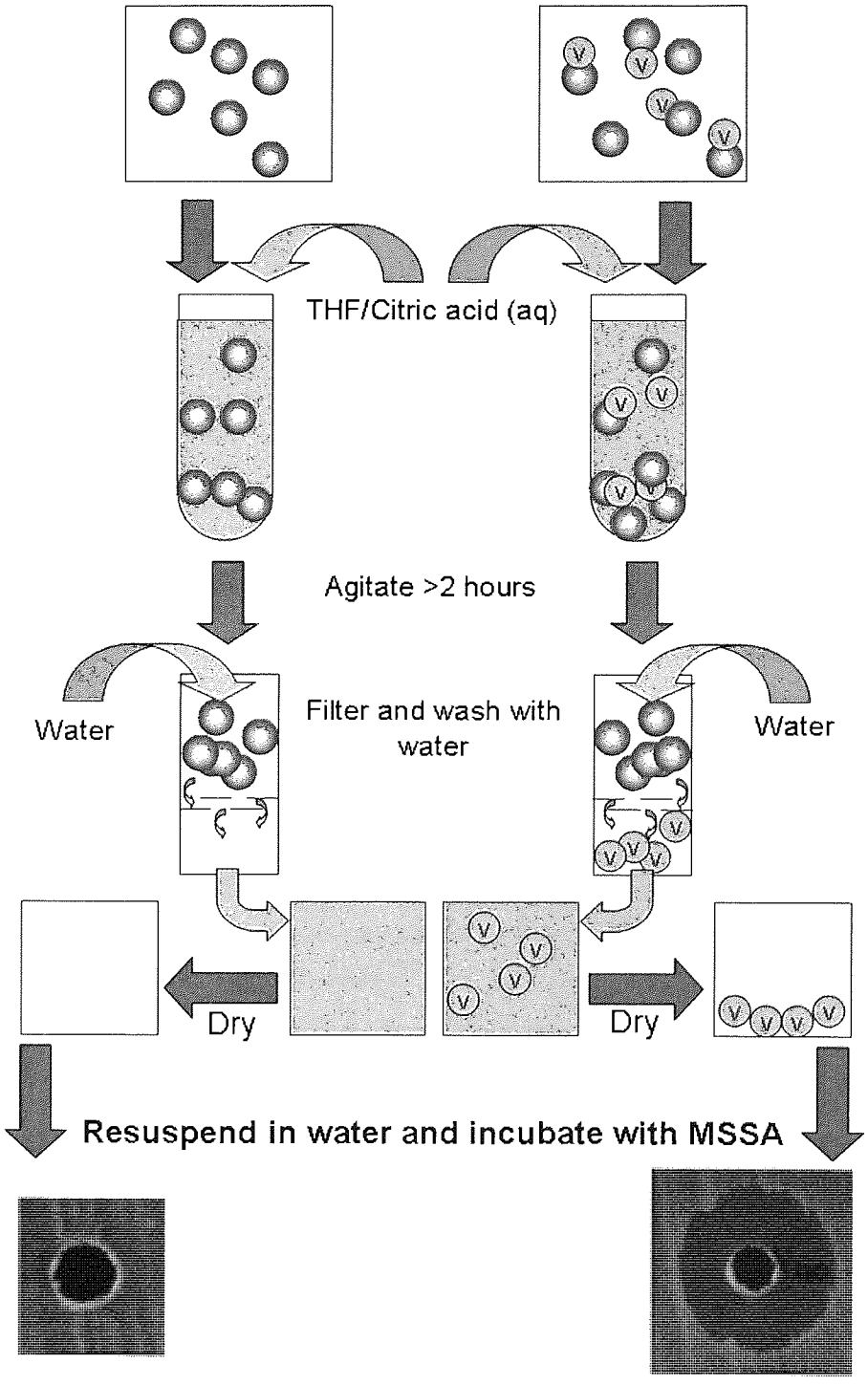

Figure 45: Schematic diagram of the process of releasing vancomycin from a library compound. The cleavage solution containing the vancomycin is then shown to cause areas of inhibition of bacterial growth after screening with a bacterial plate, whereas the citric acid control solution shows no activity.

5.3 The mathematics of diffusion in an ideal 1-D system

Quantification of the zone of inhibition requires a mathematical description of the diffusion of the solute, in this case vancomycin, through a solvent, in this case the growth media. The diffusion equation (Equation 9)[129] is a second-order differential equation with respect to space and first-order with respect to time. Specifying boundary conditions yields an equation which describes diffusion in one dimension (Equation 10)[129].

Equation 9

$$\frac{\delta c}{\delta t} = D\frac{\delta^2 c}{\delta x^2}$$

Equation 10

$$c(x,t) = \frac{n_0}{A(\pi Dt)^{1/2}} e^{\frac{-x^2}{4Dt}}$$

c, concentration is expressed in terms of the distance travelled (x), and time (t). The initial condition at t=0 is that n_0 moles are concentrated in an area A at x=0. D is the diffusion coefficient and is constant for a given system.

A bacterial plate is placed flat upon a surface occupying the *xy*-plane. Spotting the solute on the surface of the growth media causes the solute to diffuse outwards in a circular motion along the *xy*-plane. As the growth media also has an element of depth, this situation also introduces diffusion occurring along the *z*-axis; Figure 46.

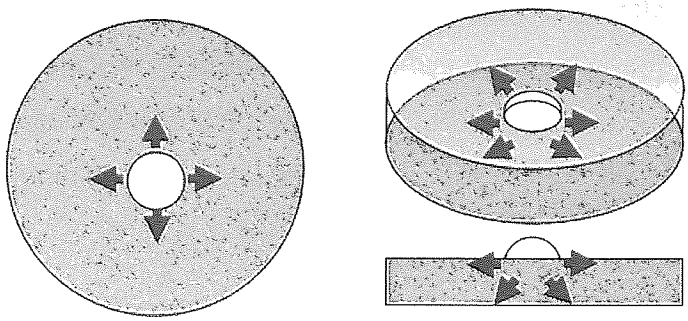

Figure 46: Spotting a solution on the surface creates diffusion over 3-dimensions.

In the current study, a bacterial plate was placed flat upon a surface occupying the *xy*-plane. The solute was placed within a well cut into the solvent medium, equal to the depth of the growth media (Figure 47). By completely filling the well, diffusion can be said to have occurred only in the *xy*-plane. The solution therefore requires a 2-dimensional expression.

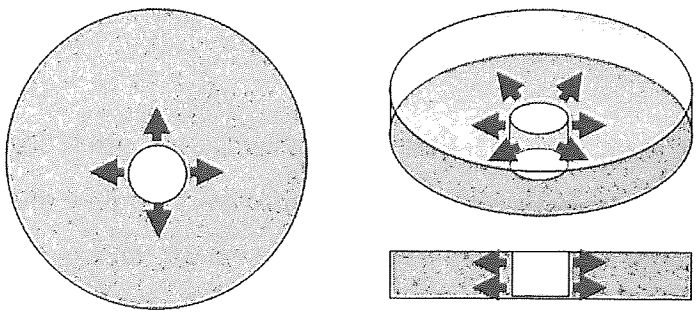

Figure 47: A bore hole is created in the media where the vancomycin solution is placed, allowing the diffusion characteristics to be approximated as diffusion in just the *xy*-plane.

The progression from an exact 2D solution to a 1D approximation depends on the relative diameters of the well and the diffusion circle. Figure 48 shows the example of a solute diffusing from a central well (black) giving rise to zone of inhibition (grey) (Figure 48a). The well can be assumed to be a point of negligible diameter at the centre of the plate. Accordingly, the well of negligible diameter also has negligible circumference. In the expansion, (Figure 48b) it can be seen that the

sectors formed by placing radial lines are in fact sectors of a circle, where the length of the external circumference is much greater than the (negligible) length of the circumference contained within the well. Any diffusion from a point in the well can therefore not be modelled one dimensionally.

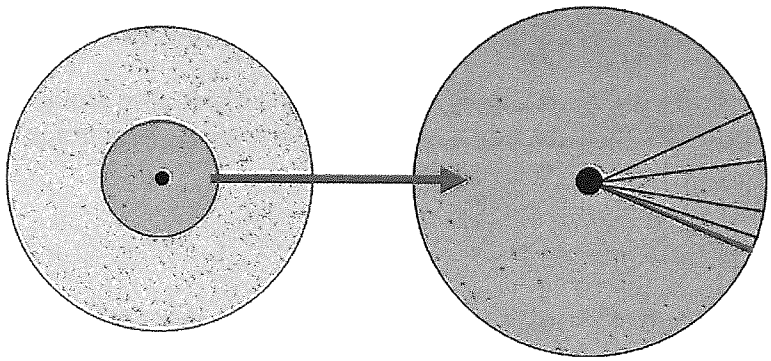

Figure 48: Expansion of the zone of inhibition (grey area) when the antibiotic is added at a point on the plate.

In the system of the study, the diameter of the well is significant, and proportionally large in comparison with the zone of inhibition of the sample (Figure 49). Placing radial lines emanating from the centre of the well again creates sectors. If the distance between radial lines tends to zero, the radial lines within the zone of inhibition become closer to being parallel. Accordingly, diffusion within this sector of parallel lines occurs in only *one* direction. Consequently, it is possible to describe the zone of inhibition as being made up of an infinite number of parallel sectors of length *(radius zone inhibition - radius well)*. As long as the diameter of the well is proportionally large (well radii:zone of inhibition radii $\geq$ 1:3) when compared with the zone of inhibition, the system can be described by the 1D mathematical model.

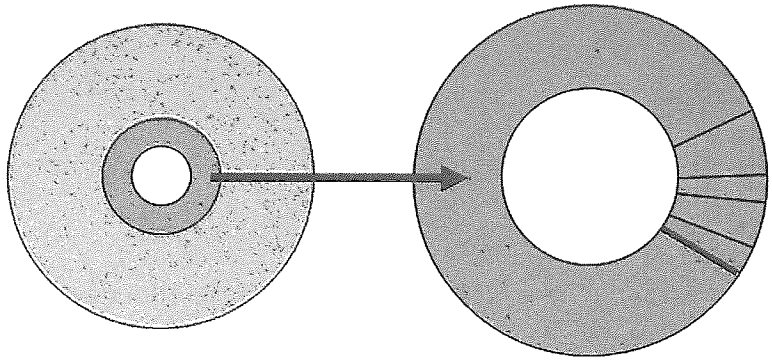

Figure 49: Expansion of the zone of inhibition (grey area) when the antibiotic is added into a well on the plate.

The initial concentration of vancomycin (c_1) can be expressed in terms of the initial time (t_1) and initial radius of the area of cell inhibition (x_1); Equation 11[129].

Equation 11

$$c_1(x_1, t_1) = \frac{n_0}{A(\pi D t_1)^{1/2}} e^{\frac{-x_1{}^2}{4Dt_1}}$$

Similarly the concentration at the boundary of cell death (c_2) at time t_2 can be expressed in terms of the radius of the area of cell inhibition (x_2) (Equation 12).

Equation 12

$$c_2(x_2, t_2) = \frac{n_0}{A(\pi D t_2)^{1/2}} e^{\frac{-x_2{}^2}{4Dt_2}}$$

Dividing Equation 12 by Equation 11 gives Equation 13.

Equation 13

$$\frac{c_2}{c_1} = \frac{{t_1}^{1/2} e^{-\frac{{x_2}^2}{4Dt_2}}}{{t_2}^{1/2} e^{-\frac{{x_1}^2}{4Dt_1}}}$$

Equation 13 can be simplified to give Equation 14.

Equation 14

$$\frac{c_2}{c_1} = \left[\frac{t_1}{t_2}\right]^{1/2} e^{\left[\frac{{x_1}^2}{4Dt_1} - \frac{{x_2}^2}{4Dt_2}\right]}$$

Taking the natural logarithms of both sides yields Equation 15.

Equation 15

$$ln\left[\frac{c_2}{c_1}\right] = \frac{1}{2} ln\left[\frac{t_1}{t_2}\right] + \frac{{x_1}^2}{4Dt_1} - \frac{{x_2}^2}{4Dt_2}$$

By definition:

Equation 16

$$ln\left(\frac{c_2}{c_1}\right) = ln\ c_2 - ln\ c_1$$

Substituting the principal established in Equation 16 into Equation 15 yields Equation 17.

Equation 17

$$-ln\ c_1 = -ln\ c_2 + \frac{1}{2} ln\left[\frac{t_1}{t_2}\right] + \frac{{x_1}^2}{4Dt_1} - \frac{{x_2}^2}{4Dt_2}$$

The initial concentration within a sample is now expressed in terms of t_1, t_2, x_1 and x_2. The concentration at the boundary of cell death (c_2) is assumed to be the same across all samples as this is the critical concentration at which there is no longer enough vancomycin to kill the cells. Similarly t_1 and t_2 are identical across the samples. Therefore the initial concentration of vancomycin (that which was bound to the resin) can be measured according to the radius of the area of cell inhibition.

Equation 18

$$-ln \propto -\frac{{x_2}^2}{4Dt_2}$$

Plotting a graph of $-\ln c_1$ as a function of ${x_2}^2$ provides a straight line of gradient $-1/4Dt_2$, with the other terms making up the intercept point of the graph.

5.4 Library calibration

In order to validate the predicted linearity over the range of concentrations, a series of calibration plates were run. Vancomycin was dissolved in a citric acid solution (1.5 mM) to afford a vancomycin stock solution (1 μg/μl, 0.67 mM). Aliquots of the stock solution were diluted with the original citric acid solution (1.5 mM) to afford a range of solutions each with an equal number of moles of citric acid, and a variable amount of vancomycin.

Table 17: Dilutions of the vancomycin stock solution for calibration purposes

Vancomycin standard	Vol. of Vancomycin stock /μl	Vol. of 1.5 mM Citric acid solution /μl	Total Volume /μl	Concentration of Vanc solution (M)
V_{40}	40	0	40	6.73E-04
V_{30}	30	10	40	5.05E-04
V_{20}	20	20	40	3.37E-04
V_{10}	10	30	40	1.68E-04
V_5	5	35	40	8.41E-05
V_2	2	38	40	3.37E-05
V_1	1	39	40	1.68E-05
$V_{0.4}$	0.4	39.6	40	6.73E-06

The methicillin sensitive *Staphylococcus aureus* bacterial inoculation assay was performed with 40 µl of each vancomycin aliquot being plated. Incubation of the bacterial plates was carried out for 24 hrs at 37 °C. Upon removal from the incubator, photographs of each plate were taken and the radii of positive results measures and recorded.

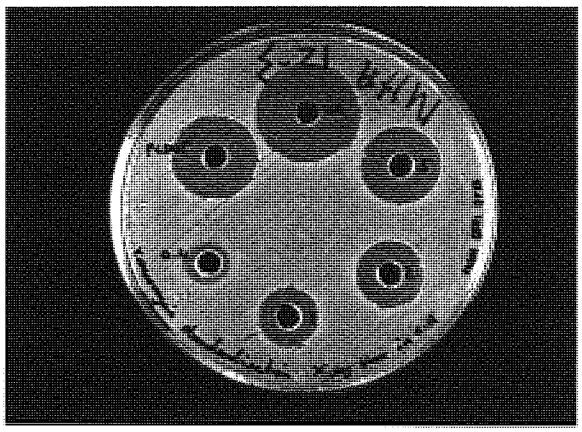

Figure 50: Plate A: Vancomycin standardisation. Clockwise from top; V_{40}, V_5, V_2, V_1, $V_{0.4}$, spare well used to test the potentially labelled vancomycin adduct 131 for biological activity.

Table 18: Incubation data of: Plate A

Vancomycin Std	Diameter /mm
V_{40}	25.5
V_5	19.8
V_2	16.7
V_1	14.6
$V_{0.4}$	10.4

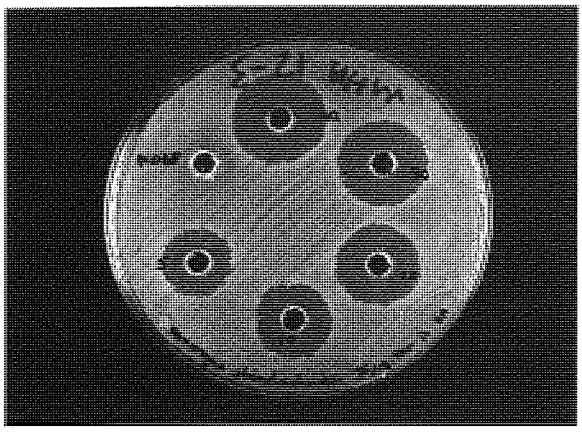

Figure 51: Plate B: Vancomycin standardisation. Clockwise from top; V_{40}, V_{30}, V_{20}, V_{10}, V_5, spare well used to test the potentially labelled vancomycin adduct 131 for biological activity.

Table 19: Incubation data of: Plate B

Vancomycin Std	Diameter /mm
V_{40}	22.8
V_{30}	21.8
V_{20}	19.7
V_{10}	18.2
V_5	16.7

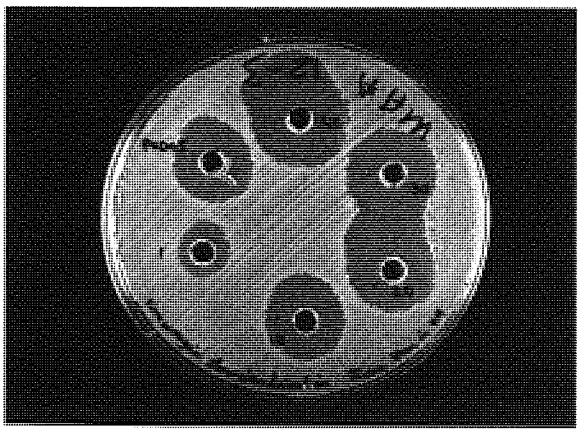

Figure 52: Plate C: Vancomycin standardisation. Clockwise from top; V_{40}, V_{30}, V_{20}, V_{10}, V_1, spare well used to test the potentially labelled vancomycin adduct 131 for biological activity.

Table 20: Incubation data of Plate C

Vancomycin Std	Diameter /mm
V_{40}	23.7
V_{30}	22.7
V_{20}	21.6
V_{10}	19.0
V_1	12.4

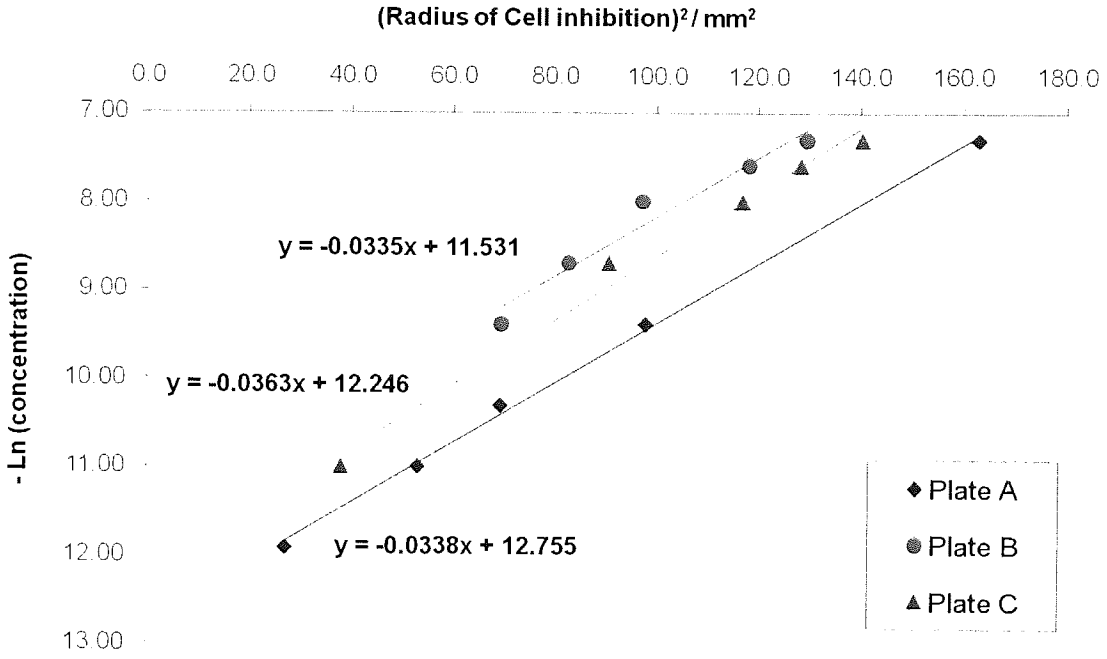

Figure 53: A graph showing the relationship between –ln concentration of vancomycin and the radius of the area of inhibition squared.

The straight line allows an unknown concentration of vancomycin (c_1) to be determined from the radius of the corresponding zone of inhibition. Since c_1 is the concentration of vancomycin solution initially plated, it corresponds to the number of moles of vancomycin cleaved from the peptidyl-resin sequence. Accordingly, the ratio of moles of vancomycin to moles of peptide/boronic acid can be calculated, affording a measure of the binding affinity under the particular conditions of this library.

The gradients of the test plates are calculated to be approximately constant across all bacterial plates, but show slight variations in the intercept points due to the slight differences in incubation time, thickness of the plate media and number of bacteria on the plate. This demonstrated the need for each individual plate to have at least two known concentrations to enable plotting of the line for each plate, thereby allowing the subsequent determination of c_1 for each library sample.

5.5 Library Results

5.5.1 L-4 sub library

The incubation of the **L-4** sub library with vancomycin was carried out in the presence of pyridine using the protocol established in the library validation. Approximately 5 mg of each library resin was utilised. The loading of the base resin was established and the number of moles of peptide calculated. A solution of vancomycin in pyridine was made and an aliquot added to each library resin, such that 0.37 molar equivalents of vancomycin was added for every peptide.

The resultant suspensions were agitated at room temperature overnight before being drained. The resins were then subjected to copious washing with pyridine via Soxhlet extraction for 4 hours before being dried to constant mass.

The THF/citric acid cleavage solution was added to each of the dry resin samples. The resulting suspensions were agitated at room temperature overnight. The supernatant was carefully removed and evaporated to dryness. Each dry residue was then resuspended in a 400 µl of water to afford a 'cleavage solution' with the original concentration of the citric acid component and an unknown vancomycin concentration.

The Methicillin sensitive *Staphylococcus aureus* bacterial assay was performed with 40 µl of each cleavage solution being plated along with 40 µl of the vancomycin standards (V_{40} & V_1). Incubation of the bacterial plates was carried out for 24 hrs at

37 °C. Upon removal from the incubator photographs of each plate were taken (Figure 54-Figure 58) and the radii of any positive results recorded (Table 21-25).

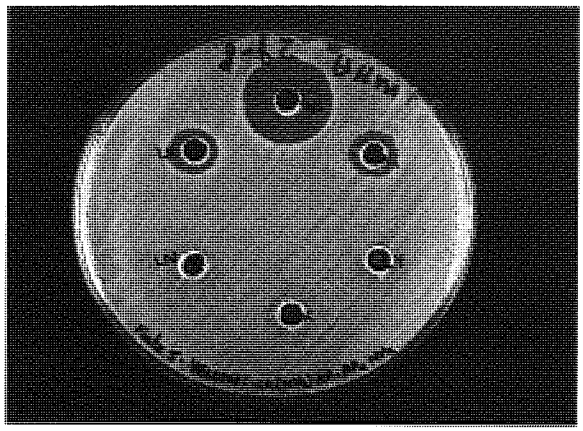

Figure 54: L-4 sub library Plate 5. Clockwise from top; V_{40}, V_1, L-4-LY, L-4-LK, L-4-LN, L-4-LR.

Table 21: Incubation data of L-4 sub library plate 5

Sample	Diameter /mm
V_{40}	21.5
V_1	11.2
L-4-LY	-
L-4-LK	-
L-4-LN	-
L-4-LR	11.2

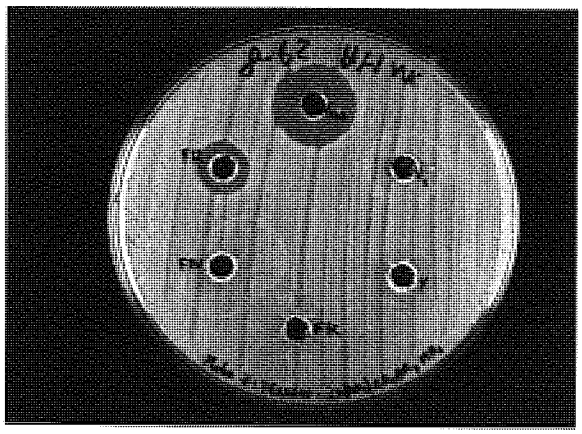

Figure 55: L-4 sub library Plate 7. Clockwise from top; V_{40}, V_1, L-4-FY, L-4-FK, L-4-FN, L-4-FR.

Table 22: Incubation data of L-4 sub library plate 7

Sample	Diameter /mm
V_{40}	20.5
V_1	7.8
L-4-FY	-
L-4-FK	-
L-4-FN	-
L-4-FR	12.7

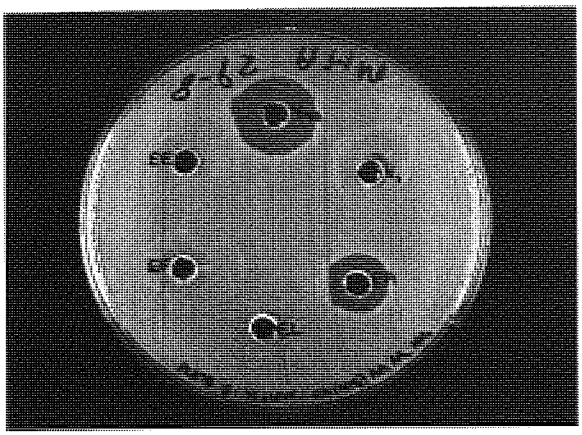

Figure 56: L-4 sub library Plate 8. Clockwise from top; V_{40}, V_1, L-4-EA, L-4-EL, L-4-EF, L-4-EE.

Table 23: Incubation data of L-4 sub library plate 8

Sample	Diameter /mm
V_{40}	19.1
V_1	8.3
L-4-EA	15.2
L-4-EL	-
L-4-EF	-
L-4-EE	-

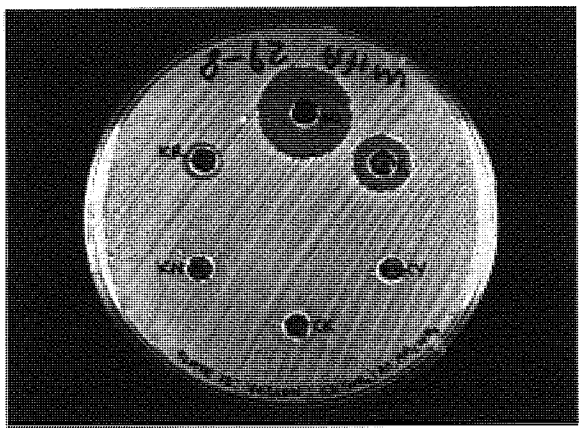

Figure 57: L-4 sub library Plate 13. Clockwise from top; V_{40}, V_1, L-4-KY, L-4-KK, L-4-KN, L-4-KR.

Table 24: Incubation data of L-4 sub library plate 13

Sample	Diameter /mm
V_{40}	22.0
V_1	13.7
L-4-KY	-
L-4-KK	-
L-4-KN	-
L-4-KR	9.3

Table 25: Incubation data of L-4 sub library plate 16

Sample	Diameter /mm
V_{40}	20.5
V_1	10.8
L-4-RA	7.8
L-4-RL	-
L-4-RF	-
L-4-RE	-

Figure 58: L-4 sub library Plate 16. Clockwise from top; V_{40}, V_1, L-4-RA, L-4-RL, L-4-RF, L-4-RE.

Incubation of the cleavage solutions with MSSA revealed that five library compounds gave rise to significant zones of inhibition. The inoculated plates had two calibration wells, each containing a different vancomycin solution of known concentration. Accordingly, Equation 18 was used as the basis for plotting the calibration line for each plate allowing the unknown, initial vancomycin concentrations of the active cleavage solutions to be calculated.

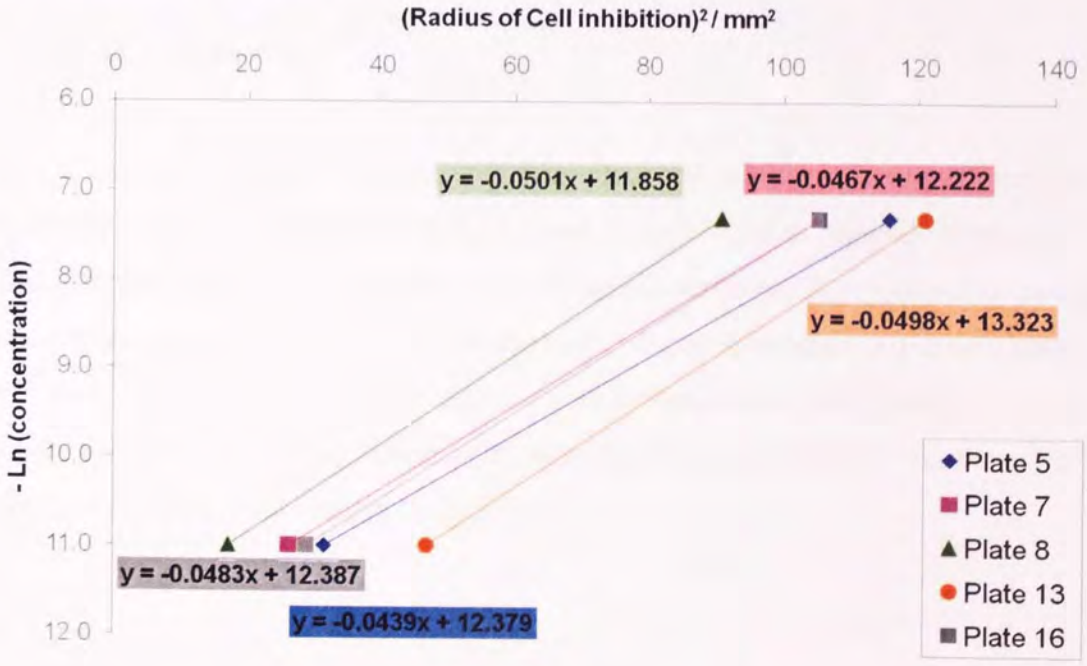

Figure 59: Calibration lines obtained for the L-4 sub library plates exhibiting zones of inhibition.

Photographs of the plates were greatly enlarged to reduce the error in the measurement of the diameter of the circular zones of inhibition. Each value of radii^2 was inputted into the calculation specific to its plate to yield a value of – ln [vancomycin]. The vancomycin concentration of the 40 µl injection sample could be ascertained and accordingly, the number of moles of vancomycin cleaved from the resin contained within the entire 400 µl cleavage solution (Table 26).

Table 26: L-4 sub library, compounds which after cleavage from the resin give rise to zones of inhibition

Sample	Plate	Diameter /mm	Radius^2 /mm^2	-Ln [Vancomycin]	[Vancomycin] /M	Total no. of moles of vancomycin in 400 µl cleavage soln
L-4-LR	5	11.2	31.6	10.99	1.69E-05	6.75E-09
L-4-FR	7	12.7	40.4	10.33	3.26E-05	1.31E-08
L-4-EA	8	15.2	57.4	8.98	1.26E-04	5.04E-08
L-4-KR	13	9.3	21.6	12.25	4.79E-06	1.91E-09
L-4-RA	16	7.8	15.3	11.65	8.72E-06	3.49E-09

5.5.2 L-4B sub library

Incubation and cleavage of vancomycin from the **L-4B** sub library was performed in an identical fashion to the **L-4** library. V_{40} and V_2 were used as internal calibration standards for each plate. Incubation with methicillin sensitive *Staphylococcus aureus* was carried out for 24 hrs at 37 °C. Photographs (Figure 60-Figure 70) showing the plates after this incubation period together with the associated data (Table 27-37) are shown below. On occasion, the zones of inhibition were only visible with the aid of greatly enlarged digital images of the plates.

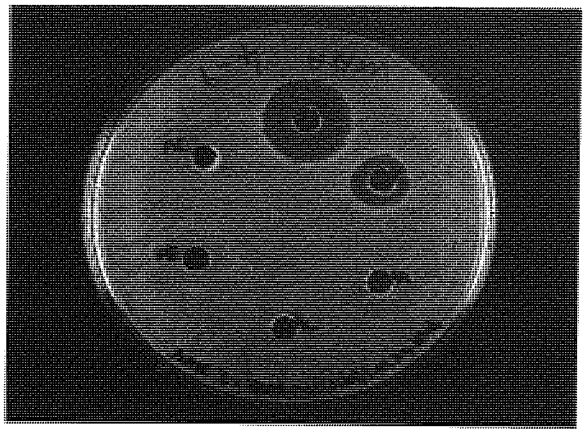

Figure 60: L-4B sub library Plate 2. Clockwise from top; V_{40}, V_2, L-4-AA, L-4-AL, L-4-AF, L-4-AE.

Table 27: Incubation data of L-4B sub library plate 2

Sample	Diameter /mm
V_{40}	19.1
V_2	12.0
L-4-AAB	-
L-4-ALB	8.0
L-4-AFB	-
L-4-AEB	-

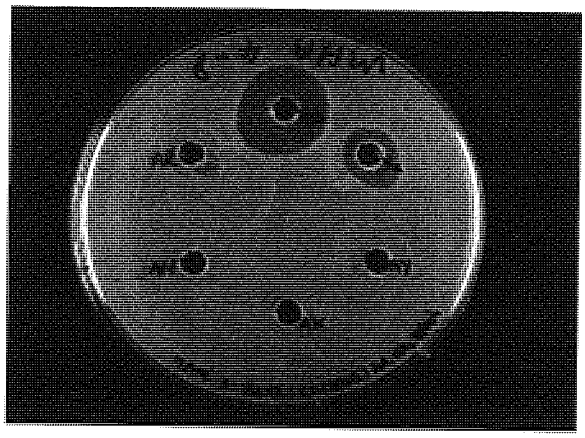

Figure 61: L-4B sub library Plate 3. Clockwise from top; V_{40}, V_2, L-4-AY, L-4-AK, L-4-AN, L-4-AR.

Table 28: Incubation data of L-4B sub library plate 3

Sample	Diameter /mm
V_{40}	18.6
V_2	12.4
L-4-AYB	-
L-4-AKB	7.5
L-4-ANB	-
L-4-ARB	8.4

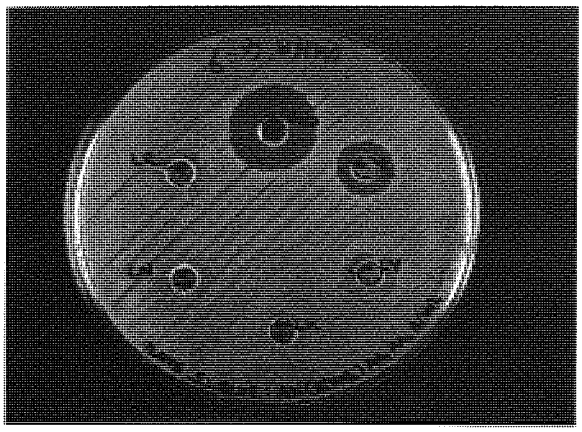

Figure 62: L-4B sub library Plate 5. Clockwise from top; V_{40}, V_2, L-4-LY, L-4-LK, L-4-LN, L-4-LR.

Table 29: Incubation data of L-4B sub library plate 5

Sample	Diameter /mm
V_{40}	20.4
V_2	12.4
L-4-LYB	8.0
L-4-LKB	7.5
L-4-LNB	-
L-4-LRB	8.4

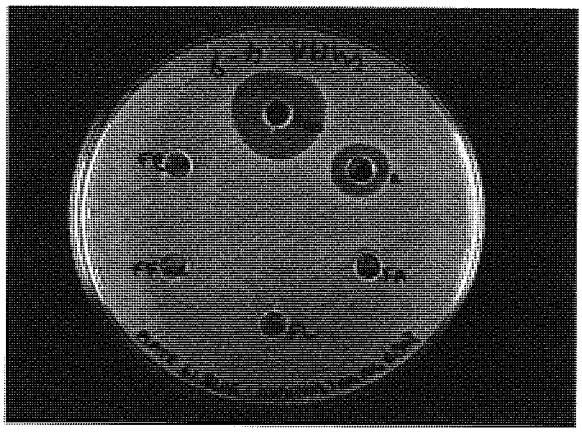

Figure 63: L-4B sub library Plate 6. Clockwise from top; V_{40}, V_2, L-4-FA, L-4-FL, L-4-FF, L-4-FE.

Table 30: Incubation data of L-4B sub library plate 6

Sample	Diameter /mm
V_{40}	20.0
V_2	12.9
L-4-FAB	8.9
L-4-FLB	-
L-4-FFB	-
L-4-FEB	-

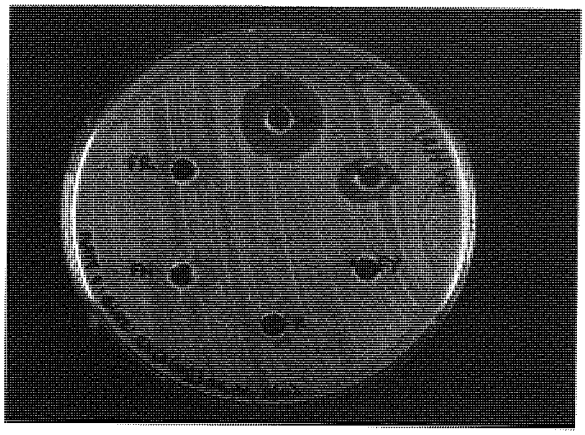

Figure 64: L-4B sub library Plate 7. Clockwise from top; V_{40}, V_2, L-4-FY, L-4-FK, L-4-FN, L-4-FR.

Table 31: Incubation data of L-4B sub library plate 7

Sample	Diameter /mm
V_{40}	18.6
V_2	12.0
L-4-FYB	-
L-4-FKB	8.0
L-4-FNB	-
L-4-FRB	-

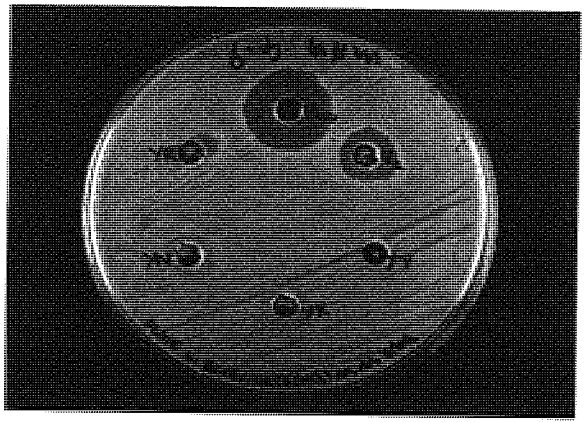

Figure 65: L-4B sub library Plate 11. Clockwise from top; V_{40}, V_2, L-4-YY, L-4-YK, L-4-YN, L-4-YR.

Table 32: Incubation data of L-4B sub library plate 11

Sample	Diameter /mm
V_{40}	19.5
V_2	12.9
L-4-YYB	-
L-4-YKB	-
L-4-YNB	-
L-4-YRB	9.3

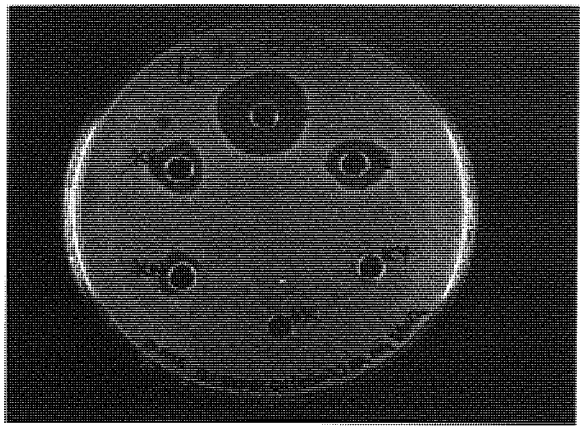

Figure 66: L-4B sub library Plate 13. Clockwise from top; V_{40}, V_2, L-4-KY, L-4-KK, L-4-KN, L-4-KR.

Table 33: Incubation data of L-4B sub library plate 13

Sample	Diameter /mm
V_{40}	20.4
V_2	11.5
L-4-KYB	8.4
L-4-KKB	-
L-4-KNB	10.2
L-4-KRB	11.1

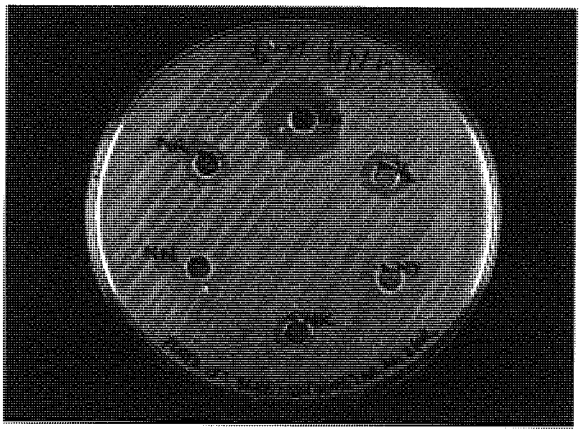

Figure 67: L-4B sub library Plate 15. Clockwise from top; V_{40}, V_2, L-4-NY, L-4-NK, L-4-NN, L-4-NR.

Table 34: Incubation data of L-4B sub library plate 15

Sample	Diameter /mm
V_{40}	18.6
V_2	11.1
L-4-NYB	-
L-4-NKB	8.9
L-4-NNB	-
L-4-NRB	10.7

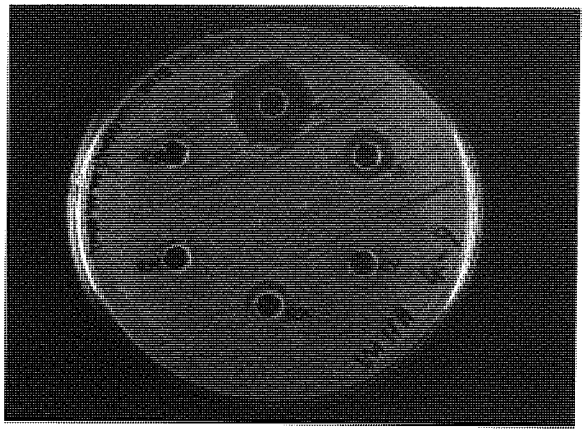

Figure 68: L-4B sub library Plate 17. Clockwise from top; V_{40}, V_2, L-4-RY, L-4-RK, L-4-RN, L-4-RR.

Table 35: Incubation data of L-4B sub library plate 17

Sample	Diameter /mm
V_{40}	18.2
V_2	11.1
L-4-RYB	-
L-4-RKB	9.3
L-4-RNB	8.0
L-4-RRB	8.4

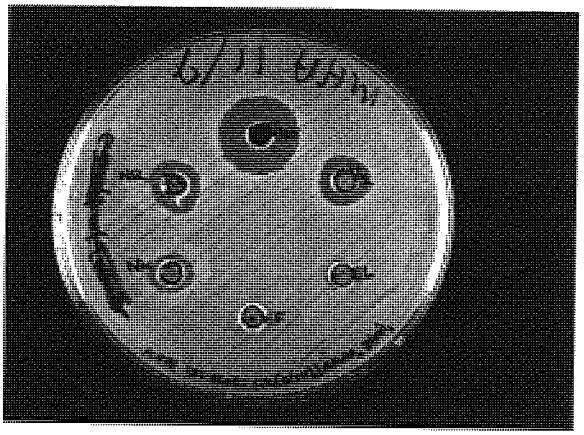

Figure 69: L-4B sub library Plate 28. Clockwise from top; V_{40}, V_2, L-4-EL, L-4-EF, L-4-NK, L-4-NR.

Table 36: Incubation data of L-4B sub library plate 28

Sample	Diameter /mm
V_{40}	19.1
V_2	12.2
L-4-ELB	7.8
L-4-EFB	-
L-4-NKB	10.8
L-4-NRB	12.7

Figure 70: L-4B sub library Plate 29. Clockwise from top; V_{40}, V_2, L-4-RA, L-4-RL, L-4-RF, L-4-RE

Table 37: Incubation data of L-4B sub library plate 29

Sample	Diameter /mm
V_{40}	21.5
V_2	14.2
L-4-RAB	9.3
L-4-RLB	10.3
L-4-RFB	9.3
L-4-REB	-

Incubation of the cleavage solutions obtained from the boronic acid containing library **L-4B** with MSSA revealed 21 compounds that gave rise to significant zones of inhibition. Again, Equation 18 was used as the basis for constructing calibration lines for each plate showing the relationship of inhibition to the sample solution's vancomycin concentration (Figure 71 & Figure 72).

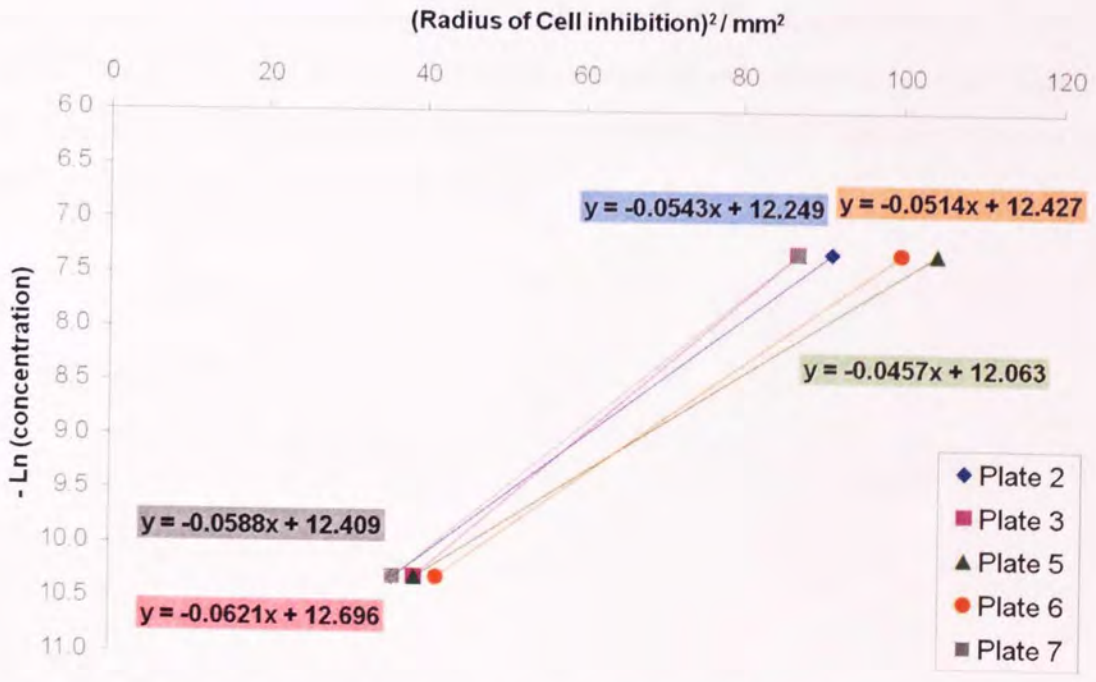

Figure 71: Calibration lines obtained for plates 2, 3, 5-7 of the L-4B sub library which exhibited zones of inhibition.

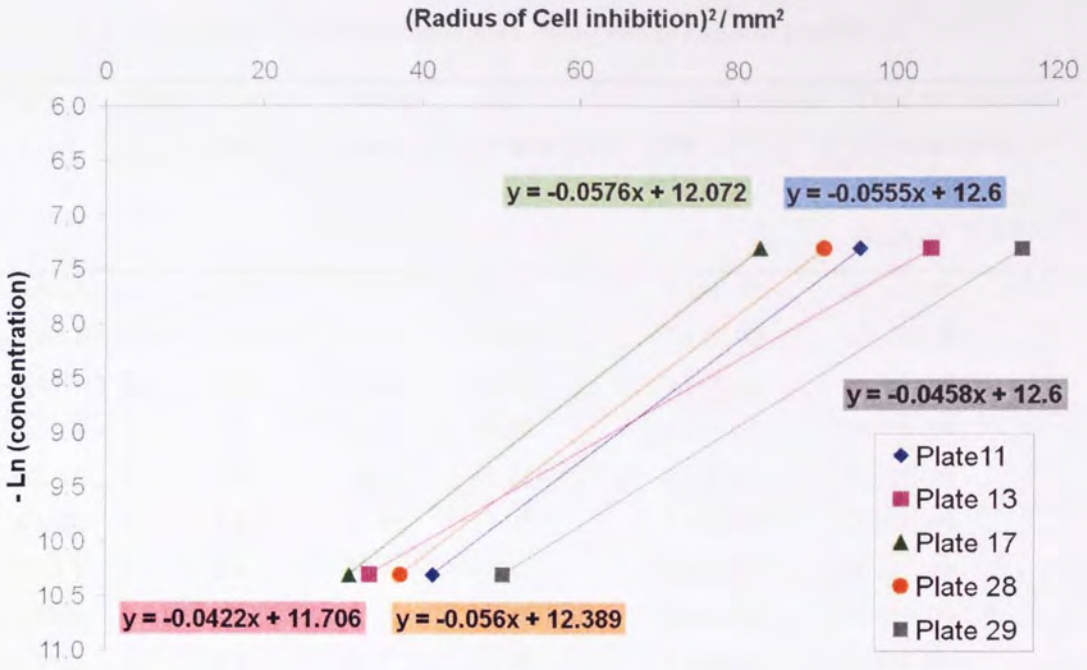

Figure 72: Calibration lines obtained for plates 11, 13, 17, 28, 29 of the L-4B sub library which exhibited zones of inhibition.

As with the **L-4** sub library, photographs of the plates were greatly enlarged to reduce the error in the measurement of the diameter of the circular zones of inhibition. Calculations for vancomycin concentration and the subsequent calculation for the amount of vancomycin in the cleavage solution (Table 37) were performed in an identical fashion to the **L-4** sub library.

Table 37: L-4 sub library cleavage compounds giving rise to zones of inhibition

Sample	Plate	Diameter /mm	Radius^2 /mm^2	-Ln [Vancomycin]	[Vancomycin] /M	Total no. of moles of vancomycin in 400 µl cleavage solution
L-4-ALB	2	8.0	16.0	11.38	1.14E-05	4.56E-09
L-4-AKB	3	7.5	14.2	11.81	7.42E-06	2.97E-09
L-4-ARB	3	8.4	17.8	11.59	9.24E-06	3.70E-09
L-4-LYB	5	8.0	16.0	11.33	1.20E-05	4.79E-09
L-4-LKB	5	7.5	14.2	11.41	1.11E-05	4.42E-09
L-4-LRB	5	8.4	17.8	11.25	1.30E-05	5.20E-09
L-4-FAB	6	8.9	19.7	11.41	1.10E-05	4.41E-09
L-4-FKB	7	8.0	16.0	11.47	1.04E-05	4.17E-09
L-4-YRB	11	9.3	21.7	11.39	1.13E-05	4.50E-09
L-4-KYB	13	8.4	17.8	10.96	1.75E-05	6.98E-09
L-4-KNB	13	10.2	26.1	10.61	2.48E-05	9.90E-09
L-4-KRB	13	11.1	30.8	10.41	3.02E-05	1.21E-08
L-4-RKB	17	9.3	21.7	10.82	2.00E-05	7.99E-09
L-4-RNB	17	8.0	16.0	11.15	1.43E-05	5.73E-09
L-4-RRB	17	8.4	17.8	11.05	1.59E-05	6.37E-09
L-4-ELB	28	7.8	15.3	11.53	9.80E-06	3.92E-09
L-4-NKB	28	10.8	28.9	10.77	2.10E-05	8.41E-09
L-4-NRB	28	12.7	40.4	10.13	3.99E-05	1.60E-08
L-4-RAB	29	9.3	21.6	11.61	9.05E-06	3.62E-09
L-4-RLB	29	10.3	26.3	11.39	1.13E-05	4.51E-09
L-4-RFB	29	9.3	21.6	11.61	9.05E-06	3.62E-09

5.6 Discussion

5.6.1 Possible errors within the bioassay

The library calibration conducted with 6 solutions of known concentration of vancomycin permitted the construction of a straight line graph using Equation 18. The three calibration plates show that the line, as expected, is one of best fit.

Due to the nature of the assay there were slight but unavoidable differences between plates such as differences in thickness of the plate media and the number of bacteria on the plate. This situation necessitated the inclusion of calibration samples on each plate. To minimise the number of plates required for the library and to make such an approach experimentally and resource viable, only two calibration wells were included on each plate. As such, the gradient is no longer one of best fit, but becomes absolute. This may go someway to establishing why the calculated gradients of the samples plates are different from those of the original calibration plates. However there is no way of knowing that the gradients are incorrect without repetition of the incubations with at least three calibration solutions per plate. The general trend of close agreement between plates is maintained, however the gradients of the library plates are generally greater than those of the calibration plates.

The Minimum Inhibitory Concentration (MIC) is the lowest concentration of vancomycin in solution that will create a visible area of cell death. The calibration plates indicated that a solution with a concentration of greater than or equal to 0.4 μg/μl would provide a visible zone of inhibition, however the variation of the radius of inhibition made by identical standard solutions across the plates suggested that such a concentration may not always inhibit cell growth. Accordingly, the 1 μg/μl solution was utilised as the most dilute calibration standard.

The unknown concentration of each of the samples can give rise to a situation where the radius of the zone of inhibition of a sample solution is outside the calibration range. Given that the calibration line is constructed using only two points, the errors

introduced are no greater than for those solutions whose radius does fall within the two calibration points.

A number of solutions exhibiting zones of inhibition were identified; however it is not possible to say with absolute certainty that any of the cleavage solutions contain no vancomycin. Plates where the concentration of vancomycin is slightly above or below the MIC are subject to the specific conditions of that plate. Those plates demonstrating zones of inhibition may not positively indicate the presence of vancomycin if they were repeated. Similarly, sample solutions regarded as negative may in fact demonstrate inhibition if repeated. For example, positive results may not have been visible on a plate with a thicker layer of growth media, while those showing negative results may have shown zones of inhibition if inoculated on thinner plates.

5.6.2 Analysis of 'positive' sequences

The results confirm previously reported results[98] regarding the lack of any complex formation between vancomycin and the **L-4-AA** sequence. While it is not unknown that sequences other than D-Ala-D-Ala-OH can bind to vancomycin[98], albeit not as effectively, the sequences tend to consist of glycine or other D-amino acids[98]. Results obtained from our library assay demonstrated that 26 compounds, the majority of which contained amino acids other than D-alanine, bound to and subsequently released the vancomycin antibiotic.

Analysis of the distribution of amino acids within the compounds which afforded positive library hits shows a high frequency of arginine. Over 30 % of the recorded hits contained at least one alanine moiety in either the L-3 or L-4 position, making it the most prevalent amino acid within the positive samples. Indeed, of the 30 sequences containing one or more arginine residues across the **L-4** and **L-4B** libraries, 53 % demonstrated zones of inhibition. Sequences containing glutamic acid are the least common, with both positive sequences expressing the amino acid in the L-3 residue position. The uniqueness of glutamic acid to position three, along with other residues which have a reasonable bias towards one position (F, Y) occurs only

in amino acids which are low in frequency, and as such, is probably down to statistical distribution rather than an actual trend.

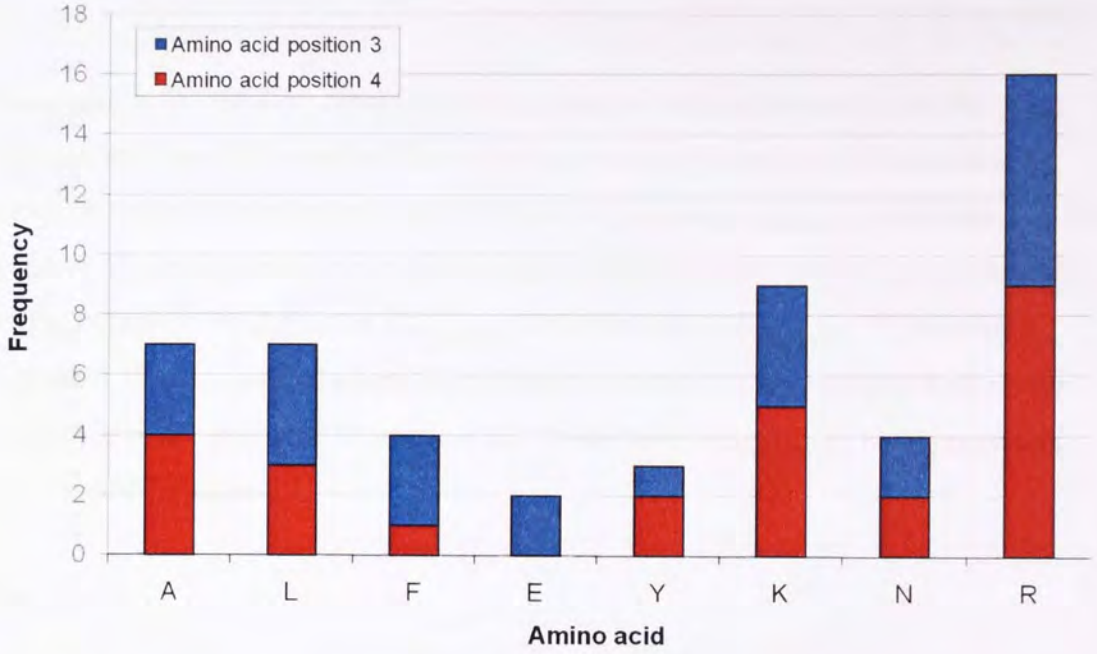

Figure 73: Frequency chart, showing the total number of occurrences of an amino acid in a sequence which binds sufficiently to and releases sufficient vancomycin to produce zones of inhibition. The tally is sub divided to show the number of occurrences of the amino acid in positions 3 and 4.

5.6.3 Energies of the systems

In a chemical reaction, the reaction can broadly be described in terms of Equation 19, where chemical entities are expressed in capital letters, with their molecular ratio in lower case letters.

Equation 19

$$aA + bB \rightleftharpoons cC + dD$$

The reaction constant, in this instance the association of the vancomycin and the peptide chain expressed on the resin beads, can be described using Equation 20.

Equation 20

$$K_{association} = \frac{[C]^c[D]^d}{[A]^a[B]^b}$$

$K_{dissociation}$ is the reaction constant of the release of the vancomycin from the vancomycin-peptide complex. Given that one mole of complex will dissociate to form one mole of vancomycin and one mole of peptide, $K_{dissociation}$ is expressed as the product of the concentration of the two end components divided by the concentration of the complex. By definition $K_{dissociation}$ is the inverse of $K_{association}$[130], therefore Equation 19 contains no factors, even though Equation 20 is expressed with molar ratios which are not equal to one another. This allows $K_{association}$ to be expressed in the form of Equation 21.

Equation 21

$$K_{association} = \frac{[vancomycin - peptide\ complex]}{[peptide][vancomycin\ in\ incubation\ soln.]} M^{-1}$$

The concentration of peptide is calculated as the mass of resin multiplied by the loading, in the volume of solvent in which the incubation is carried out. The number of moles of vancomycin released must be the same as the number of moles of complexes formed and is therefore calculated from the calibration graphs and Equation 18.

The reaction constant can then be used in conjunction with Equation 22 to calculate the free energy change of the system – a measure of the thermodynamic favourability of a reaction.

Equation 22

$$\Delta G^o = -RT\ lnK$$

If the Gibbs free energy of the system decreases as the reaction proceeds, the reaction has a spontaneous tendency to convert from the reactants (the mixture of vancomycin and resin bound peptide) to the product (the peptide-vancomycin complex).

Table 38: The reaction constant $K_{association}$ and the standard free energy change of the L-4 library-vancomycin complexes.

Derivative	$K_{association}$ / M^{-1}	**Change in Gibbs free energy, ΔG° /kJmol^{-1}**
L-4-EA	5.91	**-4.40**
L-4-FR	1.55	**-1.09**
L-4-LR	0.90	**0.27**
L-4-RA	0.45	**2.00**
L-4-KR	0.35	**2.58**

Table 39: The reaction constant $K_{association}$ and the standard free energy change of the L-4B library-vancomycin complexes.

Derivative	$K_{association}$ / M^{-1}	**Change in Gibbs free energy, ΔG° /kJmol^{-1}**
L-4-NRB	3.25	**-2.92**
L-4-KRB	1.81	**-1.47**
L-4-NKB	1.76	**-1.40**
L-4-KNB	1.52	**-1.04**
L-4-RKB	1.45	**-0.92**
L-4-RRB	1.13	**-0.31**
L-4-KYB	1.02	**-0.05**
L-4-FAB	0.97	**0.07**
L-4-LRB	0.85	**0.41**
L-4-RNB	0.84	**0.43**
L-4-YRB	0.84	**0.43**
L-4-FKB	0.71	**0.86**
L-4-LYB	0.70	**0.89**
L-4-RLB	0.69	**0.93**
L-4-RFB	0.68	**0.96**
L-4-LKB	0.62	**1.18**
L-4-ALB	0.59	**1.32**
L-4-ELB	0.57	**1.40**
L-4-RAB	0.56	**1.44**
L-4-AKB	0.46	**1.94**
L-4-ARB	0.29	**3.11**

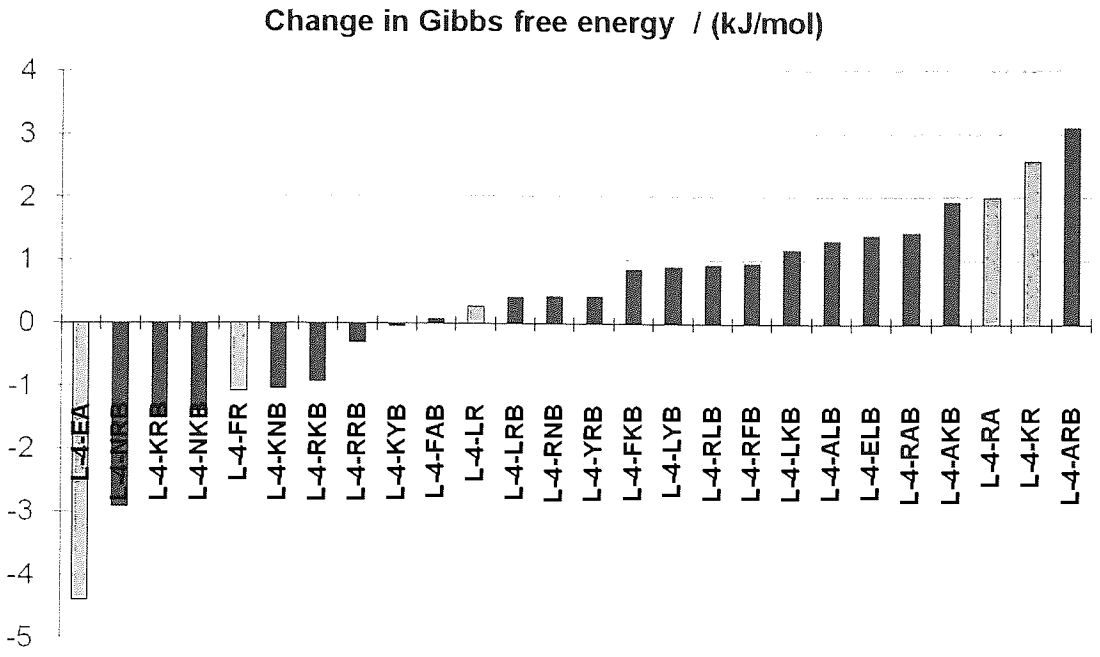

Figure 74: The trend of ΔG^{o} across the different library compounds, where those with the lowest ΔG^{o} value form the most stable complexes. A positive ΔG^{o} indicates that energy is required to drive the reaction and thus will not occur spontaneously.

The most favourable of the vancomycin-peptide complexes is provided by the **L-4-EA** compound. The least favourable but spontaneous complex is formed with the **L-4-ARB** sequence. Interestingly a number of sequences appear to have ΔG values greater than zero. This implies that the formation of the vancomycin-peptide complex is not a spontaneous event, and will not occur. Since the complexes were formed, as evidenced by the zones of inhibition, there is a need to be cautious with the adoption of this method of calculation.

Previously reported results[98] put the binding constant, $K_{association}$, of vancomycin to the D-Ala-D-Ala-OH sequence in the region of 1.5×10^{6} M^{-1} while another[110] cites the K_d as 12μM, corresponding to a K_a of ~80000 M^{-1}. The values obtained using our bacterial assays are much lower than the other studies, but recognition of the differences between the assays used to calculate these values may shed light on any errors within the analysis methods employed in the current study.

1. **Polymer vs. solution**

   In the current assay, consideration must be given to the possible effects of the polymer matrix on library compound-vancomycin interaction. Issues such as diffusion into the polymer matrix, solvent compatibility and polarity may collectively or individually affect the binding of the antibiotic.

2. **–OH vs. NH_2/boronic acid**

   Due to the linear construction of the sequences from Fmoc protected amino acids, the peptide chains terminate with either an amine (**L-4** library) or a boronic acid (**L-4B** library). The studies reported previously were conducted in solution whereby cleavage from the resin afforded the *C*-terminal hydroxide.

3. **Detection**

   Methods employed to determine the amount of vancomycin complex also differ. The literature sources favour a UV or fluorescence based approach. Although of much greater sensitivity, this technique only provides a value for the amount of complex formed. Without the subsequent cleavage operation such an approach does not recognise the efficiency of the cleavage reaction and thus the amount of 'useful' vancomycin. The presence of beads may also hinder this approach.

4. **Calculation of the peptide 'concentration'**

   The calculation of the peptide concentration for each library is based on the experimentally measured mass changes associated with the addition of amino acid residues and cleavage of protecting groups. While the loading of the original base resin **62** was accurately established, loading values of subsequent derivatisations are calculated using the theoretical number of moles in each sub library after splitting and the mass of the resin actually obtained. As each loading is calculated sequentially from the preceding calculation any errors are maintained and potentially exacerbated. Perceived errors in mass cannot be taken into account since it cannot be attributed to the loss of product or to a poor reaction yield.

   For example:

   1 g of resin has 1 mmol of reactive sites, giving it a loading of 1 mmol/g.

   Reacting 1 mmol of compound X (MW: 500, 0.5 g) should yield a product resin

with a mass of 1.5 g, with the number of reacting sites maintained at 1 mmol. The new loading of this resin is thus 0.667 mmol/g.

Consider further the case where rather than 1.5 g of product resin, a mass of 1.4 g is recorded. This implies that 0.1 g has been 'lost'.

If the reaction went to 100 % completion, and 0.1 g was lost in transferring the product to the balance, the resin loading is maintained at 0.667 mmol/g. 1.4 g of resin would therefore contain 0.93 mmol of reactive sites to carry forward to the next step. However, it could also be the case that the reaction yield was 80 %; a mass increase of 0.4 g corresponds to only 0.8 mmol of the reactive sites being used.

Evidence obtained as a result of the Fmoc-loading studies suggests that in our laboratory the propagation of the peptide chains can be carried out in a near quantitative method. This suggests that the theoretical loading values are close to the actual values, and the mass discrepancies are due to handling errors, rather than low yields. As Quadragel **59** and its derivatives do not contain a cleavable linker, thereby precluding the possibility of deconvoluting sequences, and sulphur containing residues were avoided, there is no possibility of ascertaining the true library loadings, and therefore the number of reaction sites, with any certainty.

Since the 'concentration' of peptide used in the calculation of K_a is the number of moles of peptide in the reaction volume, there are inherent errors in the calculations of the change in Gibbs free energy values.

Consequently, a different method of quantifying the binding efficiency of the sequences, most notably by the percentage immobilisation of the available vancomycin, provides a more reliable data set.

5.6.4 Vancomycin immobilisation

Perhaps of greater importance is the comparison of the various sequences by vancomycin uptake. The percentage immobilisation of vancomycin affords a method

of directly comparing the different resin sequences, identifying those with the most efficient uptake.

Table 40: % of vancomycin immobilised during the resin incubation period for the L-4 library

Derivative	Moles of vancomycin in cleavage solution	Moles of vancomycin in incubation solution	**% of vancomycin immobilised**
L-4-EA	5.04E-08	1.44E-06	**3.50**
L-4-FR	1.31E-08	1.41E-06	**0.92**
L-4-LR	6.75E-09	1.27E-06	**0.53**
L-4-RA	3.49E-09	1.32E-06	**0.26**
L-4-KR	1.91E-09	9.14E-07	**0.21**

Table 41: % of vancomycin immobilised during the resin incubation period for the L-4B library

Derivative	Moles of vancomycin in cleavage solution	Moles of vancomycin in incubation solution	**% of vancomycin immobilised**
L-4-NRB	1.60E-08	8.30E-07	**1.93**
L-4-KRB	1.21E-08	1.13E-06	**1.07**
L-4-NKB	8.41E-09	8.06E-07	**1.04**
L-4-KNB	9.90E-09	1.10E-06	**0.90**
L-4-RKB	7.99E-09	9.29E-07	**0.86**
L-4-RRB	6.37E-09	9.49E-07	**0.67**
L-4-KYB	6.98E-09	1.16E-06	**0.60**
L-4-FAB	4.41E-09	7.65E-07	**0.58**
L-4-LRB	5.20E-09	1.04E-06	**0.50**
L-4-YRB	4.50E-09	9.04E-07	**0.50**
L-4-RNB	5.73E-09	1.15E-06	**0.50**
L-4-FKB	4.17E-09	9.97E-07	**0.42**
L-4-LYB	4.79E-09	1.16E-06	**0.41**
L-4-RLB	4.51E-09	1.11E-06	**0.41**
L-4-RFB	3.62E-09	9.00E-07	**0.40**
L-4-LKB	4.42E-09	1.20E-06	**0.37**
L-4-ALB	4.56E-09	1.31E-06	**0.35**
L-4-ELB	3.92E-09	1.16E-06	**0.34**
L-4-RAB	3.62E-09	1.09E-06	**0.33**
L-4-AKB	2.97E-09	1.10E-06	**0.27**
L-4-ARB	3.70E-09	2.19E-06	**0.17**

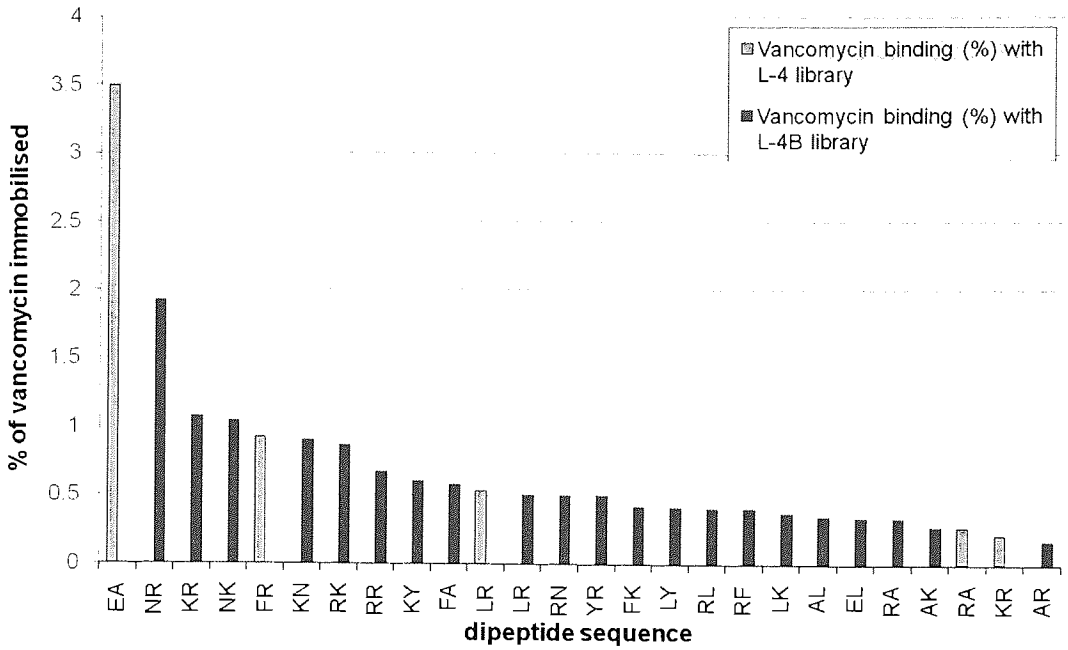

Figure 75: % of vancomycin immobilised by sequences of the L-4 library (yellow) and the boronic acid containing L-4B library (Blue) in descending order of immobilisation.

While it was assumed that the inclusion of boronic acid would create a large number of hits, it was pleasing to see that the **L-4B** library did not become a 'brute force' method for binding vancomycin, and that there were sequences which showed binding and others that showed none. Furthermore, the variable degree of binding between different sequences enhanced the result, demonstrating that the binding of vancomycin with the library was dependent on simultaneous interactions with both the boronic acid and peptide chain.

By far the most efficient scavenger of vancomycin was the **L-4-EA** library sequence, immobilising nearly twice as much as the next best sequence. The majority of sequences (85 %) immobilised less than 1 % of the vancomycin they were exposed to, while just under half of the sequences had efficiencies of less than 0.5 %. The sequence **L-4-ARB** showed only $1/20^{th}$ of the affinity for vancomycin that the best sequence did.

Presenting the data according to amino acid sequence clearly shows that three sequences afford positive library hits in both sub libraries.

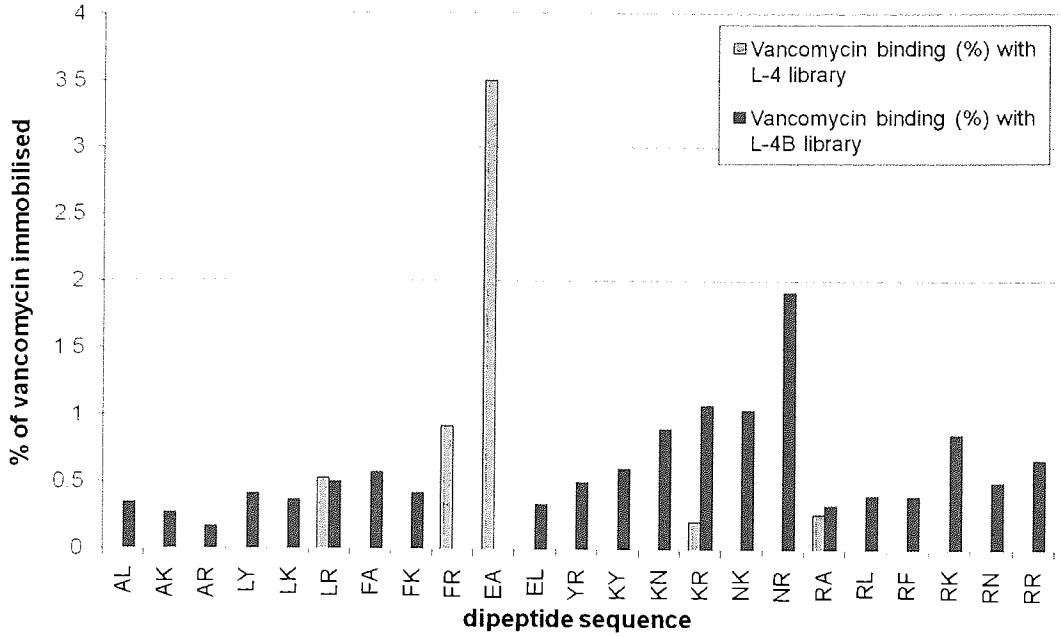

Figure 76: % of vancomycin immobilised by sequences of the L-4 library (yellow) and the boronic acid containing L-4B library (Blue) arranged by dipeptide sequence.

Table 42: Peptide sequences which bind sufficiently to vancomycin to produce zones of inhibition from both L-4 and L-4B sub libraries

Derivative	**% of vancomycin immobilised**	Derivative	**% of vancomycin immobilised**
L-4-LR	**0.53**	**L-4-LRB**	**0.50**
L-4-RA	**0.26**	**L-4-RAB**	**0.33**
L-4-KR	**0.21**	**L-4-KRB**	**1.07**

The data demonstrates the full range of eventualities for the inclusion of boronic acid in the library. The boronic acid can cause previously non-binding sequences to form vancomycin complexes, and also remove the ability to bind completely (**L-4-EAB**, **L-4-FRB**). It can also show moderate effects; binding of **L-4-KR** was greatly enhanced with the inclusion of boronic acid, while **L-4-RAB** showed a slight increase in its affinity for vancomycin when compared with **L-4-RA**. The sequences **L-4-LR** and **LRB** show very similar binding affinity, indicating a negligible effect.

5.6.5 Comparison of the methods

Although calculation of the change in free energy provides a measure of the thermodynamic favourability of a reaction, it does not yield any information on the rate of reaction. A negative ΔG indicates that a reaction *can* occur spontaneously, but does not signify whether it will occur at a perceptible rate. Accordingly, it is possible that the formation of the vancomycin-peptide complex has occurred, but at a lower rate than the formation of a thermodynamically less favourable complex, which given the finite timeframe, would appear to have a better affinity. The rate depends on the free energy of activation ($\Delta G^{\ddagger}$), which is unrelated to ΔG, leaving ΔG as a suboptimal method of calculating the effectiveness of the binding of a given library compound.

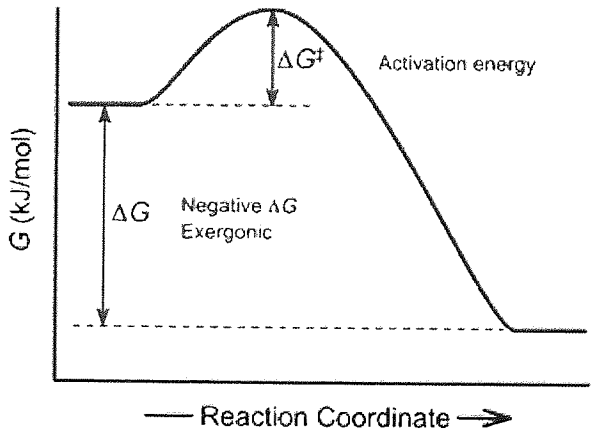

Figure 77[131]: The free energy profile of a reaction going from reactants to products.

The calculations which were utilised also contain an unavoidable inaccuracy; ΔG was calculated from the amount of vancomycin present in the cleavage solution and not from the amount of peptide-vancomycin complex, which was not directly measured in this study. Accordingly, the calculation relies on the literature description of a 1:1 vancomycin:peptide binding. While this may hold true with the **L-4** compounds, the effect of the two boronic acids in library **L-4B** is unknown. It is feasible that each binds to the carbohydrate of separate vancomycin molecules, affording a binding ratio of as much as 2:1. Steric hindrance would undoubtedly

bring this ratio down, but without absolute measurement any numbers are guesses and cast serious doubt on the merit of such calculated values.

Any calculation is also dependent on the accurate calculation of the loading of each sub library compound, which as previously discussed, is not easily assessed or verified.

Ultimately the percentage immobilisation provides a better reflection of the actual assay result. The calculation relies solely on the ratio of vancomycin before incubation and after cleavage. Accordingly, it is unaffected by the precise, and unknown mechanisms of binding of vancomycin to the peptide and boronic acid sequences, and automatically accounts for the different rates of complex formation.

The analysis of both data sets would be advisable during the design of any future library compounds.

5.6.6 Binding efficiency of the rotated peptide sequences 108 & 113

Resin compounds **108** and **113** were added to the combinatorial library as stand-alone compounds. Incubation with vancomycin and subsequent cleavage with citric acid solution were performed in an identical fashion to the other 128 library compounds. The MSSA assay was performed in triplicate with 40 µl of each cleavage solution being plated along with 40 µl of the vancomycin standards (V_{40} & V_2) on three separate plates. Incubation of the bacterial plates was carried out for 24 hrs at 37 °C.

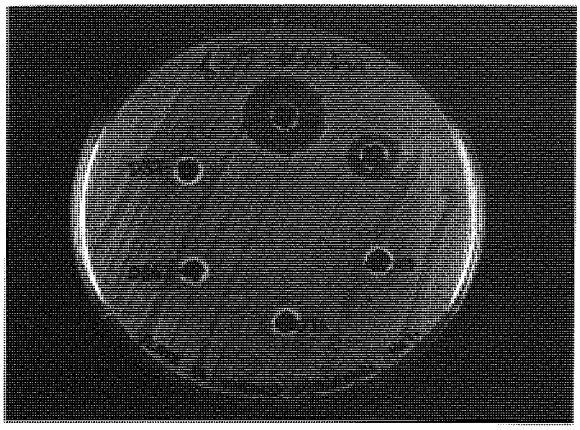

Figure 78: Stand-alone library compounds Plate 29. Clockwise from top; V_{40}, V_2, test sequence, test sequence, 108, 113.

Table 43: Incubation data of L-4B sub library plate 17

Sample	Diameter /mm
V_{40}	18.2
V_2	11.1
Test	-
Test	-
108	-
113	-

High resolution photography and image expansion showed that there were no zones of inhibition other than those caused by the vancomycin standard solutions. This result does not conclusively prove that either the synthesis or the incubation failed; it merely highlights some of the limiting factors discussed in **section 5.6.1**. Accordingly, vancomycin could have bound efficiently to a very low loaded polymer or the binding of vancomycin to the D-Ala-D-Ala sequence is not as fruitful as believed.

Post-synthesis colorimetric staining of resin compounds **108** and **113** had indicated the successful coupling of the tetrapeptide to the NHS activated resin **107**. Subsequent addition of boronic acid to the peptidyl-resin was also indicated by colorimetric staining, however quantifying the yield from the mass gain of the resin was deemed unreliable due to the scale of synthesis. Without quantitative data the success of the reaction cannot be assured. Accordingly, the lack of visible zones of inhibition is likely to be the result of an unsuccessful synthetic strategy, rather than a 'non-binding' event.

5.6.7 Incubation with *Escherichia coli*

As a control experiment, a selection of the library solutions which exhibited zones of inhibition against the Gram-positive Methicillin sensitive *Staphylococcus aureus*

were inoculated with the Gram-negative *Escherichia Coli*. As vancomycin is only effective against Gram-positive bacteria[132], the use of *E. coli* would enable zones of inhibition not attributable to vancomycin to come to light.

The sub library compounds selected had all previously shown activity against MSSA. Incubation of the bacterial plates was carried out for 24 hrs at 37 °C.

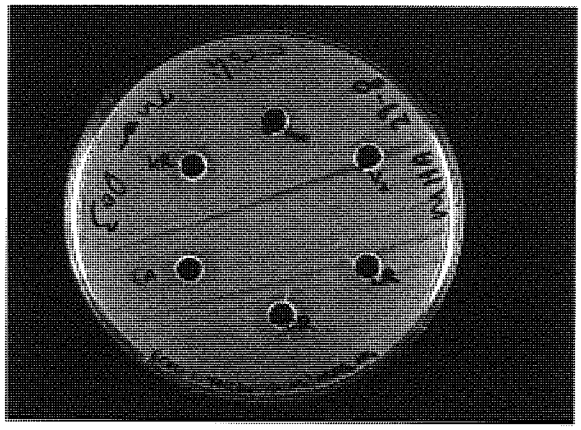

Figure 79: Incubation of L-4 sub library compounds with *E. coli*. Clockwise from top: V_{40}, V_2, L-4-LR, L-4-FR, L-4-EA & L-4-KR.

Table 44: Incubation data of L-4 sub library with *E. coli*

Sample	Diameter /mm
V_{40}	-
V_2	-
L-4-LR	-
L-4-FR	-
L-4-EA	-
L-4-KR	-

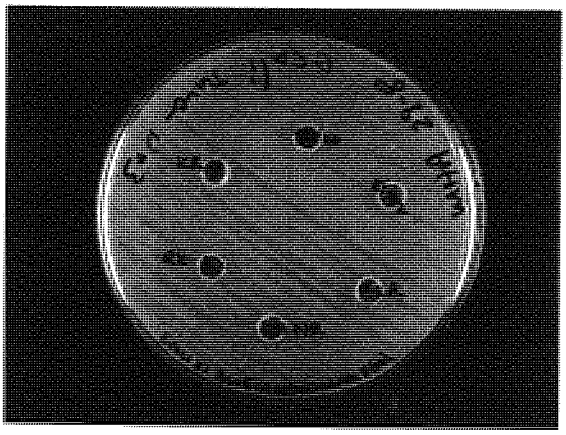

Figure 80: Incubation of L-4B sub library compounds with *E. coli*. Clockwise from top: V_{40}, V_2, L-4-LRB, L-4-NRB, L-4-RKB & L-4-KRB.

Table 45: Incubation data of L-4B sub library with *E. coli*

Sample	Diameter /mm
V_{40}	-
V_2	-
L-4-LRB	-
L-4-NRB	-
L-4-RKB	-
L-4-KRB	-

None of the library compounds displayed any biological activity towards the *E. coli*. Furthermore, the vancomycin standards failed to inhibit the growth of the bacteria. The result indicates that the cell death observed for the MSSA assays employing the 'active' library compounds is entirely due to the presence of vancomycin, as the selective nature of bacterial cell growth inhibition by the 'active' library compounds strongly indicates that the observed activity cannot be attributed to any substances leaching from the resin. Similarly neither the incubation nor cleavage processes have any observable affect on bacterial cell growth.

Chapter 6

Conclusion

Conclusions

The results generated over the course of this research can be subdivided into six areas. They key findings in each of these areas are outlined below.

6.1 Polymer synthesis and derivatisation

Chloromethyl(poly)styrene-based solid support resins were successfully synthesised in multi-gram scales. The beads were converted to the aminomethyl-functionalised derivative using a variation of the Ing-Manske procedure. The hydrophobicity of the amine-functionalised resin made it less than ideal for aqueous systems, however the low cost and ease of synthesis made it an ideal tool for establishing and enhancing all of the necessary reaction protocols to be used during library synthesis.

Resins containing polyethylene glycol were also investigated with Quadragel ultimately synthesised in collaboration with Avecia and Reaxa. Conversion of the hydroxyl-functionalised resin to the amino-functionalised resin using the Ing-Manske procedure afforded a resin suitable for peptide coupling, but with the added advantage of improved compatibility with aqueous systems; which would prove critical for its use as the base resin of all of the library compounds.

The collaboration with Avecia and Reaxa determined that Quadragel resin would be the focus of attention with regards to solid support resins. Its lack of cleavable linker prevented the deconvolution of resin bound sequences. The ability to cleave and identify an 'active' on-resin compound would allow library construction to proceed through the faster 'split and mix' method, rather than the linear 'positionally fixed' type method employed in this study. Accordingly, one avenue for future resin development would centre on the inclusion of such a cleavable linker.

6.2 Comparative loading assessments

A series of compounds was synthesised to enable the quantification of polymer loadings to be directly assessed by a number of different techniques. Previously established quantification methods in common use were scrutinised, and the loading results obtained compared with the theoretical loading values. The study highlighted the large disparity between values obtained for the same resin when using different techniques.

It appears from the study that there is a good correlation between establishing a resin loading by sulfur elemental analysis and by performing a calibration of Fmoc release products in a DBU/DMF solvent system when compared with the actual amount of material isolated after cleavage from the resin. Since the elemental analysis method takes into account the mass increase due to the covalent attachment of amino acids, it must be regarded as the most accurate pre-production method for determining resin loading values.

Ideally for assessing a batch of resin, these two methods should be used in concert with a small sample of the material being converted into the sulfur-containing Fmoc-Met- or Fmoc-Cys- derivative and subjected to both modes of analysis. For small scale syntheses where the financial implications of the resin loading are not so vital and where S is not incorporated within the initially immobilised species, a calibrated DBU method is the most time and cost effective method.

6.3 Peptide and Library Synthesis

The Dde protecting group was successfully synthesised. Subsequent protection of *N*-α-Fmoc-Lys-OH with Dde at the *N*-ε-amine saw the target compound isolated in extremely low yields due to a sub-optimised purification method. Accordingly, commercially obtained N^{α}-Fmoc-Lys(Dde)-OH was used when synthesising peptide sequences and library compounds.

Successful peptide synthesis was undertaken using a variety of coupling agents, to produce peptides of up to 6 amino acids in length. PyBOP, TBTU, HBTU, DCB and DCC were all utilised during various syntheses with great success, even when more challenging sulfur-containing peptides were synthesised for quantifying resin loading in quantitative yields (**Section 2.2**).

The recognition motif of vancomycin requires the dipeptide sequence D-Ala-D-Ala-OH to effect binding. Standard Fmoc protocols create a stepwise addition of a resin-bound amine to a free carboxylic acid, resulting in another resin-bound amine (subject to deprotection). To present the carboxy terminus using Fmoc methodology, two methods of rotating the cleaved peptide and reattaching at the amine terminus to a different resin were devised. The first strategy, employing tritylation of the carboxy anion, failed to work. Protection of the acid with the trityl group was not achieved, possibly due to the residual TFA from the cleavage of the peptide from the resin. Had the reaction been successful, resin coupling using HBTU was to follow, creating the possibility of self-coupling of the peptide or peptide elongation in solution.

A second, less protracted method using an *N*-hydroxysuccinimide-activated carboxyl-resin was attempted. Here the amine of the cleaved peptide displaced the NHS group to form a new amide bond. The advantages of this approach were that the synthesis did not require the post-cleavage addition of protecting groups, while the activated resin negated the need for the coupling agent, HBTU. Although colorimetric analysis suggested the reaction had proceeded as planned, quantification was not achievable in the absence of a cleavable resin linker.

6.4 Boronic acid incorporation

Phenyl boronic acid was successfully attached to a solid support using standard peptide coupling chemistry. The stability of the boronic acid moiety to other conditions commonly used within peptide synthesis was investigated. In all cases, except treatment with TFA, the boronic acid residues remained intact. Reaction with

TFA to produce a trifluoromethyl boron ester was shown to be reversible by incubation with a tertiary amine in a resin-compatible solvent.

The affinity of solid-supported boronic acids to 1,2- and 1,3-*cis* diols was also investigated. Immobilisation and liberation rates of sugars encompassing a furanose, pyranose and oligosaccharide were investigated and found to be comparable with previous, solution-based studies.

A novel and reproducible colorimetric assay for the determination of the on-bead presence of boronic acid was developed. The carminic acid assay allowed for absolute verification of successful boronic acid coupling, even in the presence of other functional groups. Furthermore, visualisation under UV light produced bright fluorescence which enabled positive determination, even if colours viewed under visible light could not be differentiated.

6.5 The fluorescent tagging of substrates

Attempts were made to tag a number of carbohydrates and glycopeptides with fluorescent compounds. Whilst a degree of success was witnessed, as evidenced by TLC and/or mass spectrometry, the process of purification and separation of pure product was much more challenging than had been anticipated. The equilibrium-based nature of carbohydrates in solution made characterisation, particularly by ^{1}H NMR, exceedingly difficult. Reproducing spectra was effectively impossible due to the shift in equilibrium as conditions fluctuated.

Characterisation of vancomycin derivatives was not achieved, even when following literature methods. TLC analysis suggested that a fluorescent form of vancomycin had been synthesised, but complete failure in characterisation led to the abandonment of the labelling strategy in favour of cell inhibition studies.

Questions over the effects of fluorophores on the binding abilities of sugars and glycopeptides mean that future work must be approached with the knowledge that

the investigation of fluorescent systems may not directly relate to the non-fluorescent 'real' systems.

6.6 Bioassay

A library comprising of 128 different peptidyl and peptidyl-boronic acid compounds was synthesised and incubated with vancomycin. Acid-mediated cleavage of any immobilised vancomycin afforded solutions which, when inoculated on plates inoculated with Methicillin susceptible *Staphylococcus aureus*, produced quantifiable zones of inhibition.

The affinity of vancomycin for each sequence was calculated in terms of Gibbs free energy and % immobilisation. The values for Gibbs free energy are calculated, in part, from the number of moles of peptide exposed to vancomycin. Accurate quantification of the loading of the base resin using elemental sulfur analysis allowed the theoretical maximum concentration of each sequence to be calculated.

The values of Gibbs free energy were deemed to be less reliable than the % immobilisation, for a number of reasons; firstly, the concentration of peptide is a theoretical maximum, and cannot be measured. Secondly, the value is dependent on the stoichiometry of binding; something that cannot be established for the boronic acid containing libraries due to the unknown binding ratio that the presence of two boronic acid moieties can present. It is possible that the 1:1 binding ratio of the L-4 library is preserved, but it is also possible that each boronic acid binds to an individual vancomycin molecule, thereby doubling the ratio. Any equilibrium between the two states of binding will be unique to each library compound, and is not measurable within this particular assay.

The percentage immobilisation provides a better reflection of the actual assay result. The calculation relies solely on the ratio of vancomycin before incubation and after cleavage. Accordingly, it is unaffected by the precise and unknown mechanisms of binding to the peptide and boronic acid sequences.

6.7 General Conclusions

The original aims of the research were conclusively met:

1) Can a polymer-based recognition motif be synthesised, such that it can reversibly bind to carbohydrates?
2) Can such a recognition motif be modified, so that it has a greater affinity for particular carbohydrates?
3) Can such a recognition system be used to reversibly bind glycosylated peptides without compromising their biological activity?
4) Can a moiety with a proven affinity for particular a glycopeptide have its selectivity altered by design, such that it enhances the binding to a specific glycopeptide?
5) Can such a recognition system be used as a means of purifying one glycopeptide from a mixture of glycopeptides with differing glycosylation?

Quadragel resin **59** was appended with boronic acid to produce resin **62** which reversibly bound to a range of carbohydrates. This binding was shown to be selective, with strong preferences for certain carbohydrates over others.

Resin **62** also demonstrated reversible binding to the antibiotic vancomycin without compromising its biological activity towards MSSA. The inoculation results of the binding if vancomycin to the library compounds demonstrated that the affinity for vancomycin could also be enhanced and removed.

Future research would fully establish a recognition motif unique to vancomycin and investigating the technology of producing a method for purifying it from complex glycopeptide mixtures.

Chapter 7

Experimental

Experimental

7.1.1 Reagents

Organic reagents used for polymer synthesis and polyvinyl alcohol (PVA, MW 85000-146000) were purchased from Sigma-Aldrich. All polymer supports for SPPS which were not manufactured 'in house' (Wang resin, MBHA Rink Amide) were purchased from Merck Biosciences (NovaBiochem). The Quadragel monomer was supplied by Avecia/Reaxa as a gift.

Amino acids and the aminium/phosphonium were purchased from Merck Biosciences (NovaBiochem) and were of >98.5% purity as assessed 'in-house' by reverse phase HPLC. 4-Carboxybenzeneboronic acid was purchased from Lancaster. All other compounds were obtained in the highest purity possible from Fischer Scientific, Lancaster, Avocado or Sigma Aldrich and used without further purification.

All solvents employed were HPLC grade and used as received. Anhydrous solvents were prepared by distillation and condensed under a positive pressure of nitrogen. Anhydrous reactions were performed in oven-dried glassware and performed under a positive pressure of nitrogen.

Mueller Hinton Agar was obtained from Oxoid (Basingstoke). Agar was prepared as per manufactures instructions and sterilised by autoclaving for 20 mins at 121°C.

Mueller Hinton Broth was obtained from Oxoid (Basingstoke) and prepared as per manufactures instructions before it was sterilised by autoclaving for 20 mins at 121°C.

7.1.2 Apparatus

All weighing procedures were carried out on a Sartorius CP124S, 4 d.p. (0.1 mg) balance.

Nuclear magnetic resonance (NMR) spectra were recorded on a Bruker AC300 at 300.13 MHz for proton frequency and 75.45 MHz for carbon frequency. Chemical shifts are reported in δ units (ppm) relative to tetramethylsilane (external standard) for proton and for carbon-13 (external standard). Spectra were conducted at 303K in either deuterated chloroform ($CDCl_3$), deuterated dimethyl sulfoxide (DMSO-d6) or deuterium oxide (D_2O).

Low Resolution Mass spectroscopy measurements were made with a Hewlett Packard HP5989B MS engine quadrupole mass spectrometer coupled to an HP59987A electrospray unit. Spectra in negative electrospray mode were acquired using nitrogen as the drying gas. The capillary exit voltage (CapEx) was –150V for tuning, then dynamically ramped. Samples were injected via flow injection analysis into a mobile phase of 95 % v/v methanol/water. The quadrupole was at 100 °C and the drying gas heater at 375 °C. Positive and negative APCI utilise nitrogen as the drying gas at 350 °C, with a nebuliser heater at 375 °C. The capEx is -100V for –ve, and +100V for +ve.

High Resolution Mass spectroscopy measurements were made with a Waters LCT Premier TOF (Time of Flight) mass spectrometer featuring Z spray source with electrospray ionisation (+ve and – ve) and a modular LockSpray™ interface. The system is capable of achieving less than 3 ppm, but routinely achieves 5 ppm.

IR spectra of samples were performed as KBr disks or thin film dispersion on NaCl plates in a Perkin Elmer IR spectrometer. Polymer samples were analysed by Attenuated internal refraction (ATR) using diamond compression cells (Golden Gate) with a Perkin Elmer Spectrum One spectrometer.

UV-Visible spectra were recorded on a Perkin Elmer UV/VIS Lambda 12 spectrometer, using a matched pair of quartz glass cuvettes with 1 cm path length.

Fluorescence spectra were recorded on a Molecular Devices, Spectra Max Gemini XS spectrofluorometer.

Thin-layer chromatography was performed on ALUGRAM© CEL 300 UV_{254} plates, purchased from Whatman, were visualised using UV light of 254 nm. Stains specific to the functional groups being identified were used to visualise spots. K6F silica gel 60 A 250 μm glass plates were visualised by UV, or iodine vapour.

Flash column chromatography of Dde **76** was performed using 70-230 mesh silica gel.

High Performance Liquid Chromatography purification of peptide sequences was performed using a Hewlett Packard series 1100 HPLC machine controlled by HPChem software. Mobile Phase A was 0.1 % trifluoroacetic acid in acetonitrile and mobile phase B was 0.1 % trifluoroacetic acid in water. Monitoring was performed via UV absorbance measurements.

Library cleavage solutions were concentrated by evaporation with a rotary evaporator, manufactured by Büchi, (Genevac technologies) under high vacuum

pH measurements were recorded using a Mettler Delta 340 pH meter at room temperature. Calibration was carried out using 0.993 N sodium hydroxide and 0.993 N hydrochloric acid at room temperature.

7.2 Chapter 2 Experimental

7.2.1 Chloromethyl(poly)styrene (2 % DVB crosslinked) 43

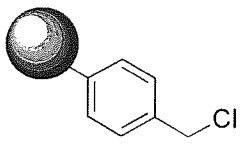

Partially hydrolysed poly(vinyl alcohol) solution (500 ml, 1 % w/v H_2O) was prepared, and stirred at room temperature. Nitrogen was passed though the solution for 30 minutes to remove any dissolved gases. Styrene (99.5 % purity, 41.3 ml, 0.355 mol, 86.7 eqv.), DVB (80 % purity, 1.46 ml, 0.0082 mol, 2.0 eqv), 4-vinylbenzylchloride (90 %, 7.26 ml, 0.0464 mol, 11.3 eqv) and AIBN (0.514 g, 3.13 mmol) were combined and degassed with nitrogen for 30 minutes. The monomer mixture was then added to the stirring aqueous solution and placed under a nitrogen atmosphere. The suspension formed was stirred for a further 30 minutes before the reaction temperature was increased linearly to 75 °C and left stirring for a further 16 hours. The mixture was cooled to room temperature, poured over a 38 μm sieve and washed with copious amounts of water. The resultant polymer beads were transferred to a sintered glass filter and successively washed with H_2O, MeOH, 50:50 MeOH:THF, THF, DCM and MeOH. The polymer was dried to constant weight to yield 19.8 g of white polymer beads with a theoretical loading of 1.00 mmol/g.

Yield: 19.8 g, 42 % by weight

FTIR (ATR) ν_{max}/cm^{-1}: 3028m (Ar. C-H stretch), 2922s (Aliph. C-H stretch), 2855m (Aliph. C-H stretch), 1598m (Benzene ring stretch), 1493s (Benzene ring stretch), 1449s, 1418w, 1265m (CH_2 wag from CH_2Cl), 1027m, 905m, 825s, 754s, 696vs.

Loading Determination: 0.96 mmol/g (%S)

7.2.2 Phthalimido-protected Aminomethyl (poly)styrene 44

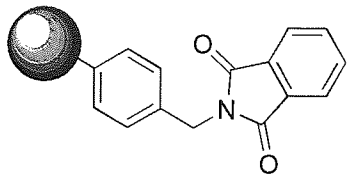

Chloromethyl(poly)styrene **43** (5.04 g, theoretical loading 1.00 mmol/g, 5.04 mmol Rn sites) and potassium phthalimide (3.73 g, 20.2 mmol, 4.0 eqv.) was placed in a round bottomed flask. DMF (300 ml) was added to the flask and the suspension was refluxed under a nitrogen atmosphere for 8 hours. The beads were subsequently washed with 50 % THF in H_2O, THF and methanol before being dried to constant weight in a vacuum oven to yield 5.20 g of polymer beads.

Yield: 5.20 g, 93.6 %

FTIR (ATR) ν_{max}/cm^{-1}: 3057w, 3025m (Ar. C-H stretch), 2921s (Aliph. C-H stretch), ~2848m (Aliph. C-H stretch), 1771w (C=O imide), 1716vs (C=O imide), 1601m (Benzene ring stretch), 1511m, 1493m (Benzene ring stretch), 1451m, 1392m, 1347m, 1327m, 1182w, 1154m, 1085w, 1028w, 937w, 907w, 834m, 756s.

7.2.3 Aminomethyl(poly)styrene (AMPS) 46

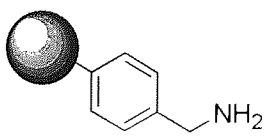

Phthalimido-protected Aminomethyl(poly)styrene **44** (3.0997 g, theoretical loading 0.91 mmol/g, 2.82 mmol reaction sites) was placed under an inert atmosphere in a 3-neck round bottomed flask and swollen in 1,4 dioxane (150 ml). Hydrazine monohydrate (5.00 ml, 103 mmol, 36.5 eqv.) was injected through a seal into the suspended resin. The mixture was allowed to equilibrate for 5 minutes then refluxed for overnight. The resin was then washed with 50 % THF in H_2O, THF and methanol

before being dried to constant weight in a vacuum oven to yield 2.81 g of polymer beads.

Yield: 2.81 g, 97.1 %

FTIR (ATR) ν_{max}/cm^{-1}: 3058w, 3024m (Ar. C-H stretch), 2917s (Aliph. C-H stretch), 2848m (Aliph. C-H stretch), 1601m (Benzene ring stretch), 1492s (Benzene ring stretch), 1451s, 1418w, 1367m/br, 1180w, 1068w, 1028m, 905m, 837w, 755s, 696vs.

Colorimetric test: Kaiser = Blue, TNBS = Orange

7.2.4 Quadragel Resin 59

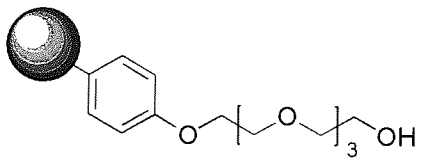

Partially hydrolysed poly(vinyl alcohol) (Airvol 540; 9.0 g, 2.5 % w/v) and sodium chloride (8.04 g, 2.5 % w/v) were charged into a 2 litre cylindrical baffled reactor containing deionised water (304.6 ml) and equipped with a mechanical stirrer. Quadragel monomer **56** (79.7 %, 20.27 g), styrene (17.5 g), 4-divinylbenzene (80 %, 0.4 g), and lauroyl peroxide initiator (1.4 g) were placed into the reactor and stirred at 400 rpm. After 20 minutes the stirrer speed was reduced to 300 rpm, and the reaction heated to 80 °C with a water bath (~ 50 min). After 16 hours, the reaction mixture was cooled, transferred to a 50 μm filter cloth bag and washed with copious amounts of deionised water. The polymer beads were then washed with THF (4 x 200 ml) followed by DCM (2 x 200 ml) and stirred at room temperature under a nitrogen atmosphere in a 500 ml flask with an overhead stirrer with a mix of DCM (450.0 ml), TFA (32.0 g) and triethylsilane (13.1 g) for 4 hours. The polymer beads were then washed with THF (4 x 200 ml) followed by DCM (2 x 200 ml). The beads were placed in a round bottom flask and a 5 % v/v TEA/DCM solution was added and stirred at room temperature under a nitrogen atmosphere for 24 hours. The product was then washed with DCM (4 x 200 ml) and hexane (5 x 200 ml) before

drying to constant weight in a vacuum oven, yielding 24.2 g of white polymer beads with a hydroxyl loading of 0.89 mmol/g.

Yield: 24.2 g, 61 %

FTIR (ATR) ν_{max}/cm^{-1}: 3391m/br (OH stretch), 3060 (ar. C-H), 3026m (Ar. C-H stretch), 2921m (Aliph. C-H stretch), ~2890w (Aliph. C-H stretch), 1602m (Benzene ring stretch), 1509m, 1493m (Benzene ring stretch), 1452m, 1300m, 1244m (C-O-C Ether Stretch), 1177w, 1106m, 1066w, 1027s, 943w, 907w, 829m, 758s, 697vs.

7.2.5 Quadragel-Tosylate 60

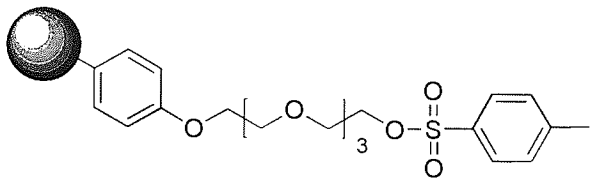

Quadragel resin **59** (5.00 g; theoretical loading 0.89 mmol/g, 4.45 mmol Rn sites) was weighed into a 3-neck round bottomed flask, and swollen with 120 ml THF. A solution of TEA (6.07 ml, 83.7 mmol, 18.8 eqv.) and DMAP (0.14 g, 1.07 mmol, 0.24 eqv.) was added to the reaction vessel. The mixture was stirred and cooled to 1 °C. A solution of *p*-toluenesulfonyl chloride (4.62 g, 24.2 mmol, 5.45 eqv.) in 60 ml THF was added dropwise to the reaction mixture, maintaining the temperature of the solution below 5 °C. After complete addition of the *p*-toluenesulfonyl chloride in THF, the reaction was brought slowly up to room temperature and stirred for 16 hours. The polymer beads were then washed with 50 % THF in H_2O, THF and methanol before being dried to constant weight in a vacuum oven yielding 5.90 g of white polymer beads.

Yield: 5.67 g, 99.8 %

FTIR (ATR) ν_{max}/cm^{-1}: 3025m (Ar. C-H stretch), 2920s (Aliph. C-H stretch), ~2890m (Aliph. C-H stretch), 1600m (Benzene ring stretch), 1509s, 1492s (Benzene ring stretch), 1451s, 1358s (SO_2 Antisym. Stretch), 1297w, 1244s (C-O-C Ether

Stretch), 1188w, 1175s (SO_2 Sym. Stretch), 1097m, 1065m, 1027m, 918s (S-O-C stretch), 815s, 757s, 697vs, 663m (C-S stretch)

Elemental Analysis: 79.7 % w/w Carbon, 7.9 % w/w Hydrogen, <0.1 % w/w Nitrogen, 2.4 % w/w Sulphur.

Loading Determination: 0.85 mmol/g (%S)

7.2.6 Phthalimido-Protected Quadragel 61

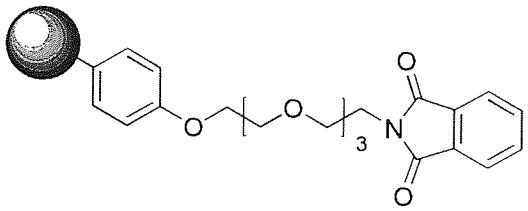

Quadragel-Tosylate **60** (3.00 g, theoretical loading 0.79 mmol/g, 2.37 mmol Rn sites) and potassium phthalimide (2.20 g, 11.9 mmol, 5.0 eqv.) was placed in a round bottomed flask. DMF (300 ml) was added to the flask and the suspension was refluxed under a nitrogen atmosphere for 8 hours. The beads were subsequently washed with 50 % THF in H_2O, THF and methanol before being dried to constant weight in a vacuum oven to yield 3.00 g of polymer beads.

Yield: 3.00 g, 98 %

FTIR (ATR) ν_{max}/cm^{-1}: 3025m (Ar. C-H stretch), 2920s (Aliph. C-H stretch), ~2890m (Aliph. C-H stretch), 1773w (C=O imide), 1712vs (C=O imide), 1601m (Benzene ring stretch), 1509m, 1492m (Benzene ring stretch), 1451m, 1392m, 1244m (C-O-C Ether Stretch), 1177w, 1111m, 1066w, 1027w, 907w, 829m, 757s, 720m, 697vs.

7.2.7 Quadramine 62

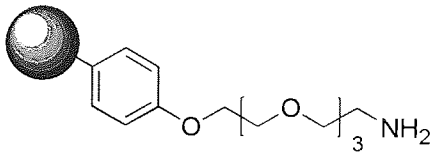

Phthalimido-protected Quadragel **61** (2.00 g, theoretical loading 0.81 mmol/g, 1.62 mmol Rn sites) was placed under an inert atmosphere in a 3-neck round bottomed flask and swollen in 1,4 dioxane (360 ml). Methylamine (40 % w/v in H_2O) (4.5 ml, 58.1 mmol, 35.8 eqv.) was injected through a seal into the suspended resin. The mixture was allowed to equilibrate for 5 minutes then refluxed for overnight. The resin was then washed with 50 % THF in H_2O, THF and methanol before being dried to constant weight in a vacuum oven to yield 1.82 g of polymer beads.

Yield: 1.81 g, 98.8 %

FTIR (ATR) ν_{max}/cm^{-1}: 3059w, 3025m (Ar. C-H stretch), 2919s (Aliph. C-H stretch), ~2890m (Aliph. C-H stretch), 1601m (Benzene ring stretch), 1509m, 1492m (Benzene ring stretch), 1451m, 1371w, 1350w, 1300w, 1244m (C-O-C Ether Stretch), 1177w, 1110m, 1066w, 1028w, 908w, 828m, 756s, 697vs.

Colorimetric test: Kaiser = Blue, TNBS = Orange

7.2.8 On-bead assays for determining primary amines - TNBS Test

2,4,6-Trinitrobenzenesulfonic acid (TNBS, 20 µl) and *N,N*-diisopropylethylamine (DIPEA) (10 % v/v in DMF, 20 µl) were added to a small test sample (~1-3 mg) of polymer beads. The presence of free primary amine groups was indicated by an orange/red colouration (positive) of the beads.

7.2.9 On-bead assays for determining primary amines - Kaiser Test

Ninhydrin (5 % w/v in EtOH, 40 µl), pyridine (20 µl) and phenol (80 % w/v in EtOH, 20 µl) were added to a small test sample (~1-3mg) of polymer beads and the resultant mixture heated at 105°C for 3 mins. in an oven. The presence of free primary amine groups was indicated by a dark blue/purple colouration (positive) of the beads and liquor.

7.2.10 Fmoc-Met-AMS (64 and 64a)

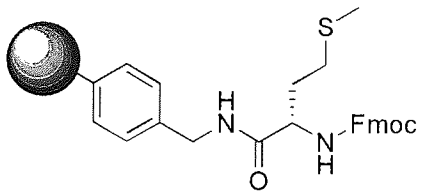

Aminomethyl(poly)styrene **46** (0.500 g, theoretical loading 1.0 mmol / g, ~0.5 mmol reaction sites) was weighed into a frit-containing polypropylene tube (10 ml) and swollen in DMF (7 ml) for one hour. After this duration the DMF was drained. A coupling solution of Fmoc-Met-OH (0.744 g, 2.00 mmol), *N*-hydroxybenzotriazole (HOBT, 0.306 g, 2.00 mmol), 2-(1H-benzotriazole-1-yl)-1,1,3,3-tetramethyluronium hexafluorophosphate (HBTU, 0.743 g, 2.00 mmol), and DIPEA (0.520 ml, 3.00 mmol) in DMF (2.5 ml) was added to the resin and the mixture agitated for 45 mins. Successful coupling of the Fmoc-protected amino acid was confirmed by a negative TNBS test for free primary amine. The coupling solution was drained and the resin washed with successive aliquots of DMF (10 x 7 ml). A capping solution consisting of Ac_2O (0.710 ml, 7.5 mmol), triethylamine (TEA, 1.05 ml, 7.5 mmol) in DMF (0.580 ml) was then added to the resin. The resultant suspension was agitated for 30 mins. The capping solution was then drained and the resin washed with successive aliquots of DMF (10 x 7 ml) and collapsed with MeOH (5 x 7 ml.). The resin was dried under vacuum to yield derivative **64** (0.544 g).

Derivative **64a** (0.524 g) was synthesised using the same method but utilizing resin **46a** (0.503 g, theoretical loading 1.2 mmol / g, ~0.6 mmol reaction sites). A coupling solution of Fmoc-Met-OH (0.897 g, 2.41 mmol), HOBT (0.370 g, 2.41 mmol), HBTU (0.897 g, 2.41 mmol), DIPEA (0.630 ml, 3.62 mmol) in DMF (3.0 ml) was employed for 45 mins. Similarly, capping was undertaken with a solution of Ac_2O (0.860 ml, 9.0 mmol) and TEA (1.27 ml, 9.0 mmol) in DMF for 15 mins.

7.2.11 Fmoc-Met-Met-AMS (65 and 65a)

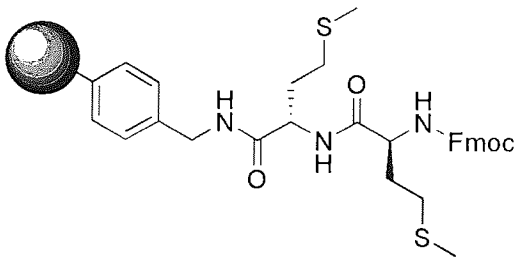

Fmoc-Met-AMPS **64** (0.250 g, theoretical loading 1.0 mmol / g, ~0.25 mmol reaction sites) was weighed into a frit-containing polypropylene tube (10 ml) and swollen in DMF (7 ml) for one hour before draining the DMF. The *N*-Fmoc-protecting group was removed by exposure to 20 % v/v piperidine in DMF solution (5 ml) with agitation over 5 mins. The resin was collected by filtration and exposed to a second identical *N*-Fmoc deprotection cycle. In a third and final deprotection step, the solution containing the remaining DBF-piperidine adduct was drained and the resin washed successively with DMF (10 x 7 ml). Successful removal of the Fmoc protecting group was confirmed by a positive TNBS test. A coupling solution of Fmoc-Met-OH (0.373 g, 1.00 mmol), HOBT (0.153 g, 1.00 mmol), HBTU (0.372 g, 1.00 mmol) and DIPEA (0.260 ml, 1.50 mmol) in DMF (1.25 ml) was added to the afforded resin and the suspension agitated for 45 mins. Successful coupling of the Fmoc-protected amino acid was confirmed by a negative TNBS test. The coupling solution was drained and the resin washed with DMF (10 x 7 ml). A capping solution consisting of Ac_2O (0.360 ml, 3.0 mmol) and TEA (0.530 ml, 3.0 mmol) in DMF (0.290 ml) was added to the resin and agitated for 30 mins. The capping solution was drained and the resin washed with DMF (10 x 7 ml) then

collapsed with MeOH (5 x 7 ml). The resultant resin was dried under vacuum to yield derivative **65** (0.298 g).

Derivative **65a** (0.328 g) was synthesised in an identical manner utilizing derivative **64a** (0.250 g, theoretical loading 1.2 mmol / g, ~0.3 mmol reaction sites). A coupling solution of Fmoc-Met-OH (0.449 g, 1.20 mmol), HOBT (0.185 g, 1.20 mmol), HBTU (0.448 g, 1.20 mmol), DIPEA (0.440 ml, 0.75 mmol) in DMF (1.25 ml), and a capping solution of Ac_2O (0.430 ml, 4.5 mmol) and TEA (0.640 ml, 4.5 mmol) in DMF (0.350 ml).

7.2.12 Synthesis of resin bound oligo-peptide sequences

Assembly of Fmoc-[Met^5]-Enkephalin-OH [133] and Fmoc-[Met^5Met^6]-Enkephalin-OH was performed using standard uronium methodologies upon identical batches of 2-chlorotrityl chloride PS support **63**.

The first amino acid in both sequences was added to the support via a facile S_N1 reaction. Firstly, Fmoc-Met-OH (10.03 g, 27 mmol) was dissolved in DMF/DCM (100 ml, 4:1 respectively). A single aliquot of DIPEA (9.400 ml, 54 mmol) was added to this solution and the basic mixture agitated for 1 min with stirring. This mixture was then added to dry 2-chlorotrityl chloride polystyrene resin **63** (15.002 g, theoretical loading 1.2 mmol / g). The resulting resin derivative was washed successively with DMF (10 x 30 ml), DCM (5 x 30ml) then collapsed with MeOH (5 x 30 ml). The resultant resin Fmoc-Met-O-2-Cl Trt PS **66** was then dried to constant weight (18.704 g).

A sample of derivative **66** (5.009 g) was weighed into a glass column (~100 ml) containing a glass sinter (porosity 4) and swollen in DMF (70 ml) for one hour. After draining the DMF the *N*-Fmoc-protecting group was removed by 2 separate exposures of the resin to 20 % v/v piperidine in DMF solution (for 3 mins., 40 ml and 7 mins. 40 ml respectively). The final deprotection solution containing any remaining DBF adduct was drained and the resultant resin washed with DMF (10 x

30 ml). Qualitative removal of the Fmoc group was confirmed with a positive Kaiser test for free primary amines.

For both sequences the peptide elongation was performed in a stepwise manner employing the TBTU / DIPEA technique. Fmoc-amino acid activations (Table 1) were performed in the minimum volume of DMF (10 ml – 20 ml). Coupling times were minimised and deemed to have reached full completion within 20 mins. for all steps during the assembly. Following each coupling cycle and the second of the deprotection cycles, the peptidyl-resin was washed successively with DMF (10 x 30 ml). Propagation of the chain continued with the subsequent removal of the *N*-Fmoc protecting group with 20 % v/v piperidine in DMF (for 3 mins., 40 ml and 7 mins. 40 ml respectively) and coupling of the ensuing amino acid. Indicative Kaiser resin tests confirmed successful progression of the stepwise peptide assemblies. Both resin bound sequences Fmoc-Tyr(^{t}Bu)-Gly-Gly-Phe-Met-O-2Cl Trt PS and Fmoc-Tyr(^{t}Bu)-Gly-Gly-Phe-Met-Met-O-2Cl Trt PS were left *N*-Fmoc protected. Both completed resin bound sequences were washed with DMF (10 x 30 ml) then collapsed with DCM (10 x 30 ml) and MeOH (10 x 30 ml) and air dried to yield derivative **68** (6.021 g) and **69** (6.620 g) respectively

Table 46: Masses of Fmoc-amino acids coupled to derivative 66 in order to synthesise derivatives 68 and 69.

Coupling sequence	Derivative	Met / g	Phe / g	Gly / g	Gly / g	Tyr(^{t}Bu) / g
1	**68**	-	5.8132	4.4568	4.4579	6.8939
2	**69**	5.582[a]	5.8157	4.4600	4.4620	6.9028

The molar equivalents of all of the reagents used in the coupling procedure, with respect to the theoretical resin loading value were as follows: Fmoc-amino acid (see Table above, 2.50 eq.), 2-(1H-benzotriazole-1-yl)-1,1,3,3-tetramethyluronium tetrafluoroborate (TBTU) (4.528 g, 2.35 eq.), DIPEA (3.08 ml, 3.00 eq.) in DMF (~20 ml). [a] A small aliquot of resin (0.072 g) was removed from the bulk after the methionine coupling. This Fmoc-Met-Met resin is derivative **67**.

Fmoc-[Met^5]-Enkephalin -O-2Cl Trt PS **68** (5.0027 g) and Fmoc-[Met^{5}Met^6]-Enkephalin -O-2Cl Trt PS **69** (5.0012 g) were cleaved from the resin via acidolysis. Separately, each peptidyl-resin was incubated with a pre-mixed solution of TFA/EDT/TIPS (95/2.5/2.5, 100 ml) over 90 mins. After this time the spent resin

was removed by filtration and the filtrate concentrated under reduced pressure to a volume of <10 ml. The crude peptidic cleavage products were precipitated from diethyl ether (100 ml), triturated and collected by filtration through a DVPP membrane filter cloth. Reverse phase HPLC analysis suggested only minor alkylation of the methionine residues by the ^{t}Bu cation had occurred[134]. Accordingly both peptides were incubated for four hours in 0.5M AcOH in water/MeCN (1:1, 100 ml, 55°C)[120], successfully reducing the methionine residues. Both crude peptides were lyophilised affording the desired peptides Fmoc-[Met^{5}]-Enkephalin-OH (MW.796 Yield: 1.7091 g, 2.15 mmol) and Fmoc-[Met^{5}Met^{6}]-Enkephalin-OH (MW.927 Yield: 2.043 g, 2.20 mmol) as white, fluffy solids. In each case analysis by HPLC indicated a single product of purity >95 %.

7.2.13 Fmoc-Met-Quadramide 70

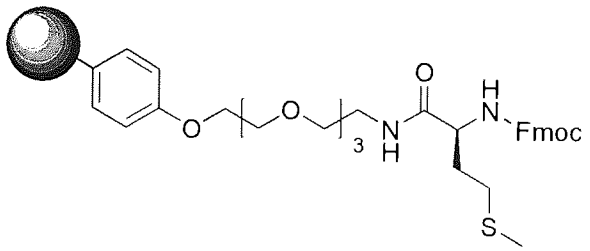

Quadramine **62** (0.0995 g, theoretical loading 0.89 mmol / g, ~ 0.089 mmol reaction sites), was weighed into a frit-containing polypropylene tube (2 ml) and swollen in DMF (7 ml) for one hour. After this duration the DMF was drained. A coupling solution of Fmoc-Met-OH (0.133 g, 0.37 mmol), *N*-hydroxybenzotriazole (HOBT, 0.055 g, 0.37 mmol), 2-(1H-benzotriazole-1-yl)-1,1,3,3-tetramethyluronium hexafluorophosphate (HBTU, 0.138 g, 0.37 mmol), and DIPEA (0.10 ml, 0.53 mmol) in DMF (2.0 ml) was added to the resin and the mixture agitated for 45 mins. Successful coupling of the Fmoc-protected amino acid was confirmed by a negative TNBS test for free primary amine. The coupling solution was drained and the resin washed with successive aliquots of DMF (10 x 7 ml) and collapsed with MeOH (5 x 7 ml.). The resin was dried under vacuum to yield derivative **70** (0.117 g).

7.2.14 On-support Fmoc release assays

The polymer-supported amino acids, **64, 64a, 65** and **65a,** were subjected to two Fmoc release assays which employed piperidine or 1,8-diazabicyclo[5.4.0]undec-7-ene (DBU) as the Fmoc-cleavage agent respectively. Polymer-supported peptides **66-70** were subjected to just the DBU-mediated method.

The assay procedures employing piperidine utilised a previously reported method for resin samples of about 3 mg[82]. This methodology was also repeated on a larger scale utilizing resin samples of about 17 mg to enable greater accuracy. Reagent amounts and solvent volumes were scaled accordingly. All of the assay procedures employing DBU were performed on resin samples of about 50 mg (accurately weighed) using a previously reported method[78].

7.2.15 Calibrated Fmoc release assay employing piperidine

To calculate accurate resin loading, by piperidine-mediated Fmoc release assay, it was first necessary to construct a calibration curve for the DBF-piperidine adduct released from Fmoc-Met-OH. To establish whether or not this calibration curve was amino acid dependent, similar curves were constructed for Gly and Nle. Accordingly, approximately 25 mg of each Fmoc-AA-OH (one of Met (0.0261 g, 0.070 mmol), Gly (0.0252 g, 0.085 mmol) and Nle (0.0252 g, 0.071 mmol)) was transferred to a 100 ml volumetric flask and dissolved in 20 % v/v piperidine in DMF (80.000 ml). After stirring for 30 mins. the solution was made up to volume with 20 % v/v piperidine in DMF, to yield stock solution $A_{(pip.)}$. An aliquot of $A_{(pip.)}$ (0.500, 1.000, 2.000, 3.000,..., 12.000 ml) was transferred to a 25 ml volumetric flask and further diluted to volume with 20 % v/v piperidine in DMF. This procedure afforded sample solutions with a range of known Fmoc concentrations. In each case the UV/vis absorbance of each sample solution was measured in quadruplicate at 290 and 300 nm. The average absorbance values obtained for each sample were plotted against the known Fmoc concentration to produce a series of calibration curves (Figure. 19 & 20) each with a gradient of ε_{Fmoc}. By averaging the calibration curve

gradients at each wavelength a good estimation of the (amino acid-independent) extinction coefficient ($\varepsilon_{piperidine/DMF}$) of Fmoc in 20 % v/v piperidine in DMF is provided.

7.2.16 Calibrated Fmoc release assay employing DBU[78]

Calibration curves were constructed for DBU-mediated Fmoc release in an analogous fashion to those constructed for piperidine mediated Fmoc release. Accordingly, approximately 25 mg of each Fmoc-AA-OH (one of Met (0.0254 g, 0.068 mmol), Gly (0.0258 g, 0.087 mmol) and Nle (0.0250 g, 0.071 mmol)) was transferred to a 100 ml volumetric flask and dissolved in DMF (20.000 ml). After stirring for 30 mins. DBU (0.400 ml) was added to this flask furnishing a 2 % v/v DBU in DMF solution. This resultant media was stirred for a further 30 mins. before being diluted to volume with MeCN to yield stock solution $A_{(DBU)}$. An aliquot of $A_{(DBU)}$ (0.500, 1.000, 2.000, 3.000, 4.000 ml) was transferred to a 25 ml volumetric flask, and diluted to volume with MeCN to yield sample solutions with a range of known Fmoc concentrations. For each amino acid the UV/vis absorbance of each sample solution was measured in quadruplicate at both 294 and 305 nm. The average absorbance values obtained for each sample were plotted against the known Fmoc concentrations to produce a series of calibration curves (Figure 21) each with a gradient of ε_{Fmoc}. Averaging the calibration curve gradients at each wavelength provides a good estimation of the extinction coefficient ($\varepsilon_{DBU/DMF/MeCN}$) of Fmoc in the DBU/DMF/MeCN solvent system. The same procedure was employed for the analysis of resin samples (~50 mg, accurately weighed) except that in each case 2.000 ml of the deprotection reaction solution (the sample equivalent solution to $A_{(DBU)}$) was diluted to a volume of 25 ml prior to UV analysis by the addition of MeCN.

7.3 Chapter 3 Experimental

7.3.1 2-acetyldimedone (Dde) 76

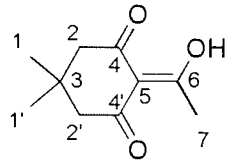

Dimedone (10.0 g, 71.5 mmol, 1.1 eqv.), DCC (13.4 g, 65 mmol, 1 eqv.) and DMAP (7.93 g, 64.9 mmol, 1 eqv.) were dissolved in DMF (100 ml). To this, a solution of glacial acetic acid (3.72 ml, 65 mmol, 1 eqv.) in DMF (150 ml) was added drop wise (0.5 ml/min) under an inert atmosphere. The clear solution was stirred at room temperature for 48 hours and the colourless precipitate removed by suction filtration. The solvent was removed *in vacuo* to yield a red waxy solid which was dissolved in a minimum of ethyl acetate and washed with $KHSO_4$ (1M, 200 ml). The crude produce was then extracted into a sat. $NaHCO_3$ solution (200 ml) which was neutralised with 5M HCl prior to extraction with DCM (200 ml). The organic extract was dried over $MgSO_4$ and the solvent removed *in vacuo* to give the crude product as a thick yellow oil (7.15 g). A small sample of crude product (0.679 g) was purified by flash column chromatography (100 % DCM) to afford the title compound as a yellow oil (0.337 g, 1.85 mmol, 28.5 %).

Yield: 0.337 g (1.85 mmol, 28.5 %)

^{1}H NMR: (250 MHz, $CDCl_3$) δ_H 1.04 (s, 6H, **H-1/H-1'**), 2.32 (s, 2H, CH_2), 2.50 (s, 2H, CH_2), 2.57 (s, 3H, **H-7**), 5.27 (s, 0.5 H, **H-5** equilibrium to ketone tautomer)

^{13}C NMR: (75 MHz, d-DMSO, PENDANT) δ_C 28.0 (s, CH_3, **C-1** & **C-1'**), 28.6 (s, CH_3, **C-7**), 30.8 (s, C, **C-3**), 46.3 (s, CH_2, **C-2/C-2'**) 52.2 (s, CH_2, **C-2/C-2'**), 102.9 (s, C, **C-5** keto), 112.5 (s, C, **C-5** enol) 195.3 (s, C, **C-4/C-4'**), 198.7 (s, C, **C-4/C-4'**), 202.3 (s, C, **C-6**)

FW: 182.2164, **Exact Mass:** 182.0943

MS: HRMS (ES-): ***m/z*** 181.0781 (100 % $[M-H]^-$), 181.2169 (50 % $[M-H]^-$), calculated for $C_{10}H_{13}O_3$ 181.0865

FTIR (Thin film, NaCl plate) ν_{max}/cm^{-1}: 3626w/br (H-Bonded OH Stretch), 3318w, 2959vs (Aliph. C-H. Stretch), 2872s (Aliph. C-H Stretch), 1668vs (C=O Ketone), 1560vs (C=O β diketone in Enol form), 1444vs (CH_3 Antisymm. Deformation), 1407w, 1370s (CH_3 Symm. Deformation), 1333w, 1237w, 1148m, 1125w, 1047s (C-O stretch of alcohol), 1028m, 976w, 947m/s, 924m, 848w, 704w, 667w.
Rf: 0.23 (Mobile Phase: 100 % DCM) visualised under UV_{254}

7.3.2 Phenylboronic acid-*N*-α-Lysine(NH_2)-Alanine-Glycine-O-NH_2 87

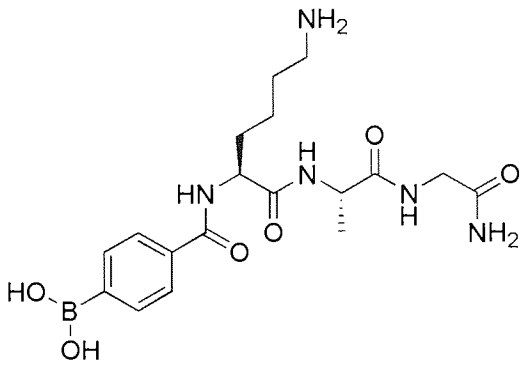

Fmoc-protected Rink Amide MBHA resin (0.100 g, loading 0.8 mmol/g, 0.08 mmol Rn sites) was treated with 20 % v/v piperidine in DMF (2 x 10 ml, 3 & 7 mins. respectively) to afford the amine functionalised resin **84**. Peptide elongation was performed in a stepwise manner employing the PyBOP / DIPEA technique. Fmoc-amino acid activations (Table 47) were performed in the minimum volume of DMF (5 ml – 10 ml). Coupling times were minimized and deemed to have reached full completion within 20 mins. for all steps during the assembly. Following each coupling cycle and the second of the deprotection cycles, the peptidyl-resin was washed successively with DMF (10 x 10 ml). Propagation of the chain continued with the subsequent removal of the *N*-Fmoc protecting group with 20 % v/v piperidine in DMF (for 3 mins., 20 ml and 7 mins. 20 ml respectively) and coupling of the ensuing amino acid. Indicative TNBS resin tests confirmed successful progression of the stepwise peptide assemblies, with carminic acid being used to confirm the addition of the boronic acid.

Table 47: Masses of Fmoc-amino acids used coupled to resin Rink Amide MBHA resin in order to synthesise derivative 86

Component	Gly/g	Ala/g	Lys(Boc)/g	4-Carboxyphenylboronic acid/g
Amino Acid	0.1012	0.1008	0.1507	0.0534
PyBOP	0.1506	0.1508	0.1501	0.1494
DIPEA	0.084 ml	0.084 ml	0.084 ml	0.084 ml

The resultant resin bound sequence $(HO)_2B$-Ph-CONH-Lys(NHBoc)-Ala-Gly-Rink Amide MBHA **86** was then dried to constant weight (0.104 g).

The sequence was cleaved from the resin via acidolysis. The peptidyl resin was incubated with a pre-mixed solution of TFA/EDT/TIPS (95/2.5/2.5, 10.0 ml) over 90 mins. After this time the spent resin was removed by filtration and the filtrate concentrated under reduced pressure to a volume of <1 ml. The crude peptidic cleavage products were precipitated from diethyl ether/hexane (1:1 10.0 ml). The precipitate was centrifuged for 10 minutes at 5000 rpm and the supernatant removed. The peptide was dissolved in water and shell-frozen before being lyophilised to afford 0.0331 g of drawn peptide **87**.

Yield: 0.0326 g (0.0773 mmol, 98.4 %)

FW: 421.2558, **Exact Mass:** 421.2133

MS: LRMS (ES+): ***m/z*** 423 (ES+; $[M+H]^+$), 445 (ES+; $[M+Na]^+$), calculated for $C_{18}H_{28}BN_5O_6$

7.3.3 Quadramide-phenylboronic acid 88

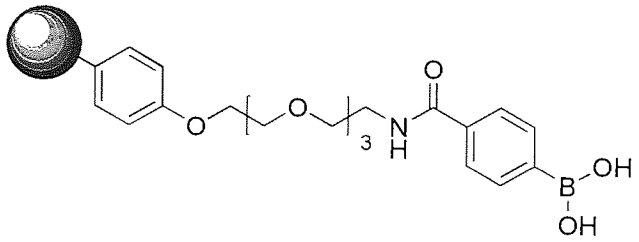

Quadramine **62** (1.9993 g, theoretical loading 0.89 mmol/g, 1.78 mmol Rn sites) was swollen in DMF for 1 hour prior to coupling. Separately, 4-carboxyphenylboronic acid (0.8513 g, 5.13 mmol, 2.88 eqv.) and TBTU (1.5221 g, 4.74 mmol, 2.66 eqv.) were dissolved in a minimum volume of DMF (~15 ml), before adding DIPEA (1.05 ml, 6.02 mmol, 3.39 eqv.). The resin was drained and the boronic acid containing solution was transferred quantitatively to the resin, where the mixture was agitated. The reaction was monitored by removing a small amount of resin (~ 3 mg) and subjecting it to a Kaiser assay. After approximately 20 mins the reaction was deemed complete. The coupling solution was drained and the resin washed with DMF (10 x 30 ml), DCM (10 x 30 ml) and methanol (5 x 30 ml) before air drying to yield 2.1661 g of white polymer beads.

Yield: 2.1661 g, 95.7 %

FTIR (ATR) ν_{max}/cm^{-1}: 3356m/br (H Bonded OH Stretch), 3026m (Ar. C-H stretch), 2919s (Aliph. C-H stretch), ~2890w (Aliph. C-H stretch), 1661s (C=O stretch 2° amide), 1602m (Benzene ring stretch), 1509m, 1493m (Benzene ring stretch), 1452m, 1348m (B-O Stretch), 1301m, 1244m (C-O-C Ether Stretch), 1178w, 1107s (C-O-C Aliph. Ether Stretch), 1028m, 909w, 829m, 756s, 697vs, 667w.

Colorimetric test: Kaiser = White, TNBS = White, Carminic acid = Red

7.3.4 Fmoc-Glycine-Lysine(Dde)-D-Alanine-D-Alanine-OH 95

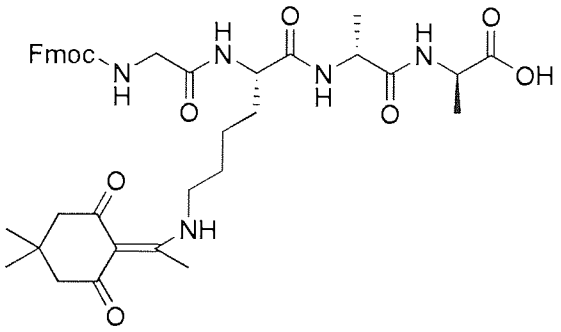

The first amino acid was added to the support via a facile S_N1 reaction. Firstly, Fmoc-D-Ala-OH (0.65 g, 2.1 mmol) was dissolved in DMF/DCM (10.0 ml, 4:1 respectively). A single aliquot of DIPEA (0.73 ml, 4.2 mmol) was added to this solution and the basic mixture agitated for 1 min with stirring. This mixture was then added to dry 2-chlorotrityl chloride polystyrene resin **63** (1.00 g, theoretical loading 1.4 mmol / g) and agitated gently for 1 hour. The resulting resin derivative was washed successively with DMF (10 x 10 ml).

The peptide elongation was performed in a stepwise manner employing the TBTU / DIPEA technique. Fmoc-amino acid activations (Table 48) were performed in the minimum volume of DMF (5 ml – 10 ml). Coupling times were minimized and deemed to have reached full completion within 20 mins. for all steps during the assembly. Following each coupling cycle and the second of the deprotection cycles, the peptidyl-resin was washed successively with DMF (10 x 10 ml). Propagation of the chain continued with the subsequent removal of the *N*-Fmoc protecting group with 20 % v/v piperidine in DMF (for 3 mins., 20 ml and 7 mins. 20 ml respectively) and coupling of the ensuing amino acid. Indicative Kaiser resin tests confirmed successful progression of the stepwise peptide assemblies. The resin bound Fmoc-D-Ala-D-Ala-O-2-Cl Trt PS was dried to constant weight (1.72 g) and divided in two with 0.85 g being used to continue the sequence.

Table 48: Masses of Fmoc-amino acids used coupled to resin 63 in order to synthesise derivative 94

Component	D-Ala/g	Lys(Dde)/g	Gly/g
Amino Acid	0.6537	0.9321	0.5203
TBTU	1.0564	0.5282	0.5282
DIPEA	0.73 ml	0.37 ml	0.37 ml

The resultant resin bound sequence Fmoc-Gly-Lys(Dde)-D-Ala-D-Ala-O-2-Cl Trt PS **94** was then dried to constant weight (0.80 g).

The sequence was cleaved from the resin via acidolysis. The peptidyl resin was incubated with a pre-mixed solution of TFA/EDT/TIPS (95/2.5/2.5, 10.0 ml) over 90 mins. After this time the spent resin was removed by filtration and the filtrate concentrated under reduced pressure to a volume of <1 ml. The crude peptidic cleavage products were precipitated from diethyl ether (10.0 ml), triturated and collected by filtration through a DVPP membrane filter cloth to yield the peptidic product **95**.

Yield: 0.41 g (0.56 mmol, 80 %)
FW: 731.83, **Exact Mass:** 731.35
MS: LRMS (ES+): ***m/z*** 732 (100 % $[M+H]^+$), 754 (97 % $[M+Na]^+$), calculated for $C_{39}H_{49}N_5O_9$ 731.3530

7.3.5 Quadramide-butanoic acid 98

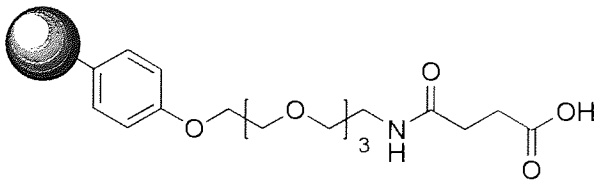

Quadramine **62** (0.994 g, loading 0.89 mmol/g, 0.885 mmol Rn sites) was added to a solution of succinic anhydride (1.00 g, 10.0 mmol) in DMF (20.0 ml). DIPEA (1.74 ml, 10 mmol) was added and the suspension was agitated at room temperature

overnight. The coupling solution was drained and the beads were washed with copious amounts of DMF, DCM and methanol. The resin was dried to constant mass to yield 1.05 g of white polymer beads.

Yield: 1.05 g, 97.2 %

FTIR (ATR) ν_{max}/cm^{-1}: 3334 s/br (H Bonded OH Stretch), 3059w, 3025m (Ar. C-H stretch), 2921s (Aliph. C-H stretch), ~2890m (Aliph. C-H stretch), 1727s (C=O stretch carboxylic acid), 1649s (C=O stretch 2° amide), 1602m (Benzene ring stretch), 1582w, 1546w, 1509s, 1492s (Benzene ring stretch), 1452s, 1349w, ~1240m (C-O-C Ether Stretch), 1177m, 1098s (C-O-C Aliph. Ether Stretch), 1028m, 945w, 829m,

Colorimetric Assay: Kaiser = Colourless, TNBS = Colourless

7.3.6 H_2N-Glycine-Lysine(NH_2)-D-Alanine-D-Alanine-OH 106

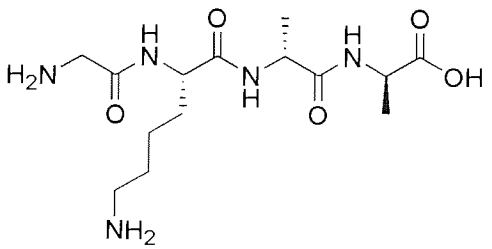

Fmoc-D-Ala-OH (0.996 g, 1.0 mmol) and pyridine (0.66 ml, 8.25 mmol) was dissolved in DMF (15.0 ml). This mixture was then added to dry Wang resin (100-200 mesh, 2 % DVB; 1.00 g, theoretical loading 0.6-1.0 mmol / g).
2,6 dichlorobenzoyl chloride (DCB, 0.71 ml, 5 mmol) was added to the flask and the mixture was agitated for 18 hours. The resulting resin derivative was washed successively with DMF (10 x 10 ml).

The peptide elongation was performed in a stepwise manner employing the TBTU / DIPEA technique. Fmoc-amino acid activations (Table 49) were performed in the minimum volume of DMF (5 ml – 10 ml). Coupling times were minimized and deemed to have reached full completion within 20 mins. for all steps during the assembly. Following each coupling cycle and the second of the deprotection cycles,

the peptidyl-resin was washed successively with DMF (10 x 10 ml). Propagation of the chain continued with the subsequent removal of the *N*-Fmoc protecting group with 20 % v/v piperidine in DMF (for 3 mins., 20 ml and 7 mins. 20 ml respectively) and coupling of the ensuing amino acid. Indicative Kaiser resin tests confirmed successful progression of the stepwise peptide assemblies.

Table 49: Masses of Fmoc-amino acids used coupled to resin Wang resin in order to synthesise derivative 105

Component	D-Ala/g	Lys(Mtt)/g	Gly/g
Amino Acid	0.7845	1.5634	0.7578
TBTU	0.7597	0.7706	0.7602
DIPEA	0.53 ml	0.51 ml	0.51 ml

The resultant resin bound sequence H_2N-Gly-Lys(NH_2)-D-Ala-D-Ala-O-Wang **105** was then dried to constant weight (1.064 g).

The sequence was cleaved from the resin via acidolysis. The peptidyl resin was incubated with a pre-mixed solution of TFA/EDT/TIPS (95/2.5/2.5, 10.0 ml) over 90 mins. After this time the spent resin was removed by filtration and the filtrate concentrated under reduced pressure to a volume of <1 ml. The crude peptidic cleavage products were precipitated from diethyl ether (10.0 ml), triturated and collected by filtration through a DVPP membrane filter cloth. The peptide was dissolved in water and shell-frozen before being lyophilised to afford a drawn peptide **106**.

Yield: 0.062 g (0.18 mmol, 18-30 % based on resin loading; 97 % based on mass gain)

FW: 345.3947, **Exact Mass:** 345.2012

MS: HRMS (ES+): ***m/z*** 346.2077 (100 % $[M+H]^+$) calculated for $C_{14}H_{27}N_5O_5$

7.3.7 Quadramide-PEG$_4$carboxylic acid 112

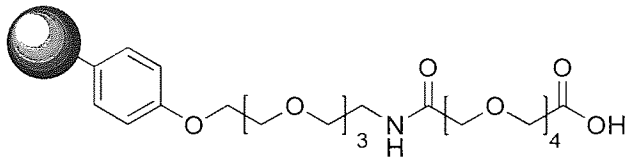

Quadramine **62** (0.10 g, loading 0.89 mmol/g, 0.089 mmol Rn sites) was added to a solution of Poly(ethylene glycol) bis(carboxymethyl)ether (0.106 g, 0.50 mmol) and TBTU (0.398 g, 1.2 mmol) in DMF (1.2 ml). DIPEA (0.21 ml, 1.2 mmol) was added and the suspension was agitated at room temperature overnight. The coupling solution was drained and the beads were washed with copious amounts of DMF, DCM and methanol. The resin was dried to constant mass to yield 0.119 g of white polymer beads.

Yield: 0.119 g, 95.2 %

FTIR (ATR) ν_{max}/cm^{-1}: 3364 m/br (H Bonded OH Stretch), 3059w, 3025m (Ar. C-H stretch), 2920s (Aliph. C-H stretch), 2868m (Aliph. C-H stretch), 1750m (C=O stretch carboxylic acid), 1674s (C=O stretch 2° amide), 1602m (Benzene ring stretch), 1509s, 1492s (Benzene ring stretch), 1452s (aliphatic CH_2, CH_2 scissors vibration), 1349w, 1244s (C-O-C Ether Stretch), 1178w, 1110s (C-O-C Aliph. Ether Stretch), 1029w, 942w, 829m, 757s

Colorimetric Assay: Kaiser = Colourless, TNBS = Colourless

7.3.8 Quadramide-PEG$_4$carboxy-N-Hydroxysuccinimde 107

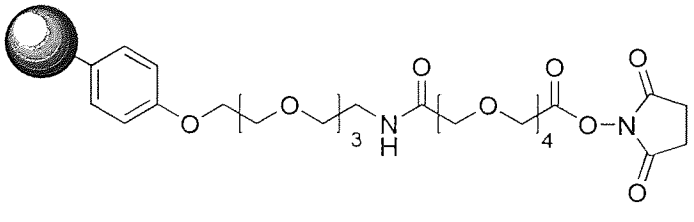

A solution of *N*-hydroxysuccinimide (0.0261 g, 0.23 mmol), TBTU (0.1443 g, 0.45 mmol) and DIPEA (0.075 ml, 0.45 mmol) in DMF (0.10 ml) was charged to dry

Quadramide-PEG_4carboxylic acid resin **112** (0.039 g, loading 0.75 mmol/g, 0.029 mmol Rn sites) and agitated for 16 hours.

As an intermediate compound, no analysis was performed.

7.3.9 Quadramide-PEG_4CONH-Peptide 108

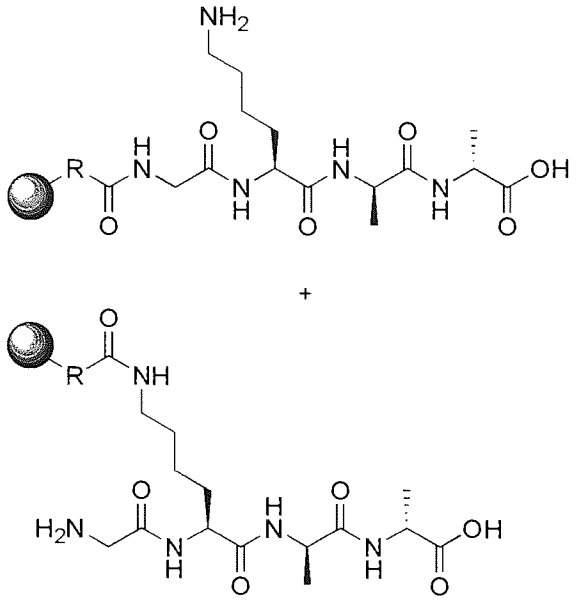

A solution of H_2N-Glycine-Lysine(NH_2)-D-Alanine-D-Alanine-OH **106** (0.062 g, 0.18 mmol) and DIPEA (0.10 ml, 0.60 mmol) in DMF (1.0 ml) was charged to dry sample of Quadramide-PEG_4carboxy-*N*-Hydroxysuccinimde **107** (0.038 g, loading 0.75 mmol/g, 0.029 mmol Rn sites) and the suspension was agitated at room temperature overnight. The coupling solution was drained and the beads were washed with copious amounts of DMF, DCM and methanol. The resin was dried to constant mass to yield 0.0389 g of white polymer beads.

Yield: 0.039 g, 11 %

FTIR (ATR) ν_{max}/cm^{-1}: 3318 w/br (H-Bonded OH Stretch, H-Bonded N-H stretch 1° amine), 3022m (Ar. C-H stretch), 3001m, 2897s (Aliph. C-H stretch), 1737w, 1657s (C=O stretch 2° amide), 1589m, 1497s (Benzene ring stretch), 1480, 1440s (OH carboxylic acid, in plane OH bending), 1338w, 1234s (C-O-C Ether Stretch), 1169w, 1100s (C-O-C Aliph. Ether Stretch), 1021w, 933w, 823m, 750s

Colorimetric Assay: Kaiser = Blue, TNBS = Orange

7.3.10 Quadramide-PEG$_4$CONH-Peptide-Boronic acid 113

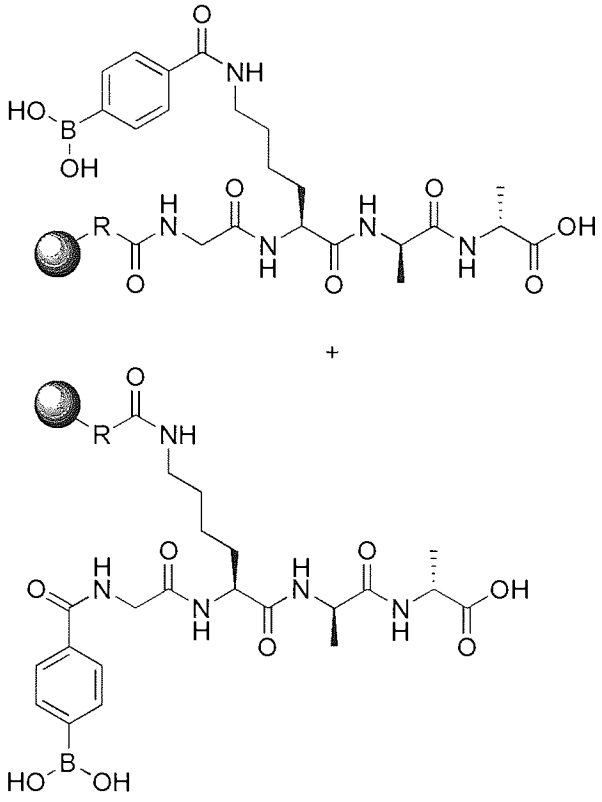

A solution of 4-carboxyphenylboronic acid (0.0067 g, 0.038 mmol), TBTU (0.013 g, 0.035 mmol) and DIPEA (0.006 ml, 0.45 mmol) was charged to dry sample of the peptidyl resin **108** (0.0149 g, loading 0.75 mmol/g, 0.011 mmol Rn sites) and agitated at room temperature for 20 minutes. The coupling solution was drained and the beads were washed with copious amounts of DMF, DCM and methanol. The resin was dried to constant mass to yield 0.0156 g of white polymer beads.

Yield: 0.0156 g, >95 %

FTIR (ATR) ν_{max}/cm^{-1}: ~3320 w/br (H-Bonded OH Stretch), 3032m (Ar. C-H stretch), 3001m, 2899s (Aliph. C-H stretch), 1657s (C=O stretch 2° amide), 1589m, 1497s (Benzene ring stretch), 1480, 1440s (OH carboxylic acid, in plane OH bending), 1374m, 1337w, 1234s (C-O-C Ether Stretch), 1087s (C-O-C Aliph. Ether Stretch), 1054s 1021w, 933w, 902m, 823m, 750s

Colorimetric Assay: Kaiser = Colourless, Carminic acid = Red, fluorescent under UV.

7.4 Chapter 4 Experimental

7.4.1 Quadramide Boronic acid / Fructose Complex 114

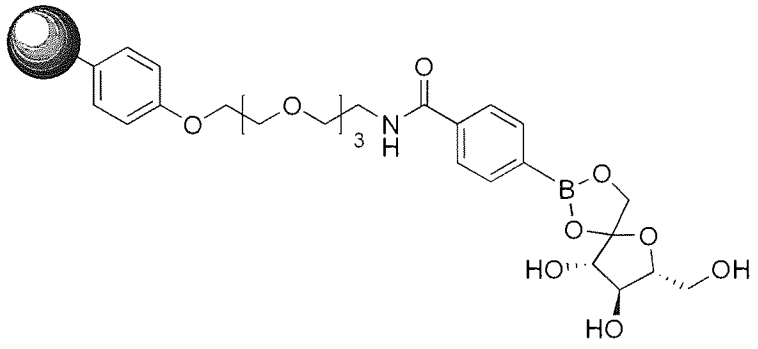

Quadramide-phenyl boronic acid **88** (1.0039 g, loading 0.79 mmol/g, 0.793 mmol Rn sites) was swollen in pyridine (20 ml). After 1 hour the solvent was removed and D-(-)-fructose (1.605 g, 8.91 mmol) in pyridine (50 ml) was added to the resin and agitated for 1 hour. The solvent was again removed, and the resin washed with pyridine (2 x 50 ml) before being dried to constant weight to yield 1.0888 g of the target conjugate.

Yield: 1.0888 g (0.573 mmol fructose, 74 %)
FTIR (ATR) ν_{max}/cm^{-1}: 3388m/br (H Bonded OH Stretch), 3026m (Ar. C-H stretch), 2919s (Aliph. C-H stretch), ~2890w (Aliph. C-H stretch), 1649m (C=O stretch 2° amide), 1602m (Benzene ring stretch), 1510m, 1493m (Benzene ring stretch), 1452m, 1358m (B-O Stretch), 1301m, 1244m (C-O-C Ether Stretch), 1178w, 1097s (C-O-C Ether Stretch), 1029s (CH_2-OH in 1° alcohol, C-O Stretch), 829m, 756s, 697vs, 668w.
Colorimetric test: Carminic acid = White

7.4.2 Quadramide Boronic acid / Glucose Complex 115

Quadramide-phenyl boronic acid **88** (0.9928 g, loading 0.79 mmol/g, 0.784 mmol Rn sites) was swollen in pyridine (50 ml). After 1 hour the solvent was removed and D-(+)-glucose (1.6090 g, 8.93 mmol) in pyridine (50 ml) was added to the resin and

agitated for 1 hour. The solvent was again removed, and the resin washed with pyridine (2 x 50 ml) before being dried to constant weight to yield 1.0411 g of the target conjugate.

Yield: 1.0411 g (0.326 mmol glucose, 43 %)
FTIR (ATR) ν_{max}/cm^{-1}: 3322m/br (H Bonded OH Stretch), 3026m (Ar. C-H stretch), 3002s (Aliph. C-H stretch), 2896w (Aliph. C-H stretch), 1641m (C=O stretch 2° amide), 1589m (Benzene ring stretch), 1497m (Benzene ring stretch), 1481s, 1440s, 1339m (B-O Stretch), 1292m, 1234m (C-O-C Ether Stretch), 1169w, 1092s (C-O-C Aliph. Ether Stretch), 1059s (CH_2-OH in 1° alcohol, C-O Stretch), 1020m, 823m, 749s.
Colorimetric test: Carminic acid = White

7.4.3 Quadramide Boronic acid / Raffinose Complex 116

Quadramide-phenyl boronic acid **88** (0.9981 g, loading 0.79 mmol/g, 0.788 mmol Rn sites) was swollen in pyridine (30 ml). After 1 hour the solvent was removed and D-(+)-Raffinose pentahydrate (2.6344 g, 4.43 mmol) in pyridine (30 ml) was added to the resin and agitated for 1 hour. The solvent was again removed, and the resin washed with pyridine (2 x 30 ml) before being dried to constant weight to yield 1.1633 g of the target conjugate.

Yield: 1.1633 g (0.353 mmol Raffinose, 45 %)
FTIR (ATR) ν_{max}/cm^{-1}: 3328s/br (H Bonded OH Stretch), 3026m (Ar. C-H stretch), 3002s (Aliph. C-H stretch), 2896w (Aliph. C-H stretch), 1624m (C=O stretch 2° amide), 1589m (Benzene ring stretch), 1497m (Benzene ring stretch), 1480s, 1440s, ~1340m (B-O Stretch), 1303m, 1234m (C-O-C Ether Stretch), 1039s (CH_2-OH in 1° alcohol, C-O Stretch), 1059, 1020m, 823m, 749s.
Colorimetric test: Carminic acid = White beads

7.5 Chapter 5 Experimental

7.5.1 L-2 sub library, library construction

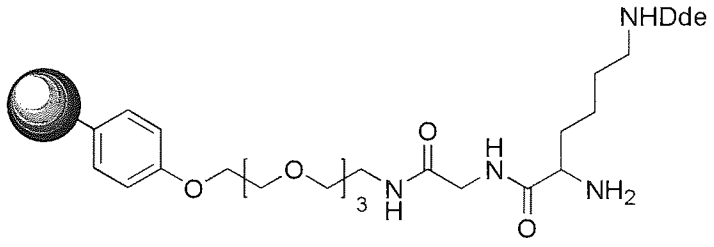

A solution of Fmoc-Gly-OH (1.17 g, 3.75 mmol), TBTU (1.13 g, 3.53 mmol) and DIPEA (0.78 ml, 4.5 mmol) in the minimum volume of DMF (~20 ml) was added to pre-swollen Quadramine resin **62** (1.50 g, loading 0.89 mmol/g, 1.5 mmol Rn sites) and agitated at room temperature for 20 minutes. The coupling solution was drained and the beads were washed with copious amounts of DMF to afford the Fmoc-protected library compound **L-1***.

Removal of the *N*-α-Fmoc protecting group was afforded with 20 % v/v piperidine in DMF (for 3 mins., 20 ml and 7 mins. 20 ml respectively). The deprotected compound **L-1** was then mixed with a solution of Fmoc-Lys(Dde)-OH **76** (2.00 g, 3.75 mmol), TBTU (1.13 g, 3.53 mmol) and DIPEA (0.78 ml, 4.5 mmol) in the minimum volume of DMF (~10 ml). Coupling was deemed to have reached completion after 20 minutes, after which the resin was washed with DMF (10 x 10 ml). Subsequent removal of the *N*-Fmoc protecting group was again afforded with 20 % v/v piperidine in DMF. Indicative Kaiser resin tests confirmed successful progression of the stepwise peptide assemblies. The resin was washed with copious amounts of DMF, DCM and methanol and dried to constant mass to yield 1.99 g of the title **L-2** compound.

Yield: 1.99 g (0.013 mmol, 100 %)

FTIR (ATR) ν_{max}/cm^{-1}: 3287m/br (N-H stretch 1° amine), 3002m (Ar. C-H stretch), 2900s (Aliph. C-H stretch), ~2890w (Aliph. C-H stretch), 1626s (C=O stretch 2° amide), 1558s (C=O β diketone in Enol form), 1497m/sharp (Benzene ring stretch), 1481m, 1440s (CH_3 Antisymm. Deformation), 1356m, 1324m, 1292m, 1233m (C-O-

C Ether Stretch), 1169w, 1092s (C-O-C Aliph. Ether Stretch), 1020m, 900w, 823m, 751s, 692vs

Colorimetric test: Kaiser = Blue, TNBS = Orange

7.5.2 L-3 sub library; library construction

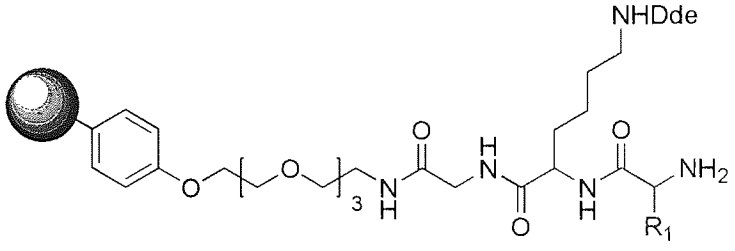

Quadramide-Gly-Lys(Dde)-NH_2 **L-2** (loading 0.67 mmol/g) was divided into 8 groups of approximately equal mass. Each group of resin was extended by a single amino acid using the TBTU/DIPEA methodology. Each group of the pre-swollen resin was mixed with a solution of an N-α-Fmoc amino acid (Table 50), TBTU (2.35 eq.), DIPEA (3.0 eq.) dissolved in the minimum volume of DMF (~2 ml) and agitated at room temperature for 20 minutes. The coupling solution was drained and the peptidyl-resin was washed successively with DMF (10 x 10 ml). to afford the Fmoc-protected library compounds **L-3-X***, where X is any amino acid.

Table 50: Amino acids coupled to L-2 with respective masses of amino acid and resin used.

Amino Acid	Amino acid /g	L-2 Resin /g
Fmoc-D-Ala-OH	0.1488	0.1878
Fmoc-Leu-OH	0.1686	0.1886
Fmoc-Phe-OH	0.1837	0.1886
Fmoc-Glu(OtBu)-OH	0.2049	0.1891
Fmoc-Tyr(tBu)-OH	0.2159	0.1878
Fmoc-Lys(Boc)-OH	0.2239	0.1886
Fmoc-Asn(Trt)-OH	0.2825	0.1883
Fmoc-Arg(Pbf)-OH	0.3088	0.1894

Removal of the *N*-Fmoc protecting groups of the **L-3-X*** compounds were afforded with 20 % v/v piperidine in DMF (for 3 mins., 20 ml and 7 mins. 20 ml respectively).

Indicative Kaiser resin tests confirmed successful progression of the stepwise peptide assemblies. The peptidyl-resin was washed successively with DMF (10 x 10 ml), DCM (10 x 10 ml) and methanol (5 x 10 ml) and dried to constant mass to yield the *N*-α-amine **L-3-X*** compounds.

Table 51: Yields of L-3-X* sub library

Derivative	Yield /g	Loading/ mmol/g
L-3-A*	0.1906	0.660
L-3-L*	0.1963	0.644
L-3-F*	0.1913	0.661
L-3-E*	0.2025	0.626
L-3-Y*	0.2010	0.626
L-3-K*	0.2467	0.512
L-3-N*	0.2349	0.537
L-3-R*	0.2279	0.557

7.5.3 L-4 sub library; library construction

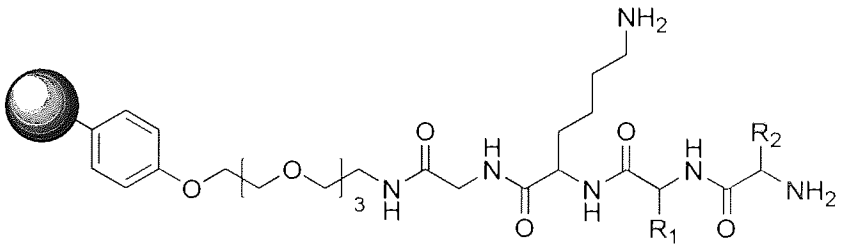

Each of the 8 Quadramide-Gly-Lys(Dde)-AA_1-NH_2 **L-3-X*** compounds were divided into 8 separate groups of approximately equal mass to afford a total of 64 groups. Each group of resin was extended by a single amino acid using the TBTU/DIPEA methodology. Each group of the pre-swollen resin was charged with a solution of an *N*-α-Fmoc amino acid (Table 52-Table 59), TBTU (2.35 eq.), DIPEA (3.0 eq.) dissolved in the minimum volume of DMF (~2 ml) and agitated at room temperature for 20 minutes. The coupling solution was drained and the peptidyl-resin was washed successively with DMF (10 x 2 ml) to afford the Fmoc-protected library compounds **L-4-XX***, where X is any amino acid.

Table 52: Amino acids coupled to L-3-A with respective masses of amino acid and resin used.

Amino Acid	Amino acid /g	**L-3-A** Resin /g
Fmoc-D-Ala-OH	0.0281	0.0239
Fmoc-Leu-OH	0.0302	0.0238
Fmoc-Phe-OH	0.0338	0.0237
Fmoc-Glu(OtBu)-OH	0.0375	0.0237
Fmoc-Tyr(tBu)-OH	0.0410	0.0239
Fmoc-Lys(Boc)-OH	0.0393	0.0233
Fmoc-Asn(Trt)-OH	0.0470	0.0214
Fmoc-Arg(Pbf)-OH	0.0387	0.0155

Table 53: Amino acids coupled to L-3-L with respective masses of amino acid and resin used.

Amino Acid	Amino acid /g	**L-3-L** Resin /g
Fmoc-D-Ala-OH	0.0193	0.0164
Fmoc-Leu-OH	0.0259	0.0204
Fmoc-Phe-OH	0.0210	0.0147
Fmoc-Glu(OtBu)-OH	0.0286	0.0181
Fmoc-Tyr(tBu)-OH	0.0276	0.0161
Fmoc-Lys(Boc)-OH	0.0329	0.0195
Fmoc-Asn(Trt)-OH	0.0306	0.0139
Fmoc-Arg(Pbf)-OH	0.0387	0.0155

Table 54: Amino acids coupled to L-3-F with respective masses of amino acid and resin used.

Amino Acid	Amino acid /g	**L-3-F** Resin /g
Fmoc-D-Ala-OH	0.0180	0.0153
Fmoc-Leu-OH	0.0200	0.0158
Fmoc-Phe-OH	0.0243	0.0170
Fmoc-Glu(OtBu)-OH	0.0242	0.0153
Fmoc-Tyr(tBu)-OH	0.0258	0.0150
Fmoc-Lys(Boc)-OH	0.0258	0.0153
Fmoc-Asn(Trt)-OH	0.0358	0.0163
Fmoc-Arg(Pbf)-OH	0.0429	0.0172

Table 55: Amino acids coupled to L-3-E with respective masses of amino acid and resin used.

Amino Acid	Amino acid /g	**L-3-E** Resin /g
Fmoc-D-Ala-OH	0.0176	0.0150
Fmoc-Leu-OH	0.0201	0.0159
Fmoc-Phe-OH	0.0224	0.0157
Fmoc-Glu(OtBu)-OH	0.0253	0.0160
Fmoc-Tyr(tBu)-OH	0.0276	0.0161
Fmoc-Lys(Boc)-OH	0.0258	0.0153
Fmoc-Asn(Trt)-OH	0.0356	0.0162
Fmoc-Arg(Pbf)-OH	0.0424	0.0170

Table 56: Amino acids coupled to L-3-Y with respective masses of amino acid and resin used.

Amino Acid	Amino acid /g	**L-3-Y** Resin /g
Fmoc-D-Ala-OH	0.0165	0.0140
Fmoc-Leu-OH	0.0185	0.0146
Fmoc-Phe-OH	0.0211	0.0148
Fmoc-Glu(OtBu)-OH	0.0226	0.0143
Fmoc-Tyr(tBu)-OH	0.0268	0.0156
Fmoc-Lys(Boc)-OH	0.0254	0.0151
Fmoc-Asn(Trt)-OH	0.0336	0.0153
Fmoc-Arg(Pbf)-OH	0.0404	0.0162

Table 57: Amino acids coupled to L-3-K with respective masses of amino acid and resin used.

Amino Acid	Amino acid /g	**L-3-K** Resin /g
Fmoc-D-Ala-OH	0.0149	0.0127
Fmoc-Leu-OH	0.0175	0.0138
Fmoc-Phe-OH	0.0201	0.0141
Fmoc-Glu(OtBu)-OH	0.0199	0.0126
Fmoc-Tyr(tBu)-OH	0.0216	0.0126
Fmoc-Lys(Boc)-OH	0.0231	0.0137
Fmoc-Asn(Trt)-OH	0.0306	0.0139
Fmoc-Arg(Pbf)-OH	0.0357	0.0143

Table 58: Amino acids coupled to L-3-N with respective masses of amino acid and resin used.

Amino Acid	Amino acid /g	L-3-N Resin /g
Fmoc-D-Ala-OH	0.0174	0.0148
Fmoc-Leu-OH	0.0200	0.0158
Fmoc-Phe-OH	0.0210	0.0147
Fmoc-Glu(OtBu)-OH	0.0225	0.0142
Fmoc-Tyr(tBu)-OH	0.0259	0.0151
Fmoc-Lys(Boc)-OH	0.0249	0.0148
Fmoc-Asn(Trt)-OH	0.0330	0.0150
Fmoc-Arg(Pbf)-OH	0.0364	0.0146

Table 59: Amino acids coupled to L-3-R with respective masses of amino acid and resin used.

Amino Acid	Amino acid /g	**L-3-R** Resin /g
Fmoc-D-Ala-OH	0.0178	0.0151
Fmoc-Leu-OH	0.0190	0.0150
Fmoc-Phe-OH	0.0217	0.0152
Fmoc-Glu(OtBu)-OH	0.0234	0.0148
Fmoc-Tyr(tBu)-OH	0.0263	0.0153
Fmoc-Lys(Boc)-OH	0.0256	0.0152
Fmoc-Asn(Trt)-OH	0.0343	0.0156
Fmoc-Arg(Pbf)-OH	0.0392	0.0157

Simultaneous removal of the *N*-α-Fmoc and *N*-ε-Dde protecting groups of the **L-4-XX*** compounds were afforded with 2 % hydrazine in DMF (2 x 2 ml, 3 mins each). Indicative Kaiser resin tests confirmed successful progression of the stepwise peptide assemblies. The peptidyl-resin was washed successively with DMF (10 x 2 ml), DCM (10 x 2 ml) and methanol (5 x 2 ml) and dried to constant mass to yield the *N*-α-amine-*N*-ε-amine **L-4-XX*** compounds.

Each **L-4-XX*** compound was split into two groups; one half of which were coupled with boronic acid to yield the **L-4-XXB*** library.

The remaining half of the compounds were fully deprotected by charging the resin with a solution of 95 % v/v TFA, 2.5 % v/v TIPS and 2.5 % v/v water (1 ml) and agitating at room temperature for 60 minutes. Each peptidyl-resin was washed with

DMF (10 x 2 ml), charged with a 5 % v/v TEA/DCM solution and agitated at room temperature 2 hours. The basic solution was drained and the peptidyl-resin was washed with DMF (10 x 2 ml), DCM (10 x 2 ml) and methanol (5 x 2 ml) and dried to constant mass to yield the **L-4-XX** compounds.

Table 60-Table 67 detail the yield and respective loading of each product.

Table 60: Yields of L-4-AX sub library

Derivative	Yield /g	Loading / mmol/g
L-4-AA	0.0081	0.6463
L-4-AL	0.0084	0.6144
L-4-AF	0.0075	0.6259
L-4-AE	0.0059	0.5983
L-4-AY	0.0079	0.5841
L-4-AK	0.0098	0.5680
L-4-AN	0.0084	0.5536
L-4-AR	0.0058	0.5697

Table 61: Yields of L-4-LX sub library

Derivative	Yield /g	Loading / mmol/g
L-4-LA	0.0074	0.591
L-4-LL	0.0062	0.620
L-4-LF	0.0060	0.578
L-4-LE	0.0057	0.585
L-4-LY	0.0065	0.529
L-4-LK	0.0066	0.510
L-4-LN	0.0054	0.562
L-4-LR	0.0062	0.547

Table 62: Yields of L-4-FX sub library

Derivative	Yield /g	Loading / mmol/g
L-4-FA	0.0050	0.606
L-4-FL	0.0059	0.625
L-4-FF	0.0057	0.623
L-4-FE	0.0053	0.622

Derivative	Yield /g	Loading / mmol/g
L-4-FY	0.0070	0.552
L-4-FK	0.0059	0.584
L-4-FN	0.0068	0.574
L-4-FR	0.0067	0.563

Table 63: Yields of L-4-EX sub library

Derivative	Yield /g	Loading / mmol/g
L-4-EA	0.0070	0.548
L-4-EL	0.0058	0.564
L-4-EF	0.0060	0.583
L-4-EE	0.0055	0.612
L-4-EY	0.0072	0.535
L-4-EK	0.0066	0.539
L-4-EN	0.0052	0.561
L-4-ER	0.0055	0.603

Table 64: Yields of L-4-YX sub library

Derivative	Yield /g	Loading / mmol/g
L-4-YA	0.0061	0.580
L-4-YL	0.0066	0.585
L-4-YF	0.0059	0.564
L-4-YE	0.0055	0.612
L-4-YY	0.0061	0.578
L-4-YK	0.0056	0.577
L-4-YN	0.0065	0.567
L-4-YR	0.0060	0.553

Table 65: Yields of L-4-KX sub library

Derivative	Yield /g	Loading / mmol/g
L-4-KA	0.0050	0.425
L-4-KL	0.0052	0.475
L-4-KF	0.0056	0.451
L-4-KE	0.0053	0.477
L-4-KY	0.0051	0.479
L-4-KK	0.0056	0.434

Derivative	Yield /g	Loading / mmol/g
L-4-KN	0.0057	0.448
L-4-KR	0.0052	0.470

Table 66: Yields of L-4-NX sub library

Derivative	Yield /g	Loading / mmol/g
L-4-NA	0.0056	0.554
L-4-NL	0.0055	0.580
L-4-NF	0.0053	0.535
L-4-NE	0.0052	0.554
L-4-NY	0.0060	0.521
L-4-NK	0.0057	0.529
L-4-NN	0.0059	0.466
L-4-NR	0.0037	0.722

Table 67: Yields of L-4-RX sub library

Derivative	Yield /g	Loading / mmol/g
L-4-RA	0.0060	0.589
L-4-RL	0.0063	0.574
L-4-RF	0.0055	0.599
L-4-RE	0.0059	0.522
L-4-RY	0.0057	0.522
L-4-RK	0.0055	0.512
L-4-RN	0.0054	0.568
L-4-RR	0.0052	0.564

7.5.4 L-4B sub library; library construction

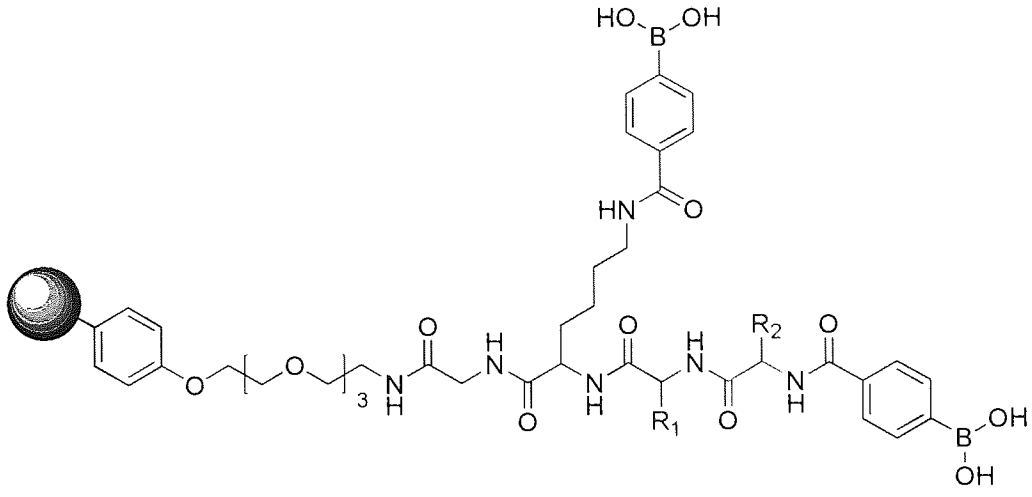

Each of the 64 Quadramide-Gly-Lys(Dde)-AA_1-NH_2 **L-4-XX*** pre-swollen sub library compounds was charged with a solution of 4-carboxyphenylboronic acid (Table 68-Table 75), TBTU (2.35 eq.), DIPEA (3.0 eq.) dissolved in the minimum volume of DMF (~2 ml) and agitated at room temperature for 20 minutes. The coupling solution was drained and the peptidyl-resin was washed successively with DMF (10 x 2 ml). to afford the protected *N*-α-*N*-ε-phenylboronic acid library compounds **L-4-XXB***, where X is any amino acid.

Table 68: L-4-AX* with respective masses of 4-carboxyphenylboronic acid amino acid and resin used.

Library Compound	**L-4-AX*** Resin /g	4-Carboxyphenylboronic acid /g
L-4-AA*	0.0167	0.0022
L-4-AL*	0.0172	0.0023
L-4-AF*	0.0182	0.0024
L-4-AE*	0.0206	0.0026
L-4-AY*	0.0194	0.0025
L-4-AK*	0.0171	0.0023
L-4-AN*	0.0177	0.0022
L-4-AR*	0.0134	0.0018

Table 69: L-4-LX* with respective masses of 4-carboxyphenylboronic acid amino acid and resin used.

Library Compound	**L-4-LX*** Resin /g	4-Carboxyphenylboronic acid /g
L-4-LA*	0.0101	0.0013
L-4-LL*	0.0155	0.0021
L-4-LF*	0.0102	0.0013
L-4-LE*	0.0145	0.0018
L-4-LY*	0.0123	0.0016
L-4-LK*	0.0164	0.0022
L-4-LN*	0.0113	0.0014
L-4-LR*	0.0130	0.0017

Table 70: L-4-FX* with respective masses of 4-carboxyphenylboronic acid amino acid and resin used.

Library Compound	**L-4-FX*** Resin /g	4-Carboxyphenylboronic acid /g
L-4-FA*	0.0112	0.0015
L-4-FL*	0.0110	0.0015
L-4-FF*	0.0128	0.0017
L-4-FE*	0.0116	0.0015
L-4-FY*	0.0105	0.0013
L-4-FK*	0.0116	0.0015
L-4-FN*	0.0128	0.0016
L-4-FR*	0.0147	0.0020

Table 71: L-4-EX* with respective masses of 4-carboxyphenylboronic acid amino acid and resin used.

Library Compound	**L-4-EX*** Resin /g	4-Carboxyphenylboronic acid /g
L-4-EA*	0.0093	0.0012
L-4-EL*	0.0114	0.0015
L-4-EF*	0.0110	0.0014
L-4-EE*	0.0119	0.0015
L-4-EY*	0.0113	0.0014
L-4-EK*	0.0110	0.0015
L-4-EN*	0.0141	0.0018
L-4-ER*	0.0148	0.0020

Table 72: L-4-YX* with respective masses of 4-carboxyphenylboronic acid amino acid and resin used.

Library Compound	**L-4-YX*** Resin /g	4-Carboxyphenylboronic acid /g
L-4-YA*	0.0087	0.0012
L-4-YL*	0.0090	0.0012
L-4-YF*	0.0104	0.0014
L-4-YE*	0.0100	0.0013
L-4-YY*	0.0113	0.0014
L-4-YK*	0.0114	0.0015
L-4-YN*	0.0115	0.0014
L-4-YR*	0.0138	0.0019

Table 73: L-4-KX* with respective masses of 4-carboxyphenylboronic acid amino acid and resin used.

Library Compound	**L-4-KX*** Resin /g	4-Carboxyphenylboronic acid /g
L-4-KA*	0.0089	0.0012
L-4-KL*	0.0095	0.0013
L-4-KF*	0.0099	0.0013
L-4-KE*	0.0084	0.0011
L-4-KY*	0.0087	0.0011
L-4-KK*	0.0100	0.0013
L-4-KN*	0.0105	0.0013
L-4-KR*	0.0116	0.0016

Table 74: L-4-NX* with respective masses of 4-carboxyphenylboronic acid amino acid and resin used.

Library Compound	**L-4-NX*** Resin /g	4-Carboxyphenylboronic acid /g
L-4-NA*	0.0094	0.0012
L-4-NL*	0.0105	0.0014
L-4-NF*	0.0102	0.0013
L-4-NE*	0.0097	0.0012
L-4-NY*	0.0104	0.0013
L-4-NK*	0.0103	0.0014
L-4-NN*	0.0118	0.0015
L-4-NR*	0.0118	0.0016

Table 75: L-4-RX* with respective masses of 4-carboxyphenylboronic acid amino acid and resin used.

Library Compound	L-4-RX* Resin /g	4-Carboxyphenylboronic acid /g
L-4-RA*	0.0090	0.0012
L-4-RL*	0.0090	0.0012
L-4-RF*	0.0099	0.0013
L-4-RE*	0.0101	0.0013
L-4-RY*	0.0110	0.0014
L-4-RK*	0.0113	0.0015
L-4-RN*	0.0118	0.0015
L-4-RR*	0.0126	0.0017

Complete deprotection of each the compounds was afforded by charging the resin with a solution of 95 % v/v TFA, 2.5 % v/v TIPS and 2.5 % v/v water (1 ml) and agitating at room temperature for 60 minutes. Each peptidyl-resin was washed with DMF (10 x 2 ml), charged with a 5 % v/v TEA/DCM solution and agitated at room temperature 2 hours. The basic solution was drained and the peptidyl-resin was washed with DMF (10 x 2 ml), DCM (10 x 2 ml) and methanol (5 x 2 ml) and dried to constant mass to yield the **L-4-XXB** compounds.

Table 76-Table 83 detail the yield and respective loading of each product.

Table 76: Yields of L-4-AXB sub library

Derivative	Yield /g	Loading / mmol/g
L-4-AAB	0.0162	0.650
L-4-ALB	0.0181	0.584
L-4-AFB	0.0198	0.553
L-4-AEB	0.0168	0.721
L-4-AYB	0.0170	0.658
L-4-AKB	0.0161	0.609
L-4-ANB	0.0152	0.622
L-4-ARB	0.0071	0.974

Table 77: Yields of L-4-LXB sub library

Derivative	Yield /g	Loading / mmol/g
L-4-LAB	0.0111	0.560
L-4-LLB	0.0198	0.470
L-4-LFB	0.0112	0.536
L-4-LEB	0.0144	0.579
L-4-LYB	0.0130	0.534
L-4-LKB	0.0158	0.583
L-4-LNB	0.0065	0.910
L-4-LRB	0.0126	0.522

Table 78: Yields of L-4-FXB sub library

Derivative	Yield /g	Loading / mmol/g
L-4-FAB	0.0166	0.426
L-4-FLB	0.0118	0.573
L-4-FFB	0.0149	0.517
L-4-FEB	0.0121	0.564
L-4-FYB	0.0111	0.546
L-4-FKB	0.0120	0.555
L-4-FNB	0.0121	0.566
L-4-FRB	0.0134	0.567

Table 79: Yields of L-4-EXB sub library

Derivative	Yield /g	Loading / mmol/g
L-4-EAB	0.0084	0.404
L-4-ELB	0.0125	0.545
L-4-EFB	0.0115	0.492
L-4-EEB	0.0130	0.538
L-4-EYB	0.0108	0.521
L-4-EKB	0.0113	0.529
L-4-ENB	0.0129	0.541
L-4-ERB	0.0136	0.543

Table 80: Yields of L-4-YXB sub library

Derivative	Yield /g	Loading / mmol/g
L-4-YAB	0.0089	0.586

Derivative	Yield /g	Loading / mmol/g
L-4-YLB	0.0108	0.487
L-4-YFB	0.0106	0.563
L-4-YEB	0.0120	0.468
L-4-YYB	0.0119	0.523
L-4-YKB	0.0119	0.525
L-4-YNB	0.0108	0.545
L-4-YRB	0.0133	0.514

Table 81: Yields of L-4-KXB sub library

Derivative	Yield /g	Loading / mmol/g
L-4-KAB	0.0061	0.721
L-4-KLB	0.0071	0.648
L-4-KFB	0.0072	0.655
L-4-KEB	0.0057	0.690
L-4-KYB	0.0070	0.572
L-4-KKB	0.0076	0.604
L-4-KNB	0.0076	0.599
L-4-KRB	0.0091	0.537

Table 82: Yields of L-4-NXB sub library

Derivative	Yield /g	Loading / mmol/g
L-4-NAB	0.0082	0.495
L-4-NLB	0.0106	0.485
L-4-NFB	0.0092	0.465
L-4-NEB	0.0094	0.554
L-4-NYB	0.0095	0.489
L-4-NKB	0.0100	0.501
L-4-NNB	0.0092	0.532
L-4-NRB	0.0112	0.493

Table 83: Yields of L-4-RXB sub library

Derivative	Yield /g	Loading / mmol/g
L-4-RAB	0.0094	0.513
L-4-RLB	0.0094	0.502
L-4-RFB	0.0106	0.481

Derivative	Yield /g	Loading / mmol/g
L-4-REB	0.0089	0.573
L-4-RYB	0.0108	0.506
L-4-RKB	0.0108	0.517
L-4-RNB	0.0100	0.548
L-4-RRB	0.0112	0.507

7.5.5 Incubation of the library compounds with vancomycin

Approximately 5 mg of each library resin was utilised. The loading of each resin was established and the number of moles of peptide calculated. A solution of vancomycin (0.330 g, 2.2 mM) in pyridine (100.0 ml) in pyridine was made and a volume charged to each resin, such that 0.37 equivalents of vancomycin was added for every peptide.

The suspensions were agitated at room temperature overnight before being drained. The resins were then subjected to copious washing with pyridine via Soxhlet extraction for 4 hours then dried to constant mass.

7.5.6 L-4 sub library; incubation

Table 84: Incubation of L-4-AX sub library

Derivative	mass /g	Loading / mmol/g	Moles peptide	Moles Vancomycin required	Vol. Vancomycin solution (2.2 mM) /ml
L-4-AA	0.0081	0.6463	5.24E-06	1.96E-06	0.88
L-4-AL	0.0084	0.6144	5.16E-06	1.93E-06	0.87
L-4-AF	0.0075	0.6259	4.69E-06	1.76E-06	0.79
L-4-AE	0.0059	0.5983	3.53E-06	1.32E-06	0.59
L-4-AY	0.0079	0.5841	4.61E-06	1.73E-06	0.78
L-4-AK	0.0098	0.5680	5.57E-06	2.08E-06	0.94
L-4-AN	0.0084	0.5536	4.65E-06	1.74E-06	0.78
L-4-AR	0.0058	0.5697	3.30E-06	1.24E-06	0.56

Table 85: Incubation of L-4-LX sub library

Derivative	mass /g	Loading / mmol/g	Moles peptide	Moles Vancomycin required	Vol. Vancomycin solution (2.2 mM) /ml
L-4-LA	0.0074	0.591	4.37E-06	1.64E-06	0.74
L-4-LL	0.0062	0.620	3.84E-06	1.44E-06	0.65
L-4-LF	0.0060	0.578	3.47E-06	1.30E-06	0.58
L-4-LE	0.0057	0.585	3.34E-06	1.25E-06	0.56
L-4-LY	0.0065	0.529	3.44E-06	1.29E-06	0.58
L-4-LK	0.0066	0.510	3.37E-06	1.26E-06	0.57
L-4-LN	0.0054	0.562	3.04E-06	1.14E-06	0.51
L-4-LR	0.0062	0.547	3.39E-06	1.27E-06	0.57

Table 86: Incubation of L-4-FX sub library

Derivative	mass /g	Loading / mmol/g	Moles peptide	Moles Vancomycin required	Vol. Vancomycin solution (2.2 mM) /ml
L-4-FA	0.0050	0.606	3.03E-06	1.13E-06	0.51
L-4-FL	0.0059	0.625	3.69E-06	1.38E-06	0.62
L-4-FF	0.0057	0.623	3.55E-06	1.33E-06	0.60
L-4-FE	0.0053	0.622	3.30E-06	1.23E-06	0.56
L-4-FY	0.0070	0.552	3.87E-06	1.45E-06	0.65
L-4-FK	0.0059	0.584	3.44E-06	1.29E-06	0.58
L-4-FN	0.0068	0.574	3.90E-06	1.46E-06	0.66
L-4-FR	0.0067	0.563	3.77E-06	1.41E-06	0.64

Table 87: Incubation of L-4-EX sub library

Derivative	mass /g	Loading / mmol/g	Moles peptide	Moles Vancomycin required	Vol. Vancomycin solution (2.2 mM) /ml
L-4-EA	0.0070	0.548	3.83E-06	1.44E-06	0.65
L-4-EL	0.0058	0.564	3.27E-06	1.23E-06	0.55
L-4-EF	0.0060	0.583	3.50E-06	1.31E-06	0.59
L-4-EE	0.0055	0.612	3.36E-06	1.26E-06	0.57
L-4-EY	0.0072	0.535	3.85E-06	1.44E-06	0.65
L-4-EK	0.0066	0.539	3.56E-06	1.33E-06	0.60
L-4-EN	0.0052	0.561	2.92E-06	1.09E-06	0.49
L-4-ER	0.0055	0.603	3.32E-06	1.24E-06	0.56

Table 88: Incubation of L-4-YX sub library

Derivative	mass /g	Loading / mmol/g	Moles peptide	Moles Vancomycin required	Vol. Vancomycin solution (2.2 mM) /ml
L-4-YA	0.0061	0.580	3.54E-06	1.32E-06	0.60
L-4-YL	0.0066	0.585	3.86E-06	1.44E-06	0.65
L-4-YF	0.0059	0.564	3.33E-06	1.24E-06	0.56
L-4-YE	0.0055	0.612	3.37E-06	1.26E-06	0.57
L-4-YY	0.0061	0.578	3.52E-06	1.32E-06	0.59
L-4-YK	0.0056	0.577	3.23E-06	1.21E-06	0.54
L-4-YN	0.0065	0.567	3.69E-06	1.38E-06	0.62
L-4-YR	0.0060	0.553	3.32E-06	1.24E-06	0.56

Table 89: Incubation of L-4-KX sub library

Derivative	mass /g	Loading / mmol/g	Moles peptide	Moles Vancomycin required	Vol. Vancomycin solution (2.2 mM) /ml
L-4-KA	0.0050	0.425	2.13E-06	7.96E-07	0.36
L-4-KL	0.0052	0.475	2.47E-06	9.25E-07	0.42
L-4-KF	0.0056	0.451	2.53E-06	9.45E-07	0.43
L-4-KE	0.0053	0.477	2.53E-06	9.46E-07	0.43
L-4-KY	0.0051	0.479	2.44E-06	9.14E-07	0.41
L-4-KK	0.0056	0.434	2.43E-06	9.10E-07	0.41
L-4-KN	0.0057	0.448	2.56E-06	9.57E-07	0.43
L-4-KR	0.0052	0.470	2.44E-06	9.14E-07	0.41

Table 90: Incubation of L-4-NX sub library

Derivative	mass /g	Loading / mmol/g	Moles peptide	Moles Vancomycin required	Vol. Vancomycin solution (2.2 mM) /ml
L-4-NA	0.0056	0.554	3.10E-06	1.16E-06	0.52
L-4-NL	0.0055	0.580	3.19E-06	1.19E-06	0.54
L-4-NF	0.0053	0.535	2.84E-06	1.06E-06	0.48
L-4-NE	0.0052	0.554	2.88E-06	1.08E-06	0.49
L-4-NY	0.0060	0.521	3.12E-06	1.17E-06	0.53
L-4-NK	0.0057	0.529	3.01E-06	1.13E-06	0.51
L-4-NN	0.0059	0.466	2.75E-06	1.03E-06	0.46
L-4-NR	0.0037	0.722	2.67E-06	1.00E-06	0.45

Table 91: Incubation of L-4-RX sub library

Derivative	mass /g	Loading / mmol/g	Moles peptide	Moles Vancomycin required	Vol. Vancomycin solution (2.2 mM) /ml
L-4-RA	0.0060	0.589	3.54E-06	1.32E-06	0.60
L-4-RL	0.0063	0.574	3.62E-06	1.35E-06	0.61
L-4-RF	0.0055	0.599	3.29E-06	1.23E-06	0.56
L-4-RE	0.0059	0.522	3.08E-06	1.15E-06	0.52
L-4-RY	0.0057	0.522	2.98E-06	1.11E-06	0.50
L-4-RK	0.0055	0.512	2.82E-06	1.05E-06	0.47
L-4-RN	0.0054	0.568	3.07E-06	1.15E-06	0.52
L-4-RR	0.0052	0.564	2.93E-06	1.10E-06	0.49

7.5.7 L-4B sub library; incubation

Table 92: Incubation of L-4-AXB sub library

Derivative	mass /g	Loading / mmol/g	Moles peptide	Moles Vancomycin required	Vol. Vancomycin solution (2.2 mM) /ml
L-4-AAB	0.0055	0.650	3.58E-06	1.34E-06	0.60
L-4-ALB	0.0060	0.584	3.50E-06	1.31E-06	0.59
L-4-AFB	0.0051	0.553	2.82E-06	1.06E-06	0.48
L-4-AEB	0.0055	0.721	3.97E-06	1.49E-06	0.67
L-4-AYB	0.0064	0.658	4.21E-06	1.58E-06	0.71
L-4-AKB	0.0048	0.609	2.93E-06	1.10E-06	0.49
L-4-ANB	0.0065	0.622	4.05E-06	1.51E-06	0.68
L-4-ARB	0.0060	0.974	5.85E-06	2.19E-06	0.99

Table 93: Incubation of L-4-LXB sub library

Derivative	mass /g	Loading / mmol/g	Moles peptide	Moles Vancomycin required	Vol. Vancomycin solution (2.2 mM) /ml
L-4-LAB	0.0056	0.560	3.14E-06	1.17E-06	0.53
L-4-LLB	0.0051	0.470	2.40E-06	8.97E-07	0.40
L-4-LFB	0.0051	0.536	2.73E-06	1.02E-06	0.46
L-4-LEB	0.0054	0.579	3.13E-06	1.17E-06	0.53
L-4-LYB	0.0058	0.534	3.10E-06	1.16E-06	0.52
L-4-LKB	0.0055	0.583	3.20E-06	1.20E-06	0.54
L-4-LNB	0.0065	0.910	5.92E-06	2.22E-06	1.00

Derivative	mass /g	Loading / mmol/g	Moles peptide	Moles Vancomycin required	Vol. Vancomycin solution (2.2 mM) /ml
L-4-LRB	0.0053	0.522	2.77E-06	1.04E-06	0.47

Table 94: Incubation of L-4-FXB sub library

Derivative	mass /g	Loading / mmol/g	Moles peptide	Moles Vancomycin required	Vol. Vancomycin solution (2.2 mM) /ml
L-4-FAB	0.0048	0.426	2.04E-06	7.65E-07	0.34
L-4-FLB	0.0045	0.573	2.58E-06	9.65E-07	0.43
L-4-FFB	0.0043	0.517	2.22E-06	8.33E-07	0.37
L-4-FEB	0.0058	0.564	3.27E-06	1.23E-06	0.55
L-4-FYB	0.0048	0.546	2.62E-06	9.81E-07	0.44
L-4-FKB	0.0048	0.555	2.66E-06	9.97E-07	0.45
L-4-FNB	0.0055	0.566	3.11E-06	1.16E-06	0.52
L-4-FRB	0.0058	0.567	3.29E-06	1.23E-06	0.55

Table 95: Incubation of L-4-EXB sub library

Derivative	mass /g	Loading / mmol/g	Moles peptide	Moles Vancomycin required	Vol. Vancomycin solution (2.2 mM) /ml
L-4-EAB	0.0049	0.404	1.98E-06	7.42E-07	0.33
L-4-ELB	0.0057	0.545	3.11E-06	1.16E-06	0.52
L-4-EFB	0.0055	0.492	2.71E-06	1.01E-06	0.46
L-4-EEB	0.0053	0.538	2.85E-06	1.07E-06	0.48
L-4-EYB	0.0047	0.521	2.45E-06	9.16E-07	0.41
L-4-EKB	0.0048	0.529	2.54E-06	9.51E-07	0.43
L-4-ENB	0.0051	0.541	2.76E-06	1.03E-06	0.47
L-4-ERB	0.0057	0.543	3.09E-06	1.16E-06	0.52

Table 96: Incubation of L-4-YXB sub library

Derivative	mass /g	Loading / mmol/g	Moles peptide	Moles Vancomycin required	Vol. Vancomycin solution (2.2 mM) /ml
L-4-YAB	0.0051	0.586	2.99E-06	1.12E-06	0.50
L-4-YLB	0.0057	0.487	2.78E-06	1.04E-06	0.47
L-4-YFB	0.0057	0.563	3.21E-06	1.20E-06	0.54
L-4-YEB	0.0041	0.468	1.92E-06	7.18E-07	0.32
L-4-YYB	0.0051	0.523	2.67E-06	9.98E-07	0.45
L-4-YKB	0.0047	0.525	2.47E-06	9.23E-07	0.42

Derivative	mass /g	Loading / mmol/g	Moles peptide	Moles Vancomycin required	Vol. Vancomycin solution (2.2 mM) /ml
L-4-YNB	0.0052	0.545	2.83E-06	1.06E-06	0.48
L-4-YRB	0.0047	0.514	2.41E-06	9.04E-07	0.41

Table 97: Incubation of L-4-KXB sub library

Derivative	mass /g	Loading / mmol/g	Moles peptide	Moles Vancomycin required	Vol. Vancomycin solution (2.2 mM) /ml
L-4-KAB	0.0044	0.721	3.17E-06	1.19E-06	0.53
L-4-KLB	0.0047	0.648	3.05E-06	1.14E-06	0.51
L-4-KFB	0.0048	0.655	3.14E-06	1.18E-06	0.53
L-4-KEB	0.0057	0.690	3.93E-06	1.47E-06	0.66
L-4-KYB	0.0054	0.572	3.09E-06	1.16E-06	0.52
L-4-KKB	0.0049	0.604	2.96E-06	1.11E-06	0.50
L-4-KNB	0.0049	0.599	2.93E-06	1.10E-06	0.49
L-4-KRB	0.0056	0.537	3.01E-06	1.13E-06	0.51

Table 98: Incubation of L-4-NXB sub library

Derivative	mass /g	Loading / mmol/g	Moles peptide	Moles Vancomycin required	Vol. Vancomycin solution (2.2 mM) /ml
L-4-NAB	0.0047	0.495	2.33E-06	8.72E-07	0.39
L-4-NLB	0.0047	0.485	2.28E-06	8.53E-07	0.38
L-4-NFB	0.0047	0.465	2.19E-06	8.18E-07	0.37
L-4-NEB	0.0056	0.554	3.11E-06	1.16E-06	0.52
L-4-NYB	0.0051	0.489	2.50E-06	9.35E-07	0.42
L-4-NKB	0.0043	0.501	2.15E-06	8.06E-07	0.36
L-4-NNB	0.0060	0.532	3.19E-06	1.19E-06	0.54
L-4-NRB	0.0045	0.493	2.22E-06	8.30E-07	0.37

Table 99: Incubation of L-4-RXB sub library

Derivative	mass /g	Loading / mmol/g	Moles peptide	Moles Vancomycin required	Vol. Vancomycin solution (2.2 mM) /ml
L-4-RAB	0.0057	0.513	2.92E-06	1.09E-06	0.49
L-4-RLB	0.0059	0.502	2.96E-06	1.11E-06	0.50
L-4-RFB	0.0050	0.481	2.40E-06	9.00E-07	0.41
L-4-REB	0.0051	0.573	2.92E-06	1.09E-06	0.49
L-4-RYB	0.0048	0.506	2.43E-06	9.08E-07	0.41

Derivative	mass /g	Loading / mmol/g	Moles peptide	Moles Vancomycin required	Vol. Vancomycin solution (2.2 mM) /ml
L-4-RKB	0.0048	0.517	2.48E-06	9.29E-07	0.42
L-4-RNB	0.0056	0.548	3.07E-06	1.15E-06	0.52
L-4-RRB	0.0050	0.507	2.54E-06	9.49E-07	0.43

7.5.8 Cleavage of the library compounds

Citric acid solution (52.0 ml, 1.5 mM) was dissolved in THF (104.0 ml) to make the cleavage solution. The cleavage solution (1200 µl) was charged to each resin sample and agitated at room temperature overnight. The supernatant was carefully removed and taken to dryness. Each residue was then redissolved in water (400 µl) which afforded a solution with the original concentration of the citric acid component and an unknown vancomycin concentration.

7.5.9 Preparation of vancomycin standards

Vancomycin was dissolved in a citric acid solution (1.5 mM) to afford a vancomycin stock solution (1 µg/µl, 0.67 mM). Aliquots of the stock solution were diluted with the original citric acid solution (1.5 mM) to afford a range of solutions with an equal number of moles of citric acid, and a variable amount of vancomycin.

Table 100: Dilutions of the vancomycin stock solution for calibration purposes

Vancomycin standard	Vol. of Vancomycin stock /µl	Vol. of 1.5 mM Citric acid solution /µl	Total Volume /µl	Concentration of Vanc. solution (M)
V_{40}	40	0	40	6.73E-04
V_{30}	30	10	40	5.05E-04
V_{20}	20	20	40	3.37E-04
V_{10}	10	30	40	1.68E-04
V_{5}	5	35	40	8.41E-05
V_{2}	2	38	40	3.37E-05
V_{1}	1	39	40	1.68E-05
$V_{0.4}$	0.4	39.6	40	6.73E-06

7.5.10 Library Assay

All experiments were carried out using the Oxford strain (NCTC 6571, ATCC 9144) of methicillin sensitive *Staphylococcus aureus* (MSSA)

The *S. aureus* was grown overnight at 37°C on Muller Hinton agar, and subsequently an individual colony was used to inoculate 10 ml of Mueller Hinton Broth. This was incubated overnight at 37 °C with shaking at 220 rpm.

The following day the overnight culture was used to inoculate a suspension of MSSA by dilution with sterile Mueller Hinton broth until the broth reached an OD of 0.13 at 600nm. This corresponds to a McFarland Standard of 0.5 or approximately 1.5×10^8 cells.

Mueller Hinton Agar plates (8.7 cm diameter) were inoculated with a sterile swab of the inoculation culture (OD 0.13 at 600nm) to form a confluent lawn of bacteria.

The plates were allowed to dry and six equidistant wells, of 6.0 mm diameter and a depth equal to that of the growth media, were cut and removed from each plate using sterilised glass Pasteur pipettes.

The six wells consisted of four cleavage solutions and two vancomycin standards (V_{40} & V_1; **L-4** library and V_{40} & V_2 **L-4B** library). 40 µl of the appropriate solution was injected into the corresponding well and the plates were incubated for 24 hrs at 37 °C.

After 24 hours, zones of inhibition were measured and recorded using a GeneSnap transiluminator Gel photographic system (GeneSnap UK)

Chapter 8

References

[1] Davis, B. G.; Fairbanks, A. J.; *Carbohydrate Chemistry*; Oxford: Oxford University Press; **2002**; ISBN 0-19-855833-3

[2] Berg, J. M.; Tymoczko, J. L.; Stryer, L.; *Biochemistry 5th Edition*; W. H. Freeman & co., New York; **2002**; ISBN: 0-7167-4684-0

[3] McMurry J.; *Organic Chemistry 4th Edition*; Brooks/Cole Publishing; **1996**; ISBN 0-534-23832-7

[4] Saunders, J.; *Top Drugs; Top Synthetic routes*; Oxford: Oxford University Press; **2001**; ISBN 0-19-850100-5

[5] Kuivula, H. G.; Keough, A. H.; Soboczenski, E. J.; *J. Org. Chem.*; **1954**; 19; 780

[6] James, T. D.; Samankumara Sandanayake, K. R. A.; Shinkai, S.; *Angew. Chem. Int. Ed.*; **1994**; 33; 21; 2207-9

[7] Ward, C. J.; Patel, P.; Ashton, P. R.; James, T. D.; *Chem. Commun.*; **2000**; 229-30

[8] Ward, C. J.; Patel, P.; James, T. D.; *J. Chem. Soc., Perkin Trans 1*; **2002**; 462-70

[9] Yang, W.; Yan, J.; Fang, H.; Wand, B.; *Chem. Commun.*; **2003**; 792-3

[10] Zhao, J.; Fyles, T. M.; James, T. D.; *Angew. Chem. Int. Ed*; **2004**; 43; 3461-4

[11] Kawanishi, T.; Romey, M. A.; Zhu, P. C.; Holody, M. Z.; Shinkai, S.; *Journal of Fluorescence*; **2004**; 14; 5; 499-512

[12] Zhoa, J.; Davidson, M. G.; Mahon, M. F.; Kociok-Köhn, G.; James, T. D.; *J. Am. Chem. Soc.*; **2004**; 126; 16179-86

[13] Norrild, J. C.; Eggert, H.; *J. Am. Chem. Soc.*; **1995**; 117; 1479

[14] Springsteen, G.; Wang, B.; *Tetrahedron*; **2002**; 58; 5291-300

[15] Eggert, H.; Friederiksen, J.; Morin, C.; Norrild, J. C.; *J. Org. Chem.*; **1999**; 64; 3846-52

[16] Lorand, J. P.; Edwards, J. O.; *J. Org. Chem.*; **1959**; 24; 769-74

[17] Bosch, L. I.; Fyles, T. M.; James, T. D.; *Tetrahedron*; **2004**; 60; 11175-90

[18] James, T. D.; Shinkai, S.; *Topics in Current Chemistry*; **2002**; 218; 159-200

[19] Liu, X.; Scouten, W.; *J Chromatogr. A*; **1994**; 687; 61-9

[20] Springsteen, G.; Wang, B.; *Chem. Commun.*; **2001**; 1608-9

[21] Singhal, R. P.; Ramamurthy, B.; Govindraj, N.; Sarwar, Y.; *J. Chromatogr, A*; **1991**; 543; 17-38

[22] Yan, J.; Springsteen, G.; Deeter, S.; Wang, B.; *Tetrahedron*; **2004**; 60; 11205-9

[23] Springsteen, G.; Deeter, S.; Wang, B.; *Tetrahedron*; **2004**; 60; 11205-9

[24] Yang, W.; He, H.; Drueckhammer, D. G.; *Angew. Chem. Int. Ed.*; **2001**; 40; 9; 1714-8

[25] Tsukagoshi, K.; Shinkai, S.; *J. Org. Chem.*; **1991**; 56; 4089

[26] Takeuchi, M.; Imada, T.; Shinkai, S.; *J. Am. Chem. Soc.*; **1996**; 118; 10658

[27] James, T. D.; Samankumara Sandanayake, K. R. A.; Shinkai, S.; *Supramolecular Chemistry*; **1995**; 6; 1-2; 141-157

[28] Springsteen, G.; Ballard, C. E.; Gao, S.; Wang, W.; Wang, B.; *Bioorganic Chemistry*; **2001**; 29; 259-70

[29] James, T. D.; Samankumara Sandanayake, K. R. A.; Shinkai, S.; *J. Chem. Soc., Chem. Commun.*; **1994**; 477-8

[30] Cooper, C. R.; James, T. D.; *Chemistry Letters*; **1998**; 883-4

[31] Samankumara Sandanayake, K. R. A.; Imazu, S.; James, T. D.; Mikami, M.; Shinkai, S.; *Chemistry Letters*; **1995**; 139-40

[32] Cooper, C. R.; James, T. D.; *J. Chem. Soc., Perkin Trans 1*; **2000**; 963-9

[33] James, T. D.; Samankumara Sandanayake, K. R. A.; Shinkai, S.; *Nature*; **1995**; 374; 345-7

[34] Zhao, J.; James, T. D.; *J. Mater. Chem.*; **2005**; 15; 2896-901

[35] Hatcher, J. T.; Wilcox, L. V.; *Analytical Chemistry*; **1950**; 22; 4; 567-9

[36] Smith Jr., W. C.; Goudie, A. J.; Siverston, J. N.; *Analytical Chemistry*; **1955**; 27; 2; 295-7

[37] Kubo, Y.; Kobayashi, A.; Ishida, T.; Misawa, Y.; James, T. D.; *Chem. Commun.*; **2005**; 2846-8

[38] Koumoto, K.; Shinkai, S.; *Chemistry Letters*; **2000**; 8; 856-7

[39] James, T. D.; Samankumara Sandanayake, K. R. A.; Shinkai, S.; *Supramolecular Chemistry*; **1998**; 9; 3; 203-10

[40] James, T. D.; Harada, T.; Shinkai, S.; *J. Chem. Soc. Chem. Commun.*; **1993**; 1176

[41] Takeuchi, M.; Mizuno, T.; Shinkai, S.; Shirakami, S.; Itoh, T.; *Tetrahedron: Asymmetry*; **2000**; 11; 3311-3322

[42] Sugasaki, A.; Sugiyasu, K.; Ikeda, M.; Takeuchi, M.; Shinkai, S.; *J. Am. Chem. Soc.*; **2001**; 123; 10239-44

[43] Kimaru, T.; Takeuchi, M. Nagasaki, T.; Shinkai, S.; *Tetrahedron Letters*; **1995**; 559-62

[44] Kobayashi, H.; Nakashima, K.; Ohshima, E.; Hisaeda, Y.; Hamachi, I.; Shinkai, S.; *J. Chem. Soc., Perkin Trans. 2*; **2000**; 997-1002

[45] Arimori, S.; Hartley, J. H.; Bell, M. L.; Oh, C. S.; James, T. D.; *Tetrahedron Letters*; **2000**; 10291-4

[46] Yang, W.; Gao, X.; Springsteen, G.; Wang, B.; *Tetrahedron Letters*; **2002**; 6339-42

[47] Stones, D.; Manku, S.; Lu, X.; Hall, D. G.; *Chem. Eur. J.*; **2004**; 10; 92-100

[48] Merrifield, R. B.; *J. Am. Chem. Soc.*; **1963**, 85; 14; 2149–54

[49] Atherton, E.; Fox, H.; Harkiss, D.; Logan, C. J.; Sheppard, R. C.; Williams, B. J.; *J. Chem. Soc. Chem. Comm.*; **1978**; 13; 537-9

[50] Jones, J.; *Amino Acid and Peptide Synthesis*; Oxford: Oxford University Press; **1994**; p 18; ISBN 0-19-855668-3

[51] Chan, W. C.; White, P. D.; In: Chan, W. C.; White, P. D.; Editors. *Fmoc Solid Phase Peptide Synthesis; A Practical Approach*; Oxford: Oxford University Press; **2000**; ISBN: 0-19-963724-5

[52] Atherton, E.; Holder, J.; Meldal, M.; Sheppard, R. C.; Valerio, R. M.; *J. Chem. Soc. Perkin Trans. 1*; **1988**; 2887

[53] Carpino, L. A.; Beyermann, M.; Wenschuh, H.; Bienert, M.; *Acc. Chem. Res.*; **1996**; 29; 268

[54] Coste, J.; Le-Nguyen, D.; Castro, B.; *Tetrahedron Letters*; **1990**; 31; 205

[55] Knorr, R.; Trzeciak, A.; Bannwarth, W.; Gillessen, D.; *Tetrahedron Letters*; **1989**; 30; 1927

[56] Fields, C. G.; Lloyd, D. H.; Macdonald, R. L.; Otteson, K. M.; Noble, R. L.; *Pept. Res.*; **1991**; 4; 95

[57] Carpino, L.; *J. Am. Chem. Soc.*; **1993**; 115; 4397

[58] Albericio, F.; Cases, M.; Alsina, J.; Triolo, S. A.; Carpino, L. A.; Kates, S. A.; *Tetrahedron Letters*; **1991**; 38; 4853

[59] Carpino, L.; Han, G. Y.; *J. Org. Chem.*; **1972**; 37; 3404-9

[60] Bycroft, B. W.; *J. Chem. Soc. Chem. Comm.*; **1993**; 778

[61] Sherrington, D. C.; *Chem. Commun.*; **1998**; 2275-86

[62] Balkenhohl, F.; von dem Bussche-Hunnefeld, C.; Lansky, A.; Zechel, C.; *Angew. Chem. Int. Engl.*; **1996**; 35; 2288

[63] Ing, H. R.; Manske, R. H. F.; *J. Chem. Soc.*; **1926**: 2348

[64] Wilson, M. E.; Paech, K.; Jing Zhou, W.; Kurth, M. J.; *J. Org. Chem.* **1998**; 63, 5094

[65] McCairn, M. C.; Tonge, S. R.,; Sutherland, A. J.; *J. Org. Chem.* **2002**; 67; 4847-4855

[66] Adams, J. H.; Cook, R. M.; Hudson, D.; Jammalamadaka, V.; Lyttle, M. H.; Songster, M. F.; *J. Org. Chem.*; **1998**; 63; 11; 3706-16

[67] Kaiser, E.; Colescott, R. L.; Bossinger, C. D.; Cook, P. I.; *Anal. Biochem.*; **1970**; 34; 595

[68] Hancock, W. S.; Battersby, J. E.; *Anal. Biochem.*; **1976**; 71 260

[69] MSDS; www.sigmaaldrich.com

[70] Joo, S. H.; Pei, D.; *Biochemistry*; **2008**; 47; 3061-72

[71] *Resins and Reagents for accelerating Synthesis and Purification Catalogue*; Argonaut Technologies; Foster City, CA; **2000**

[72] Zaplinsky, S.; Chang, J. L.; Albericio, F.; Barany, G.; *React. Polym.*; **1994**; 22; 243

[73] Buchardt, J.; Meldal, M.; *Tetrahedron Lett.*; **1998**; 39; 8695-8

[74] Patent / PCT/GB03/01774

[75] Renil, M.; Meldal, M. *Tetrahedron Lett.*; **1992**; 37; 6185

[76] Gaggini, F.; Porcheddu, A.; Reginato, G.; Rodriquez, M.; Taddei, M.; *J. Comb. Chem.* **2004**; 6; 805-10

[77] Lambert, J. B.; Shurvell, H. F.; Lightner, D. A.; Cooks, R. G.; *Organic Structural Spectroscopy*; 1st Edition; Prentice Hall; ISBN 0-13-258690-8

[78] Gude, M.; Ryf, J.; White, P. D.; *Letters in Peptide Science*; **2002**; 9 (4-5); 203-6

[79] Marx, V.; *Chemical and Engineering News*; **2005**; 83 (11); 16-7 and *C&EN online* http://pubs.acs.org/cen/business/83/i11/8311bus1box1.html

[80] Alesso, S. M.; Zhanru, Y.; Pears, D.; Worthington, P. A.; Luke R. W. A.; Bradley, M.; *J Comb. Chem.*; **2001**; 3 (6); 631-3

[81] Jotterland, N.; Pearce, D. A.; Imperiali, B.; *J. Org. Chem.*; **2001**; 66 (9); 3224-8

[82] Novabiochem. Synthesis Notes. In: *Novabiochem Catalogue and Peptide Synthesis Handbook*. CA: La Jolla; **1998**, p.S37

[83] Kates, S. A.; Sole, N. A.; Beyermann, M.; Barany, G.; Albericio, F.; *Pept. Res.*; **1996**; 9 (3); 106-13

[84] Wade, J. D.; Bedford, J.; Sheppard, R. C.; Tregear, G. W.; *Pept. Res.*; **1991**;4 (3); 194-9

[85] Tickler, A. K.; Barrow, C. J.; Wade, J. D.; *J. Pept. Sci*; **2001**; 7; 488-94

[86] Várady, L.; Shranabasava, B. R.; Nicewonger, R. B.; Guo, M.; Ditto, L.; *J. Chromatogr. A*; **2000**; 869 (1-2); 171-9

[87] Freeman, C. E.; Howard, A. G.; *Talanta*; **2005**; 65; 574-7

[88] Newcomb, W. S.; Deegan, T. L.; Miller, W.; Porco Jr., J. A.; *Biotech. Bioeng*; **1998**;61; 55-60

[89] Diaz-Monchón, J. J.; *Organic letters*; **2004**; 6; 1127

[90] Kellam, B.; Chan, W. C.; Chhabra, S. R.; Bycroft, B. W.; *Tetrahedron Letters*; **1997**; 30; 30; 5391-4

[91] www.sigmaaldrich.com [Product specification; CAS 126-81-8; FT-NMR]

[92] Arimori, S.; James, T. D.; *Tetrahedron Letters*; **2002**; 43; 507-9

[93] Arimori, S.; Consiglio, G. A.; Phillips, M. D.; James, T. D.; *Tetrahedron Letters*; **2003**; 44; 4789-92

[94] Smoum, R.; Rubinstein, A.; Srebnik, M,; *Bioorganic Chemistry*; **2003**; 31; 464-74

[95] Riggs, J. A.; Hossler, K. A.; Smith, B. D.; Karpa, M. J.; Griffin, G.; Duggan, P. J.; *Tetrahedron Letters*; **1996**; 35; 6303-6

[96] Draffin, S. P.; Duggan, P. J.; Duggan, S. A. M.; Norrild, J. C.; *Tetrahedron*; **2003**; 59; 9075-82

[97] Sarin, V. K.; Kent, S. B. H.; Tam, J. P.; Merrifield, R. B.; *Anal. Biochem.*; **1981**; 117; 147-57

[98] Perkins, H. R.; Nieto, M.; *Biochem. J.*; **1971**; 123; 789-803

[99] Sheldrick, G. M.; Jones, P. G., Kennard, O.; Williams, D. H.; Smith, G. A.; *Nature*; **1978**; 271; 223-5

[100] Arthur, M.; Reynolds, P.; Courvalin, P.; *Trends in Microbiology*; **1996**; 4; 10; 401-7

[101] Chu, Yen-Ho; Whitesides, G. M.; *J. Org. Chem.*; **1992**; 57; 3524-5

[102] Hermanson, G., T.; *Bioconjugate Techniques: 2nd Ed.*; Published by Academic Press; **2008**; ISBN 0-12-370501-0; p.103

[103] Sieber, P.; *Tetrahedron Letters*; **1987**; 28; 49; 6147-50

[104] Wormald, M. R.; Petrescu, A. J.; Pao, Y.; Glithero, A.; Elliott, T.; Dwek, R. A.; *Chem. Rev.*; **2002**; 120; 371-86

[105] Hayes, W.; Osborn, H. M. I.; Osborne, S. D.; Rastall, R. A.; Romagboli, B.; *Tetrahedron*; **2003**; 59; 7983-7996

[106] Grandjean, C.; Rommens, C.; Gras-Masse, H.; Melnyk, O.; *Tetrahedron Letters*; **1999**; 40; 7235-8

[107] Bertozzi, C. R.; Bednarski, M. D.; *J. Org. Chem.*; **1991**; 56; 4326-9

[108] Cao, S.; Tropper, F. D.; Roy, R.; *Tetrahedron*; **1995**; 51; 24; 6679-86

[109] Cotté, A.; Bader, B.; Kuhlmann, J.; Waldmann, H.; *Chem. Eur. J.*; **1999**; 5; 3; 922-36

[110] Gutheil, W. G.; Stefanova, M. E.; Nicholas, R. A.; *Analytical Biochemistry*; **2000**; 287; 196-202

[111] Kao, J. C.; Geroski, D. H.; Edelhauser, H. F.; *Journal of Ocular Pharmacology and Therapeutics*; **2005**; 21; 1; 1-10

[112] Pereira, P. M.; Filipe, S. R.; Tomasz, A.; Pinho, M. G.; *Antimicrobial Agents and Chemotherapy*; **2007**; 51; 10; 3627-33

[113] DeDent, A. C.; McAdow, M.; Schneewind, O.; *Journal of Bacteriology*; **2007**; 189; 12; 4473-84

[114] Jefferson, K. K.; Goldmann, D. A.; Pier, G. B.; *Antimicrobial Agents and Chemotherapy*; **2005**; 49; 6; 2467-73

[115] Thanky, N. R.; Young, D. B.; Robertson, B. D.; *Tuberculosis*; **2007**; 87; 231-6

[116] Tiyanont, K.; Doan, T.; Lazarus, M. B.; Fang, X.; Rudner, D. Z.; Walker, S.; *PNAS*; **2006**; 103; 29; 11033-8

[117] Metallo, S. J.; Kane, R. S.; Holmlin, R. E.; Whitesides, G. M.; *J. Am. Chem. Soc.*; **2003**; 125; 4534-40

[118] Nagarjan, R.; Schabel, A. A.; Occolowitz, J. L.; *The Journal of Antibiotics*; **1988**; 41; 10; 1430-8

[119] Fernández, J. M. G.; Mellet, C. O.; Diaz Pérez, V. M.; Jiménez Blanco, J. L.; Fuentes, J.; *Tetrahedron*; **1996**; 52; 40; 12947-70; **see compound 40, 41.**

[120] Noble, R. L.; Yamashiro, D.; Li, C. H.; *J. Am. Chem. Soc.*; **1976**; 98; 2324-8

[121] Schwyzer, R.; Dietrich, H.; *Helv. Chim. Acta.*; **1961**; 44; 2003

[122] Callahan, F. M.; Anderson, G. W.; Paul, R.; Zimmermann, J. E.; *J. Am. Chem. Soc.*; **1963**; 85; 201

[123] Chang, C. D.; Wakai, M.; Ahmed, M.; Meienhofer, J.; Lundell, E. D.; Huang, J. D.; *Int. J. Pep. Protein. Res.*; **1980**; 15; 59

[124] Sieber, P.; Riniker, B.; *Tetrahedron Letters*; **1991**; 32; 739

[125] Carpino, L. A; Shroff, H.; Triolo, S. A.; Mansour, M. E.; Wenschurch, H.; Albericio, F.; *Tetrahedron Letters*; **1993**; 34; 7829

[126] Sundram, U. N.; Griffin, J. H.; *J. Org. Chem.*; **1995**; 60; 1102-3

[127] Roberts, P. J.; Kennard, O.; Smith, K. A.; Williams, D. H.; *J. C. S. Chem Comm.*; **1973**; 772-4

[128] Waltho, J. P.; Williams, D. H.; Stone, D. J.; Skelton, N. J.; *J. Am. Chem. Soc.*; **1988**; 110; 5638-43

[129] Atkins, P. W.; *Physical Chemistry 6th Ed.*; Oxford University Press; **1998**; p.752; ISBN: 0-19-850101-3

[130] Shriver, D. F.; Atkins, P. W.; Langford, C. H.; *Inorganic chemistry 2nd Ed.*; Oxford University Press; **1998**; ISBN: 0-19-855396-X; p.262

[131] http://www.wiley.com/college/pratt/0471393878/student/review/thermodynamics/4_gibbs.html

[132] Nicas, T. I.; Cole, C. T.; Preston, D. A.; Schabel, A. A.; Nagarajan, R.; *Antimicrobial Agents and Chemotherapy*; **1989**; 1477-81

[133] Hughes, J.; Smith, T. W.; Kosterlitz, H. W.; Fothergill, L. A.; Morgan, B. A.; Morris, H. R.; *Nature*; **1975**; 258 (5536); 577-80

[134] Albericio, F.; Annis, I.; Royo, M.; Barany, G.; Preparation and handling of peptides containing methionine and cysteine. In: Chan, W. C.; White, P. D, Editors. *Fmoc Solid Phase Peptide Synthesis; A Practical Approach*. Oxford: Oxford University Press; **2000**, p.77-114